



National Library  
of Canada

Acquisitions and  
Bibliographic Services Branch

395 Wellington Street  
Ottawa, Ontario  
K1A 0N4

Bibliothèque nationale  
du Canada

Direction des acquisitions et  
des services bibliographiques

395, rue Wellington  
Ottawa (Ontario)  
K1A 0N4

*Your file* *Votre référence*

*Our file* *Notre référence*

## NOTICE

The quality of this microform is heavily dependent upon the quality of the original thesis submitted for microfilming. Every effort has been made to ensure the highest quality of reproduction possible.

If pages are missing, contact the university which granted the degree.

Some pages may have indistinct print especially if the original pages were typed with a poor typewriter ribbon or if the university sent us an inferior photocopy.

Reproduction in full or in part of this microform is governed by the Canadian Copyright Act, R.S.C. 1970, c. C-30, and subsequent amendments.

## AVIS

La qualité de cette microforme dépend grandement de la qualité de la thèse soumise au microfilmage. Nous avons tout fait pour assurer une qualité supérieure de reproduction.

S'il manque des pages, veuillez communiquer avec l'université qui a conféré le grade.

La qualité d'impression de certaines pages peut laisser à désirer, surtout si les pages originales ont été dactylographiées à l'aide d'un ruban usé ou si l'université nous a fait parvenir une photocopie de qualité inférieure.

La reproduction, même partielle, de cette microforme est soumise à la Loi canadienne sur le droit d'auteur, SRC 1970, c. C-30, et ses amendements subséquents.

# **The Evaporation of Crude Oil and Petroleum Products**

Mervin F. Fingas

In Partial Fulfilment of the  
Requirements for the Degree of

Doctor of Philosophy

Department of Natural Resource Sciences  
McGill University, Montreal

February, 1996

© Mervin F. Fingas



National Library  
of Canada

Acquisitions and  
Bibliographic Services Branch

395 Wellington Street  
Ottawa, Ontario  
K1A 0N4

Bibliothèque nationale  
du Canada

Direction des acquisitions et  
des services bibliographiques

395, rue Wellington  
Ottawa (Ontario)  
K1A 0N4

*Your file* *Votre référence*

*Our file* *Notre référence*

The author has granted an irrevocable non-exclusive licence allowing the National Library of Canada to reproduce, loan, distribute or sell copies of his/her thesis by any means and in any form or format, making this thesis available to interested persons.

L'auteur a accordé une licence irrévocable et non exclusive permettant à la Bibliothèque nationale du Canada de reproduire, prêter, distribuer ou vendre des copies de sa thèse de quelque manière et sous quelque forme que ce soit pour mettre des exemplaires de cette thèse à la disposition des personnes intéressées.

The author retains ownership of the copyright in his/her thesis. Neither the thesis nor substantial extracts from it may be printed or otherwise reproduced without his/her permission.

L'auteur conserve la propriété du droit d'auteur qui protège sa thèse. Ni la thèse ni des extraits substantiels de celle-ci ne doivent être imprimés ou autrement reproduits sans son autorisation.

ISBN 0-612-12368-5

Canada

## Abstract

The physics of oil and petroleum evaporation are investigated. Literature on oil spill evaporation shows that most workers use boundary-layer equations adapted from water evaporation work. These equations predict a constant evaporation mass-transfer rate, dependent on scale size and wind speed. Evaporation was studied further by measuring evaporation of commercial oil products. An experimental apparatus for the study of evaporation was developed. Evaporation was determined by weight loss measured on a balance and recorded constantly on a computer. Examination of the data shows that most oil and petroleum products evaporate at a logarithmic rate with respect to time. This is attributed to the overall logarithmic appearance of many components evaporating at different linear rates. Petroleum products with fewer chemical components such as diesel fuel, evaporate at a rate which is square root with respect to time. The particular behaviour is shown to be a result of the number of components evaporating. Oils with greater than seven to ten components can be predicted with logarithmic equations, those with three to seven components, with square root equations. Evaporation of oils and petroleum products is not strictly boundary-layer regulated. This is largely a result of the high saturation concentrations of oil components in air, which is associated with a high boundary-layer regulated rate. Typical oil evaporation rates do not exceed that of molecular diffusion, and thus turbulent diffusion does not increase the evaporation rates. Some volatile oils and petroleum products show some effect of boundary-layer regulation at the start of the evaporation process, but after several minutes, evaporation slows because of the loss of the more volatile components, at which point evaporation ceases to be boundary-layer regulated. Overall, boundary-layer regulation can be ignored in the prediction of oil and petroleum evaporation. A simple equation relating only the logarithm of time (or square root of time for narrow-cut products) and temperature can accurately describe oil evaporation. Methods to calculate the constants for the equation using only conventional distillation data are described. Empirical and calculated evaporation equations for several common world crude oils are given.

## Resumé

La physique de l'évaporation des huiles et du pétrole a été étudiée. Une revue de la littérature démontre que la majorité des auteurs utilisent des équations adaptées de travaux portant sur l'évaporation de l'eau. Ces équations prédisent un taux constant de transfert de masse dû à l'évaporation, dépendant de l'échelle spatiale et de la vitesse du vent. Le processus d'évaporation a été étudié en utilisant des huiles industrielles. Un appareil expérimental a été développé à cette fin. L'évaporation a été suivie en mesurant sur une base continue la perte de masse à l'aide d'une balance informatisée. L'examen des données montre que la plupart des huiles et produits pétroliers s'évaporent selon une fonction logarithmique du temps. Ceci est attribué à l'apparence logarithmique générale de plusieurs composantes s'évaporant selon des taux linéaires. Les produits pétroliers contenant moins de composantes, comme le diesel, s'évaporent selon la racine carrée du temps. Ce comportement particulier découle du nombre de composantes qui s'évaporent. Les huiles formées de plus de sept à dix composantes peuvent être évaluées selon un taux logarithmique alors que celles contenant de trois à sept composantes peuvent l'être selon une puissance une-demi. L'évaporation des huiles et produits pétroliers n'est pas régulée par la couche aérodynamique au sens strict du mot. Ceci est dû en grande partie aux fortes concentrations de saturation des composantes s'évaporant dans l'air, d'où une influence importante de la couche de surface. Les taux typiques d'évaporation ne dépassent pas ceux de la diffusion moléculaire, donc la turbulence en terme de diffusion n'accroît pas le taux d'évaporation. Quelques huiles et produits pétroliers légers montrent un effet de la couche de surface au début du processus d'évaporation mais, après plusieurs minutes, le taux diminue en fonction de la perte de composantes volatiles et l'évaporation n'est plus dépendante de la couche de surface. De façon générale, la régulation par couche de surface peut être ignorée dans les prédictions d'évaporation d'huiles et de produits pétroliers. Une équation simple reliant le temps (logarithme - ou encore la racine carrée du temps pour des produits bien définis) et la température peut décrire adéquatement le processus d'évaporation. Des méthodes pour calculer les constantes de ces équations utilisant seulement des résultats de distillation sont décrites et des équations d'évaporation - empiriques et théoriques - sont présentées pour plusieurs huiles brutes en utilisation dans partout le monde.

## Statement of Originality

This thesis presents a new method for the measurement of oil evaporation, a new mathematical model for the evaporation process, and new findings on the evaporation of oils including the relationship of temperature, boundary layer effect, curvilinear behaviour of evaporating oils and the relationship of the evaporation equations to distillation data.

The literature section presents the first comprehensive review ever compiled on the physics and modelling of oil spill evaporation.

The methodology section describes a new procedure for continuous measurement of oil evaporation. Several innovations are presented, including the use of a new generation of accurate balances, development of a software package that enables geometric progress of time intervals between data times, and the filtering of balance data in real time to remove fluctuating values.

Chapter 4 presents confirmation that oil and petroleum products evaporate in a curvilinear fashion rather than linear as do pure chemicals. This curvilinear behaviour is demonstrated to be the envelope of many components evaporating linearly, but at different rates.

This thesis shows, for the first time, that the evaporation of oils and petroleum products is not strictly boundary-layer regulated. The physical reasons for this phenomenon are demonstrated to be the result of rate as well as more fundamental differences between oils and water, including the difference in air saturation concentration.

This thesis shows that the relationship between temperature and evaporation rate for oils is linear and not  $\log T/T$  which was previously noted in the literature. This thesis

This thesis presents a new mathematical model for oil evaporation. This model is very different from any previous work and does not include components related to boundary-layer regulation. The model is simple, but results in highly-accurate predictions of evaporation rate and loss. This model has constants which are shown to be predictable from oil and petroleum distillation data. This is the first time such relationships have been suggested.

## Acknowledgements

I thank Dr. Peter Schuepp, my supervisor, for his constant encouragement and enthusiasm for the work. I particularly wish to thank him for taking on an off-campus student whom he did not know. His trust and support throughout this project were outstanding.

I thank my wife, Brenda, and my three children, Jonathan, Roger, and Karen, for their patience and understanding during the four years of this work. My schedule during this time was not conducive to a leisurely family life. A typical day consisted of leaving home at 8:00 a.m., returning at 7:00 p.m. and then immediately retreating to the computer for data analysis and paper writing. All day Saturday and Sunday were similar, with only a short time taken out for family events. Only in this way could I put in a full day on the evaporation project and take care of my work duties.

I thank my co-workers at Environment Canada, first for allowing me to take on this onerous task and secondly for showing patience and help during the project. First, I should acknowledge my immediate supervisor, Dr. Thornton, for allowing me to do both jobs, knowing that he would have to shoulder some additional management tasks. Second, I acknowledge my staff who offered me so much encouragement and support during the project. I name Dr. Paré, Dr. Bélanger, Dr. Wang, Dr. Carl Brown, Dr. Richard Lawuyi, Paula Jokuty, Pat Lambert, Dave Roy and Steve Whiticar.

I also thank Dr. Yaylayan, who provided advice on this project, and my fellow graduate students at McGill for support, helpful discussions and for helping me do many things by 'remote control'.

## Preface

This thesis presents the results of experimental, statistical and theoretical investigation into the physics of oil and petroleum evaporation. The thesis is divided into chapters. Each chapter is written with abstract, introduction, conclusions and references - where appropriate. The introduction introduces the topic and explores the theoretical relationships of evaporation. The second chapter presents an extensive literature review on the topics of evaporation physics and the application to prediction modelling. The third chapter presents the methodology developed to measure evaporation and the characterization of turbulence in the experiments. The fourth chapter presents the methodology and results from experiments designed to examine the overall nature of oil evaporation. The relationship between the curve describing oil evaporation and the nature of the oil itself is described for the first time. Chapter 5 describes experiments testing whether or not oil evaporation is boundary-layer regulated. The findings that oil evaporation is not specifically boundary-layer regulated are explained in physical terms. Chapter 6 reports on experiments to delineate the effect of temperature on oil evaporation rate. Chapter 7 describes outdoor experiments to confirm the laboratory findings. Chapter 8 describes experiments on various oils and petroleum products and correlations of evaporation rate to distillation data. Equations to predict oil evaporation are developed. The overall conclusions of the thesis are summarized in Chapter 9.

Some earlier findings of this work were published as separate papers. All work in this thesis is newer and more comprehensive than presented in these three papers. The references for these are:

Fingas, M.F., "Studies on the Evaporation of Oil Spills," in *Proceedings of the Seventeenth Arctic and Marine Oil Spill Program Technical Seminar*, Environment Canada, Ottawa, Ontario, pp. 189-212, 1994.

Fingas, M.F., "The Evaporation of Oil Spills," *Journal of Hazardous Materials*, Vol. 42, pp. 157-175, 1995.

Fingas, M.F., "The Evaporation of Oil Spills," in *Proceedings of the Eighteenth Arctic and Marine Oil Spill Program Technical Seminar*, Environment Canada, Ottawa, Ontario, pp.43-60, 1995.

## Table of Contents

Abstract	ii
Resumé	iii
Claims of Originality	iv
Acknowledgements	vi
Preface	vii
Table of Contents	viii
List of Tables	x
List of Figures	xii
Glossary of Symbols and Abbreviations	xvii
Chapter 1 Introduction	1
1.1 Introduction	1
1.2 Physics of Evaporation	2
1.3 Thermodynamic Aspects of Evaporation	5
1.4 References	7
Chapter 2 Literature Review	9
2.1 Abstract	9
2.2 Physics and Chemistry of Oil Evaporation	9
2.3 Use of Evaporation Equations in Spill Models	20
2.4 Discussion	30
2.5 References	31
Chapter 3 Experimental Methodology and Turbulence Characterization	36
3.1 Experimental	36
3.2 Evaporation Data Handling	36
3.3 Air Flow and Turbulence Measurements	44
Chapter 4 Evaporation Behaviour of Oils and Petroleum	54
4.1 Abstract	54
4.2 Experimental	54

4.3 Results and Discussion	54
4.4 Conclusions	62
Chapter 5 The Application of Traditional Boundary Layer Regulation	64
5.1 Abstract	64
5.2 Introduction	64
5.3 Experimental	66
5.3 Results and Discussion	68
5.4 Conclusions	111
Chapter 6 The Relationship Between Evaporation Rate and Temperature	114
6.1 Abstract	114
6.2 Introduction	114
6.3 Experimental	115
6.4 Results and Discussion	118
6.5 Conclusions	139
Chapter 7 Field Confirmation of Laboratory Methodology	143
7.1 Abstract	143
7.2 Introduction	143
7.3 Experimental	144
7.4 Results and Discussion	144
7.5 Conclusions	154
Chapter 8 Development of Evaporation Prediction Equations	155
8.1 Abstract	155
8.2 Introduction	155
8.3 Experimental	155
8.4 Results and Discussion	156
8.5 Conclusions	174
Chapter 9 Overall Conclusions	175
Recommendations for Further Research	181

<b>List of Tables</b>	<b>Page</b>
Table 2.1 Data from the Bobra Evaporation Experiments	20
Table 2.2 Correlation Equation Constants for the Characterization of Narrow Boiling Point Fractions	26
Table 3.1 Example Calculation Spreadsheet for an Evaporation Experiment	41
Table 3.2 Example Curve Fit Table for an Evaporation Experiment	43
Table 3.3 Data Obtained from the NRC Anemometer Calibration Experiments	44
Table 3.4 Example of A Calculation Table for Air Velocity and Turbulence Analysis	47
Table 3.5 Summary of Wind Data	49
Table 4.1 Summary Table of Experiments Conducted to Delineate Oil Evaporation Behaviour	55
Table 4.2 Best Fit Equations for Each of the Oils	58
Table 4.3 Constituents of the Hydrocarbon Mixtures	60
Table 4.4 Power Exponents for Multi-Component Evaporation	60
Table 5.1 Properties of the Test Liquids	64
Table 5.2 Experiments Conducted To Test Boundary Layer Regulation	70
Table 5.3 Data From The Wind Tests	73
Table 5.4 Data From the Thickness Tests	89
Table 5.5 Data from the Area Tests	91
Table 5.6 Data from the Volume/Mass Tests	93
Table 5.7 Data from the Evaporation Tests of Pure Hydrocarbons	96
Table 5.8 Data from the Evaporation of Pure Hydrocarbons in a Weathered Oil Matrix	96
Table 5.9 Instantaneous Evaporation Rates of ASMB with Varying Winds	102
Table 5.10 Summary of Rate Comparisons	108
Table 5.11 Comparison of Maximum Evaporation Rates	109
Table 5.12 Saturation Concentration of Water and Oil Components	110

**List of Tables .. ctd.**

	Page
Table 6.1 Properties of the Test Liquids	116
Table 6.2 Experiments Conducted to Test the Temperature Effect	117
Table 6.3 Evaporation Rates or Single-Factor Equation Parameters	129
Table 6.4 Equations Relating Evaporation Rate and Temperature	129
Table 6.5 Experimental and Calculated Temperature Equations	133
Table 6.6 Evaporation Rates or Single-Factor Equation Parameters - Prediction Using Base Equations	134
Table 6.7 Evaporation Rates or Single-Factor Equation Parameters - Prediction by Use of Distillation Data	140
Table 7.1 Summary of Outdoor Confirmation Experiments	145
Table 7.2 Temperature and Wind for Outdoors Experiments	145
Table 8.1 Summary Table of Experiments Involving Different Oils	157
Table 8.2 Properties of the Test Liquids	158
Table 8.3 Distillation Data on Oil Used in the Study	159
Table 8.4 Correlation Between Distillation Data and Evaporation	164
Table 8.5 Experimental and Calculated Evaporation Rates	169
Table 8.6 Experimental and Calculated Evaporation Rates for Narrow-Cut Products	170

## List of Figures

	Page
Figure 3.1 Experimental Setup	39
Figure 3.2 Example Correlation curve for an Evaporation Experiment	45
Figure 3.3 Calibration of the Anemometer	45
Figure 3.4 The Variation of Air Velocity Over Time - An Example	48
Figure 3.5 The Spectra of Turbulence - An Example	48
Figure 3.6 Correlation of Wind Statistical Factors	48
Figure 3.7 Experimental Setup for Wind Four	51
Figure 3.8 The Variation of Air Velocity Over Time - Wind 1	52
Figure 3.9 The Variation of Air Velocity Over Time - Wind 2	52
Figure 3.10 The Variation of Air Velocity Over Time - Wind 3	52
Figure 3.11 The Variation of Air Velocity Over Time - Wind 4	52
Figure 3.12 The Spectra of Turbulence - Wind 1	53
Figure 3.13 The Spectra of Turbulence - Wind 2	53
Figure 3.14 The Spectra of Turbulence - Wind 3	53
Figure 3.15 The Spectra of Turbulence - Wind 4	53
Figure 4.1 The Evaporative Behaviour of Multiple Components	61
Figure 4.2 A Schematic Showing How Logarithmic Behaviour Can Result from Linear Multi-Component Evaporation	63
Figure 5.1 Correlation of Evaporation and Wind Velocity - ASMB Oil	74
Figure 5.2 Correlation of Evaporation and Wind Velocity - Gasoline	75
Figure 5.3 Correlation of Evaporation and Wind Velocity - FCC heavy	76
Figure 5.4 Correlation of Evaporation and Wind Velocity - Water	77
Figure 5.5 Correlation of Evaporation and Wind Velocity - ASMB by Weight	78
Figure 5.6 Correlation of Evaporation and Wind Velocity - Gasoline by Weight	79
Figure 5.7 Correlation of Evaporation and Wind Velocity - FCC Heavy by Weight	80

## List of Figures ... ctd.

	Page
Figure 5.8 Correlation of Evaporation and Wind Velocity - Water by Weight	81
Figure 5.9 Evaporation of ASMB with Varying Wind Velocities	82
Figure 5.10 Evaporation of FCC with Varying Wind Velocities	83
Figure 5.11 Evaporation of Gasoline with Varying Wind Velocities	84
Figure 5.12 Evaporation of Water (20g) with Varying Wind Velocities	85
Figure 5.13 Evaporation of Water (40g) with Varying Wind Velocities	86
Figure 5.14 Correlation of Evaporation Rates with Wind Speed	88
Figure 5.15 Correlation of Thickness with Evaporation Rate	90
Figure 5.16 Correlation of Area with Evaporation Rate	92
Figure 5.17 Correlation of Mass with Evaporation Rate	94
Figure 5.18 Evaporation Rate of Pure Hydrocarbons	97
Figure 5.19 Evaporation Rate of Pure Hydrocarbons in an Oil Matrix	99
Figure 5.20 Comparison of Evaporation Rates of Pure Hydrocarbons Neat and in a Weathered Oil Matrix	100
Figure 5.21 Plot of ASMB Evaporation Rates Versus Time - No Wind	103
Figure 5.22 Plot of ASMB Evaporation Rates Versus Time - Variable Winds	104
Figure 5.23 Comparison of Maximum Evaporation Rates at Different Wind Velocities	105
Figure 5.24 Conceptual Diagram of Oil Evaporation	113
Figure 6.1 The Variation of Evaporation Rates with Temperature	119
Figure 6.2 The Variation of Evaporation Rates with Temperature - Without Gasoline	120
Figure 6.3 The Variation of Evaporation Rates with Temperature - Linear Regression	121
Figure 6.4 The Variation of Evaporation Rates with Temperature - Without Gasoline - Linear Regression	122

## List of Figures ... ctd.

	Page
Figure 6.5 Correlation of ASMB Evaporation and Temperature	123
Figure 6.6 Correlation of Gullfaks Evaporation and Temperature	123
Figure 6.7 Correlation of Brent Evaporation and Temperature	124
Figure 6.8 Correlation of Arabian Light Evaporation and Temperature	124
Figure 6.9 Correlation of Gasoline Evaporation and Temperature	125
Figure 6.10 Correlation of Terra Nova Evaporation and Temperature	125
Figure 6.11 Correlation of Statfjord Evaporation and Temperature	126
Figure 6.12 Correlation of Diesel Evaporation and Temperature	126
Figure 6.13 Correlation of Bunker C Light Evaporation and Temperature	128
Figure 6.14 Correlation of ASMB Evaporation and Temperature: Loss of Weight Equation	128
Figure 6.15 Correlation of Percentage Temperature Equation Slope and Base Parameter	131
Figure 6.16 Correlation of Percentage Temperature Equation Intercept and Base Parameter	131
Figure 6.17 Correlation of Weight Temperature Equation Slope and Base Parameter	132
Figure 6.18 Correlation of Weight Temperature Equation Intercept and Base Parameter	132
Figure 6.19 Optimization of Distillation and Temperature Slope - Percent Equation	136
Figure 6.20 Optimization of Distillation and Temperature Slope - Weight Equation	136
Figure 6.21 Correlation of Slope of Percent Equation and the Percent Distilled at a Given Temperature	137
Figure 6.22 Correlation of Intercept of Percent Equation and the Percent Distilled at a Given Temperature	137

## List of Figures ... ctd.

	Page
Figure 6.23 Correlation of Slope of Weight Equation and the Percent Distilled at a Given Temperature	138
Figure 6.24 Correlation of Intercept of Weight Equation and the Percent Distilled at a Given Temperature	138
Figure 7.1 Log Curve Fit of October 3 Data	147
Figure 7.2 Single-Factor Log Curve Fit of October 3 Data	147
Figure 7.3 Log Curve Fit of October 4 Data	148
Figure 7.4 Square Root Curve Fit of October 4 Data	148
Figure 7.5 Log Curve Fit of October 5 Data	149
Figure 7.6 Modified Log Curve Fit of October 5 Data	149
Figure 7.7 Prediction of October 3 Results	151
Figure 7.8 Prediction of October 4 Results	152
Figure 7.9 Prediction of October 5 Results	153
Figure 8.1 Plot of Distillation Curves	160
Figure 8.2 Correlation of Evaporation Parameters with Distillation Data	162
Figure 8.3 Distillation Regression Coefficients versus Temperature	163
Figure 8.4 Comparison of Regression Coefficient and Temperatures at which these Occur - Percentage Curves and Full Set	165
Figure 8.5 Comparison of Regression Coefficient and Temperatures at which these Occur - Percentage Curves and Partial Set	165
Figure 8.6 Correlation of Percent Equation and the Percent Distilled at 180 °C	166
Figure 8.7 Correlation of Weight Equation and the Percent Distilled at 180 °C	166
Figure 8.8 Correlation of Percent Equation and the Percent Distilled at 180 °C - Narrow Cut Products	167
Figure 8.9 Correlation of Weight Equation and the Percent Distilled at 180 °C - Narrow Cut Products	167

**List of Figures ... ctd.**

	Page
Figure 8.10 Comparison of Gasoline Evaporation - Data Taken March 20, 1995	172
Figure 8.11 Comparison of ASMB Evaporation - Data Taken December 10, 1993	173

## Glossary of Symbols and Abbreviations \*

% - percentage

$\Delta H$  - heat of transition

$\Delta V$  - change in volume

$\mu$  - activity of a component or substance

A - area of the evaporating source

ASMB - Alberta Sweet Mixed Blend, a crude oil commonly used in Canada

C - commonly used for concentration or a constant

compd. - components

d - diameter or sometimes distance

D - the slick diameter or diffusivity or percent distilled

E - sometimes used to designate the evaporation rate

exp - exponential

f - fraction of a substance

FCC - Fractionated Catalytic Component, an intermediate refinery product

$F_v$  - volume fraction

g - grams

H - heat usually in context with the heat of transition, or Henry's law constant

ID - internal diameter

k - commonly used for a constant in evaporation equations or as the mass transfer rate,  
also used for the von Karman constant

K - commonly used for a constant in evaporation equations or as the mass transfer rate

lin - linear

ln - natural logarithm

Lt. - light

m/s - metres per second

M - molecular weight

min. - minutes

mm - millimetres

N - carbon number  
P - pressure or in some cases vapour pressure  
 $P_c$  - critical pressure  
 $P_{sat}$  - saturated vapour pressure  
 $P_{vap}$  - vapour pressure  
r - exponent for turbulence level, or radius  
R - universal gas constant  
 $R^2$  - regression coefficient  
S - entropy  
 $Sc$  - Schmidt number  
sq. rt. - square root  
T - temperature, usually in °C, but sometimes in K (Kelvin)  
U - wind speed, most often in m/s  
V - volume  
wt. - weight  
x - the axis x, or referring to a component of a chemical mixture  
X - distance along the evaporating path

\* Note: not all symbols can be listed in specific form because in the literature review authors' notations are usually preserved and are often used for very different applications. The standard notations for the most common notations such as temperature, T, and time, t, will not be repeated throughout the thesis if the units are respectively in degrees Celsius and in seconds. If units are different from these, this fact will be noted.

# Chapter 1

## 1.1 Introduction

Evaporation is a very important process for most oil spills. In a few days, light crude oils can be reduced by up to 75% of their initial volume and medium crudes up to 40% of their volume. In contrast, heavy or residual oils will only lose about 5% of their volume in the first few days following a spill. Most oil spill behaviour models include evaporation as a component of the process and output of the model. Despite the importance of the field, relatively little work has been conducted on the basic physics and chemistry of oil spill evaporation (Fingas, 1995). The particular difficulty with oil evaporation is that oil is a mixture of hundreds of compounds and this mixture varies from source to source and even over time. Much of the work described in the literature focuses on 'calibrating' equations developed for water evaporation. Furthermore, very little empirical data on oil evaporation is published.

Scientific and quantitative work on water evaporation is decades old (Brutsaert, 1982; Jones 1992). Furthermore, the basis for the oil work in the literature is water evaporation. There are several fundamental differences between the evaporation of a pure liquid such as water and that of a multi-component system such as crude oil. First, the evaporation rate for a single liquid such as water, is a constant with respect to time. Evaporative loss - by total weight or volume - is not linear with time for crude oils and other multi-component fuel mixtures. This is due to the depletion of more volatile components, these are exponentially (or by some similar function) depleted with time. The second major difference is the effect of atmospheric conditions. Water evaporation is strongly dependent on wind speed and relative humidity. Air can only hold a certain volume of water. The boundary layer above an evaporating water mass governs the rate at which the evaporation occurs. Once this air layer is saturated with water, evaporation ceases or slows as the saturation nears. Normal air does not contain a high level of benzene and similar oil components. Furthermore the saturation level of these components in air is often well above concentrations that can be achieved from an evaporating slick. This thesis will address these issues by examining the evaporation of

oil and comparing this with that of water, about which much is known.

## 1.2 Physics of Evaporation

Evaporation of a liquid can be considered as the movement of molecules from the surface into the vapour phase above it. The layer of air above the evaporation surface is known as the boundary layer. This is the air layer most directly affected by the surface and by oil evaporation. The characteristics of this air layer can influence evaporation. In the case of water, the air regulates the evaporation rate. Air can hold a variable amount of water, depending on temperature, as expressed by the relative humidity. At constant temperature, and constant conditions in the boundary layer, the evaporation rate of water is a constant. Under conditions where the boundary layer is not moving (no wind) or has low turbulence, the air immediately above the water quickly becomes saturated and evaporation slows or ceases. In practice, the actual evaporation of water proceeds at a small fraction of the maximum rate because of the saturation of the boundary layer. The boundary layer physics is then said to regulate the evaporation of water. This regulation manifests itself in the sensitivity of evaporation to wind or turbulence. When turbulence is weak or absent, the evaporation can slow down by orders-of-magnitude. The molecular diffusion of water molecules is generally at least  $10^3$  times slower than turbulent diffusion (Jones, 1992).

Evaporation can then be viewed as consisting of two fundamental components, basic evaporation itself and regulatory mechanisms. Basic evaporation is that process consisting of the evaporation of the liquid directly into the vapour phase without any regulation other than that by the thermodynamics of the liquid itself. Regulatory mechanisms are those processes which serve to regulate the final evaporation rate into the environment. For water, the main regulation factor is the boundary layer regulation discussed above. The boundary layer regulation is manifested by the limited rate of diffusion, both molecular and turbulent diffusion, and by saturation dynamics. Molecular diffusion is based on exchange of molecules over the mean free path in the gas. The rate of molecular diffusion for water is about  $10^5$  slower than the maximum rate of evaporation permitted, purely from thermodynamic considerations. (Jones, 1992). The

rate for turbulent diffusion, the combination of molecular diffusion and movement with turbulent air, is on the order of  $10^2$  slower than that for maximum evaporation. In fact, in the case of water, maximum evaporation is not known and has only been estimated by experiments in artificial environments or by calculation.

If the evaporation of oil was like that of water and was boundary-layer regulated one could write the mass transfer rate in semi-empirical form (also in generic and unitless form) as:

$$E \approx K C T_u S \quad (1.1)$$

where  $E$  is the evaporation rate in mass per unit area,  $K$  is the mass transfer rate of the evaporating liquid, presumed constant for a given set of physical conditions,  $C$  is the concentration (mass) of the evaporating fluid as a mass per volume,  $T_u$  is a factor characterizing the relative intensity of turbulence,  $S$  is a factor that relates to the saturation of the boundary layer above the evaporating liquid. The saturation parameter,  $S$ , represents the effects of local advection on saturation dynamics. If the air is already saturated with the compound in question, the evaporation rate is zero. This also relates to the scale length of an evaporating pool. If one views a large pool over which a wind is blowing, there is a high probability that the air is saturated downwind and the evaporation rate per unit area is lower than for a smaller pool.

Much of the pioneering work for evaporation work was performed by Sutton (1934). Sutton proposed the following equation based largely on empirical work:

$$E = K C_s U^{7/9} d^{1/9} Sc^{-r} \quad (1.2)$$

where  $C_s$  is the concentration of the evaporating fluid (mass/volume),  $U$  is the wind speed,  $d$  is the area of the pool,  $Sc$  is the Schmidt number and  $r$  is the empirical exponent assigned values from 0 to  $2/3$ . Other parameters are defined as above. The terms in this equation are analogous to the very generic equation (1.1) proposed above. The turbulence is expressed by a combination of the wind speed,  $U$ , and the Schmidt number,

Sc. The Schmidt number is the ratio of kinematic viscosity of air ( $\nu$ ) to the molecular diffusivity ( $D$ ) of the diffusing gas in air, i.e. a dimensionless expression of the molecular diffusivity of the evaporating substance in air. The coefficient of the wind power typifies the turbulence level. The value of 0.78 (7/9) as chosen by Sutton, represents a turbulent wind whereas a coefficient of 0.5 would represent a wind flow that was more laminar. The scale length is represented by  $d$  and has been given an empirical exponent of 1/9. This represents, for water, a weak dependence on size. The exponent of the Schmidt number,  $r$ , represents the effect of the diffusivity of the particular chemical, and historically was assigned values between 0 and 2/3.

This expression for water evaporation was subsequently used by those working on oil spills to predict and describe oil and petroleum evaporation. Much of the literature follows the work of Mackay (1973, and Stiver and Mackay, 1984). Mackay and Matsugu (1973) corrected the equations to hydrocarbons using the evaporation rate of cumene. It was noted that the difference in constants was related to the enthalpy differences between water and cumene. Data on the evaporation of water and cumene have been used to correlate the gas phase mass transfer coefficient as a function of wind-speed and pool size by the equation:

$$K_m = 0.0292 U^{0.78} X^{-0.11} Sc^{-0.67} \quad (1.3)$$

Where  $K_m$  is the mass transfer coefficient in units of mass per unit time and  $X$  is the pool diameter or the scale size of evaporating area. Stiver and Mackay (1984) subsequently developed this further by adding a second equation:

$$N = k_m AP / (RT) \quad (1.4)$$

Where  $N$  is the evaporative molar flux (mol/s),  $k_m$  is the mass transfer coefficient at the prevailing wind (m/s),  $A$  is the area (m<sup>2</sup>),  $P$  is the vapour pressure of the bulk liquid (Pa)  $R$  is the gas constant [8.314 Joules/(mol-K)], and  $T$  is the temperature (K).

Thus, boundary layer regulation is assumed to be the primary regulation mechanism for oil and petroleum evaporation. This assumption was never tested by experimentation, as revealed by the literature search. The implications of these assumptions are that evaporation rate for a given oil is increased by:

- increasing turbulence

- increasing wind speed
- increasing the surface area of a given mass of oil
- decreasing the scale size of the evaporating area (note the balance between this and the above factor).

These factors can then be verified experimentally to test if oil is boundary-layer regulated or not. This formed the basis of experimentation for this thesis.

### 1.3 Thermodynamic Aspects of Evaporation

The fundamental physics of evaporation is not well understood. No fundamental equations relating the thermodynamics of evaporation have been developed. There are a number of equations which, however, can be related to the fundamental physics of evaporation. The evaporation can typically be understood as being represented by a volume change, which, in fact, it is in conventional equilibrium thermodynamics:

#### 1. Clausius-Clapeyron Equation

A commonly-used relationship is the Clausius-Clapeyron equation (Smith and Van Ness, p. 182, 1987):

$$\frac{dP}{dT} = \frac{\Delta H}{T\Delta V} \quad (1.5)$$

where P is the vapour pressure,  $\Delta H$  is the heat of transition and  $\Delta V$  is the volume change accompanying the transition.

The key in interpreting the Clausius-Clapeyron equation is to examine the  $\Delta H$  relationship to temperature. Another fundamental relationship in thermodynamics is (Smith and Van Ness, p. 182, 1987):

$$\frac{dP}{dT} = \frac{\Delta H}{RT^2} \frac{1}{P_{sat}} \quad (1.6)$$

where  $P_{sat}$  is the saturated vapour pressure.

Rearranging (1.6) we obtain:

$$\Delta H = \frac{RT^2}{P_{sat}} \frac{dP}{dT} \quad (1.7)$$

Substituting this latter equation in the Clausius-Clapeyron equation,

$$\frac{dP}{dT} = \frac{RT^2}{P_{sat}} \frac{dP}{dT} \frac{1}{T\Delta V} \quad (1.8)$$

and rearranging, we get:

$$\Delta V \propto \frac{RT}{P_{sat}} \quad (1.9)$$

Thus the evaporation rate as represented by the volume change, is directly proportional to the temperature and inversely proportional to the saturation vapour pressure.

## 2. Maxwell's Equations

Maxwell's equations are direct restatements of the fundamental thermodynamic relationships. They reflect the ideal relationships between fundamental parameters. The most relevant equation is (Smith and Van Ness, p. 169, 1987):

$$\left[ \frac{dV}{dS} \right]_p = \left[ \frac{dT}{dP} \right]_s \quad (1.10)$$

where V is the volume, S is the entropy and subscripts s and p denote conditions of constant S and P, respectively.

This directly states that the change in volume with respect to entropy is directly related to the change in temperature given the constant conditions. Thus a direct relationship between volume and temperature is predicted and an inverse relationship with saturation vapour pressure.

### 3. Ideal Gas Equation

The simplest form of relationship can be given by the ideal gas equation:

$$PV = nRT \quad (1.11)$$

or

$$V = \frac{nRT}{P} \quad (1.12)$$

where V is the volume, here representing the volume evaporated, n is the number of moles and P is the pressure (equivalent to saturation vapour pressure).

Therefore, again, the volume evaporated is directly related to the temperature and inversely to pressure.

Thermodynamic and fundamental equations show that the volume change and thus the evaporation rate is directly related to the temperature and to the vapour pressure, and inversely to saturation vapour pressure.

### 1.4 REFERENCES

Brutsaert, W., *Evaporation into the Atmosphere*, Reidel Publishing Company, Dordrecht, Holland, 299 p., 1982.

Fingas, M.F., "The Evaporation of Oil Spills," *Journal of Hazardous Materials*, Vol. 42, pp. 157-175, 1995.

Jones, F.E., *Evaporation of Water*, Lewis Publishers, Chelsea, Michigan, 188 p., 1992.

Mackay, D. and R.S. Matsugu, "Evaporation Rates of Liquid Hydrocarbon Spills on Land and Water," *Canadian Journal Chemical Engineering*, Vol. 51, Canadian Society for Chemical Engineering, Ottawa, pp 434-439, 1973.

Smith, J.M. and H.C. Van Ness, *Introduction to Chemical Engineering Thermodynamics*, McGraw-Hill, Inc., New York, p. 182, 1987.

Stiver, W. and D. Mackay, "Evaporation Rate of Spills of Hydrocarbons and Petroleum Mixtures," *Environmental Science and Technology*, Vol. 18, American Chemical Society, Washington, D.C., pp 834-840, 1984.

Sutton, O.G., "Wind Structure and Evaporation in a Turbulent Atmosphere," *Proceedings of the Royal Society of London, A 146*, pp. 701-722, 1934.

## Chapter 2 - Literature Review

### 2.1 Abstract

Literature on the physics and mathematical modelling of oil spill evaporation is reviewed. Two basic approaches to the mechanism of evaporation are proposed in the literature, first-order decay and boundary-layer limited. Most workers use boundary-layer equations adapted from water evaporation work. These equations predict a constant evaporation mass transfer rate dependent on scale size and wind turbulence levels. The implementation of these equations in oil spill models is reviewed. Three primary approaches are adopted: direct use of a boundary-layer model, use of a simplified logarithmic predictor, and use of a fractionated-cut model. The last uses readily-available distillation data and estimations of how each cut evaporates. Comparison of experimental data with prediction methods shows that the accuracy is very dependent on the particular oil properties.

### 2.2 Physics and Chemistry of Oil Evaporation

The basis for most of the evaporative work is the extensive studies on the evaporation of water (Brutsaert, 1982; Jones, 1992). In fact, the currently-used equations still employ portions of these equations. The pioneering work in the development of evaporation equations was carried out by Sutton (1934). Sutton proposed the following equation:

$$E = K C_s U^{7/9} d^{1/9} Sc^{-r} \quad (2.1)$$

where  $E$  is the mean evaporation rate per unit area,  $K$  is the mass transfer coefficient,  $C_s$  is the concentration of the evaporating fluid (mass/volume),  $U$  is the wind speed,  $d$  is the area of the square or circular pool,  $Sc$  is the Schmidt number and  $r$  is an empirical exponent assigned values from 0 to 2/3.

Blokker (1964) was the first to develop oil evaporation equations for oil evaporation at sea. His starting basis was theoretical. Oil was presumed to be a one-

component liquid. The ASTM (American Society for Testing and Materials) distillation data and the average boiling points of successive fractions were used as the starting point to predict an overall vapour pressure. The average vapour pressure of these fractions was then calculated from the Clausius-Clapeyron equation to yield:

$$\log \frac{p_s}{p} = \frac{qM}{4.57} \left( \frac{1}{T} - \frac{1}{T_s} \right) \quad (2.2)$$

where  $p$  is the vapour pressure at the absolute temperature,  $T$ ,  $p_s$  is the vapour pressure at the boiling point,  $T_s$  (for  $p_s$ , 760 mm Hg was used),  $q$  is the heat of evaporation in cal/g and  $M$  is the molecular weight.

The term  $qM/(4.57 T_s)$  was taken to be nearly constant for hydrocarbons ( $=5.0 \pm 0.2$ ) and thus the expression was simplified to

$$\log p_s / p = 5.0 [ (T_s - T)/T ] \quad (2.3)$$

From the data obtained the weathering curve was calculated, assuming that Raoult's law is valid for this situation giving  $qM$  as a function of the percentage evaporated. Pasquill's equation was applied stepwise, and the total evaporation time obtained by summation:

$$t = \frac{\Delta h D^\beta}{K_{ev} U^\alpha} \sum \frac{1}{PM} \quad (2.4)$$

where  $t$  is the total evaporation time in hours,  $\Delta h$  is the decrease in layer thickness in m,  $D$  is the diameter of the oil spill,  $\beta$  is a meteorological constant (assigned a value of 0.11),  $K_{ev}$  is a constant for atmospheric stability (taken to be  $1.2 \times 10^{-8}$ ),  $\alpha$  is a meteorological constant (assigned a value of 0.78),  $P$  is the vapour pressure at the absolute temperature,  $T$ , and  $M$  is the molecular weight of the component or oil mass.

Blokker constructed a small wind tunnel and tested this equation against the evaporation of gasoline and a medium crude oil. The observed gasoline evaporation rate was much higher than was predicted and the crude oil rate was much lower than predicted. The times of evaporation, however were relatively close and the equation was

accepted for further use. The above equations were then incorporated into spreading equations to yield equations to predict the simultaneous spreading and evaporation of oil and petroleum products.

Mackay and Matsugu (1973) approached the problem by using the classical water evaporation and experimental work. The water evaporation equation was corrected to hydrocarbons using the evaporation rate of cumene. It was noted that the difference in constants was related to the enthalpy differences between water and cumene. Data on the evaporation of water and cumene have been used to correlate the gas phase mass transfer coefficient as a function of wind-speed and pool size by the equation,

$$K_m = 0.0292 U^{0.78} X^{-0.11} Sc^{-0.67} \quad (2.5)$$

Where  $K_m$  is the mass transfer coefficient in units of mass per unit time and  $X$  is the pool diameter or the scale size of evaporating area. Note that the exponent of the wind speed,  $U$ , is 0.78 which is equal to the classical water evaporation-derived coefficient. Mackay and Matsugu noted that for hydrocarbon mixtures the evaporation process is more complex, being dependent on the liquid diffusion resistance being present. Experimental data on gasoline evaporation were compared with computed rates. The computed rates showed fair agreement and suggest the presence of a liquid-phase mass-transfer resistance.

This work was subsequently extended by the same group (Goodwin, Mackay et al., 1976) to show that the evaporative loss of a mass of oil spilled can be estimated using a mass transfer coefficient, as shown above. This approach was investigated with some laboratory data and tested against some known mass transfer conditions on the sea. The conclusion was that this mass transfer approach could result in predictions of evaporation at sea.

Butler (1976) developed a model to examine evaporation of specific hydrocarbon components. The weathering rate was taken as proportional to the equilibrium vapour pressure,  $P$ , of the compound and to the fraction remaining:

$$dx/dt = -kP(x/x_0) \quad (2.6)$$

where  $x$  is the amount of a particular component of a crude oil at time,  $t$ ,  $x_0$  is the amount of that same component present at the beginning of weathering ( $t = 0$ ),  $k$  is an empirical rate coefficient and  $P$  is the vapour pressure of the oil component.

Since petroleum is a complicated mixture of compounds,  $P$  is not equal to the vapour pressure of the pure compound, but neither would there be large variations in the activity coefficient as the weathering process occurs. For this reason, the activity coefficients were subsumed in the empirical rate coefficient  $k$ .  $P$  and  $k$  were taken as independent of the amount,  $x$ , for a fairly wide range of oils. The equation was then directly integrated to give the fraction of the original compound remaining after weathering as:

$$x/x_0 = \exp(-ktP/x_0) \quad (2.7)$$

The vapour pressure of individual components was fit using a regression line to yield a predictor equation for vapour pressure:

$$P = \exp(10.94 - 1.06 N) \quad (2.8)$$

where  $P$  is the vapour pressure in Torr and  $N$  is the carbon number of the compound in question.

This combined with equation (2.7) yielded the following expression:

$$x/x_0 = \exp [-(kt/x_0)\exp(10.94 - 1.06 N)] \quad (2.9)$$

Where  $x/x_0$  is the fraction of the component left after weathering,  $k$  is an empirical constant,  $x_0$  is the original quantity of the component and  $N$  is the carbon number of the component in question.

Equation 2.9 predicts that the fraction weathered is a function of the carbon number and decreases at a rate that is faster than predicted from simple exponential decay. If the initial distribution of compounds is essentially uniform ( $x_0$  independent of  $N$ ), then the above equation predicts that the carbon number where a constant fraction

(e.g. half) of the initial amount has been lost ( $x = 0.5 x_0$ ) is a logarithmic function of the time of weathering:

$$N_{1/2} = 10.66 + 2.17 \log (kt/x_0) \quad (2.10)$$

where  $N_{1/2}$  is half the volume fraction of the oil.

The equation was tested using data from some patches of oil on shoreline, whose age was known. The equation was able to predict the age of the samples relatively well. It was suggested that the equation was applicable to open water spills; however, this was never subsequently applied in models.

Yang and Wang (1977) developed an equation using the Mackay and Matsugu molecular diffusion process. The vapour phase mass transfer process was expressed by:

$$D_{ie} = k_m (p_i - p_{i\infty}) / [RT_s] \quad (2.11)$$

where  $D_{ie}$  is the vapour phase mass transfer rate,  $k_m$  is a coefficient that lumps all the unknown factors that affect the value of  $D_{ie}$ ,  $p_i$  is the hydrocarbon vapour pressure of fraction,  $i$ , at the interface,  $p_{i\infty}$  is the hydrocarbon vapour pressure of fraction,  $i$ , at infinite altitude of the atmosphere,  $R$  is the universal gas constant and  $T_s$  is the absolute temperature of the oil slick.

The following functional relationship was proposed:

$$k_m = aA^\gamma e^{qU} \quad (2.12)$$

where  $A$  is the slick area,  $U$  is the overwater wind speed, and  $a$ ,  $q$  and  $\gamma$  are empirical coefficients. This functional relationship was based on the results of past investigations, including, for instance, those of MacKay and Matsugu (1973) who suggested the value of  $\gamma$  to be in the range from -0.025 to -0.055. Further experiments were performed by Yang and Wang to determine the values of 'a' and 'q'. The results were found to be two-fold. Experiments showed that a film formed on evaporating oils and that this film severely retarded evaporation. Before the surface film has developed ( $\rho_t/\rho_o < 1.0078$ ):

$$K_{mb} = 69A^{-0.0055} e^{0.42U} \quad (2.13)$$

where  $K_{mb}$  is the coefficient that groups all factors affecting evaporation before the surface film has formed and  $A$  is the area.

After the surface film has developed ( $\rho_t/\rho_o > 1.0078$ )

$$K_{ma} = 1/5 k_{mb} \quad (2.14)$$

where  $\rho_o$  is initial oil density,  $\rho_t$  is weathered oil density at time  $t$ , and  $K_{ma}$  is the coefficient that groups all factors affecting evaporation after the surface film has formed. The evaporation rate was found to be reduced fivefold after the formation of the surface film.

Drivas (1982) compared the Mackay and Matsugu equation with data found in the literature and noted that the equations yielded predictions that were close to the experimental data. Rheijnhart and Rose (1982) developed a simple predictor model for the evaporation of oil at sea. They proposed the following simple relationship:

$$Q_{ei} = \alpha C_o \quad (2.15)$$

where  $Q_{ei}$  is the evaporation rate of the component of interest,  $\alpha$  is a constant incorporating wind velocity and other factors (taken as  $0.0009 \text{ m s}^{-1}$ ) and  $C_o$  is the equilibrium concentration of the vapour at the oil surface.

Several pan experiments were run to simulate evaporation at sea and the data used to test the equation. No means were given for calculating the essential value,  $C_o$ .

Brighton (1985) proposed that the standard formulation used by many workers required refining. His starting point for water evaporation was similar to that proposed by Sutton (1934):

$$E = K C_s U^{7/9} d^{1/9} Sc^{-r} \quad (2.16)$$

where  $E$  is the mean evaporation rate per unit area,  $K$  is an empirically-determined constant,  $C_s$  is the concentration of the evaporation fluid (mass/volume),  $d$  is the area of the square or circular pool and  $r$  is an empirical exponent assigned values from 0 to 2/3. Brighton suggested that this equation does not conform to the basic dimensionless form

involving the parameters  $U$  and  $Z_0$  (wind speed and roughness length, respectively) which define the boundary layer conditions. The key factor in Brighton's analysis was to use a linear eddy-diffusivity profile. This feature implied that concentration profiles become logarithmic near the surface, which is suspected to be more realistic compared to the more finite values previously used. Using a power profile to provide an estimation of the turbulence, Brighton was able to substitute the following identities into the classical relationship

$$U = \frac{u^*}{k} z^n \quad (2.17)$$

$$n = \left( \ln \frac{z_1}{z_0} \right)^{-1} \quad (2.18)$$

Where  $u^*$  is the friction velocity,  $z_1$  is the reference height above the surface,  $z_0$  is the roughness length and  $n$  is the power law dimensionless term.

The evaporation equation now became

$$U \left( \frac{z}{z_1} \right) \frac{\delta X}{\delta x} = \frac{\delta}{\delta z} \left( \frac{k u^* z}{\sigma} \frac{\delta X}{\delta z} \right) \quad (2.19)$$

where  $z$  is the height above the surface,  $X$  is the concentration of the evaporating compounds,  $x$  is the dimension of the evaporating pool,  $k$  is given by  $K/u^*z$ , and is the von Karman constant and  $\sigma$  is the turbulent Schmidt number (taken as 0.85).

Brighton (1990) subsequently compared his model with several runs of experimental evaporation experiments in the field and in the laboratory, this included laboratory oil evaporation data. The model only correlated well with laboratory water evaporation data and the reason given was that other data sets were 'noisy'.

Tkalin (1986) proposed a series of equations to predict evaporation at sea:

$$E_i = \frac{K_a M_i P_{oi} x_t}{RT} \quad (2.20)$$

where  $E_i$  is the evaporation rate of component  $i$  (or the sum of all components) ( $\text{kg/m}^2\text{s}$ ),  $K_a$  is the mass transfer coefficient ( $\text{m/s}$ ),  $M_i$  is the molecular weight,  $P_{oi}$  is the vapour pressure of the component  $i$ , and  $x_t$  is the amount of component  $i$  at time,  $t$ .

Using empirical data, relationships were developed for some of the factors in the equation:

$$P_{oi} = 10^3 e^A \quad (2.21)$$

$$\text{where } A = -(4.4 + \log T_b) [1.803 \{T_b/T - 1\} - 0.803 \ln(T_b/T)] \quad (2.22)$$

and where  $T_b$  is the boiling point of the hydrocarbon, given as

$$K_a = 1.25 \times 10^{-3} \quad (2.23)$$

The equations were verified using empirical data from the literature.

The most frequently used work in spill modelling is that of Stiver and Mackay (1984). It is based on some of the earlier work by Mackay and Matsugu (1973) but significant additions were made. Additional information is given in a thesis by Stiver (1984). The formulation was initiated with assumptions about the evaporation of a liquid. If a liquid is spilled, the rate of evaporation is given by:

$$N = KAP/(RT) \quad (2.24)$$

where  $N$  is the evaporative molar flux ( $\text{mol/s}$ ),  $K$  is the mass transfer coefficient under the prevailing wind ( $\text{ms}^{-1}$ ) and  $A$  is the area ( $\text{m}^2$ ),  $P$  is the vapour pressure of the bulk liquid.

This equation was arranged to give:

$$dF_v/dt = KAPv/(V_o RT) \quad (2.25)$$

where  $F_v$  is the volume fraction evaporated,  $v$  is the liquid's molar volume ( $\text{m}^3/\text{mol}$ ) and  $V_o$  is the initial volume of spilled liquid ( $\text{m}^3$ ).

By rearranging we obtain

$$dF_v = [Pv/(RT)](KA dt/V_o) \quad (2.26)$$

$$\text{or } dF_v = Hd\theta \quad (2.27)$$

where H is Henry's law constant and  $\theta$  is the evaporative exposure (defined below).

The right-hand side of the second last equation has been separated into two dimensionless groups. The group,  $KA dt/V_o$ , represents the time-rate of what has been termed the "evaporative exposure" and was denoted as  $d\theta$ . The evaporative exposure is a function of time, the spill area and volume (or thickness), and the mass transfer coefficient (which is dependent on the wind speed). The evaporative exposure can be viewed as the ratio of exposed vapour volume to the initial liquid volume.

The group  $Pv/(RT)$  or H is a dimensionless Henry's law constant or ratio of the equilibrium concentration of the substance in the vapour phase [ $P/(RT)$ ] to that in the liquid ( $l/v$ ). H is a function of temperature. The product  $\theta H$  is thus the ratio of the amount which has evaporated (oil concentration in vapour times vapour volume) to the amount originally present. For a pure liquid, H is independent of  $F_v$  and equation 2.26 was integrated directly to give:

$$F_v = H \theta \quad (2.28)$$

If K, A, and temperature are constant, the evaporation rate is constant and evaporation is complete ( $F_v$  is unity) when  $\theta$  achieves a value of  $1/H$ .

If the liquid is a mixture, H depends on  $F_v$  and the basic equation can only be integrated if H is expressed as a function of  $F_v$ ; i.e., the principal variable of vapour pressure is expressed as a function of composition. The evaporation rate slows as evaporation proceeds in such cases.

Equation 2.26 was replaced with a new equation developed using data from evaporation experiments:

$$F_v = (T/K_1) \ln (1 + K_1 \theta/T) \exp(K_2 - K_3/T) \quad (2.29)$$

where  $F_v$  is the volume fraction evaporated and  $K_{1,2,3}$  are empirical constants.

A value for  $K_1$  was obtained from the slope of the  $F_v$  vs.  $\log \theta$  curve from pan or bubble evaporation experiments. For  $\theta$  greater than  $10^4$ ,  $K_1$  was found to be

approximately  $2.3T$  divided by the slope. The expression  $\exp(K_2 - K_3/T)$  was then calculated, and  $K_2$  and  $K_3$  determined individually from evaporation curves at two different temperatures. Variations of all the above equations have been used extensively by many other experimenters and for model application.

Hamoda and co-workers (1989) performed theoretical and experimental work on evaporation. An equation was developed to express the effects of API° (American Petroleum Institute gravity - a unit of density) of the crude oil, temperature, and salinity on the mass transfer coefficient  $K$ :

$$K = 1.68 \times 10^{-5} (\text{API}^\circ)^{1.253} (T)^{1.80} e^{0.1441} \quad (2.30)$$

where  $K$  is the mass transfer coefficient,  $\text{cm h}^{-1}$ , API° is the density in API units, unitless, and  $e$  is the water salinity in degrees salinity or parts-per-thousand. The exponents of the equation were determined by multiple linear regression on experimental data.

Quin and co-workers (1990) weathered oils in a controlled environment and correlated the data with equations developed starting with Fick's diffusion law and the Clausius-Clapeyron equation. Crude oil was divided into a series of pseudo fractions by boiling point. Each fraction was taken to be equivalent to an  $n$ -paraffin in evaporation behaviour. The  $n$ -paraffin distributions of a number of naturally weathered crude oils were determined by capillary gas-liquid chromatography. The actual evaporation determined by this procedure was compared with those generated by computer simulation of weathering. Good agreement was obtained for oil film thicknesses between  $10 \mu\text{m}$  and  $1 \text{ mm}$ , weathered for periods of up to 4 weeks.

Brown and Nicholson (1991) studied the weathering of a heavy oil, Bitumen. They compared experimental data using a large-scale weathering tank with two spill model outputs. In the FOOS model, the evaporative exposure concept is used in which the fraction of oil evaporated is given by a variant of the Mackay equation:

$$F = [\ln(P) + \ln(CE) + 1/P]/C \quad (2.31)$$

where  $F$  is the fraction evaporated,  $C$  is an empirical constant and  $E$  is a measure of the evaporative exposure, defined as

$$E = (K_m A v t) / (R T V_o) \quad (2.32)$$

where 
$$K_m = 0.0048 U^{0.78} Z^{-0.11} Sc^{0.67} \quad (2.33)$$

and where  $K_m$  is the mass transfer coefficient,  $A$  is the slick area,  $v$  is the oil molar volume,  $V_o$  is the initial slick volume,  $Z$  is the pool size scale factor, and  $Sc$  is the Schmidt number (taken as 2.7).

Brown and Nicholson compared the measured evaporation for a  $5 \text{ ms}^{-1}$  wind at an ambient temperature of  $20^\circ\text{C}$ , and evaluation was done with the equation above. A spill volume of  $100 \text{ m}^3$  was assumed. A value of about  $10^{-5} \text{ m}^3/\text{mol}$  was used for the average molar volume. The model generally described the observed evaporation quite well, particularly during the first few hours. Later however, the model consistently over-predicted the evaporation rate. A simple method of correcting the equation was implemented by assuming that the vapour phase Schmidt number decreases slightly as the skin on the oil thickens. In response, the evaporative exposure was modified to:

$$K_m = (0.0025 - 0.000021 t) U^{0.78} \quad (2.34)$$

The predicted evaporation then compared favourably with the measured values.

The ASA model was also compared to the experimental data (Brown and Nicolson, 1991). This model assumed that the oil consists of a series of components each with a distinct boiling point, API gravity, and molecular weight. A mass transfer rate from the slick was then written for each component as:

$$dm/dt = K_m P_i A F_i \text{Mass}_i / RT \quad (2.35)$$

where  $dm/dt$  is the mass transfer rate,  $K_m$  is the mass transfer coefficient of Mackay,  $P_i$  is the vapour pressure of each component,  $F_i$  is the fraction of each component remaining and  $\text{Mass}_i$  is the mass of each component.

For this simulation, boiling points, volume percent, and API gravities were input for 13 boiling ranges. The general shape of the model curve agreed well with the measured data but the model predicts a slightly higher overall evaporation rate.

Bobra (1992) conducted laboratory studies on the evaporation of crude oils. The evaporation curves for several crude oils and petroleum products were

measured under several different environmental conditions. These data were compared to the equation developed by Stiver and Mackay (1984). The equation used was:

$$F_v = \ln[1 + B(T_G/T) \theta \exp(A - B T_o/T)] \{T/BT_G\} \quad (2.36)$$

where  $F_v$  is the fraction evaporated,  $T_G$  is the gradient of the modified distillation curve, A and B are dimensionless constants,  $T_o$  is initial boiling point of the oil and  $\theta$  is the evaporative exposure as previously defined.

The constants for the above equation and the results from several comparison runs are summarized in the following table (Table 2.1).

Table 2.1 Data from the Bobra Evaporation Experiments

Oil	Density g/mL (15 °C)	Viscosity cP (15 °C)	Agreement to Equation	To	Tg	A	B
Adgo	0.95	60	poor	551	195	24	21
Alberta	0.84	10	good	397	539	8	12
Amauligak	0.89	15	moderate	471	370	12	15
Bent Horn	0.82	25	poor	406	484	11	14
Diesel	0.83	3	moderate	517	140	20	18
Endicott	0.92	85	good	454	1400	-0.8	7
North Slope	0.89	25	good	431	722	5	10
Panuke	0.78	1	poor	268	368	7	11

This comparison showed that the Stiver and Mackay equation predicts the evaporation of most oils relatively well until time exceeds about 8 hours, after that it over-predicted the evaporation. The 'overshoot' can be as much as 10% evaporative loss at the 24-hour mark. This is especially true for very light oils. The Stiver and Mackay equation was also found to under-predict or over-predict the evaporation of oils in the initial phases. Bobra also noted that most oil evaporation follows a logarithmic curve with time.

### 2.3 Use of Evaporation Equations in Spill Models

Evaporation equations are the prime physical change equations used in spill

models. This is because evaporation is the most significant change that occurs in an oil's composition. Many recent models (after 1984) use the Stiver and Mackay (1984) approach. The equations developed by Mackay and co-workers can be implemented in a variety of ways. Often the difference in models is the manner in which the models are applied.

Fallah and Stark (1976) proposed a random model to predict the evaporation of oil at sea. The rate of evaporation from a free surface was given by:

$$\frac{dV}{dt} = KA^\beta [U(z)]^\alpha (P_s - P_a) \quad (2.37)$$

where V and t are volume and time, respectively, A is the surface area of liquid, U(z), the wind speed at height z above the liquid surface, P<sub>s</sub> is the saturation vapour pressure at liquid surface temperature, P<sub>a</sub> is the partial vapour pressure in the air upwind of the liquid surface and K, α, and β are constants.

This equation was combined with a probability density function and the Blokker equations described above. After a Mellin transform, the following equation was developed:

$$\Delta V_j = \frac{\pi}{4} K_e D_{j-1}^{2-\beta} U_j^\alpha (PM)_{j-1} \Delta t_j \quad (2.38)$$

where ΔV<sub>j</sub> is the change in volume, K<sub>e</sub> is the evaporation coefficient (~ 10<sup>-8</sup> min<sup>-1</sup> for hydrocarbons), α and β are constants (α = 0.78, and β = 0.11), D is the slick diameter and M is the molecular weight.

For oil slicks, the vapour pressure, P, was said to decrease sharply as evaporation of volatile components takes place, causing a changing oil composition.

Weathering curves were used to give values of the vapour pressure, P, and the molecular weight as a function of the evaporation fraction, M(γ). The weathering curves for crude oil and gasoline were approximated by the following exponential functions:

$$PM(\gamma) = 1900 \exp \{- 8\gamma - 200\gamma^3\} \quad \text{crude oil (20 °C)} \quad (2.39)$$

$$PM(\gamma) = 4000 \exp \{-1.2\gamma - 2.5\gamma^2\} \text{ gasoline (2 }^\circ\text{C)} \quad (2.40)$$

where PM is the change in mass of the oil and  $\gamma$  denotes the application of the gamma probability function.

Fallah and Stark applied this probabilistic approach to some literature data to demonstrate the technique.

Grose (1979) used the Mackay and Matsugu (1973) equations with some modification:

$$L = (C U^{0.78} D_o^{-0.11}) / (RK) P_i Sk M_i \quad (2.41)$$

where L is the mass of oil evaporated with time (kg/s), C is the environmental transfer constant, U is the wind speed at the surface (m/hr),  $D_o$  is the diameter of the oiled area (m), K is the oil temperature in Kelvin,  $P_i$  is the vapour pressure of the particular component, Sk is the skin factor and  $M_i$  is the molecular weight equivalent of the particular oil fraction.

The skin factor, Sk, ranges from 0.1 to 8 and accounts for the effect of skinning (the formation of a semi-permeable surface layer). Yang and Wang (1977) suggested a value of Sk = 0.2 after the density of their test oils had increased by 0.78%. A value of 1.0 was used in testing the model. In addition, mass loss rate depends on the vapour pressure,  $P_i$ , and the molecular weight,  $MW_i$ , of each fraction. C is a dimensionless environmental transfer constant whose magnitude depends on the units used. The value used for C (0.00024) includes the constant 0.015 after Mackay and Matsugu (1973).

Mackay and co-workers developed an extensive oil spill model incorporating a number of process equations including evaporation (Mackay et al. 1980). The earlier work of Leinonen and Mackay (1975) was used with the modification proposed by Yang and Wang (1977). The process includes dividing the oil into a number of different fractions and analyzing each fraction for evaporation loss. The mass transfer function used is the familiar one proposed by Mackay and Matsugu (1973).

Aravamudan and co-workers (1981a, 1981b) developed an oil spill model incorporating evaporation equations of their own design. The rate of evaporation of the

different components in crude oil can be represented by the equation:

$$\frac{d}{dt} [c_i V] = -k_o U P_i A \quad (2.42)$$

where  $c_i$  is the mass concentration of the  $i$ th species (mass per unit volume of the oil),  $V$  is the total volume of oil floating on the water surface,  $k_o$  is an empirical evaporation constant,  $P_i$  is partial pressure of the  $i$ th species and  $A$  is the total horizontal surface area of the oil slick.

Aravamudan and co-workers show that, using various volumetric relationships:

$$\frac{dV}{dt} = -k_o U A(t) \sum_{i=1}^n \frac{P_i}{\rho_i} \quad (2.43)$$

and

$$V \frac{dV}{dt} (\ln c_i) = -k_o U A(t) \left( \frac{P_i}{c_i} - \sum_{i=1}^n \frac{P_i}{\rho_i} \right) \quad (2.44)$$

where  $\rho_i$  = the density of the  $i$ th component and all other parameters are as in equation 2.42.

The partial pressure of each component was related to the saturated vapour pressure,  $P_i$ , of the  $i$ th component at the temperature  $T$ , of the oil by:

$$\frac{\rho_i}{P_i(T)} = \frac{c_i / \mu_i}{\sum_{i=1}^n c_i / \mu_i} \quad (2.45)$$

where  $\rho_i$  = the density of the  $i$ th component and  $\mu_i$  is the activity of the component  $i$ .

These equations can be solved to obtain  $V$  and  $c_i$  as functions of time. Solutions were developed by assuming a five-component crude oil that spreads on the water surface according to the correlations for the area.

Huang (1983) reviewed oil spill models and noted the state-of-the-art up to that time. Huang notes that many of the approaches are similar and can be generalized into the following:

1. The oil is assumed to be composed of a number of hydrocarbon groups, the mixture of which has physical-chemical characteristics similar to the parent oil;
2. The evaporative loss of a given hydrocarbon component is assumed to follow an exponential decay, or first-order kinetics;
3. The evaporation rate is assumed to be a function of the following key physical parameters: (a) spill area, (b) wind speed, (c) vapour pressure, (d) slick thickness, and (e) temperature.

Huang notes that the main difference among models of the second type seems to be the level of detail and sophistication by which various hydrocarbon components and various physical-chemical parameters affecting evaporation are incorporated in the model.

Payne and co-workers (1984a,b,c) developed an oil spill model using the pseudo-component approach. Given the boiling point (1 atm) and API gravity of each cut (or pseudo-component), the vapour pressure of the cut as a function of temperature was calculated. First, the molecular weight and critical temperature of the cut were calculated according to the following correlation:

$$y = C_1 + C_2X_1 + C_3X_2 + C_4X_1X_2 + C_5X_1^2 + C_6X_2^2 \quad (2.46)$$

where  $y$  is the vapour pressure of the cut,  $X_1$  is the boiling point ( $^{\circ}\text{F}$ ) at one atmosphere,  $X_2$  is the API gravity and  $C_{1-6}$  are constants whose values are shown in Table 2.2. Similarly, the critical temperature was calculated from the same equation form using the indicated constant values in Table 2.2.

Next, the equivalent paraffin carbon number,  $N_c$ , was calculated according to:

$$N_c = (M - 2) / 14 \quad (2.47)$$

where  $M$  is the molecular weight assigned to the particular cut. The critical volume,  $V_c$ , was then calculated according to:

$$V_c = (1.88 + 2.44N_c) / 0.044 \quad (2.48)$$

and the critical pressure,  $P_c$ , was calculated from:

$$P_c = \frac{20.8 T_c}{(V_c - 8)} + P'_c \quad (2.49)$$

where  $T_c$  is the critical temperature and  $P'_c$  correction factor for critical pressure.

The factor  $P'_c$  was set to 10 to correct the critical pressure correlation from a strictly paraffinic mixture to a naphtha-aromatic-paraffin mixture. Next the parameter,  $b$ , was calculated according to

$$b = b' - 0.02 \quad (2.50)$$

where

$$b' = C_1 + C_2 N_c + C_3 N_c^2 + C_4 N_c^3 \quad (2.51)$$

and the values of the constants  $C_1$  to  $C_4$  are indicated in Table 2.2.

A final parameter designated as  $A$  is then calculated according to:

$$A = \frac{T_{r_b}}{T_{r_b} - 1} \left[ \log_{10}(P_{r_b}) + \exp\left(-20(T_{r_b} - b)^2\right) \right] \quad (2.52)$$

where  $A$  is an intermediary parameter,  $T_{r_b}$  is the reduced temperature at the normal boiling point,  $P_{r_b}$  is the reduced pressure at the normal boiling point and  $b$  is an intermediary parameter determined in (2.50) above.

The vapour pressure equation which can be used down to 10 mm Hg can be expressed in terms of  $A$  and  $b$  as:

$$\log_{10} P_r = \frac{-A(1 - T_r)}{T_r} - \exp\left[-20(T_r - b)^2\right] \quad (2.53)$$

where  $P_r$  is the reduced pressure and  $T_r$  is the reduced temperature.

$A$ ,  $b$ ,  $T_c$  and  $P_c$  were determined from the normal boiling point and API gravity of the cut. The temperature at which the vapour pressure is 10 mm Hg was obtained by the root-finding algorithm of Newton-Raphson (Payne et al., 1984a).

Below 10 mm Hg, the vapour pressure between two temperatures,  $T_{r1}$  and  $T_{r2}$ , was calculated according to the Clausius-Clapeyron equation as follows:

$$\ln \frac{P_2}{P_1} = \frac{\lambda_o}{RT_c} \int_{T_{r1}}^{T_{r2}} \frac{(1 - T_r)^{0.38}}{T_r^2} dT_r \quad (2.54)$$

where  $P_1$  is the vapour pressure at temperature 1,  $P_2$  is the vapour pressure at temperature 2,  $\lambda_o$  is the heat of vaporization at 0 K, and  $T_c$  is the critical temperature. This was based on the fact that the ratio of the heat of vaporization,  $\lambda$ , to  $(1 - T)^{0.38}$  is a constant at any temperature. The latent heat of vaporization was calculated from the slope of the natural log of the vapour pressure equation with respect to the temperature where the vapour pressure is 10 mm Hg. Thus, in the above equation,  $P_2$  is the 10 mm Hg vapour pressure at the temperature,  $T_r$ , previously determined.

**Table 2.2 Correlation Equation Constants for the Characterization of Narrow Boiling Petroleum Fractions (Payne et al., (1988a, b,c))**

Property	C <sub>1</sub>	C <sub>2</sub>	C <sub>3</sub>	C <sub>4</sub>	C <sub>5</sub>	C <sub>6</sub>
molecular weight t <sub>b</sub> ≤ 500°F	6.241E+01	-4.595E-02	-2.836E-01	3.256E-03	4.578E-04	5.279E-04
molecular weight t <sub>b</sub> > 500°F	4.268E+02	-1.007	-7.491	1.380E-02	1.047E-03	2.621E-02
critical temperature, t <sub>b</sub> ≤ 500	4.055E+02	1.337	-2.662	-2.169E-03	-4.943E-04	1.454E-02
critical temperature, t <sub>b</sub> > 500	4.122E+02	1.276	-2.865	-2.888E-03	-3.707E-04	2.288E-02
b'	1.237E-02	2.513E-01	4.039E-02	-4.024E-02	—	—
kinematic vis, cS @ 122°F API ≤ 35	-4.488E-01	-9.344E-04	1.583E-02	-5.219E-05	5.268E-06	1.536E-04
kinematic vis, cS @ 122°F API > 35	6.019E-01	1.793E-03	-3.159E-03	-5.1E-06	9.067E-07	3.522E-05

Rasmusen (1985) developed an oil spill model for Danish waters and proposed an equation to describe the evaporative mass flux of a single hydrocarbon:

$$N_i = k_{mi} \frac{P_i^{SAT} - P_{i,air}}{RT} X_i^{surface} \quad (2.55)$$

where  $N_i$  is the evaporative mass flux,  $k_{mi}$  is the mass transfer coefficient of component  $i$  (in m/s),  $P_i^{sat}$  is the vapour pressure of component  $i$ ,  $P_{i,air}$  is the partial pressure of component  $i$  in the air and  $X_i^{surface}$  is the mole fraction of component  $i$  at the surface.

Rasmusen chose an equation by Mackay and Matsugu (1973) to estimate the mass transfer coefficient,  $k_{mi}$ :

$$k_{mi} = 16.076U^{0.78} R^{-0.11} Sc_i^{-0.67} \quad (2.56)$$

where  $Sc_i$  is the Schmidt number for component  $i$ .

Ross and Dickins (1988) used empirical data to model the evaporation of oil under snow. The evaporative exposure approach of Stiver and Mackay (1984) was used:

$$F_v = (T/10.3 T_G) \ln (1 + (10.3 T_G/T)) \theta \exp (6.3 - 10.3 T_o/T) \quad (2.57)$$

$$\text{and } \theta = kAt/V = kt/x \quad (2.58)$$

where  $F_v$  is the volume fraction evaporated,  $T_G$  is the slope of modified ASTM distillation curve (539 K for medium crude),  $T_o$  is the intercept of modified ASTM distillation curve (385 K for medium crude),  $\theta$  is the evaporative exposure coefficient,  $k$  is the mass transfer coefficient (m/s),  $A$  is the spill area ( $m^2$ ),  $V$  is the spill volume ( $m^3$ ) and  $x$  is the slick thickness (m).

The following relationships were defined:

$$A = (T/10.3 T_G) \quad (2.59)$$

$$B = (10.3 T_G/T) \exp (6.3 - 10.3 T_o/T) \quad (2.60)$$

$$F_v = A \ln (1 + B\theta) \quad (2.61)$$

so that by rearranging we obtain:

$$\theta = (\exp (F_v/A) - 1)/B \quad (2.62)$$

and, after substituting for  $\theta$ ,

$$x (\exp (F_v/A) - 1)/B = kt \quad (2.63)$$

A plot of  $x(\exp (F_v/A)-1)/B$  vs  $t$  yields a slope of  $k$ , the overall mass transfer coefficient. The resistance-in-series approach to mass transfer was used:

$$1/k = 1/k_w + H/k_o + L/D_s \quad (2.64)$$

where  $k_w$  is the air-side mass transfer coefficient (m/s) ( $0.002U^{0.78}$  (Mackay and Matsugu, 1973)),  $k_o$  is the oil internal mass transfer coefficient (m/s),  $H$  is Henry's law constant for the oil,  $D_s$  is the diffusivity of oil vapours in snow ( $m^2/s$ ) and  $L$  is the depth of oil below snow surface (m).

A plot of  $1/k$  against snow depth ( $L$ ) has a slope of  $1/D_s$  and intercept of  $1/k_w + H/k_o$ . The least squares fit to the small-scale data from the trays with un-compacted snow gives a slope of  $5.5 \times 10^4 \text{ s/m}^2$  or  $D_s = 1.8 \times 10^{-5} \text{ m}^2/\text{s}$ .

Reed (1989) reports on the development of an evaporation equation. He used the familiar Mackay and Matsugu (1973) approach to estimate the mass transfer coefficient:

$$K = 0.029 U^{0.78} D^{-0.11} Sc^{-0.67} \sqrt{(M+29)/M} \quad (2.65)$$

where  $K$  is the mass transfer coefficient,  $U$  is the wind speed (miles/hr),  $D$  is the slick diameter (m),  $Sc$  is the Schmidt number (Reed used 2.7, that of cumene),  $M$  is the molecular weight of the volatile portion of the spill (g/mol).

The mass transfer rate  $dm/dt$  (in g/hr) of the surface slick was then stated as:

$$dm/dt = (K P_{vp} A / RT) f M \quad (2.66)$$

where  $dm/dt$  is the mass transfer rate in g/hr,  $P_{vp}$  is vapour pressure in atm,  $A$  is the slick area in  $m^2$  and  $f$  is the fraction of the remaining slick that is composed of volatile substances.

Lunel (1991) combined the mass transfer rates of evaporation and dissolution to deal with these competing processes simultaneously. The mass transfer rate,  $dM_E/dt$ , of the evaporative portion was expressed as:

$$dM_E/dt = (k_E M P A) / RT \quad (2.67)$$

where  $k_E$  is the evaporative mass transfer coefficient and  $M$  is the relative molecular mass.

The evaporative mass transfer coefficient was solved using the work of Mackay and Matsugu (1973):

$$k_E = 0.029 U^{0.78} X^{-0.11} Sc_G^{-0.67} \quad (2.68)$$

where  $U$  is the wind speed at a height of 10 m,  $X$  is the pool diameter and  $Sc_G$  is the gas

phase Schmidt number.

Estimates of  $k_E$  and  $k_s$  were derived from work on dissolved gases. For a dissolved gas to pass into the atmosphere across the air-sea interface it has to overcome two resistances (the resistance being the reciprocal of the mass transfer coefficient): one from the water it is dissolved in ( $1/k_s$ ) and one from the air above the interface ( $1/k_E$ ). The two resistances were combined to yield an overall mass transfer coefficient,  $k_{Overall}$ , according to the formula:

$$\frac{1}{k_{Overall}} = \frac{1}{k_s} + \frac{RT}{Hk_E} \quad (2.69)$$

where H is the Henry's law constant (which is the vapour pressure divided by the solubility).

Once the overall mass transfer coefficient was calculated, the researchers obtained information on both  $k_a$  and  $k_s$ .

Luk and Kuan (1992) describe an oil spill model which incorporates an evaporative equation nearly identical to that of Reed above. Spaulding and co-workers (1992) use the same equations for the model OILMAP.

Lehr and co-workers (1992) developed an oil spill model (ADIOS) using the evaporative algorithm developed by Stiver and Mackay (1984), expressed as :

$$\frac{df}{d\theta} = \exp\left[6.3 - \frac{10.3}{T} (T_o + T_G f)\right] \quad (2.70)$$

where  $f$  is the volume fraction of oil evaporated,  $\theta$  is the evaporative exposure,  $T$  is the temperature of the oil and  $T_o$  and  $T_G$  are oil-dependent parameters derived from the fractional distillation data.

The evaporative exposure is a dimensionless variable related to time:

$$\theta = \frac{K_m A t}{V_o} \quad (2.71)$$

where  $K_m$  is the mass transfer coefficient and  $V_o$  is the initial spill volume. An adjustment was made to account for the decrease in the evaporation rate as the water content

increases to account for oil emulsification. The mass transport coefficient was scaled linearly with the oil fraction in the emulsion.

## **2.4 Discussion**

In conclusion, many models exist incorporating evaporative equations. Most recent models (after 1980) use one of three approaches to model oil spill evaporation; the Mackay and Matsugu (1973), the use of distillation cut data to simulate each fraction, and the Stiver and Mackay (1984) approach. The equations developed by Mackay and co-workers can be implemented in a variety of ways. Often the difference in models is the manner in which the models are applied. The comparison by Bobra (1992) found that the Stiver and Mackay equation predicts the evaporation of most oils relatively well until time exceeds about 8 hours, after that it over-predicts the evaporation that occurs. This is especially true for very light oils. The comparison by Brown and Nicholson (1991) found that for the heavy and mixed oils used in their study, the Mackay and Matsugu approach was better than the distillation cut approach; however, the mass transfer coefficient required adjustment.

## 2.5 References

Aravamudan, K.S., P. Raj, J. Ostlund, E. Newman and W. Tucker, *Break-up of Oil on Rough Seas - Simplified Models and Step-by-Step Calculations*, United States Coast Guard, CG-D-28-82, Washington, D.C., 1982.

Aravamudan, K.S., P.K. Raj and G. Marsh, "Simplified Models to Predict the Breakup of Oil on Rough Seas", in *Proceedings of the 1981 Oil Spill Conference*, American Petroleum Institute, Washington, D.C., pp. 153-15, 1981.

Bobra, M., *A Study of the Evaporation of Petroleum Oils*, Manuscript Report Number EE-135, Environment Canada, Ottawa, Ontario, 1992.

Blokker, P.C., "Spreading and Evaporation of Petroleum Products on Water", in *Proceedings of the Fourth International Harbour Conference*, Antwerp, Belgium, pp. 911-919, 1964.

Brighton, P.W.M., "Evaporation from a Plane Liquid Surface into a Turbulent Boundary Layer", *Journal of Fluid Mechanics*, Vol. 159, pp. 323-345, 1995.

Brighton, P.W.M., "Further Verification of a Theory for Mass and Heat Transfer from Evaporating Pools", *Journal of Hazardous Materials*, Vol. 23, pp. 215-234, 1990.

Brown, H.M. and P. Nicholson, "The Physical-Chemical Properties of Bitumen", in *Proceedings of The Fourteenth Arctic Marine Oilspill Program Technical Seminar*, Environment Canada, Ottawa, Ontario, pp. 107-117, 1991.

Brutsaert, W., *Evaporation into the Atmosphere*, Reidel Publishing Company, Dordrecht, Holland, 1982.

Butler, J.N., "Transfer of Petroleum Residues from Sea to Air: Evaporative Weathering", In *Marine Pollutant Transfer*, Ed. H.L. Windom and R.A. Duce, Lexington Books, Toronto, pp. 201-212, 1976.

Drivas, P.J., "Calculation of Evaporative Emissions from Multi-Component Liquid Spills", *Environmental Science and Technology*, Vol. 16, American Chemical Society, Washington, D.C., pp. 726-728, 1982.

Fallah, M.H. and R.M. Stark, "Random Model of Evaporation of Oil at Sea", *The Science of the Total Environment*, Vol. 5, Elsevier Scientific Publishing Company, Amsterdam, pp. 95-109, 1976.

Goodwin, S.R., D. Mackay, W.Y. Shiu, "Characterization of the Evaporation Rates of Complex Hydrocarbon Mixtures Under Environmental Conditions", *Canadian Journal of Chemical Engineering*, Vol. 54, Canadian Society for Chemical Engineering, Ottawa, pp. 290-294, 1976.

Grose, P.L., "A Preliminary Model to Predict The Thickness Distribution of Spilled Oil", in *Proceedings of A Workshop on The Physical Behaviour of Oil in The Marine Environment*, Princeton University, Princeton, National Oceanic and Atmospheric Administration, Washington, D.C., 1979.

Hamoda, M.F., S.E.M. Hamam, and H.I. Shaban, "Volatization of Crude Oil from Saline Water", *Oil and Chemical Pollution*, Vol. 5, Elsevier Science Publishers Ltd., Essex, England, pp. 321-331, 1989.

Huang, J.C., "A Review of the State-of-the-Art of Oil Spill Fate/Behaviour Models", in *Proceedings of The 1983 Oil Spill Conference*, American Petroleum Institute, Washington, D.C., pp. 313-322, 1983.

Jones, F.E., *Evaporation of Water*, Lewis Publishers, Chelsea, Michigan, 1992.

Lehr, W.J., R. Overstreet, R. Jones and G. Watabayashi, "ADIOS-Automatic Data Inquiry for Oil Spill", in *Proceedings of The Fifteenth Arctic Marine Oilspill Program Technical Seminar*, Environment Canada, Ottawa, Ontario, pp. 31-45, 1992.

Leinonen, P.J. and D. Mackay, "A Mathematical Model of Evaporation and Dissolution from Oil Spills on Ice, Land, Water and Under Ice", in *Proceedings Tenth Canadian Symposium 1975: Water Pollution Research Canada*, pp. 132-141, 1975.

Luk, G.K. and H.F. Kuan, Modelling "The Behaviour of Oil Spills in Natural Waters", *Canadian Journal of Civil Engineering*, Vol. 20, No. 2, pp. 171-342, 1992.

Lunel, T., "Eurospill: Chemical Spill Model Based on Modelling Turbulent Mixing at Sea", in *Proceedings of the Eighth Technical Seminar on Chemical Spills*, Environment Canada, Ottawa, Ontario, pp. 48-57, 1991.

Mackay, D., I. Buist, R. Mascarenhas, and S. Paterson, *Oil Spill Processes and Models*, EE-8, Environment Canada, Ottawa, Ontario, 1980.

Mackay, D. and R.S. Matsugu, "Evaporation Rates of Liquid Hydrocarbon Spills on Land and Water", *Canadian Journal of Chemical Engineering*, Vol. 51, Canadian Society for Chemical Engineering, Ottawa, pp. 434-439, 1973.

Payne, J.R., G.D. McNabb, Jr., L.E. Hachmeister, B.E. Kirstein, J.R. Clayton, Jr., C.R. Phillips, R.T. Redding, C.L. Clary, G.S. Smith and G.H. Farmer, *Development of a Predictive Model for the Weathering of Oil in the Presence of Sea Ice*, Outer Continental Shelf Environmental Assessment Program, Vol. 59, National Oceanic and Atmospheric Service, Alaska, 1988.

Payne, J.R., B.E. Kirstein, G.D. McNabb, Jr., J.L. Lambach, R. Redding, R.E. Jordan, W. Hom, C. de Oliveira, G.S. Smith, D.M. Baxter and R. Gaegel, *Multivariate Analysis of Petroleum Weathering in the Marine Environment - Subarctic*, U.S. Department of Commerce, National Oceanic and Atmospheric Administration, OCSEAP, Vol. 21, 1984.

Payne, J.R. and G.D. McNabb, Jr., *Weathering of Petroleum in the Marine Environment*, Marine Technology Society Journal, Vol. 18, Washington, D.C., pp. 24-42, 1984.

Quin, M.F., K. Marron, B. Patel, R. Abu-Tabanja and H. Al-Bahani, "Modelling of The Ageing of Crude Oils", *Oil and Chemical Pollution*, Vol. 7, pp. 119-128, 1990.

Rasmussen, D., "Oil Spill Modelling - A Tool for Cleanup Operations", in *Proceedings of the 1985 Oil Spill Conference*, American Petroleum Institute, Washington, D.C., pp. 243-249, 1985.

Reed, M., "The Physical Fates Component of the Natural Resource Damage Assessment Model System", *Oil and Chemical Pollution*, Vol. 5, Elsevier Applied Science Publishers, Great Britain, pp. 99-123, 1989.

Reijnhart, R. and R. Rose, "Evaporation of Crude Oil at Sea", *Water Research*, Vol. 16, Pergamon Press, Great Britain, pp. 1319-1325, 1982.

Ross, S.L., Environmental Research Limited and D.F. Dickins Associates Limited, *Modelling of Oil Spills in Snow*, EE-109, Environment Canada, Ottawa, Ontario, 1988.

Spaulding, M.L., E. Howlett, E. Anderson and K. Jayko, "OILMAP: A Global Approach to Spill Modelling", in *Proceedings of the Fifteenth Arctic Marine Oilspill Program Technical Seminar*, Environment Canada, Ottawa, Ontario, pp. 15-21, 1992.

Stiver, W., *Weathering Properties of Crude Oils when Spilled on Water*, Master of Applied Science Thesis, Department of Chemical Engineering and Applied Chemistry, University of Toronto, Toronto, pp. 4-7, 110-126 & 132-137, 1984.

Stiver, W. and D. Mackay, "Evaporation Rate of Spills of Hydrocarbons and Petroleum Mixtures", *Environmental Science and Technology*, Vol. 18, American Chemical Society, Washington, D.C., pp. 834-840, 1984.

Sutton, O.G., "Wind Structure and Evaporation in a Turbulent Atmosphere", *Proceedings of the Royal Society of London, A* 146, pp. 701-722, 1934.

Tkalin, A.V., "Evaporation of Petroleum Hydrocarbons From Films on a Smooth Sea Surface", *Oceanology of the Academy of Sciences of the USSR*, Vol. 26, American Geophysical Union, Washington, D.C. pp. 473-474, 1986.

Yang, W.C. and H. Wang, "Modelling of Oil Evaporation in Aqueous Environments", *Water Research*, Vol. 11, Pergamon Press, Great Britain, pp. 879-887, 1977.

## Chapter 3 Experimental Methodology and Turbulence Characterization

### 3.1 Experimental

Evaporation rate was measured by weight loss using an electronic balance. The balance was a Mettler PM4000, capable of measurements to  $0.01 \pm 0.02$  g. A new type of open-pan balance, the Mettler PM4000, provides accuracy an order of magnitude higher than previous top loading balances (0.01 grams versus 0.1 grams) with 4000-gram weight-loading capability. This is important in accurately measuring the weight loss of heavy oils which evaporate slowly, where incremental weight losses are often less than 0.1 grams. An open balance was chosen to allow for application of wind to the oil surface. The weight was recorded using a computerized system consisting of a Toshiba 3100, a serial cable to the balance and a modified version of the software program, 'Collect' (Labtronics, Richmond, Ontario). The latter consisted of an older version of the program written in Basica which could then be easily modified to incorporate new features. The software program normally acquires data at fixed time intervals. Adjustments were made to the program to allow different time multiples for data acquisition. This then allowed minimization of data quantity at times after the initial rapid evaporation period. Intervals of data acquisition could be set at multiples such that each time increment had an approximately equal weight loss increment. For example in one day, using a timing multiplier of 1.1 and an interval of 10 seconds, 75 data points were collected compared to 8640 if regular time intervals were used. It was important then to use the time increment to yield data sets which were manageable. Experiments were done to measure the effect of the number of data points on data quality. A sequence using the multiplier 1.1 was optimal. Using this timing sequence, measurements were taken at the following minute intervals, 8.3, 9.1, 10, 11.1, 13.4, etc. After one day, sequences were already at intervals of several hours. At the end of the experiment, the time sequence was re-triggered to add the last data point. Data was usually collected for 5 to 20 data points to improve the curve fits. This addition of data points on the end of the run counterbalances the many data points at the start of a run and thus the tendency

for curve fit to weigh the initial points heavier than those at the end. This method differs significantly from previous measurements noted in the literature which were taken by weighing the pan at fixed intervals, resulting in fewer data points and thus less reliable data.

Measurements were typically conducted in the following fashion. A tared petri dish of defined size was loaded with a measured amount of oil. The weight loss dishes were standard glass petri dishes from Corning. A standard 139 mm diameter (ID) dish was most frequently used. Petri dishes of other sizes were used in experiments where the area of evaporation was a variable and included those of inside diameters 44.8, 88.9, 143.2, and 162.2 mm. Diameters and other dimensions were measured using a Mitutoyo digital vernier caliper.

Oil was directly placed on the glass petri dish unless otherwise noted. Experiments were initially conducted with oil on water to evaluate the effects of the substrate. However, use of water under the oil resulted in errors if the water became exposed to the air and evaporated. The resulting evaporation curve is then an undetermined composite of oil and water evaporation. Data acquisition was started and continued to the desired endpoint (varying from a few hours for a volatile substance to several days for a less-volatile oil). At the end of the experiment, the weathered oil was saved for chemical analysis for other experiments not related to this thesis. Vessels were cleaned and rinsed with Dichloromethane and a new experiment started.

Wind and turbulence acting directly on a sensitive balance cause the apparent weight to vary somewhat. Thus special arrangements were necessary during these experiments to measure data that had an acceptable noise level. Experiments that did not evaluate the effect of wind were conducted in a fume hood cabinet which was closed to prevent the passage of air currents over the oil and with the fume hood fan off. When the experiment was moved to the cold room or to a laboratory bench, a cardboard box was placed over the balance to prevent air movement over measurement pan.

Measurements were done in one of four locations; inside a fume hood, inside a controlled temperature room, on a counter top and some were performed outside to verify that evaporation behaviour obtained was not unduly influenced by experimental

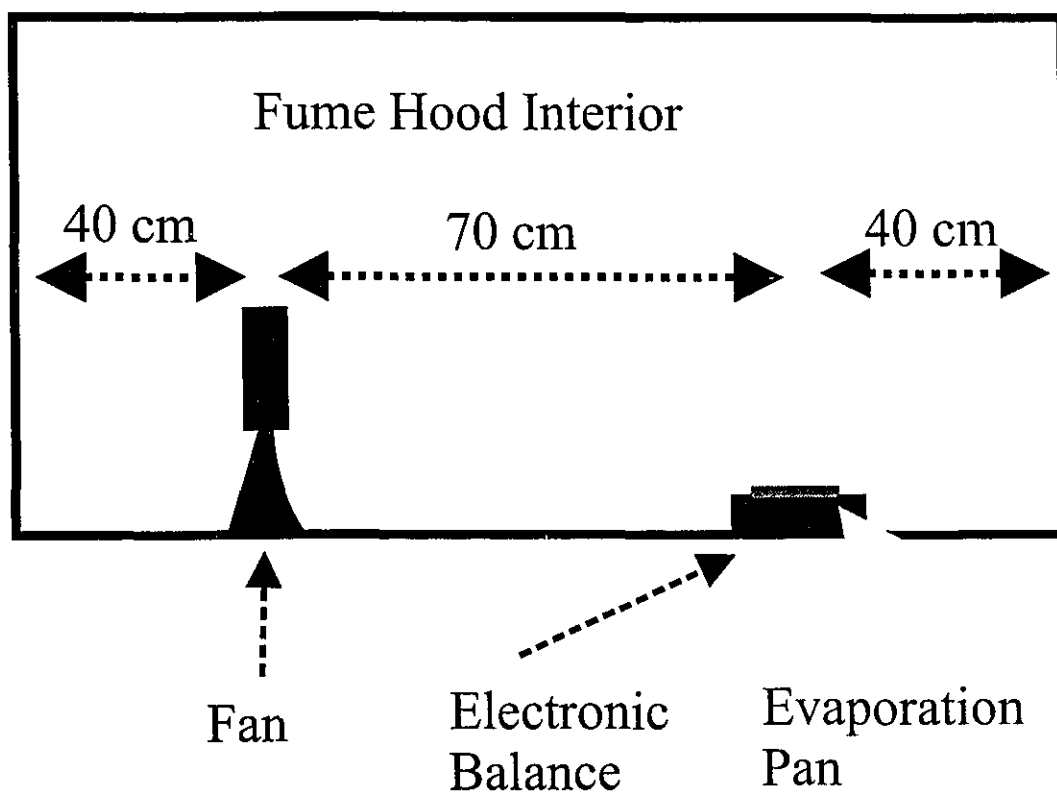
conditions. The layout of experiments conducted in the fume hood are illustrated in Figure 3.1. The fan and velocity measuring equipment were not always employed, depending on the experiment conducted.

Many experiments were conducted in the fume hood, where there was no temperature regulation. Temperatures were measured using a Keithley 871 digital thermometer with a thermocouple supplied by the same firm. Temperatures at the fume hood location were relatively constant at 20°C except during the coldest of winter months. During these times, experiments of a different nature were generally carried out such as those involving variable temperatures using the cold room. Temperatures were taken at the beginning and the end of a given experimental run, and were occasionally measured in the middle of runs to verify that they had not changed.

The constant temperature chamber (room) employed was a Constant Temperature model constructed in 1993. It could maintain temperatures from -40°C to +60°C and regulate the chosen temperature within  $\pm 1^\circ\text{C}$ . The chamber was also capable of controlling relative humidity. At relative humidities of 40 to 70%, the unit could maintain set humidities within  $\pm 2\%$ , at other levels this precision decreased. The relative humidity was maintained at 40% when relative humidity was not a parameter of concern.

In experiments involving wind, air velocities were measured using a Taylor vane anemometer (no model number on the unit) and a Tadi, 'Digital Pocket Anemometer'. These velocities were later confirmed using a hot wire anemometer and appropriate data manipulations of the outputs. The anemometer was a TSI - Thermo Systems model 1053b, with power supply (TSI model 1051-1), averaging circuit (TSI model 1047) and signal linearizing circuit (TSI model 1052). The voltage from the averaging circuit was read with a Fluke 1053 voltmeter. The hot wire sensor (TSI model 1213-60) was angled at 45°. The sensor probe resistance at 0°C was 7.21 ohms and the sensor was operated at 12 ohms for a recommended operating temperature of 250°C. Data from the hot wire anemometer was collected on a Campbell Scientific CR-10 data logger at a rate of 64 Hz. At this data rate about 8000 data points, or about 2 ½ minutes of data, could be collected before the CR-10 was overwriting data. These data were subsequently down-loaded to a lap top computer and saved for subsequent analysis.

Figure 3.1 **Experimental Setup**



Scale   
25 cm

For some experiments a mixing device was used. This device consisted of an air flow through a syringe at a flow rate varying from 70 to 150 cc/min. The flow was established using a Gilian 'Gilibrator' which is a bubble flow meter. The syringe was placed in a stand and flow directed 1 cm above the oil at a 30° angle. This was sufficient to cause a rotation and mixing of the oil in the pan and avoid an early formation of a 'skin' on the oil. This stirrer was only used where specifically noted.

Quality control on instruments was maintained throughout the experiments. The balance was levelled on each installation. It was periodically checked using a set of standard weights from Mettler and no deviation or drift was noted. The data downloading and software were checked during this time as well. The computer clock was checked for correspondence to time on a wrist watch each time a new run was started and no discrepancies were noted. Both the balance and data acquisition computer were powered through an uninterruptable power supply. The Keithley thermometer was calibrated on two occasions using ice water and boiling water as described in the manufacturers instructions. The controlled temperature chamber temperature always corresponded to readings on the Keithley thermometer, within 0.2 degrees. The vane anemometers had been calibrated in the National Research Council wind tunnel. Subsequently, the TSI hot wire anemometer was also calibrated there.

### **3.2 Evaporation Data Handling**

Evaporation data were collected on the Toshiba 3100 laptop computer and subsequently transferred to other computers for analysis. The 'Collect' program records time and the weight directly. Data was recorded in ASCII format and converted to Excel format, Microsoft Incorporated, Redmond, Washington. Table 3.1 shows a typical spread sheet. The first two columns are the ASCII data from the data loggers, for time and weight, respectively. The 'converted time' in column 6 is usable by a spread sheet macro and is converted to a total time in minutes in Column 7. Column 8 shows the conversion of the data to a time interval and Column 9 to a cumulative time in minutes. The data subsequently used in analysis are the cumulative time in minutes, transposed to column 3; the weight change in percentage lost ('Delta wt %') in column 4 and the weight

Table 3.1 Example Calculation Spreadsheet for an Evaporation Experiment

(Data taken from an actual experiment conducted November 16, 1993, using Alberta crude oil)

Time (original)	Weight	Time (min)	Delta Wt %	Delta weight	converted time	time in minutes	time interval (min)	cumulative time (min)
14:23:00	28.42	0	0	0	14:23:00	863	0	0
14:25:07	24.74	2.1	12.95	3.68	14:25:07	865.11667	2.1	2.1
14:25:12	24.71	2.2	13.05	3.71	14:25:12	865.2	0.1	2.2
14:25:22	24.65	2.4	13.27	3.77	14:25:22	865.36667	0.2	2.4
14:25:31	24.6	2.5	13.44	3.82	14:25:31	865.51667	0.1	2.5
14:25:48	24.52	2.8	13.72	3.9	14:25:48	865.8	0.3	2.8
14:26:13	24.44	3.2	14	3.98	14:26:13	866.21667	0.4	3.2
14:26:51	24.33	3.8	14.39	4.09	14:26:51	866.85	0.6	3.8
14:27:48	24.17	4.7	14.95	4.25	14:27:48	867.8	0.9	4.7
14:29:13	23.99	6.1	15.59	4.43	14:29:13	869.21667	1.4	6.1
14:31:21	23.72	8.2	16.54	4.7	14:31:21	871.35	2.1	8.2
14:34:34	23.32	11.4	17.95	5.1	14:34:34	874.56667	3.2	11.4
14:39:22	22.88	16.2	19.49	5.54	14:39:22	879.36667	4.8	16.2
14:46:34	22.38	23.4	21.25	6.04	14:46:34	886.56667	7.2	23.4
14:57:23	21.87	34.2	23.05	6.55	14:57:23	897.38333	10.8	34.2
15:13:35	21.27	50.4	25.16	7.15	15:13:35	913.58333	16.2	50.4
15:37:55	20.79	74.7	26.85	7.63	15:37:55	937.91667	24.3	74.7
16:14:23	20.09	111.2	29.31	8.33	16:14:23	974.38333	36.5	111.2
17:09:06	19.44	165.9	31.6	8.98	17:09:06	1029.1	54.7	165.9
18:31:11	18.95	248	33.32	9.47	18:31:11	1111.1833	82.1	248
20:34:18	18.49	371.1	34.94	9.93	20:34:18	1234.3	123.1	371.1
23:38:58	18.03	555.8	36.56	10.39	23:38:58	1418.9667	184.7	555.8
4:15:59	17.68	832.8	37.79	10.74	4:15:59	255.98333	277	832.8
11:11:29	17.29	1248.3	39.16	11.13	11:11:29	671.48333	415.5	1248.3
21:34:45	16.86	1871.6	40.68	11.56	21:34:45	1294.75	623.3	1871.6
13:09:39	16.48	2806.55	42.01	11.94	13:09:39	789.65	934.95	2806.55
12:31:59	16.13	4208.95	43.24	12.29	12:31:59	751.98333	1402.4	4208.95
23:35:30	15.6	6312.55	45.11	12.82	23:35:30	1415.5	2103.6	6312.55
20:01:29	15.25	8978.55	46.34	13.17	20:01:29	1201.4833	2666	8978.55
20:01:34	15.27	8978.65	46.27	13.15	20:01:34	1201.5667	0.1	8978.65
20:01:41	15.27	8978.75	46.27	13.15	20:01:41	1201.6833	0.1	8978.75

change in grams ('Delta Weight') in column 5, were calculated from the raw weight values in column 2.

Curve fitting was performed using the software program "TableCurve", Jandel Scientific Corporation, San Raphael, California. The weight percent and the absolute weight were always fitted separately and statistics on these parameters recorded separately. This was done to enable subsequent analysis of dimensionless and absolute evaporation. It is important to note that the absolute weight calculation still relates to the weight of the starting substance. If oil were boundary-layer regulated, evaporation rate as a weight loss, would relate to the specific area. The program "TableCurve" enables the user to fit hundreds of relationships to a set of data and rank the resulting fit in order of regression coefficient ( $R^2$ ). In this study, the 'common' functions were generally used, although the complete set of equations (several thousand) was also used. The latter consist largely of higher-order polynomials, which are typically used for data interpolation, rather than for determining the physical relationships applicable to a given set of experimental data. A sample output of the equations fit and their regression coefficients are shown in Table 3.2 and illustrated in Figure 3.2. The data are from an actual experimental run and are complete for that experiment. The particular best equation was the logarithmic one and the regression coefficient (correlation coefficient) was 0.996. Equations with only one constant or single-parameter equations were also calculated for correlation work.

### **3.3 Air Flow and Turbulence Measurements**

Winds were used for some experiments. A standard household electric fan was used to generate the winds and velocities were measured as previously described above in Section 3.1.

The wind velocity data from the hot wire anemometer was down loaded to a computer in the form of relative velocity measurements and time intervals. The hot wire anemometer was taken to the Aerodynamics Section of the National Research Council for calibration. This section has a wind tunnel which serves as a primary standard for air

**Table 3.2 Example Curve Fit Table for An Evaporation Experiment**

(Data taken from an actual experiment conducted November 16, 1993, using Alberta crude oil)

(Fit equations and ranks taken directly from the Output of the 'Table Curve' Program)

Rank	R <sup>2</sup> - regression coefficient	Equation
1	0.995829324	$y=a+blnx$
2	0.99287119	$y=a+bx^c$ [Power]
3	0.989777065	$y^2=a+b(lnx)^2$
4	0.987272996	$y^{0.5}=a+blnx$
5	0.977832304	$1/y=a+b/x^{0.5}$
6	0.965780474	$lny=a+blnx$
7	0.965419857	$y^2=a+blnx$
8	0.958893505	$1/y=a+blnx/x$
9	0.941410007	$y=a+b(lnx)^2$
10	0.936231391	$1/y=a+b/lnx$
11	0.908286321	$lny=a+blnx/x$
12	0.90798645	$lny=a+b/x^{0.5}$
13	0.904816948	$y^{0.5}=a+b(lnx)^2$
14	0.879167925	$1/y=a+blnx$
15	0.879090597	$y^{0.5}=a+blnx/x$
16	0.861142978	$y^{0.5}=a+b/x^{0.5}$
17	0.85556315	$lny=a+b(lnx)^2$
18	0.855461104	$y^2=a+bx^{0.5}$
19	0.848314518	$y=a+blnx/x$
20	0.809798613	$y=a+b/x^{0.5}$
21	0.80843424	$lny=a+b/lnx$
22	0.773327469	$y^2=a+bx^{0.5}lnx$
23	0.770084832	$y=a+bx^{0.5}$
24	0.766373386	$y^2=a+blnx/x$
25	0.760603938	$1/y=a+b/x$
26	0.742206905	$y^{0.5}=a+b/lnx$
27	0.714472007	$y^{0.5}=a+bx^{0.5}$
28	0.704069814	$y=a+bx^{0.5}lnx$
29	0.688320674	$1/y=a+b(lnx)^2$
30	0.679705624	$lny=a+b/x$
31	0.674016236	$y=a+b/lnx$
32	0.650215149	$y^{0.5}=a+b/x$
33	0.646522963	$y^{0.5}=a+bx^{0.5}lnx$
34	0.623475348	$y^2=a+bx/lnx$
35	0.622649671	$lny=a+bx^{0.5}$
36	0.613328071	$y=a+b/x$
37	0.595467281	$y=a+bx/lnx$
38	0.587054023	$1/y=a+blnx/x^2$
39	0.569425518	$lny=a+blnx/x^2$
40	0.568783904	$y^{0.5}=a+blnx/x^2$
41	0.563036884	$y^2=a+bx$
42	0.557679938	$y=a+bx$
43	0.557679844	$y=a+bexp(-x/c)$ [Exponential]
44	0.551978583	$y=a+blnx/x^2$
45	0.542137066	$lny=a+bx^{0.5}lnx$
46	0.539521227	$1/y=a+b/x^{1.5}$

velocity measurements. The accuracy of velocity measurements is stated to be 2%. Table 3.3 summarizes the average voltage and wind measurements from the wind tunnel. The voltages are averages of 1024 data points taken from the time interval that the wind tunnel was set to a specific time period. These were recorded using the CR-10 data logger and were checked using a voltmeter, also described above. Instantaneous voltage readings agreed with subsequent data averages within 3%. The data in Table 3.3 were subsequently fit with a curve using the software program, 'TableCurve', sold by Jandel Corporation, San Raphael, California. The results are illustrated in Figure 3.3. This resulted in the calibration curve of:

$$Y = -0.672 + 0.995 * \exp(-x/-170) \quad (3.1)$$

where Y is the air velocity in m/s and x is the anemometer reading in millivolts.

---

**Table 3.3 Data Obtained From the NRC Anemometer Calibration Experiments**

<b>Air Velocity (m/s)</b>	<b>Anemometer Response (mv)</b>
0.5	35.65
1	80.47
1.5	128.36
2	174.28
3	219.72

---

Equation 3.1 was used in subsequent calculations to convert anemometer readings to air velocity units. The hot wire anemometer was used to measure all four air velocities used in the experiments. The air velocity was measured at the centre of the standard evaporation pan used and at the height of the rim, for two perpendicular orientations of the film, ie. for the vector components xy and xz, where x is the direction of the turbulent flow. The hot wire is sensitive to the vector sum of the two components perpendicular to the axis of the wire. Because the turbulence was relatively isotropic in all axes, these measurements are similar. The net wind velocity is, however along the x axis, and this is the axis of primary interest. For these experiments, the axis differentiation was not

Figure 3.2 Example Correlation Curve for An Evaporation Experiment

Rank 1 Eqn 13  $y=a+blnx$

$r^2=0.996$  FitStdErr=0.813 Fstat=6690

a=9.05

b=4.16

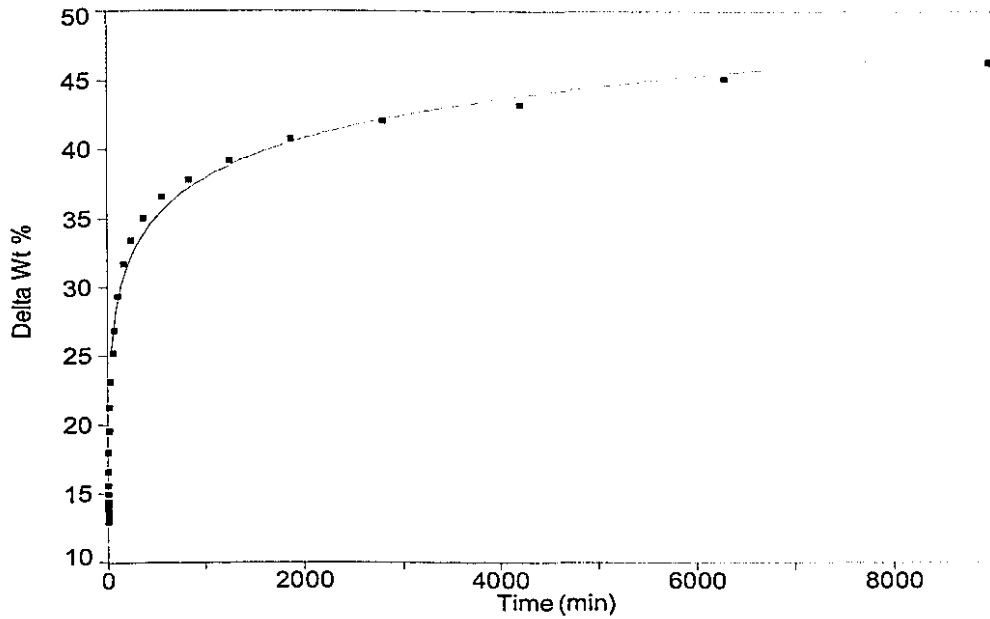


Figure 3.3

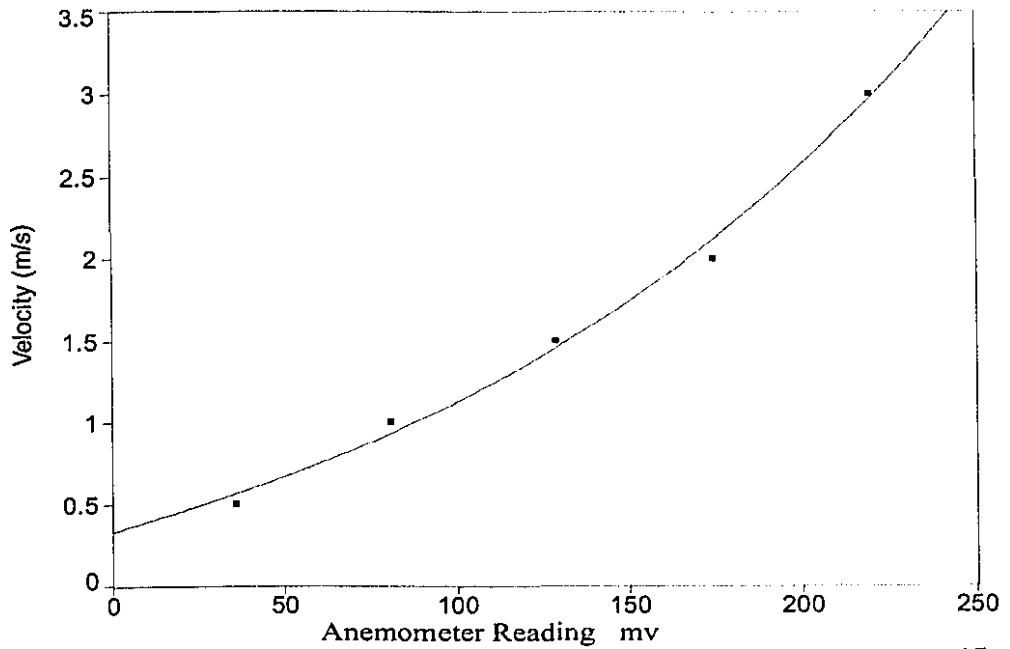
Calibration of The Anemometer

Rank 3 Eqn 8002  $y=a+bexp(-x/c)$  [Exponential]

$r^2=0.993$  FitStdErr=0.110 Fstat=152

a=-0.672 b=0.995

c=-170



important, so data analysis for turbulence on each axis was not performed. Data are, however, reported with the axis designation to ensure that the orientation is apparent. Anemometer data from each air velocity (wind) setup were recorded as described above and data transferred to a computer for subsequent analysis. The spreadsheet program, Excel, Microsoft Incorporated, Redmond, Washington, was used to perform the final calculations. Table 3.4 illustrates the calculations used to characterize the wind conditions. The first two columns show the raw time and voltages collected by the data logger. The raw time is converted to a time step for illustrative purposes only. The raw voltage is converted to velocity using equation 3.1. The velocities are listed in column 4 with an average given below. The sub-table which appears below the main table lists the summary statistics on the velocities. Column 5 provides the wave number from the Fourier transform performed on the velocities. The data here are of the conventional complex number form. Column 6 shows the modulus of the Fourier transform, which is calculated as the square root of the sum of the squares of the real and imaginary components. Column 7, rounded wave number, is the Fourier transform rounded to a whole number. Column 8, sorted wave number, is the sorted wave number. Sorting is necessary to draw a histogram using Excel. Column 9, frequency, contains the sorted frequencies used to plot a histogram. Column 10, log wave number, is the logarithm of the wave number and column 11, log frequency, is the logarithm of the frequency.

A typical plot of wind velocity versus time is shown in Figure 3.4 and the histogram of the log abundance versus the logarithm of the Fourier transform is shown in Figure 3.5. This shows that this particular velocity regime has a slight resemblance to the  $-5/3$  slope characteristic of a 'natural', fully-developed turbulence. This is not typical of the winds measured here and a fully-developed turbulence would not be expected from the wind created directly in front of the fan. The wind shows strong harmonics characteristics of a fan, related to the number of blades and the rotational velocity of the fan.

Standard analyses were performed on all four wind velocity structures and these data are summarized in Table 3.5. The average of the xy and xz root mean square values of the winds shown here were used for further calculations and correlations of the wind

Table 3-4 Example of A Calculation Table for Air Velocity and Turbulence Analysis

Raw Time	Raw Voltage	Time Diff. (sec.)	Velocity (m/s)	Wavenumber <sup>1</sup>	Modulus <sup>2</sup>	Rounded Wave number <sup>3</sup>	Sorted Wave number	Frequency <sup>4</sup>	Log Wave number	Log Frequency
38.63	60.96		0.693	869.888	869.888	870	0	1	2.94	0
38.63	68.09	0.01563	0.752	13.9204693151362+62.7233201127121i	64.24947	64	6	1	1.81	0
38.63	96.6	0.03125	1.012	6.05027205017693+37.9293932922428i	38.40891	38	14	2	1.58	0.3
38.63	61.61	0.04688	0.698	-88.1919675267281-14.2305882233706i	89.33271	89	14	2	1.95	0.3
38.63	69.39	0.0625	0.763	34.0057546721765-75.533278927712i	82.83518	83	31	2	1.92	0.3
38.63	45.4	0.07813	0.573	11.4849909075221+42.7667410318293i	44.28204	44	31	2	1.64	0.3
38.63	64.85	0.09375	0.725	-6.13440478386466+30.7530816759023i	31.35894	31	38	2	1.49	0.3
38.63	33.07	0.10938	0.486	27.3557014289584+54.7904950394074i	61.23996	61	38	2	1.79	0.3
38.75	65.5	0.125	0.73	17.8693739758018+34.926823654299i	39.23261	39	39	2	1.59	0.3
38.75	75.9	0.14063	0.819	-10.3383062608518-10.0724509588746i	14.43381	14	39	2	1.15	0.3
<i>Data points 13 to 1013 eliminated - for illustration purposes</i>										
54.38	51.23	15.8281	0.617	4.72233509553238+40.5168598060684i	40.79113	41	44	2	1.61	0.3
54.5	36.32	15.8438	0.509	3.00051543984517+5.03291763884389i	5.859467	6	44	2	0.78	0.3
54.5	100.5	15.8594	1.051	-10.3383062608517+10.0724509588746i	14.43381	14	61	2	1.15	0.3
54.5	165.4	15.875	1.854	17.8693739758016-34.926823654299i	39.23261	39	61	2	1.59	0.3
54.5	136.8	15.8906	1.462	27.3557014289579-54.7904950394076i	61.23996	61	64	1	1.79	0
54.5	143.3	15.9063	1.546	-6.13440478386487-30.7530816759023i	31.35894	31	83	2	1.49	0.3
54.5	98.6	15.9219	1.032	11.4849909075218-42.7667410318294i	44.28204	44	83	2	1.64	0.3
54.5	114.1	15.9375	1.195	34.005754672177+75.5332789277118i	82.83518	83	89	2	1.92	0.3
54.5	187.4	15.9531	2.204	-88.191967526728+14.2305882233711i	89.33271	89	89	2	1.95	0.3
54.63	35.67	15.9688	0.504	6.05027205017667-37.9293932922429i	38.40891	38	810	1	1.58	0
54.63	19.46	15.9844	0.397	810.169	810.169	810	870	1	2.91	0

raw voltage	velocity	Statistics on the velocity					
71.4	0.85	AVERAGE	AVERAGE	Mean	0.8495	Skewness	1.818
				Standard Error	0.01639	Range	3.134
				Median	0.662	Minimum	0.314
				Mode	0.401	Maximum	3.448
				Standard Deviation	0.5246	Sum	869.9
				Sample Variance	0.2752	Count	1024
				Kurtosis	3.543	Confidence Level (95%)	0.03213

- 1 - Wave number with real and imaginary components
- 2 - Modulus is the resolved value converted to a real number
- 3 - Wave number rounded to a whole number
- 4 - Frequency of a given wave number

Figure 3.4 The Variation of Air Velocity over Time - An Example  
(Data from the xz component of wind 2)

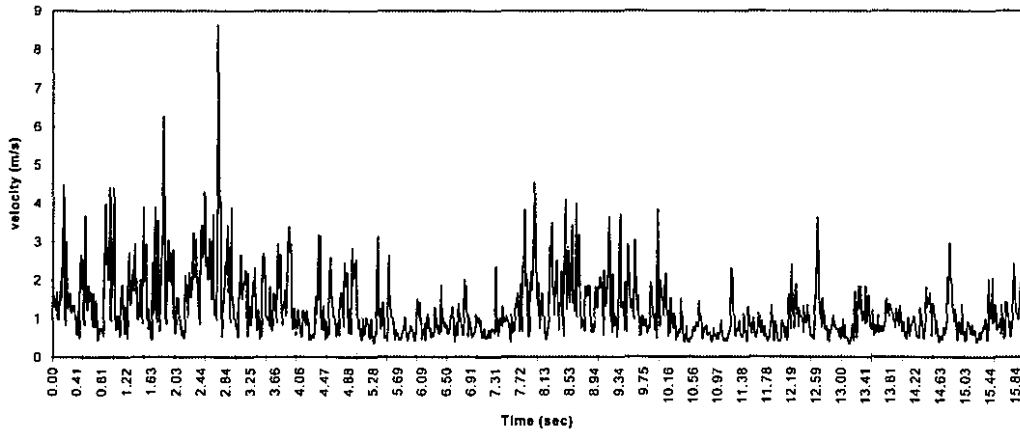


Figure 3.5 The Spectra of Turbulence - Wind 2  
(Data from the xz component of wind 2)

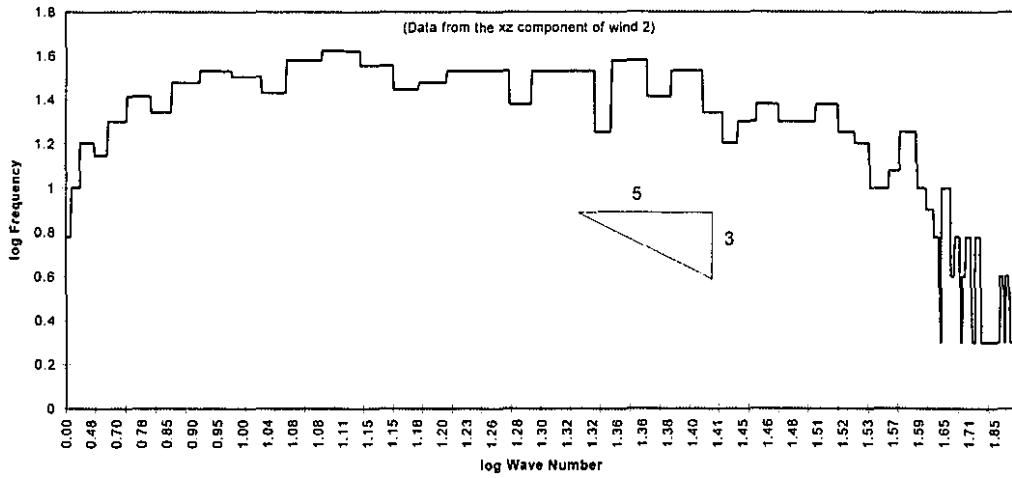


Figure 3.6 Correlation of Wind Statistical Factors

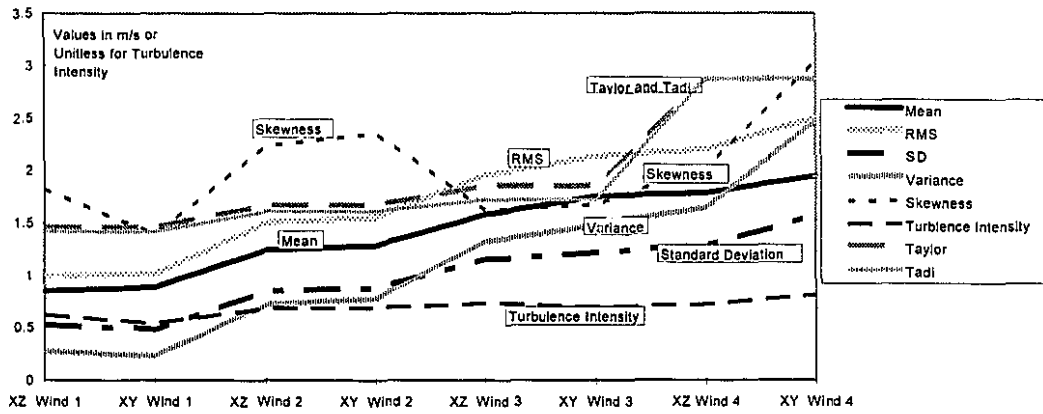


Table 3.5

**Summary of Wind Data**

all data in m/s unless otherwise indicated

	<b>XZ Wind 1</b>	<b>XY Wind 1</b>	<b>XZ Wind 2</b>	<b>XY Wind 2</b>
<b>Mean</b>	0.8495	0.8889	1.243	1.284
<b>RMS</b>	0.9983	1.011	1.505	1.557
<b>SD</b>	0.5246	0.4813	0.8497	0.8812
<b>Variance (unitless)</b>	0.2752	0.2316	0.7219	0.7764
<b>Skewness (unitless)</b>	1.818	1.392	2.233	2.354
<b>Kurtosis (unitless)</b>	3.543	1.876	8.846	9.944
<b>Turbulence Intensity</b> (unitless)	0.618	0.541	0.684	0.686
<b>Taylor Anemometer</b>	1.465	1.465	1.67	1.67
<b>Tadi Anemometer</b>	1.418	1.418	1.61	1.61
	<b>XZ Wind 3</b>	<b>XY Wind 3</b>	<b>XZ Wind 4</b>	<b>XY Wind 4</b>
<b>Mean</b>	1.578	1.751	1.784	1.942
<b>RMS</b>	1.952	2.131	2.197	2.498
<b>SD</b>	1.149	1.215	1.282	1.571
<b>Variance (unitless)</b>	1.32	1.476	1.643	2.467
<b>Skewness (unitless)</b>	1.619	1.673	2.018	3.035
<b>Kurtosis (unitless)</b>	2.924	3.483	5.724	16.75
<b>Turbulence Intensity</b> (unitless)	0.728	0.694	0.719	0.809
<b>Taylor Anemometer</b>	1.85	1.85	2.87	2.87
<b>Tadi Anemometer</b>	1.72	1.72	2.87	2.87

with evaporation rate. The correlation between the wind velocities and their statistics are shown in Figure 3.6. This shows high correlations for all factors with the minor exception of the velocities read by the two vane anemometers, the Tadi and Taylor, for the wind designated number 4 (below).

Four wind velocities were used. The first three velocities were adjusted by using the three speeds available on the fan switch and with the experimental set up shown in Figure 3.1. The fourth wind setup was adjusted to create a relatively higher velocity level by readjusting the distances between the fan and the evaporation pan. This experimental setup is illustrated in Figure 3.7. The geometry of the fan and pan may account for the slight differences noted between the vane anemometer readings (Tadi and Taylor) noted for wind 4 compared to that for other winds. Both vane anemometers have relatively large physical dimensions and the air impacts more directly on the measuring vanes in wind number 4 compared to the previous setups.

The velocity diagrams and the logarithmic histograms for the xy components of the 4 winds, prepared in the manner described above, are presented in Figures 3.8 to 3.15.

This shows that the winds generated here, had a high turbulent intensity. This is due to the use of a standard electric fan as well as flow over the evaporation pan lip. A high turbulence content was desirable for these experiments so that the effect of winds was pronounced. There was no need to or attempt to develop similarity criteria for wind conditions. It should be noted that all findings related to winds, are true for those wind conditions noted here. Effects such as very high winds or 'gusty' winds were not investigated.

Figure 3.7 **Experimental Setup  
for Wind Four**

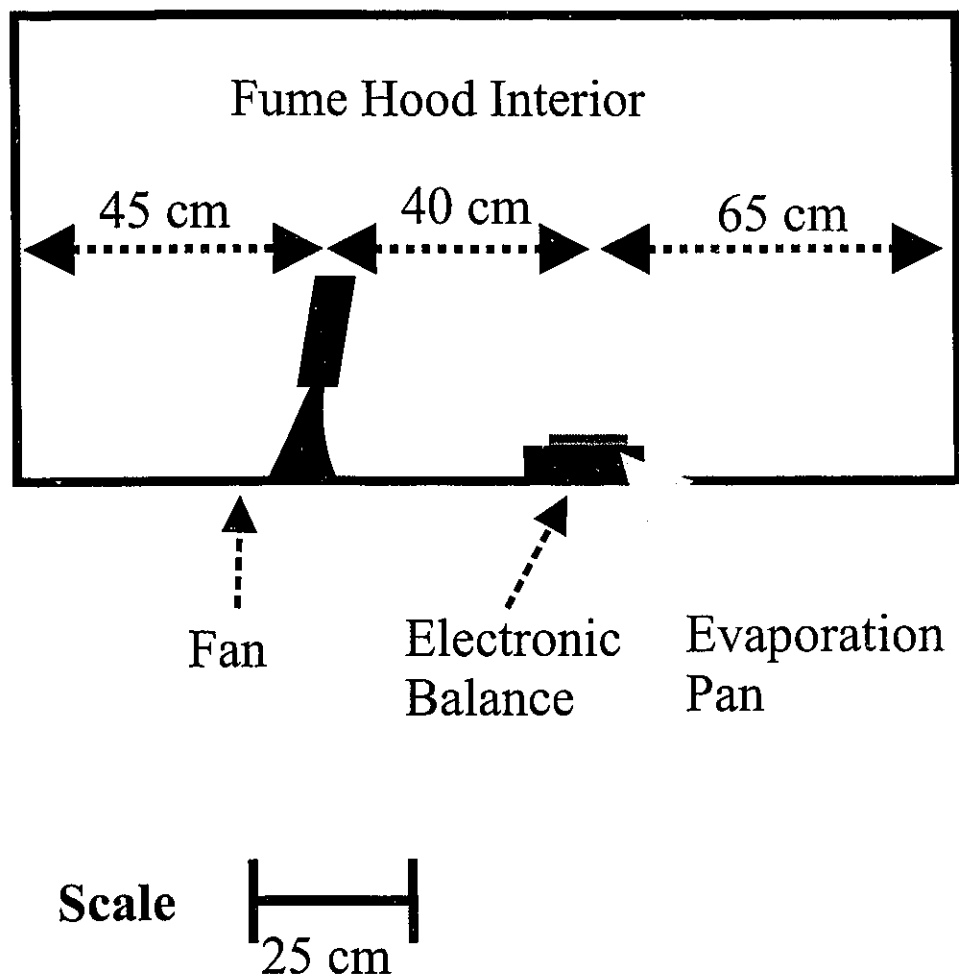


Figure 3.8

The Variation of Air Velocity Over Time - Wind 1

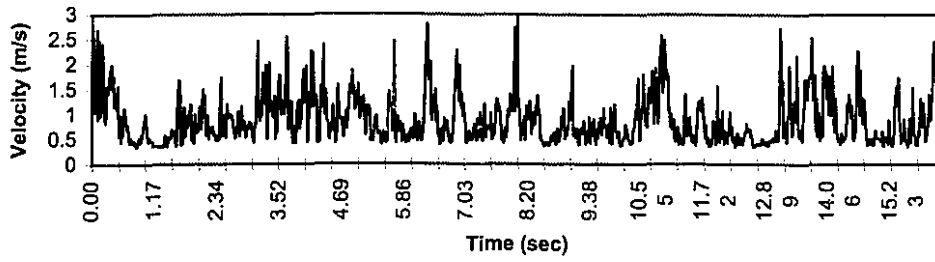


Figure 3.9

The Variation of Air Velocity Over Time - Wind 2

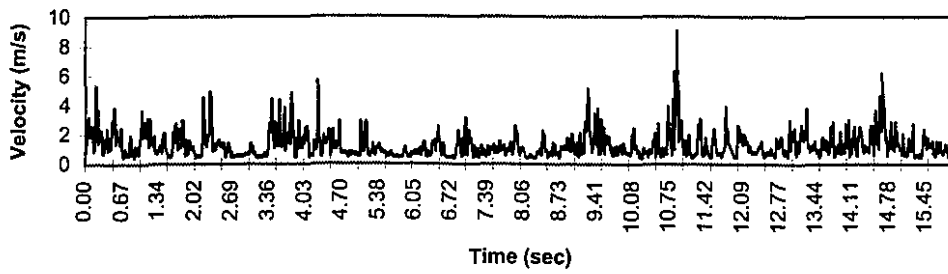


Figure 3.10

The Variation of Air Velocity Over Time - Wind 3

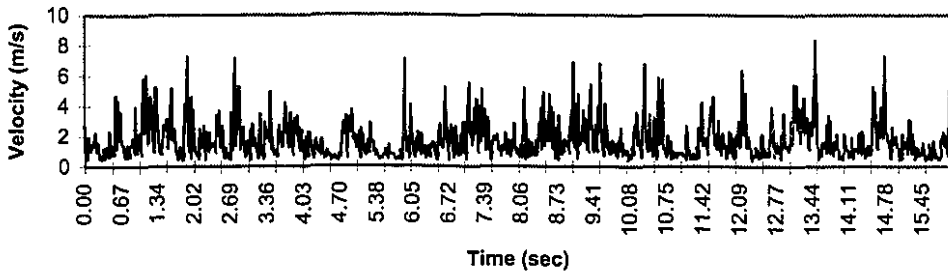


Figure 3.11

The Variation of Air Velocity Over Time - Wind 4

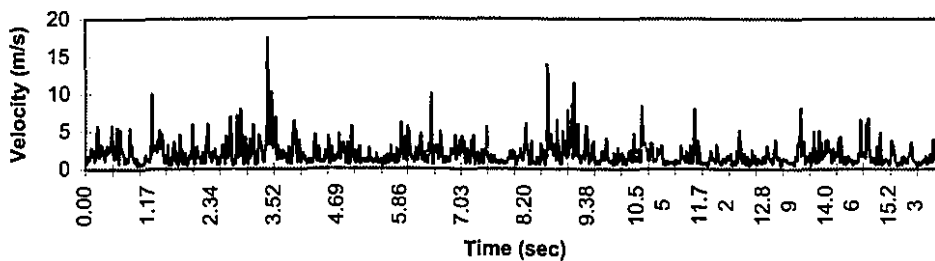


Figure 3.12

The Spectra of Turbulence - Wind 1

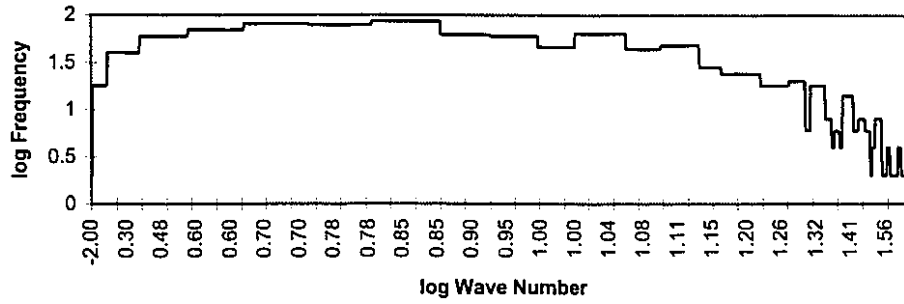


Figure 3.13

The Spectra of Turbulence - Wind 2

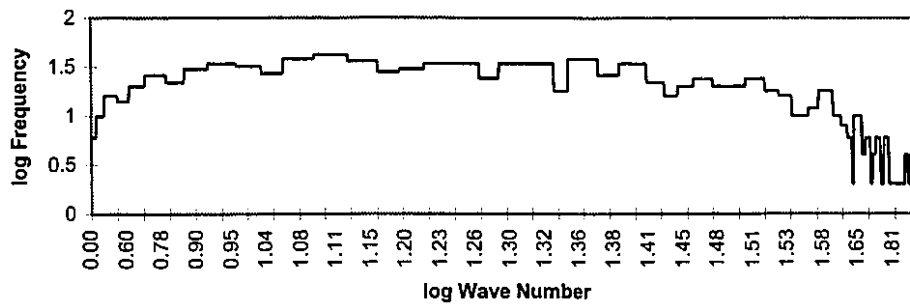


Figure 3.14

The Spectra of Turbulence - Wind 3

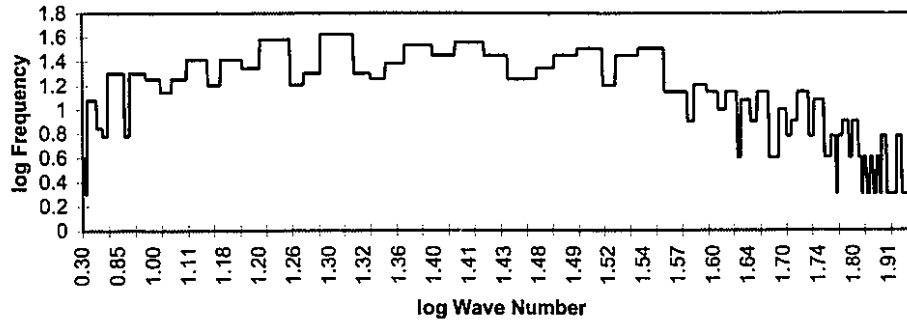
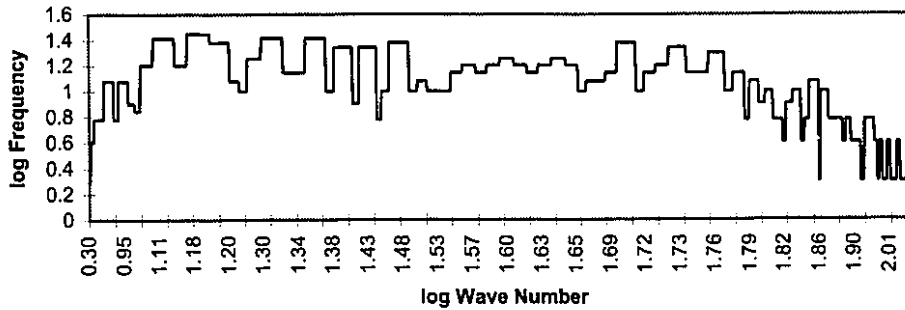


Figure 3.15

The Spectra of Turbulence - Wind 4



## **Chapter 4 Evaporation Behaviour of Oils and Petroleum**

### **4.1 Abstract**

Experiments were conducted with several crude oils and petroleum products to ascertain their evaporative behaviour. Pure compounds such as water, evaporate in a linear manner with time. Most crude oils evaporate in a logarithmic manner, i.e. the loss of mass is a logarithmic function of time. This behaviour is due to the number of components evaporating at once, each of which has a linear evaporation behaviour. The envelope of these linear rates results in a logarithmic curve.

The study of evaporative curves shows that 'best' fit largely depends on the number of components evaporating at once. Pure compounds evaporate in a direct linear fashion as was known. Mixtures of components between about 3 and 7 evaporate in square root manner with time. Logarithmic equations result when approximately 7 or more components evaporate simultaneously.

### **4.2 Experimental**

Experiments were conducted using the methods outlined in Chapter 3. Two series of experiments were conducted, the first to delineate the general nature of oil evaporation and a second to ascertain the reason for the logarithmic behaviour of oil evaporation.

Oils were taken from supplies of the Emergencies Science Division and were supplied by various oil companies for environmental testing. Properties of the oils can be found in standard references (Whiticar, Bobra et al., 1993).

Table 4.1 lists the experiments, experimental parameters and summary results.

### **4.3 Results and Discussion**

Initial experiments were conducted to reexamine the nature of the evaporative loss with time. The literature review, as summarized in Chapter 2, indicates that the weight loss of an evaporating oil may be logarithmic; however, there is no consensus on this, nor any proposition as to the reason. In this study, a variety of fluids were evaporated and the curves of evaporative loss versus time evaluated. This was done by

Table 4.1

Summary Table of Experiments to Delineate Oil Evaporation Behaviour

Date	Prime	Oil	Days	Total	Fan (cm <sup>2</sup> )	Initial	Initial (mm)	End	%	Temp	Wind	R' Best	Best	Equation
1993	Purpose	Type	Length	Time (hr)	Area	Weight (g)	Thickness	Wt.	Evap	C	m/s	Equation	Equation	Parameter
June 21	rate	ASMB	1	15	151	8.18	0.65	5.3	35	21.2	0	0.991	ln	5.35
June 23	rate	ASMB	1	22	268	16.29	0.72	11	34	21	0	0.978	ln	4.76
June 24	rate	ASMB	1	23	270	29.49	1.3	20	32	21.8	0	0.97	ln	4.43
June 25	rate	ASMB	7	182	151	8.04	0.63	4.5	44	22.6	0	0.99	ln	4.95
July 2	rate	ASMB	1	15	151	20.16	1.59	14	30	22.4	0	0.937	ln	4.05
July 3	rate	ASMB	2	51	151	22.52	1.78	15	35	21.9	0	0.975	ln	4.36
July 5	rate	ASMB	2	65	151	27.15	2.14	17	36	24.4	0	0.954	ln	4.26
July 9	rate	ASMB	1	25	151	34.1	2.69	21	38	23.8	0	0.952	ln	4.45
July 16	rate	ASMB	4	73	151	35.98	2.84	24	32	21.7	0	0.96	ln	3.81
July 20	rate	ASMB	2	36	151	57.67	4.55	39	32	22.8	0	0.963	ln	4.09
Aug 30	rate	ASMB	1	18	151	115.03	9.08	85	26	20.1	0	0.879	ln	3.07
Sept 1	rate	ASMB	4	73	151	96.41	7.61	62	36	20.3	0	0.886	ln	3.86
Sept 4	rate	ASMB	10	217	151	66	5.21	42	36	20	0	0.937	ln	3.56
Sept 13	rate	ASMB	4	64	151	19.35	1.53	12	38	22.1	0	0.981	ln	4.66
Sept 16	rate	ASMB	3	56	151	40.67	3.21	27	34	17.8	0	0.952	ln	3.95
Sept 18	rate	ASMB	2	47	151	16.87	1.33	11	36	19.2	0	0.987	ln	4.73
Sept 20	rate	ASMB	1	23	151	7.43	0.59	4.7	36	18.8	0	0.988	ln	5.16
Sept 21	rate	ASMB	1	25	151	7.92	0.63	5	36	20.1	0	0.985	ln	5.18
Sept 22	rate	ASMB	3	71	151	24.8	1.96	16	37	23.1	0	0.976	ln	4.49
Oct 15	rate	ASMB	1	32	151	32.2	2.54	21	35	18.6	0	0.977	ln	4.78
Oct 16	rate	ASMB	5	89	151	66.82	5.27	42	37	22.9	0	0.98	ln	4.27
Oct 20	rate	ASMB	4	76	151	18.06	1.43	10	45	20.4	0	0.993	ln	5.7
Oct 23	rate	ASMB	4	66	151	17.56	1.39	11	40	20.3	0	0.986	ln	5.26
Oct 26	rate	ASMB	3	88	151	35.44	2.8	22	37	19.1	0	0.962	ln	4.27
Dec 24	Oil	Bunker	4	99	151	252.07	17.14	250	1	11.8	0	0.687	ln	0.048
Dec 28	Oil	Gasoline	1	19	151	73.61	6.68	8.7	88	13.4	0	0.983	ln	10.1
Dec 29a	Oil	Gasoline	0.5	4	151	20	1.81	1.6	92	9.1	0	0.922	ln	12.1
Dec 29b	Oil	Gasoline	0.5	2	151	20	1.81	2.3	89	19.5	0	0.889	ln	15.9
Dec 29c	Oil	Bunker	3	72	151	20.06	1.36	19	6	19.6	0	0.875	ln	0.473
1994														
Jan 1	Oil	Prudhoe1	2	49	151	20	1.49	17	15	21.5	0	0.993	ln	1.65
Jan 3	Oil	Prudhoe2	3	71	151	20	1.49	16	19	21.3	0	0.997	ln	2.17
Jan 6	Oil	Orimulsion	1	26	151	20	1.34	9.2	54	21.2	0	0.95	ln	6.4
Jan 7	Oil	Orimulsion	1	20	151	20	1.34	15	26	12	0	0.951	ln	3.38
Jan 8	Oil	Brent	2	48	151	40	3.18	27	33	18	0	0.995	ln	3.93
Jan 10	Oil	Brent	1	27	151	20	1.59	12	38	21.6	0	0.991	ln	4.06
Jan 11	Oil	Orimulsion	1	25	151	40	2.71	12	69	6	0	0.792	ln	5.07
Jan 12	Oil	Brent	3	67	151	30	2.38	20	35	19.5	0	0.991	ln	4.03

Table 4.1 ctd.

## Summary Table of Experiments to Delineate Oil Evaporation Behaviour

Date	Prime	Oil	Days	Total	Fan (cm <sup>2</sup> )	Initial	Initial (mm)	End	%	Temp	Wind	R <sup>2</sup> Best	Best	Equation
1993	Purpose	Type	Length	Time (hr)	Area	Weight (g)	Thickness	Wt.	Evap	C	m/s	Equation	Equation	Parameter
Jan 15	Oil	Brent	3	74	151	50	3.97	33	33	18.1	0	0.986	ln	3.97
Jan 18	Oil	Endicott	2	42	151	50	3.62	46	9	20.1	0	0.972	ln	0.926
Jan 20a	Oil	Av Gas 80	1	3	151	20	1.91	0	100	5.6	0	0.974	ln	16.8
Jan 20b	Oil	Av Gas 80	1	2	151	20	1.91	0	100	18	0	0.964	ln	15.4
Jan 20c	Oil	Issungnak	2	47	151	20	1.56	16	22	19	0	0.947	ln	2.23
Jan 22	Oil	Terra Nova	2	43	151	20	1.54	17	17	18.8	0	0.971	ln	1.93
Jan 24	Oil	Heating Oil	4	95	151	20	1.53	12	39	5.6	0	0.852	sq. rt.	3
Jan 28a	Oil	Jet 40 Fuel	0.5	6	151	20	1.71	4.2	79	20.8	0	0.915	ln	9.63
Jan 28b	Oil	Prudhoe Bay	8	190	151	30	2.23	23	24	11.2	0	0.986	ln	2.36
Feb 5	Oil	Santa Clara	2	48	151	20	1.44	16	18	24.1	0	0.967	ln	2.3
Nov 14a	compon.	2-compon.	0.5	7	151	20	1.77	3.9	80	17	0	0.999	lin	0.2
Nov 14b	compon.	4-compon.	0.5	11	151	20	1.72	1.9	91	23.7	0	0.995	sq. rt.	3.2
Nov 15a	compon.	3-compon.	0.5	5	151	20	1.74	1.9	91	20	0	0.988	linear	0.353
Nov 15b	compon.	6-compon.	2	49	151	20	1.7	1.7	92	19	0	0.948	sq. rt.	1.79
Nov 17	compon.	5-compon.	1	27	151	20	1.72	1.6	92	21.2	0	0.985	sq. rt.	2.25
Dec 10	compon.	14-compon.	1	21	151	20.03	1.7	5.6	72	18.6	0	0.975	sq. rt.	2.17
Dec 11	compon.	13-compon.	1	30	151	20.14	1.71	5.9	71	19	0	0.923	sq. rt.	1.93
Dec 12	compon.	12-compon.	1	25	151	20.09	1.71	7	65	8	0	0.984	sq. rt.	1.8
Dec 13	compon.	11-compon.	4	92	151	20.2	1.72	4	80	9.2	0	0.916	sq. rt.	1.26
Dec 17	compon.	10-compon.	2	50	151	20.05	1.7	5.5	72	22.2	0	0.913	sq. rt.	1.52
Dec 19	compon.	9-compon.	2	40	151	20.17	1.71	7.4	63	18.6	0	0.954	sq. rt.	1.44
Dec 21	compon.	8-compon.	1	29	151	20	1.7	7.9	61	23.4	0	0.956	sq. rt.	1.66
Dec 22	compon.	7-compon.	1	25	151	20	1.7	7.2	64	23	0	0.968	sq. rt.	1.77
Dec 23	oil type	Komineft	5	121	151	12.88	1.02	8.8	32	23.3	0	0.995	ln	3.4
Dec 28	oil type	Federated	6	142	151	20	1.58	12	40	23.1	0	0.982	ln	4.44
1995														
Jan 3	oil type	Federated	4	95	151	20	1.58	13	34	15	0	0.985	ln	3.99
Jan 7	oil type	Federated	4	96	151	20	1.58	12	38	15	18	0.988	ln	4.42
Jan 11	oil type	Avalon	3	70	151	20	1.56	18	9	15	0	0.96	ln	2.08
Jan 14	oil type	Gulfaks	4	89	151	20	1.61	15	26	15	0	0.983	ln	2.89
Jan 18	oil type	Brent	3	79	151	20	1.58	13	36	15	0	0.995	ln	4.23
Jan 21	oil type	Amauligak	5	120	151	20.14	1.5	15	24	15	0	0.952	ln	2.3

curve fitting using the program TableCurve, as noted above. Table 4.2 shows the 'Best' fit equations for each oil used in this test. This table clearly shows that three 'simple' equations fit best for different situations. Obviously, more complex equations, that is those with more parameters, can fit the data better, and thus the criteria for best fit also includes the simplest form of an equation. For regular oils, logarithmic equations fit best in so far as they are the simplest equations that have only two parameters or less with the highest regression coefficient,  $R^2$ . Pure substances including the hydrocarbons and water, evaporate in a linear manner (loss with respect to time). Heating oil - similar to diesel fuel - fits a square root equation best. This oil was chosen to represent a different situation. Heating oil is a refinery product with a very narrow 'cut'. The oil has few compounds and probably is dominated by about 4 compounds compared to several dozen for a typical crude oil (Whiticar, Bobra et al., 1993). Other oils can also show this behaviour, FCC Heavy Cycle, or certain Bunker fuels where diesel is an ingredient (this will be demonstrated in Chapter 6).

To test whether the type (or shape) of the curve is a result of the number of components evaporating, a series of experiments was conducted using pure hydrocarbons. Table 4.3 gives the constituents of the hydrocarbon mixtures. Table 4.4 shows the number of components and the "best" power factor for each experimental run with the specific number of components. An experiment was conducted and the data fit to the equation  $Y = a + bX^e$ , where Y is the percent of the artificial component mixture evaporated, a and b are empirical constants, X is the time and e is the power exponent. The component mixture changes composition somewhat as it progresses past 10 components. More volatile components were used to produce the new mixture from 10 to 15 components. The results are shown in Figure 4.1. The best fit resulted from using a power equation. As can be seen, the number of components evaporating changes the curve type smoothly until the mixture changes to the more volatile components noted. A logarithmic curve is approximately a power factor of 0.35 for the values of time used in this study (10 to 2000 minutes), thus approximately 10 components evaporating are required to yield a logarithmic curve. The graph indicates also that those oils (such as FCC Heavy Cycle, heating oil and diesel fuel) which show a square root equation as

Table 4.2 Best-Fit Equations for Each of the Oils

Experiment Date	Oil or Substance	Best Equation*	Rank Chosen Equation	R <sup>2</sup> - Chosen Equation
June 21	ASMB	8010	3	0.991
June 23	ASMB	36	5	0.978
June 24	ASMB	57	6	0.97
June 25	ASMB	13	1	0.99
July 2	ASMB	76	9	0.937
July 3	ASMB	57	6	0.975
July 5	ASMB	57	8	0.954
July 9	ASMB	57	11	0.952
July 16	ASMB	57	6	0.96
July 20	ASMB	57	8	0.963
Aug 30	ASMB	76	13	0.879
Sept 1	ASMB	57	8	0.886
Sept 4	ASMB	57	9	0.937
Sept 13	ASMB	57	3	0.981
Sept 16	ASMB	57	6	0.952
Sept 18	ASMB	57	2	0.987
Sept 20	ASMB	57	2	0.988
Sept 21	ASMB	36	4	0.985
Sept 22	ASMB	57	4	0.976
Oct 15	ASMB	57	3	0.977
Oct 16	ASMB	57	4	0.98
Oct 20	ASMB	13	1	0.993
Oct 23	ASMB	76	2	0.986
Oct 26	ASMB	57	5	0.962
Dec 24	Bunker	11	41	0.687
Dec 28	Gasoline	59	8	0.983
Dec 29a	Gasoline	8010	23	0.922
Dec 29b	Gasoline	10	20	0.889
Dec 29c	Bunker	8010	22	0.875
Jan 1	Prudhoe1	8010	3	0.993
Jan 3	Prudhoe2	13	1	0.997
Jan 6	Orimulsion 1	60	12	0.95
Jan 7	Orimulsion 2	61	11	0.951
Jan 8	Brent	35	3	0.995
Jan 10	Brent	56	2	0.991
Jan 11	Orimulsion	59	41	0.792
Jan 12	Brent	94	3	0.991
Jan 15	Brent	58	6	0.986
Jan 18	Endicott	59	7	0.972
Jan 20a	Av Gas 80	59	6	0.974
Jan 20b	Av Gas 80	8010	25	0.964
Jan 20c	Issungnak	8010	13	0.947
Jan 22	Terra Nova	8010	2	0.971
Jan 24	Heating Oil	58	20	0.852
Jan 28a	Jet 40 Fuel	59	21	0.915
Jan 28b	Prudhoe Bay	57	3	0.986
Feb 5	Santa Clara	59	8	0.967

Table 4.2 ctd. **Best-Fit Equations for Each of the Oils**

Experiment Date	Oil or Substance	Best Equation*	Rank Chosen Equation	R <sup>2</sup> - Chosen Equation
Nov 14a	2-component	8010	3 - linear	0.999
Nov 14b	4-component	73	5 - square -12	0.995
Nov 15a	3-component	60	14 - linear	0.988
Nov 15b	6-component	36	9 -square -12	0.948
Nov 17	5-component	36	9 - square -12	0.985
Dec 10	14-component	60	6 - square -12	0.975
Dec 11	13-component	59	13 - square -12	0.923
Dec 12	12-component	59	5 - square -12	0.984
Dec 13	11-component	36	13 - square -12	0.916
Dec 17	10-component	36	13 - square -12	0.913
Dec 19	9-component	10	11 - square -12	0.954
Dec 21	8-component	59	10 - square -12	0.956
Dec 22	7-component	36	8 - square -12	0.968
Dec 23	Komineft	35	2	0.995
Dec 28	Federated	36	5	0.982
Jan 3	Federated	57	4	0.985
Jan 7	Federated	57	2	0.988
Jan 11	Avalon	8010	4	0.96
Jan 14	Gulfaks	57	6	0.983
Jan 18	Brent	35	2	0.995
Jan 21	Amauligak	10	13	0.952

\* Equations noted above are:

10= $y=a+b(\ln x^2)$	58= $1/y=a+b\ln x/x$
12= $y=a+bx^{0.5}$ (nar. cut)	59= $1/y=a+b/x$
13= $a + b \ln x$ (standard log)	60= $1/y=a+b/x^{1.5}$
35= $\ln y=x+b/\ln x$	73= $y^{0.5}=a+b(\ln x)^2$
36= $\ln y=a + b/x^{0.5}$	76= $y^{0.5}=a+b\ln x$
56= $1/y=a+b/\ln x$	94= $y^2=a+b(\ln x^2)$
57= $1/y=y+a+b/x^{0.5}$	8010= $y=a+bx^c$

Table 4.3

**Constituents of the Hydrocarbon Mixtures**

<b>Number of Components</b>	<b>Equal Mass Constituents</b>
1	Heptane
2	Heptane, Octane
3	Heptane, Octane, Nonane
4	Heptane, Octane, Nonane, Decane
5	Heptane, Octane, Nonane, Decane, Undecane
6	Heptane, Octane, Nonane, Decane, Undecane, Hexadecane
7	#5 above and Dodecane
8	#5 above and Dodecane, Tridecane
9	#5 above and Dodecane, Tridecane, Benzene
10	#5 above and Dodecane, Tridecane, Benzene, Toluene
11	#9 above and p-Xylene
12	#9 above and p-Xylene, Ethyl Benzene
13	#9 above and p-Xylene, Ethyl Benzene, Decahydronaphthalene
14	#12 above and Propyl Benzene
15	#12 above and Propyl Benzene, Cyclohexane

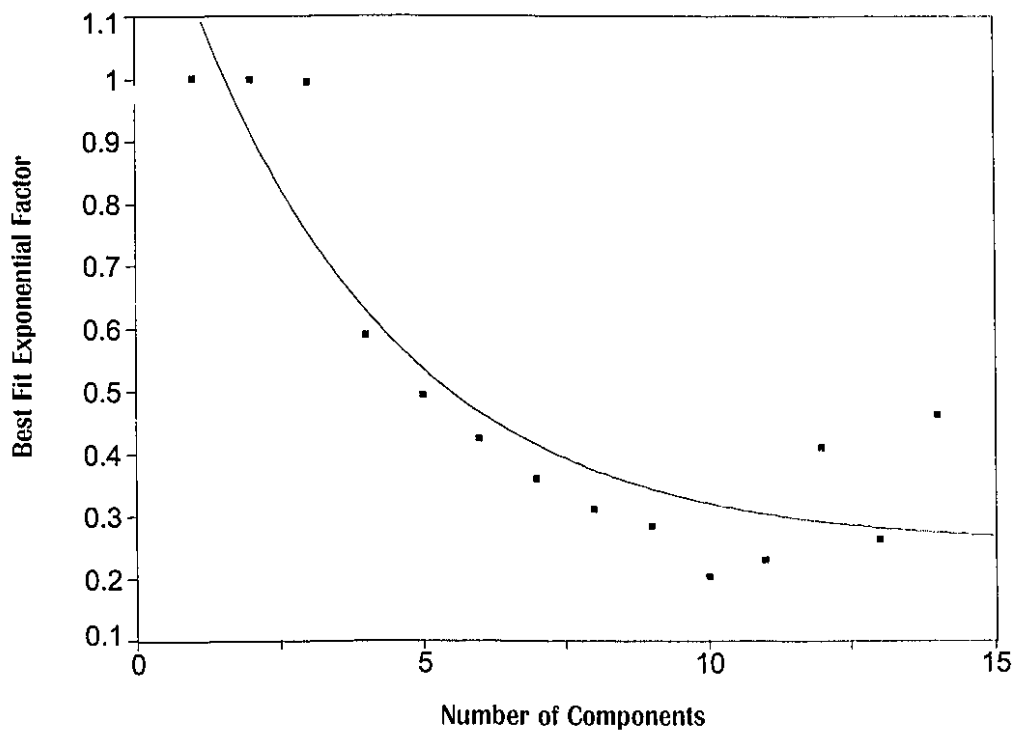
Table 4.4 **Power Exponents for Multiple-Component Evaporation**

<b>Components</b>	<b>Best-Fit Power Factor</b>
1	1
2	0.998
3	0.994
4	0.588
5	0.494
6	0.252
7	0.36
8	0.31
9	0.283
10	0.202
11	0.23
12	0.41
13	0.263
14	0.463

Figure 4.1

## The Evaporative Behaviour of Multiple Components

Rank 1 Eqn 8002  $y=a+b\exp(-x/c)$  [Exponential]  
 $r^2=0.845$   $DFAdj\ r^2=0.798$   $FitStdEr=0.124$   $Fstat=300$   
 $a=0.249$   $b=1.17$   
 $c=3.56$



having the best fit, have approximately 5 components evaporating.

#### **4.4 Conclusions**

Pure compounds evaporate in a linear manner. Most crude oils, consisting of hundreds of compounds, evaporate in a logarithmic manner, that is the loss of mass is logarithmic with time. This behaviour is due to the number of components evaporating at once, each of which has a linear evaporation behaviour. The envelope of these linear rates results in a logarithmic curve. This can be illustrated by the Figure 4.2. This figure shows the schematic of how the logarithmic curve can be formed by the envelope of several components evaporating in a linear manner.

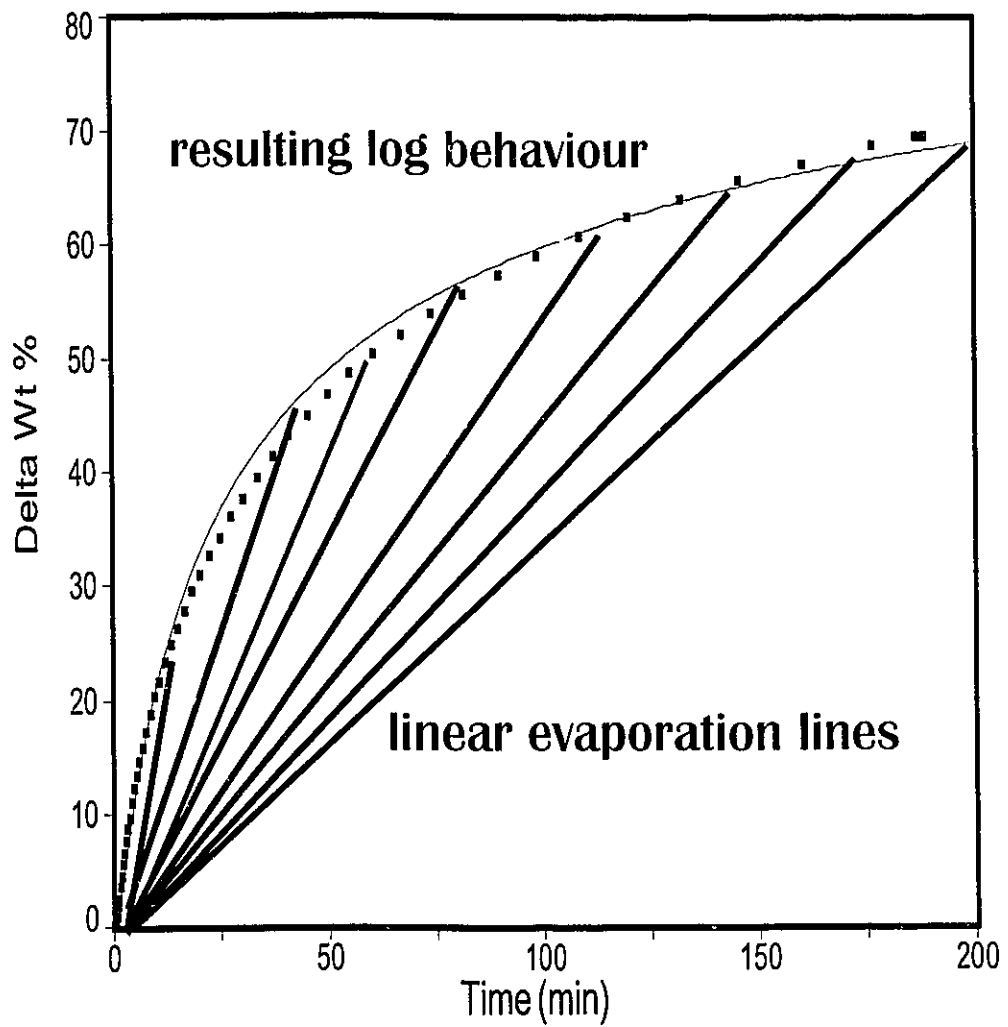
The study of the nature of the evaporative curve shows that 'best' fit largely depends on the number of components evaporating simultaneously. Pure compounds evaporate in a linear fashion. Mixtures of components between about 3 and 7 components evaporate as a square root with time. Logarithmic equations result when approximately 7 or more components evaporate simultaneously.

#### **References**

Whiticar, S., M. Bobra, M.F. Fingas, P. Jokuty, P. Liuzzo, S. Callaghan, F. Ackerman and J. Cao, *A Catalogue of Crude Oil and Oil Product Properties (1992 Edition)*, Environment Canada Manuscript Report Number EE-144, Ottawa, Ontario, 643 p., 1993.

Figure 4.2

Schematic Showing how Logarithmic Behaviour  
Can Result from Linear Multiple-Component Behaviour



## **Chapter 5 The Application of Traditional Boundary Layer Regulation**

### **5.1 Abstract**

Experiments were conducted to determine if oil and petroleum evaporation is boundary-layer regulated. Experiments included the examination of the evaporation rate with and without wind, in which case it was found that the evaporation rates were similar for all wind conditions but different for the no-wind conditions. Experiments where the area and thickness varied showed that boundary-layer regulation was applicable only for a short time after the start of evaporation. Under all experimental and environmental conditions, oils or petroleum products were not found to be strictly boundary-layer regulated. Experiments on the rate of evaporation of pure compounds showed that compounds larger than Decane, with an evaporation rate of 0.01 g/min, are not boundary-layer regulated. Most oils and petroleum products contain few compounds smaller than decane and thus their evaporation is not strictly boundary-layer limited. Other data are presented which explain the lack of boundary-layer regulation, including the length of times that an oil or petroleum evaporation exceeds boundary-layer limits and a comparison of the air saturation levels of various oils and petroleum products. The latter shows that the saturation concentration of water is significantly less than that of several petroleum hydrocarbons. Lack of boundary-layer regulation for oils is then a result of both this higher saturation concentration as well as a low (below boundary-layer value) evaporation rate on the average.

### **5.2 Introduction**

As noted in Chapter 1, evaporation can be viewed as consisting of two fundamental components, basic evaporation itself and regulatory mechanisms. Basic evaporation is that process consisting of the evaporation of the liquid directly into the vapour phase without any regulation other than by the thermodynamics of the liquid itself. Regulatory mechanisms are those processes which serve to regulate the final evaporation rate into the environment. For water, the main regulation mechanism is boundary layer regulation. Boundary layer regulation operates by limiting the rate of

diffusion, both molecular and turbulent diffusion, and by saturation dynamics. Molecular diffusion is the movement of molecules through still air. The rate for turbulent diffusion, the combination of molecular diffusion and movement with turbulent air, is on the order of  $10^2$  slower than that for maximum evaporation. (Jones, 1992).

If evaporation of oil were like that of water and were boundary-layer regulated one could write the mass transfer rate in a general form as:

$$E \approx K C T_u S \quad (5.1)$$

where E is the evaporation rate in mass per unit area, K is the mass transfer rate of the evaporating liquid (presumed constant), C is the concentration of the evaporating fluid as a mass per volume,  $T_u$  is the turbulence factor, S is a factor that relates to the saturation of the boundary layer above the evaporating liquid. If the air is already saturated with the compound in question, the evaporation rate is zero. This also relates to the scale length of an evaporating pool, considering that the air above a large pool is much more likely to be saturated than above a small pool.

Boundary layer regulation was assumed by several workers in the field to be the primary regulation for oil and petroleum evaporation. This assumption was never tested by experimentation as revealed by the literature search, detailed in Chapter 2. The implications of these assumptions are that evaporation rate for a given oil is increased by:

- increasing turbulence
- increasing wind speed (U)
- increasing the surface area of a given mass of oil
- decreasing the scale size of the evaporating area (note the balance between this and the above factor)
- decreasing the slick thickness (i.e. spreading the oil out).

These factors can then be verified experimentally to test if oil is boundary-layer regulated or not. This formed the basis of experimentation described below.

### 5.3 Experimental

The following six experiments were conducted:

1. Measurement of the evaporation rates of oils with and without wind. This experiment is a direct test of the boundary layer hypothesis. Three outcomes are possible. First, oil could evaporate at an increasing rate with increasing wind speed (evaporation rate varies as  $U^x$  where  $x$  varies between 0.5 and 0.78, depending on the turbulence level). Second, no increase with wind speed could be observed, and thus boundary layer regulation is not a factor. Third, the result could be in between, so that oil may be boundary-layer regulated under some conditions or some oils may be boundary-layer regulated and others not. Several types of oil were used, as well as water for the purpose of comparison.

2. Measurement of the variation of evaporation with slick thickness. If thinner slicks evaporate more rapidly, then oil is boundary-layer regulated. This experiment is not as definitive as the first experiment because of the simple relationship of thickness with volume and area.

3. Study of the effect of evaporation area. If increasing area increases the evaporation rate, boundary regulation is a factor. Again, there is a relationship to spill volume and thickness and thus the experiment is not definitive by itself, especially without considering the volume or mass of the spilled oil.

4. Study of the effect of volume evaporating on the evaporation rate. If the volume or mass of the spill, with the same area, increases the evaporation rate, the process is not boundary-layer regulated and vice versa.

5. Study of the evaporation of pure hydrocarbons - with and without wind. This study is to ascertain which hydrocarbons (by hydrocarbon number, eg. C6=hexane) are boundary-layer regulated and which are not. This can then be related to the oil evaporation in a quantitative way. Alberta Sweet Mixed Blend (ASMB) (a light crude oil) was used for experiments 2 to 5.

6. Study of the evaporation of a highly-evaporated ASMB (Alberta Sweet Mixed Blend - a light crude oil) residue, combined with pure hydrocarbons - with and without wind. This study is similar to that above, however is designed to both test the boundary-

layer regulation of oils and pure hydrocarbons, but also to provide indication of the cause of oil evaporation behaviour. The addition of the pure hydrocarbons to the oil will show if there are any effects of either component on the other's evaporation. As noted in the literature survey, there is concern that waxes and resins in the oil may form a capping layer and affect evaporation.

The methodology of weight loss observation has been described in Chapter 3. Experiments were conducted in the fume hood, with and without wind, also as previously described.

Since the wind caused the top-loading balance to oscillate, and therefore to introduce noise into the data, special precautions had to be taken when the wind speed exceeded 1 m/s. The electronic balance employed does not transmit data when the instantaneous variation is greater than about 5% and thus this was an indicator of excessive disturbance from wind. For wind velocities higher than 1 m/s, a timer was placed on the fan that interrupted the power to the fan every 7 minutes to record 5-7 data points, spaced at intervals of 0.2 minutes. The first data point after the wind source was stopped might not be recorded because the scale would not send the data because of excessive noise, or the first data point might be considered 'noisy'.

The oils used in the experiment series 1 included: ASMB (Alberta Sweet Mixed Blend), automotive gasoline, and FCC Heavy Cycle (a refinery intermediate of narrow cut). All oils were used from a cooler in Environment Canada laboratories where they were stored in closed Nalgene containers and kept at 15°C. The oils were obtained from various oil companies by Environment Canada over the past three years. Properties of these oils have been characterized (Whiticar et al., 1992). Oils were shaken by hand before use to ensure that the portion used was homogeneous. The 34.5% weathered ASMB was obtained from the Environment Canada laboratory. The oil had been weathered by using a rotary evaporator to a weight loss of 34.5%. The pure hydrocarbons were obtained from Aldrich Chemical, Milwaukee, Wisconsin. Properties of all the test fluids are given in Table 5.1.

Evaporation data were collected on a dedicated lab computer and subsequently transferred to other computers for analysis. As noted in Chapter 3, most data were fit with

an exponential curve on the basis of the highest regression coefficient ( $R^2$ ).

Table 5.2 summarizes the experiments conducted and the basic variables for each.

#### 5.4 Results and Discussion

The results are presented in the order of the experimental series:

1. Experiments on the evaporation of oil with and without wind, were conducted with three oils, ASMB, Gasoline, FCC Heavy Cycle, and with water. Water formed a baseline data set since much is known about its evaporation behaviour (Jones, 1992; Brutsaert, 1982). Regressions on the data were performed and the equation parameters calculated, are shown in Table 5.3. The plots of wind speed versus the evaporation rate for each oil are shown in Figures 5.1 to Figure 5.4. The equation exponent, the evaporation rate in terms of the constant in the best fit equation, is plotted in each case. The plots where the evaporation rate is given as a weight loss, are presented in Figures 5.5 to 5.8. These show that the same relationship has been determined whether one uses the percentage of oil evaporated or the actual weight. Hereinafter, both sets of values will not be plotted, since the relationship is basically the same.

Figures 5.1 to 5.8 show that the evaporation rates (taken either as a percentage or as weight loss) for oils and even the light products, gasoline and FCC Heavy Cycle, are not increased by a significant amount with increasing wind speed. In most cases, there is a rise from the 0-wind level to the 1-m/s level, but after that, the rate remains relatively constant. The FCC Heavy Cycle shows this effect to the largest degree. This can be compared to the evaporation of water, as illustrated in Figures 5.4 and 5.8. These data show the classical relationship of the water evaporation rate correlated with the wind speed. This, by itself, would appear to indicate that the oils used here are somewhat boundary-layer regulated, but only to the degree that the effect is seen in moving from 0-wind to 1 m/s, and not thereafter.

The evaporation data (percent weight loss versus time) are shown in Figure 5.9 to 5.13. These again illustrate the difference in wind effect for oils and water, and that only at the 0-wind level is there an increase in oil evaporation.

The rates of evaporation compared to the wind speed are shown for all the liquids

Table 5.1

**Properties of the Test Liquids**

<b>Name</b>	<b>Description</b>	<b>Density g/mL</b>	<b>Boiling Point °C</b>
ASMB	Alberta Sweet Mixed Blend - A common crude oil in Canada	0.839	in. 37 (in. =initial)
Water		1	100
FCC-heavy	A highly cycled refinery intermediate containing few components	0.908	
Gasoline	Standard automotive gasoline	0.709	in. 5
Benzene	Pure Hydrocarbon - C6	0.879	80.1
Dodecane	Pure Hydrocarbon - C10	0.749	213
Undecane	Pure Hydrocarbon - C11	0.742	196
p-Xylene	Pure Hydrocarbon - C8	0.861	139
Nonane	Pure Hydrocarbon - C9	0.722	151
Decane	Pure Hydrocarbon - C10	0.73	174
Heptane	Pure Hydrocarbon - C7	0.684	98
Octane	Pure Hydrocarbon - C8	0.703	126
Decahydron	Decahydronaphthalene - pure hydrocarbon C10	0.893	195
Tridecane	Pure Hydrocarbon - C13	0.755	226
Hexadecane	Pure Hydrocarbon - C16	0.773	287
WAS-34.5	Weathered Alberta Sweet Mixed Blend - 34.5% by weight removed through evaporation	0.883	

used in this study, in Figure 5.14. This figure shows the evaporation rates of all test liquids versus wind speed. The lines shown are those calculated by linear regression using the graphics software, Sigma Plot, Washington, D.C. This clearly shows that water increased, as expected, in a strong linear relationship with increasing wind velocity.

All the above figures show that oil is only slightly, if at all, boundary-layer regulated, perhaps only affecting the very initial rates after turbulence is applied. Water shows the classic boundary-layer regulation.

## 2. Experiments In Thickness Variation

A series of experiments where thickness was varied, but not the area, was conducted. Of necessity, the volume was varied and as noted above, volume alone, has the opposite effect of thickness in terms of boundary layer regulation. Data are given in Table 5.4. All data are for Alberta Sweet Mixed Blend Oil (ASMB). Data are illustrated in Figure 5.15. This figure shows large scatter between evaporation rate and thickness and thus that thickness is only weakly correlated with evaporation rate. These results are not conclusive with respect to boundary-layer regulation because the volume was directly varied with thickness.

## 3. Evaporation Rate and Area Correlation

Alberta Sweet Mixed Oil was also used to conduct a series of experiments with varying area. The mass of the oil was kept constant so that the thickness of the oil would also vary. However, the greater the area, the lesser the thickness and both factors would increase oil evaporation if it were boundary-layer regulated. Table 5.5 shows the data from these experiments and these are illustrated graphically in Figure 5.16. These data show at best a weak correlation of thickness and area with evaporation rate. Because of the driving regulation of volume, thickness and area, the upward tendency shown in Figure 5.16 may be due to correlation with thickness or volume rather than a slight increase in area. Because of the poor correlation shown in Figure 5.16 one can conclude that evaporation rate is not correlated with area, and that the evaporation of oil is not boundary-layer regulated to any significant degree.

Table 5.2

## Experiments Conducted to Test Boundary Layer Regulation

Series	Date	Prime Purpose	Oil Type	Days Length	Total Time (hr)	Fan (cm <sup>2</sup> ) Area	Initial Loading (g)	Initial (mm) Thickness	End Wt.	% Evap	Temp C	Wind m/s	Variable	Variable Value	R <sup>2</sup> Best Equation	Best Equation	Single Parameter
2	June 21	Thickness	ASMB	1	15	151	8.18	0.65	5.3	35	21.2	0	thick	0.65	0.991	ln	5.35
	June 23	Thickness	ASMB	1	22	268	16.29	0.72	11	34	21	0	thick	0.72	0.978	ln	4.76
	June 24	Thickness	ASMB	1	23	270	29.49	1.3	20	32	21.8	0	thick	1.3	0.97	ln	4.43
	June 25	Thickness	ASMB	7	182	151	8.04	0.63	4.5	44	22.6	0	thick	0.63	0.99	ln	4.95
	July 2	Thickness	ASMB	1	15	151	20.16	1.59	14	30	22.4	0	thick	1.59	0.937	ln	4.05
	July 3	Thickness	ASMB	2	51	151	22.52	1.78	15	35	21.9	0	thick	1.78	0.975	ln	4.36
	July 5	Thickness	ASMB	2	65	151	27.15	2.14	17	36	24.4	0	thick	2.14	0.954	ln	4.26
	July 9	Thickness	ASMB	1	25	151	34.1	2.69	21	38	23.8	0	thick	2.69	0.952	ln	4.45
	July 16	Thickness	ASMB	4 (5)	73	151	35.98	2.84	24	32	21.7	0	thick	2.84	0.96	ln	3.81
	July 20	Thickness	ASMB	2(8)	36	151	57.67	4.55	39	32	22.8	0	thick	4.55	0.963	ln	4.09
	Aug 30	Thickness	ASMB	1	18	151	115.03	9.08	85	26	20.1	0	thick	9.08	0.879	ln	3.07
	Sept 1	Thickness	ASMB	4	73	151	96.41	7.61	62	36	20.3	0	thick	7.61	0.886	ln	3.86
	3	Sept 4	Thickness	ASMB	10	217	151	66	5.21	42	36	20	0	thick	5.21	0.937	ln
Sept 13		Thickness	ASMB	4	64	151	19.35	1.53	12	38	22.1	0	thick	1.53	0.981	ln	4.66
Sept 16		Thickness	ASMB	3	56	151	40.67	3.21	27	34	17.8	0	thick	3.21	0.952	ln	3.95
Sept 18		Thickness	ASMB	2	47	151	16.87	1.33	11	36	19.2	0	thick	1.33	0.987	ln	4.73
Sept 20		Thickness	ASMB	1	23	151	7.43	0.59	4.7	36	18.8	0	thick	0.59	0.988	ln	5.16
Sept 21		Thickness	ASMB	1	25	151	7.92	0.63	5	36	20.1	0	thick	0.63	0.985	ln	5.18
Sept 22		Thickness	ASMB	3	71	151	24.8	1.96	16	37	23.1	0	thick	1.96	0.976	ln	4.49
Oct 15		Thickness	ASMB	1	32	151	32.2	2.54	21	35	18.6	0	thick	2.54	0.977	ln	4.78
Oct 16		Thickness	ASMB	5	89	151	66.82	5.27	42	37	22.9	0	thick	5.27	0.98	ln	4.27
Oct 20		Thickness	ASMB	4	76	151	18.06	1.43	10	45	20.4	0	thick	1.43	0.993	ln	5.7
Oct 23		Thickness	ASMB	4	66	151	17.56	1.39	11	40	20.3	0	thick	1.39	0.986	ln	5.26
Oct 26		Thickness	ASMB	3	88	151	35.44	2.8	22	37	19.1	0	thick	2.8	0.962	ln	4.27
1994																	
7	Feb 7	Area	ASMB	3	50	16	10	7.45	7.1	29	24.2	0	area	16 cm <sup>2</sup>	0.969	ln	2.95
	Feb 9	Area	ASMB	1	25	16	5	3.72	3.4	31	23.9	0	area	16 cm <sup>2</sup>	0.96	ln	3.67
	Feb 10	Area	ASMB	1	21	16	2.12	1.58	1.6	24	8	0	area	16 cm <sup>2</sup>	0.72	ln	2.89
	Feb 11	Area	ASMB	1	25	16	1.06	0.79	0.7	32	24.6	0	area	16 cm <sup>2</sup>	0.791	ln	5.23
	Feb 12	Area	ASMB	2	50	62	20	3.84	14	32	22.5	0	area	62 cm <sup>2</sup>	0.992	ln	3.52
	Feb 14	Area	ASMB	1	22	62	10	1.92	7.2	28	15.6	0	area	62 cm <sup>2</sup>	0.996	ln	3.77
	Feb 15	Area	ASMB	1	26	62	8.2	1.58	5.4	34	25.3	0	area	62 cm <sup>2</sup>	0.982	ln	4.35
	Feb 16	Area	ASMB	1	23	62	4.1	0.79	2.7	33	23.8	0	area	62 cm <sup>2</sup>	0.994	ln	4.57
	Feb 17	Area	ASMB	1	24	161	20	1.48	14	32	21	0	area	161 cm <sup>2</sup>	0.987	ln	3.98
	Feb 18	Area	ASMB	1	23	161	10.7	0.79	7.5	30	25.2	0	area	161 cm <sup>2</sup>	0.973	ln	4.07
	Feb 19	Area	ASMB	2	50	161	21.4	1.58	14	35	23.9	0	area	161 cm <sup>2</sup>	0.941	ln	3.66
	Feb 21	Area	ASMB	5	83	161	50	3.7	33	33	19.1	0	area	161 cm <sup>2</sup>	0.933	ln	3.16
	Feb 26	Area	ASMB	2	50	161	30	2.22	19	36	21	0	area	161 cm <sup>2</sup>	0.99	ln	4.7
	Feb 28	Area	ASMB	1	25	161	10	0.74	6.9	32	20	0	area	161 cm <sup>2</sup>	0.953	ln	4.06
	Mar 01	Area	ASMB	3	74	206	27.3	1.58	18	35	18	0	area	206 cm <sup>2</sup>	0.984	ln	3.63
	Mar 04	Area	ASMB	1	20	206	13.65	0.79	8.7	37	21	0	area	206 cm <sup>2</sup>	0.974	ln	5.27
	Mar 05	Area	ASMB	2	51	206	20	1.16	13	33	19.5	0	area	206 cm <sup>2</sup>	0.963	ln	3.64
	Mar 07	Area	ASMB	2	44	151	20	1.58	13	34	20.5	0	area	151 cm <sup>2</sup>	0.993	ln	4.18
	Mar 09	Area	ASMB	1	26	151	10	0.79	6.5	35	19	0	area	151 cm <sup>2</sup>	0.994	ln	4.8
8	Mar 10	Wind	ASMB	1	23	151	20	1.58	13	37	22.9	1.45	wind	1.0 m/s	0.98	ln	5.28
	Mar 11	Wind	ASMB	1	24	151	20	1.58	13	37	22	1.45	wind	1.0 m/s	0.972	ln	5.3
	Mar 12	Wind	ASMB	2	42	151	40	3.16	25	37	21.1	1.45	wind	1.0 m/s	0.99	ln	4.77
	Mar 14	Wind	ASMB	2	46	151	40	3.16	25	38	21.2	1.45	wind	1.0 m/s	0.993	ln	4.77
	Mar 16a	Wind	Water	0.5	3	151	20	1.32	1.9	91	21.8	1.45	wind	1.0 m/s	0.997	lin	0.592
	Mar 16b	Wind	Water	0.5	3	151	20	1.32	1	95	21.8	1.45	wind	1.0 m/s	0.997	lin	0.612
	Mar 16c	Wind	Water	0.5	3	151	40	2.65	18	55	21.8	1.45	wind	1.0 m/s	0.999	lin	0.34
	Mar 16d	Wind	ASMB	1	21	151	20	1.58	13	37	22.1	1.65	wind	1.6 m/s	0.981	ln	5.19
	Mar 17	Wind	ASMB	1	22	151	20	1.58	12	38	21.4	1.65	wind	1.6 m/s	0.949	ln	5.27
	Mar 18	Wind	ASMB	1	23	151	20	1.58	13	37	21.4	1.65	wind	1.6 m/s	0.996	ln	5.15
	Mar 19	Wind	ASMB	2	46	151	40	3.16	25	39	22.7	1.65	wind	1.6 m/s	0.986	ln	4.9
	Mar 21	Wind	ASMB	1	20	151	20	1.58	12	39	22.8	1.65	wind	1.6 m/s	0.977	ln	5.63
	Mar 22a	Wind	Water	0.5	1	151	20	1.32	4.6	77	21.7	1.65	wind	1.6 m/s	0.998	lin	0.512
	Mar 22b	Wind	ASMB	1	17	151	20	1.58	13	37	23.9	1.65	wind	1.6 m/s	0.978	ln	5.47
	Mar 23a	Wind	Water	0.5	3	151	20	1.32	2.7	87	22.2	1.65	wind	1.6 m/s	0.999	lin	0.515
	Mar 23b	Wind	Water	0.5	5	151	40	2.65	3.4	92	23.6	1.65	wind	1.6 m/s	0.989	lin	0.312
	Mar 23c	Wind	ASMB	1	22	151	20	1.58	12	39	24.3	1.65	wind	1.6 m/s	0.981	ln	5.54
	Mar 24a	Wind	Water	0.5	1	151	20	1.32	8.6	57	23.4	1.85	wind	2.1 m/s	0.998	lin	0.7
	Mar 24b	Wind	ASMB	2	44	151	40	3.16	25	37	23	1.85	wind	2.1 m/s	0.991	ln	4.85
	Mar 26	Wind	ASMB	1	6	151	20	1.58	14	32	21.7	1.85	wind	2.1 m/s	0.993	ln	5.78
	Mar 26b	Wind	ASMB	2	39	151	40	3.16	25	38	20.4	1.85	wind	2.1 m/s	0.993	ln	4.99
	Mar 28a	Wind	Water	0.5	2	151	20	1.32	4.5	78	21.8	1.85	wind	2.1 m/s	0.994	lin	0.603
	Mar 28b	Wind	Water	0.5	5	151	40	2.65	2.6	93	22.6	1.85	wind	2.1 m/s	0.998	lin	0.316
Mar 28c	Wind	ASMB	1	12	151	20	1.58	13	35	22.4	1.85	wind	2.1 m/s	0.993	ln	5.52	

Table 5.2 ctd.

## Experiments Conducted to Test Boundary Layer Regulation

Series	Date	Prime Purpose	Oil Type	Days Length	Total Time (hr)	Fan (cm <sup>2</sup> ) Area	Initial Loading (g)	Initial (mm) Thickness	End Wt.	% Evap	Temp C	Wind m/s	Variable	Variable Value	R <sup>2</sup> Equation	Best Equation	Best Parameter	Single
	Mar 29	Wind	FCC-heavy	1	32	151	40	2.92	30	26	21.7	1.85	wind	2.1 m/s	0.987	sq. rt.	0.557	
	Mar 30a	Wind	Gasoline	0.5	1	151	20	1.87	4.5	78	22.6	1.85	wind	2.1 m/s	0.983	ln	18.2	
	Mar 30b	Wind	Gasoline	0.5	2	151	40	3.74	9.4	77	22.4	1.85	wind	2.1 m/s	0.975	ln	15.4	
	Mar 30c	Wind	FCC-heavy	1	22	151	20	1.46	14	30	22.3	1.85	wind	2.1 m/s	0.996	sq. rt.	0.8	
	Mar 31	Wind	ASMB	1	21	151	20	1.58	12	39	23.4	3.8	wind	2.5 m/s	0.981	ln	5.82	
	April 1a	Wind	Water	0.5	1	151	20	1.32	6.6	67	22.4	3.8	wind	2.5 m/s	0.997	ln	1.02	
	April 1b	Wind	Water	0.5	2	151	40	2.65	20	50	22.2	3.8	wind	2.5 m/s	0.999	ln	0.56	
	April 1c	Wind	Gasoline	0.5	0	151	20	1.87	5.9	70	22.2	3.8	wind	2.5 m/s	0.984	ln	21.6	
	April 1d	Wind	Gasoline	0.5	1	151	40	3.74	14	64	21.9	3.8	wind	2.5 m/s	0.994	ln	16.6	
	April 2a	Wind	Water	0.5	3	151	20	1.32	13	38	21.7	0	wind	0	0.999	ln	0.186	
	April 2b	Wind	FCC-heavy	2	47	151	40	2.92	23	41	21.4	3.8	wind	2.5 m/s	0.994	sq. rt.	0.785	
	April 4	Wind	FCC-heavy	2	39	151	20	1.46	9.3	54	22	3.8	wind	2.5 m/s	0.997	sq. rt.	1.13	
	April 6	Wind	ASMB	2	34	151	20	1.58	12	40	22.5	3.8	wind	2.5 m/s	0.993	ln	5.52	
	April 7	Wind	ASMB	1	18	151	40	3.16	26	36	21	3.8	wind	2.5 m/s	0.997	ln	5.21	
	April 8a	Wind	Water	0.5	1	151	20	1.32	4.9	75	22	3.8	wind	2.5 m/s	0.986	ln	1.04	
	April 8b	Wind	Water	0.5	2	151	40	2.65	12	70	22.9	3.8	wind	2.5 m/s	0.994	ln	0.602	
	April 8c	Wind	FCC-heavy	1	19	151	20	1.46	14	31	23	3.8	wind	2.5 m/s	0.992	sq. rt.	0.905	
	April 9a	Wind	Gasoline	0.5	1	151	20	1.87	4.6	77	22.1	1.65	wind	1.6 m/s	0.996	ln	19.7	
	April 9b	Wind	Gasoline	0.5	3	151	40	3.74	6.8	83	22.4	1.65	wind	1.6 m/s	0.983	ln	16.6	
	April 9c	Wind	FCC-heavy	2	40	151	40	2.92	27	33	22.3	1.65	wind	1.6 m/s	0.997	sq. rt.	0.669	
	April 11a	Wind	Gasoline	0.5	1	151	20	1.87	4.8	76	21.8	1.45	wind	1.0 m/s	0.992	ln	19.5	
	April 11b	Wind	Gasoline	0.5	2	151	40	3.74	9.2	77	22.1	1.45	wind	1.0 m/s	0.973	ln	16	
	April 11c	Wind	FCC-heavy	1	21	151	20	1.46	14	31	23.1	1.45	wind	1.0 m/s	0.99	sq. rt.	0.887	
	April 12	Wind	FCC-heavy	2	51	151	40	2.92	25	36	24.2	1.45	wind	1.0 m/s	0.996	sq. rt.	0.66	
	April 14	Wind	FCC-heavy	2	46	151	20	1.46	16	18	24	0	wind	0	0.986	sq. rt.	0.308	
	April 16a	Wind	Water	0.5	3	151	20	1.32	14	29	23.9	0	wind	0	0.999	ln	0.179	
	April 16b	Wind	FCC-heavy	4	87	151	40	2.92	33	17	23.9	0	wind	0	0.996	ln	0.216	
	April 20a	Wind	Water	0.5	8	151	40	2.65	23	41	25	0	wind	0	0.999	ln	0.088	
	April 20b	Wind	Water	1	16	151	40	2.65	11	72	25.1	0	wind	0	0.998	ln	0.0778	
	April 21a	Wind	Gasoline	0.5	7	151	20	1.87	4.8	76	22.5	0	wind	0	0.92	ln	8.55	
	April 21b	Wind	Gasoline	1	17	151	40	3.74	8.2	80	22.5	0	wind	0	0.944	ln	9.43	
	April 22a	Wind	Water	0.5	6	151	20	1.32	7.6	62	23	0	wind	0	0.99	ln	0.178	
10	Sept 22a	Pure compd.	Benzene	0.5	2	151	20	1.51	3.5	83	23.9	0	rate	0.999	ln	0.689		
	Sept 22b	Pure compd.	Dodecane	2	45	151	20	1.77	16	18	23.3	0	rate	0.999	ln	0.0068		
	Sept 24	Pure compd.	Undecane	2	46	151	20	1.79	9.4	53	24.3	0	rate	0.999	ln	0.0193		
	Sept 26a	Pure compd.	p-Xylene	0.5	7	151	20	1.54	7.3	63	24	0	rate	0.989	ln	0.161		
	Sept 26b	Pure compd.	Nonane	1	11	151	20	1.83	3.9	80	24	0	rate	0.999	ln	0.117		
	Sept 27	Pure compd.	Decane	1	19	151	20	1.81	9.3	54	22.3	0	rate	0.998	ln	0.0498		
	Sept 28a	Pure compd.	Heptane	0.5	3	151	20	1.94	8.3	59	18.5	0	rate	0.999	ln	0.326		
	Sept 28b	Pure compd.	Octane	0.5	3	151	20	1.88	13	36	20.4	0	rate	0.997	ln	0.221		
	Sept 28c	Pure compd.	Decahydronap	1	18	151	20	1.48	13	36	21	0	rate	0.996	ln	0.0351		
	Oct 6	Pure compd.	Tridecane	1	23	151	20.36	1.79	20	2	21.1	0	rate	0.986	ln	0.0014		
	Oct 8	Pure compd.	Hexadecane	7	167	151	20	1.71	20	1	15	0	rate	0.847	ln	0.25E-05		
11	Sept 29a	Pure compd. & w.	Heptane	0.5	0	151	20	1.94	3.7	81	16.4	1.45	rate	0.999	ln	2.82		
	Sept 29b	Pure compd. & w.	Octane	0.5	2	151	20	1.88	4.9	75	18.2	1.45	rate	0.991	ln	1.27		
	Sept 29c	Pure compd. & w.	Undecane	1	17	151	20.1	1.8	8.6	57	19.8	1.45	rate	0.998	ln	0.0586		
	Sept 30a	Pure compd. & w.	Nonane	0.5	3	151	20	1.83	2.3	89	20.2	1.45	rate	0.999	ln	0.545		
	Sept 30b	Pure compd. & w.	Decane	0.5	6	151	20.5	1.86	7	66	21.6	1.45	rate	0.999	ln	0.2		
	Sept 30c	Pure compd. & w.	Hexadecane	3	63	151	20.3	1.74	20	0	22.3	1.45	rate	-	ln	0		
	Oct 7	Pure compd. & w.	Tridecane	1	25	151	20	1.75	18	12	26.2	1.45	rate	0.986	ln	0.0078		
	Oct 17a	Pure compd. & w.	Benzene	0.5	0	151	21	1.58	2.8	87	17.1	1.45	rate	0.993	ln	3.68		
	Oct 17b	Pure compd. & w.	p-Xylene	0.5	2	151	23.25	1.79	2.3	90	17.2	1.45	rate	0.999	ln	0.756		
	Oct 17c	Pure compd. & w.	Dodecane	0.5	7	151	20	1.77	18	9	21.3	1.45	rate	0.988	ln	0.0245		
	Oct 17d	Pure compd. & w.	Decahydronap	0.5	14	151	20	1.48	1.2	94	20.1	1.45	rate	0.997	ln	0.122		
13	Oct 15	Doping	WAS - 34.5	2	40	151	20	1.58	20	2	18	0	rate	0.937	sq. rt.	0.0333		
	Oct 18	Doping	Heptane+WAS	0.5	8	151	20	1.58	17	17	17.9	0	rate	0.931	sq. rt.	0.841		
	Oct 18b	Doping	Dodecane+WAS	3	64	151	20	1.58	18	9	17.8	0	rate	0.972	sq. rt.	0.137		
	Oct 21	Doping	Nonane+WAS	1	27	151	20	1.58	16	19	20.3	0	rate	0.943	sq. rt.	0.535		
	Oct 22	Doping	Tridecane+WAS	3	77	151	20	1.58	19	7	21	0	rate	0.94	sq. rt.	0.083		
	Oct 26	Doping	Decane+WAS	1.5	34	151	14.93	1.18	12	20	17.9	0	rate	0.974	sq. rt.	0.481		
	Oct 27	Doping	Undecane+WAS	3	70	151	20	1.58	16	18	16	0	rate	0.973	sq. rt.	0.251		
14	Oct 30	Dope&wind	Undecane+WAS	1.5	41	151	20	1.58	16	21	20	1	rate	0.996	sq. rt.	0.414		
	Nov 1	Dope&wind	Decane+WAS	1	24	151	20	1.58	16	21	22	1	rate	0.924	sq. rt.	0.597		
	Nov 2	Dope&wind	Dodecane+WAS	3	76	151	20	1.58	16	22	21	1	rate	0.979	sq. rt.	0.294		
	Nov 5	Dope&wind	Tridecane+WAS	5	125	151	20	1.58	16	18	23.9	1	rate	0.987	sq. rt.	0.2		
	Nov 10	Dope&wind	Nonane+WAS	1	18	151	20	1.58	16	20	21.2	1	rate	0.854	sq. rt.	0.72		
	Nov 11a	Dope&wind	Heptane+WAS	0.5	5	151	20	1.58	17	18	20.1	1	rate	0.746	sq. rt.	1.22		
	Nov 11b	Dope&wind	WAS - 34.5%	3	64	151	20	1.58	19	6	18.5	1	rate	0.923	sq. rt.	0.0967		

Table 5.3 Data from the Wind Tests

Date	Type	Loading grams	Curve Coefficients		Wind m/s	Date	Type	Loading grams	Curve Coefficients		Wind m/s
			% evap	Abs. Wt.					% evap	Abs. Wt.	
April 25	ASMB	20	4.22	0.844	0	Nov 22	FCC heavy	20	0.414	0.117	0
Mar 10	ASMB	20	5.28	1.06	1	April 11c	FCC heavy	20	0.887	0.178	1
Mar 11	ASMB	20	5.3	1.06	1	Mar 30c	FCC-heavy	20	0.8	0.161	2.1
Mar 16d	ASMB	20	5.19	1.04	1.6	April 4	FCC-heavy	20	1.13	0.225	2.5
Mar 17	ASMB	20	5.27	1.05	1.6	April 8c	FCC-heavy	20	0.905	0.181	2.5
Mar 18	ASMB	20	5.15	1.03	1.6						
Mar 21	ASMB	20	5.63	1.13	1.6	Nov 22	FCC heavy	20	0.414	0.2	0
Mar 22b	ASMB	20	5.47	1.09	1.6	April 12	FCC heavy	40	0.66	0.264	1
Mar 23c	ASMB	20	5.54	1.11	1.6	April 9c	FCC-heavy	40	0.669	0.268	1.6
Mar 26	ASMB	20	5.78	1.16	2.1	Mar 29	FCC-heavy	40	0.557	0.223	2.1
Mar 28c	ASMB	20	5.52	1.11	2.1	April 2b	FCC-heavy	40	0.785	0.314	2.5
Mar 31	ASMB	20	5.82	1.16	2.5						
April 6	ASMB	20	5.52	1.1	2.5	April 3a	Gasoline	20	12.2	3.36	0
						April 11a	Gasoline	20	19.5	3.9	1
Jul 20	ASMB	40	4.09	2	0	April 9a	Gasoline	20	19.7	3.93	1.6
Mar 12	ASMB	40	4.77	1.91	1	Mar 30a	Gasoline	20	18.2	3.64	2.1
Mar 14	ASMB	40	4.77	1.91	1	April 1c	Gasoline	20	21.6	4.32	2.5
Mar 19	ASMB	40	4.9	1.96	1.6						
Mar 24b	ASMB	40	4.85	1.94	2.1	April 3b	Gasoline	40	12.2	6	0
Mar 26b	ASMB	40	4.99	2	2.1	April 11b	Gasoline	40	16	6.4	1
April 7	ASMB	40	5.21	2.08	2.5	April 9b	Gasoline	40	16.6	6.65	1.6
						Mar 30b	Gasoline	40	15.4	6.15	2.1
April 2a	Water	20	0.186	0.0372	0	April 1d	Gasoline	40	16.6	6.64	2.5
April 16e	Water	20	0.179	0.0357	0						
April 22e	Water	20	0.178	0.0356	0	April 20a	Water	40	0.088	0.0354	0
Mar 16a	Water	20	0.592	0.118	1	April 20b	Water	40	0.0778	0.0311	0
Mar 16b	Water	20	0.612	0.112	1	Mar 16c	Water	40	0.34	0.136	1
Mar 22a	Water	20	0.512	0.102	1.6	Mar 23b	Water	40	0.312	0.137	1.6
Mar 23a	Water	20	0.515	0.103	1.6	Mar 28b	Water	40	0.316	0.127	2.1
Mar 24a	Water	20	0.7	0.14	2.1	April 1b	Water	40	0.56	0.224	2.5
Mar 28a	Water	20	0.603	0.12	2.1	April 8b	Water	40	0.602	0.241	2.5
April 1a	Water	20	1.02	0.206	2.5						
April 8a	Water	20	1.04	0.209	2.5						

Figure 5.1 **Correlation of Evaporation and Wind Velocity - ASMB Oil**

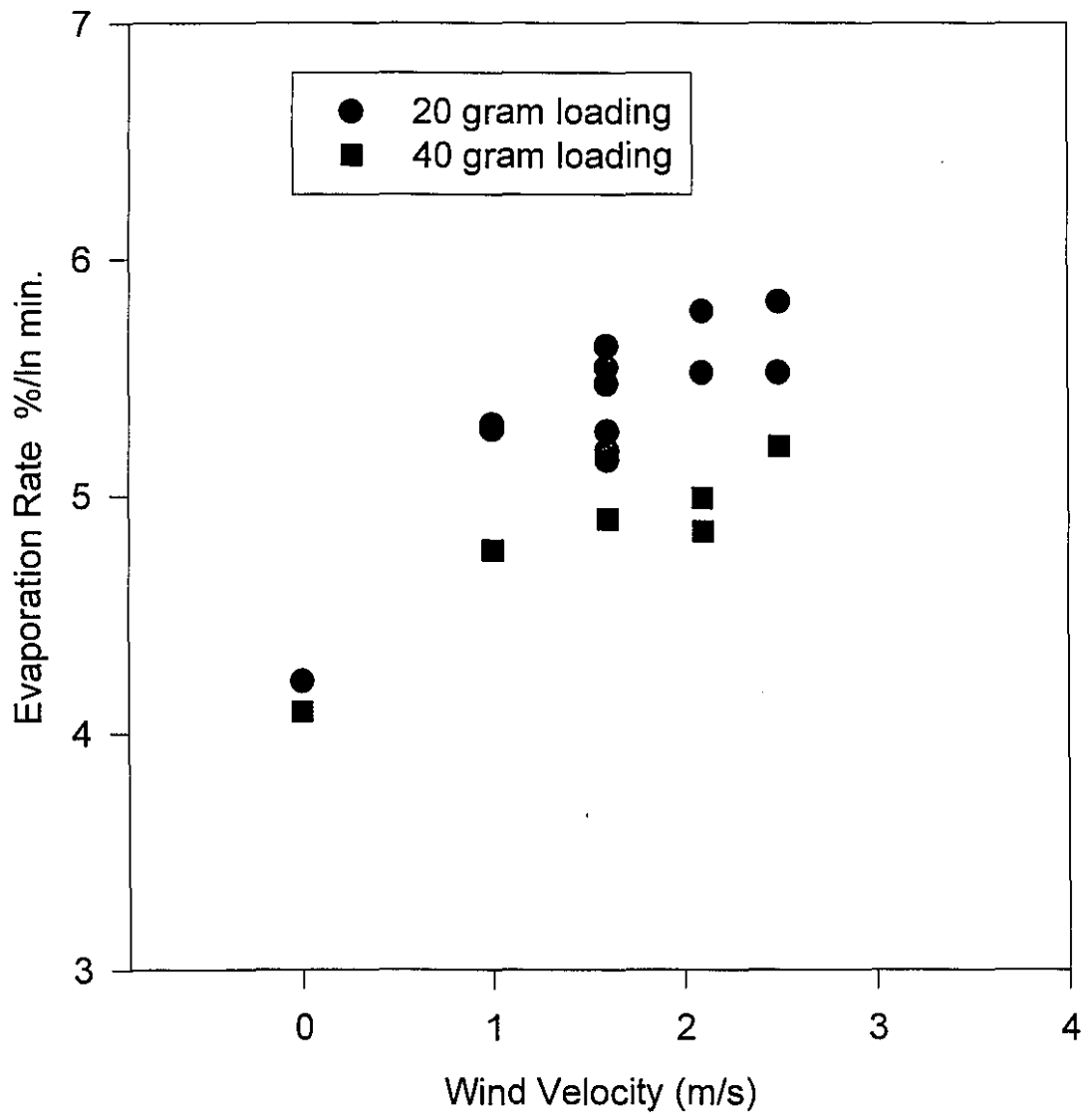


Figure 5.2

### Correlation of Evaporation and Wind Velocity - Gasoline

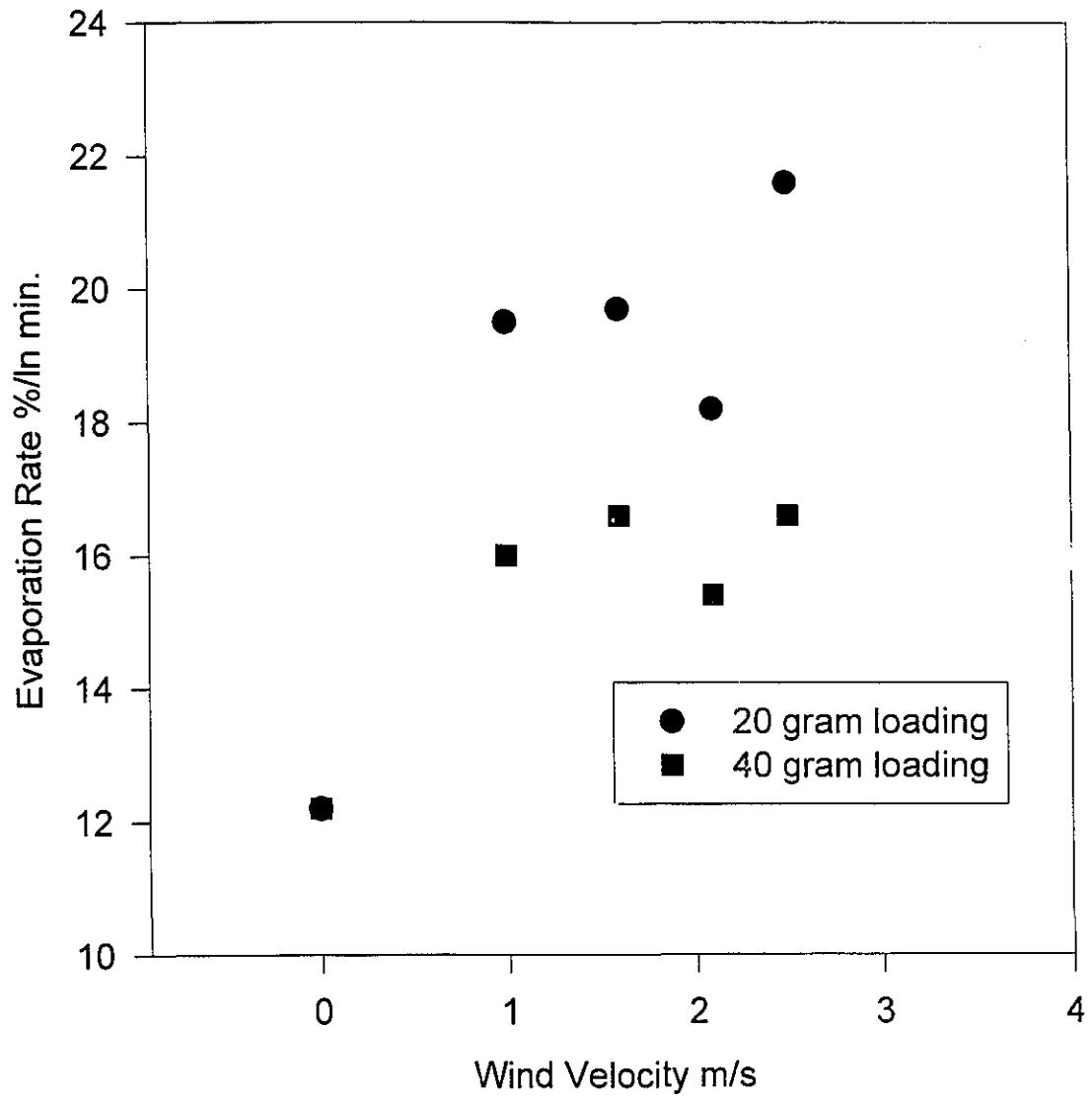


Figure 5.3

### Correlation of Evaporation and Wind Velocity - FCC Heavy

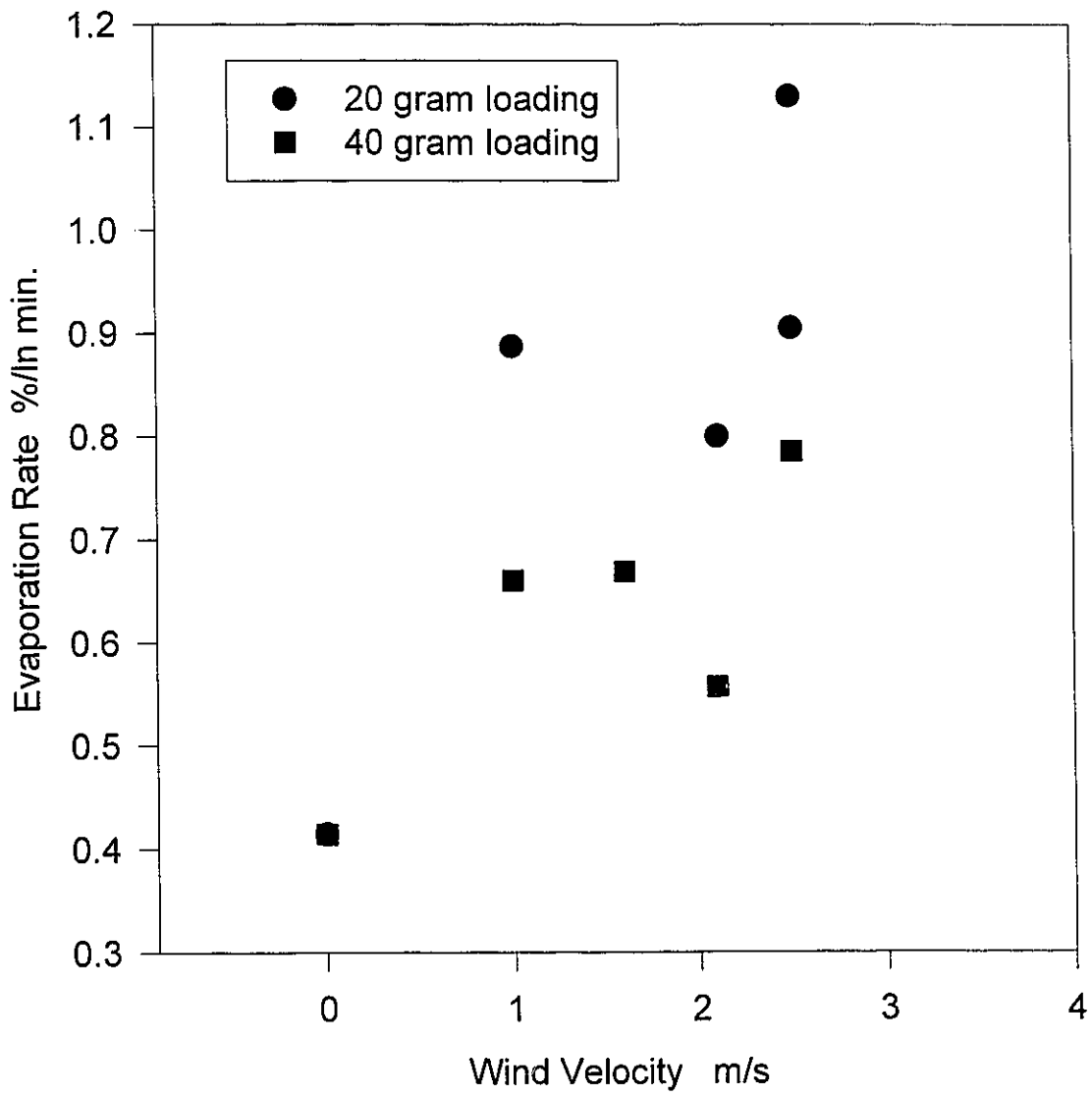


Figure 5.4

### Correlation of Evaporation and Wind Velocity - Water

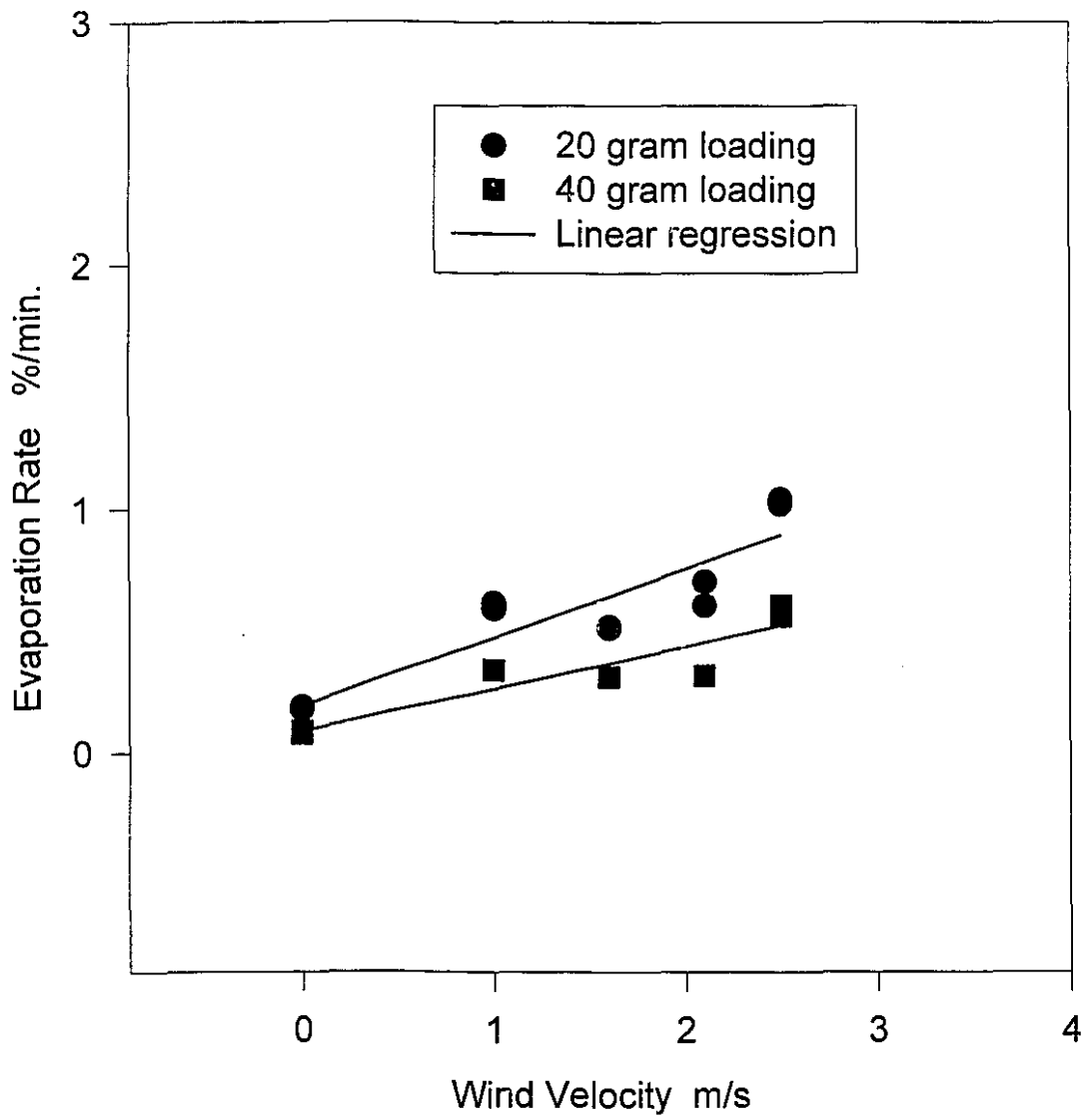


Figure 5.5

### Correlation of Evaporation and Wind Velocity - ASMB Oil - by Weight

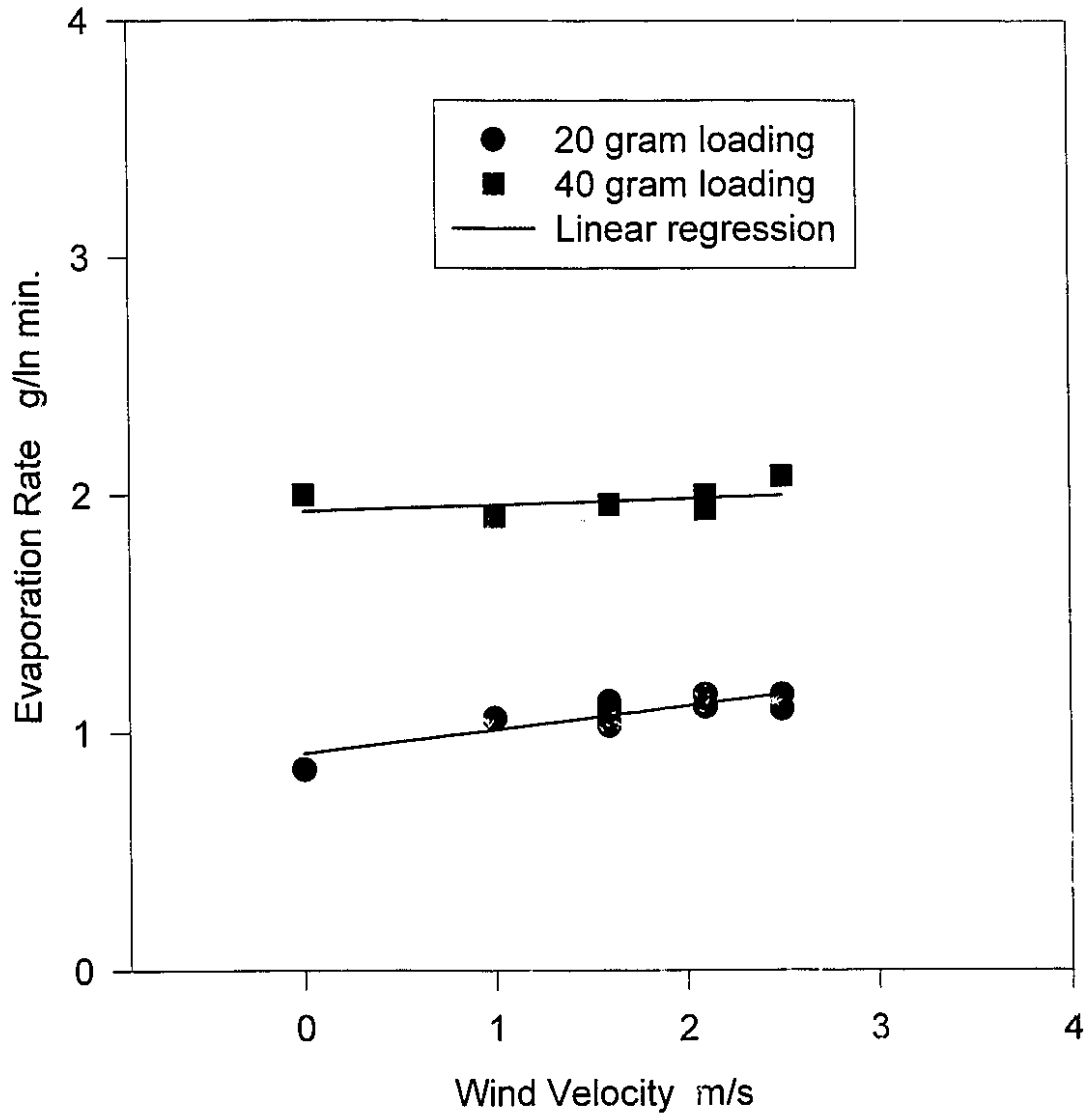


Figure 5.6

### Correlation of Evaporation and Wind Velocity - Gasoline - by Weight

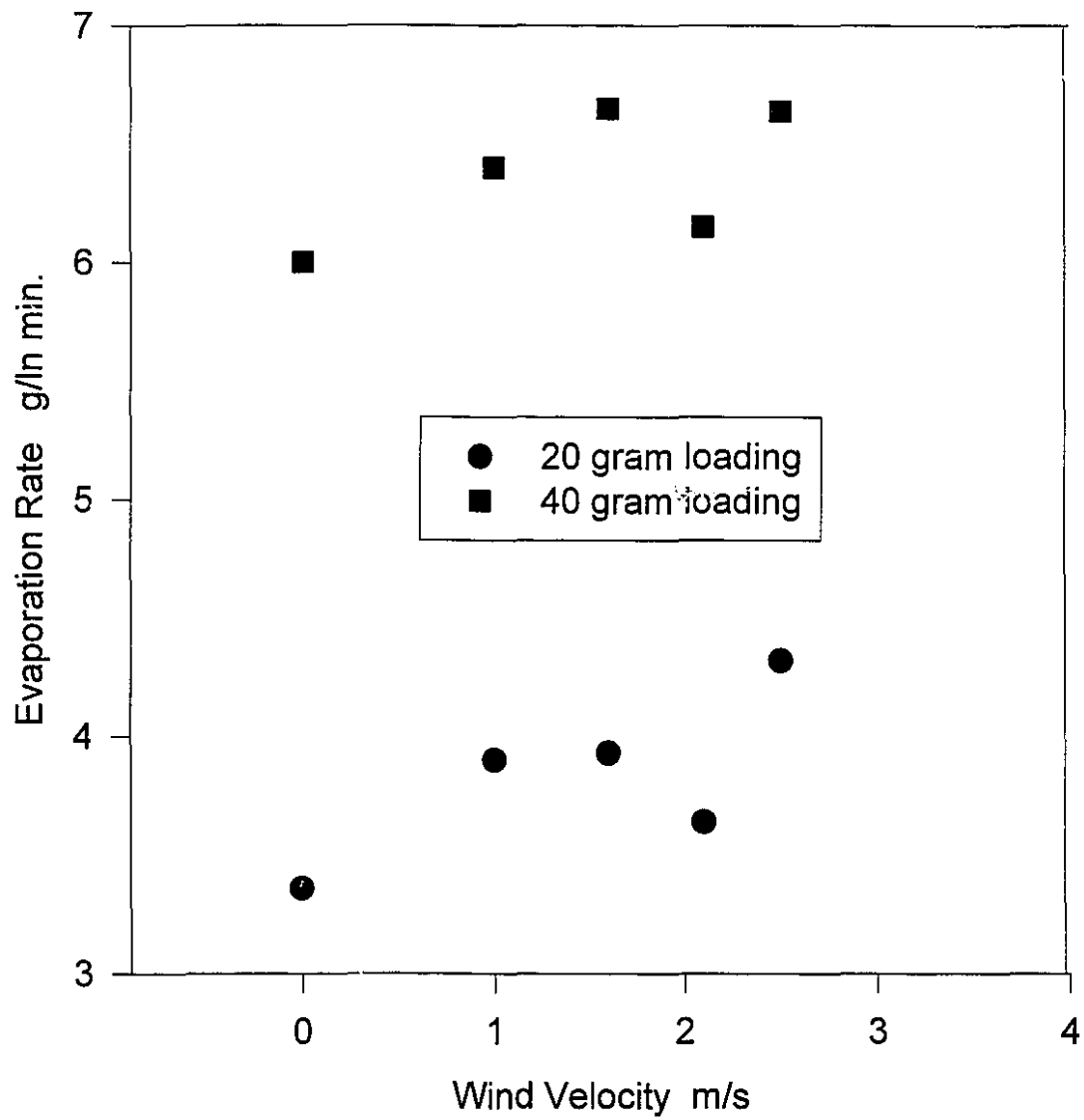


Figure 5.7

### Correlation of Evaporation and Wind Velocity - FCC Heavy - by Weight

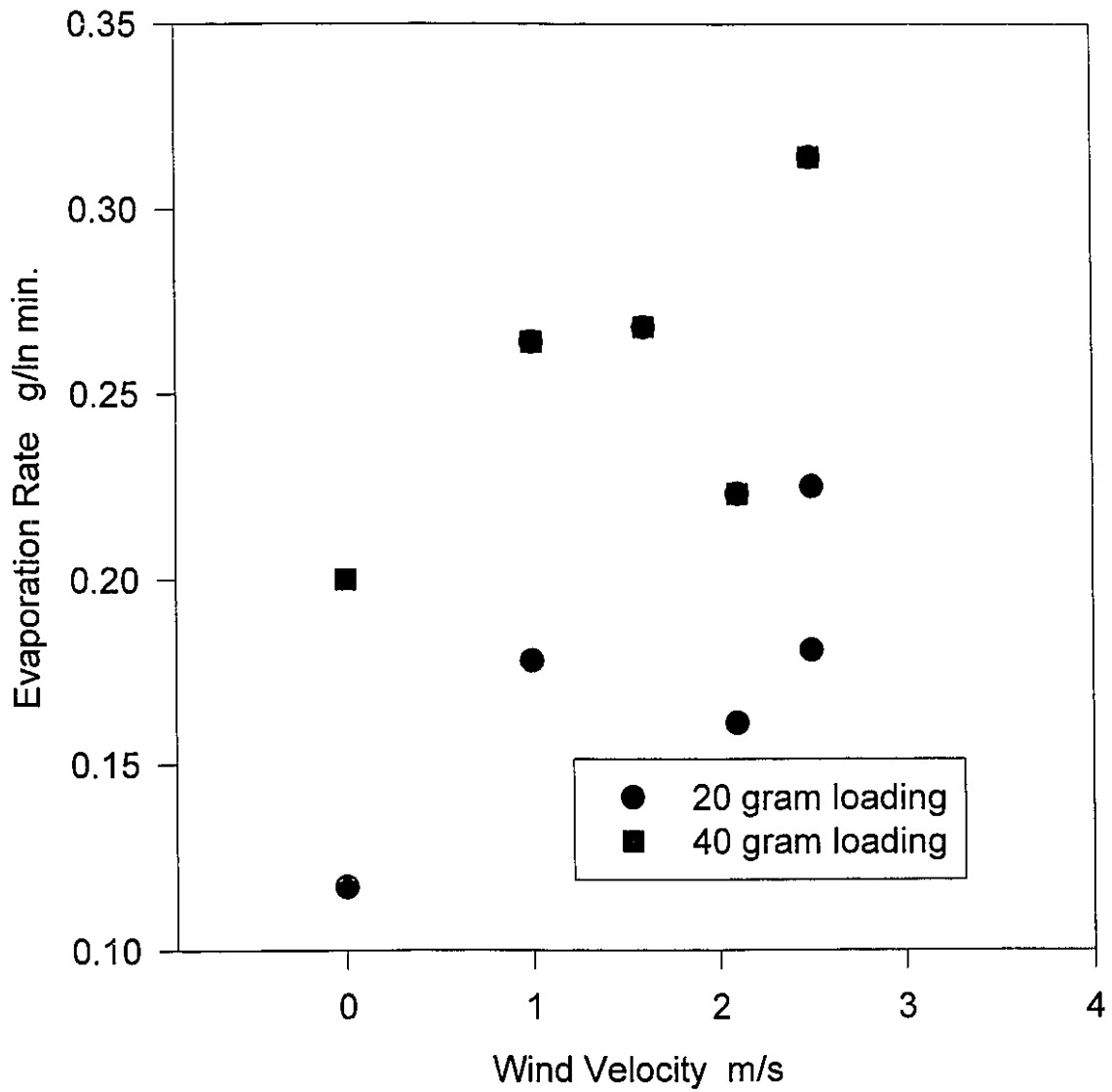


Figure 5.8

### Correlation of Evaporation and Wind Velocity - Water - by Weight

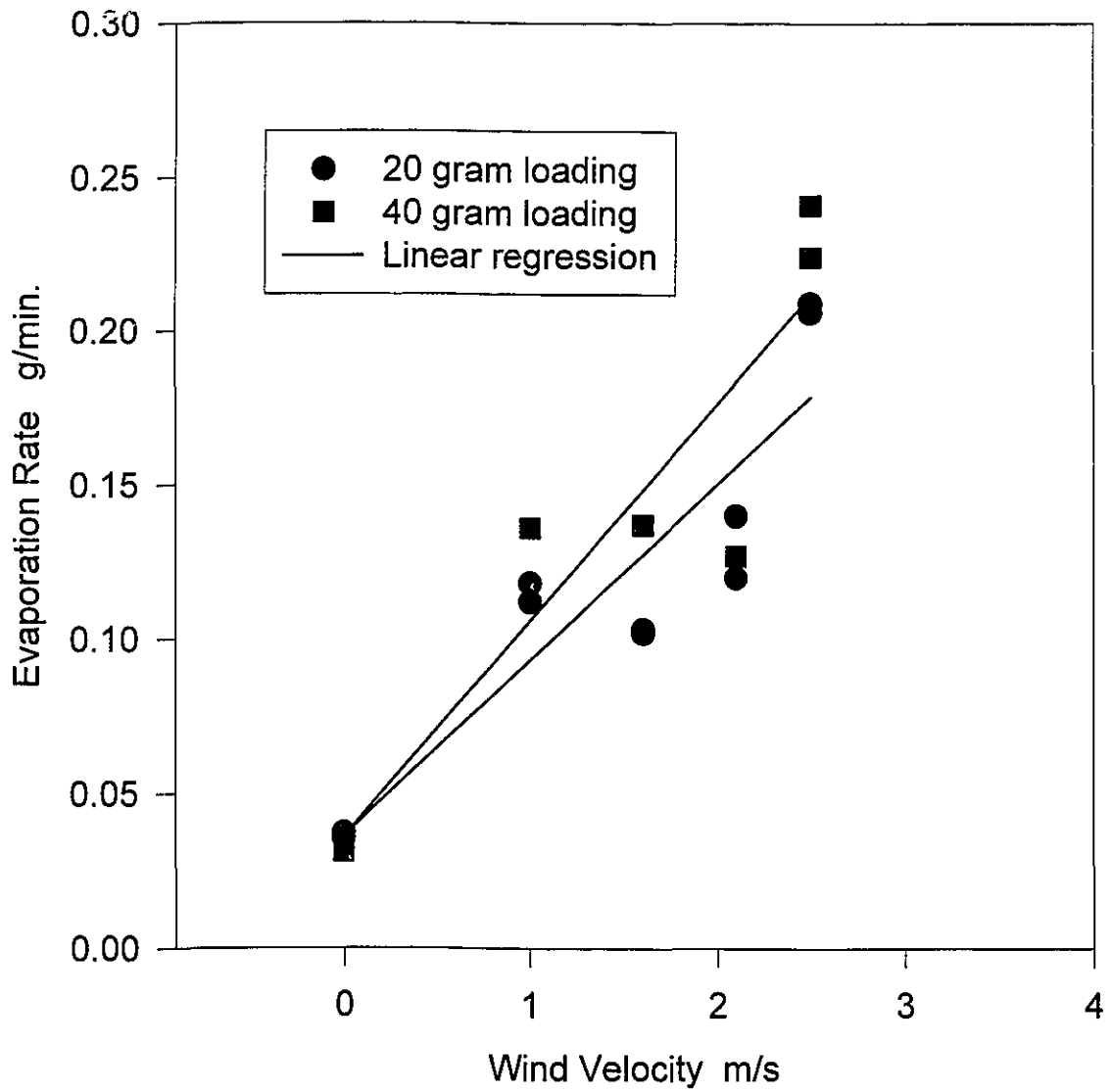


Figure 5.9

### Evaporation of ASMB with Varying Wind Velocities

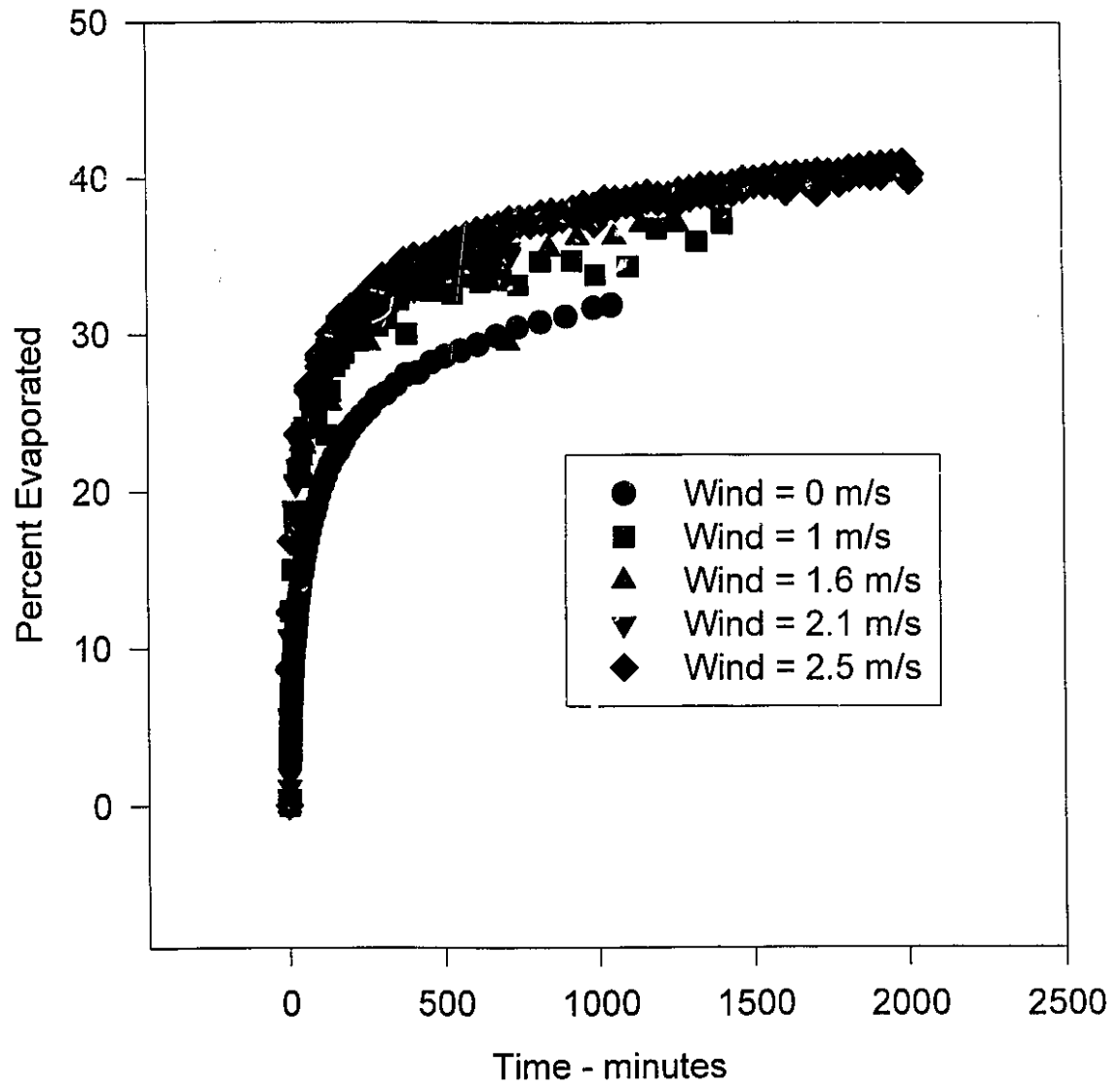


Figure 5.10

### Evaporation of FCC-Heavy with Varying Wind Velocities

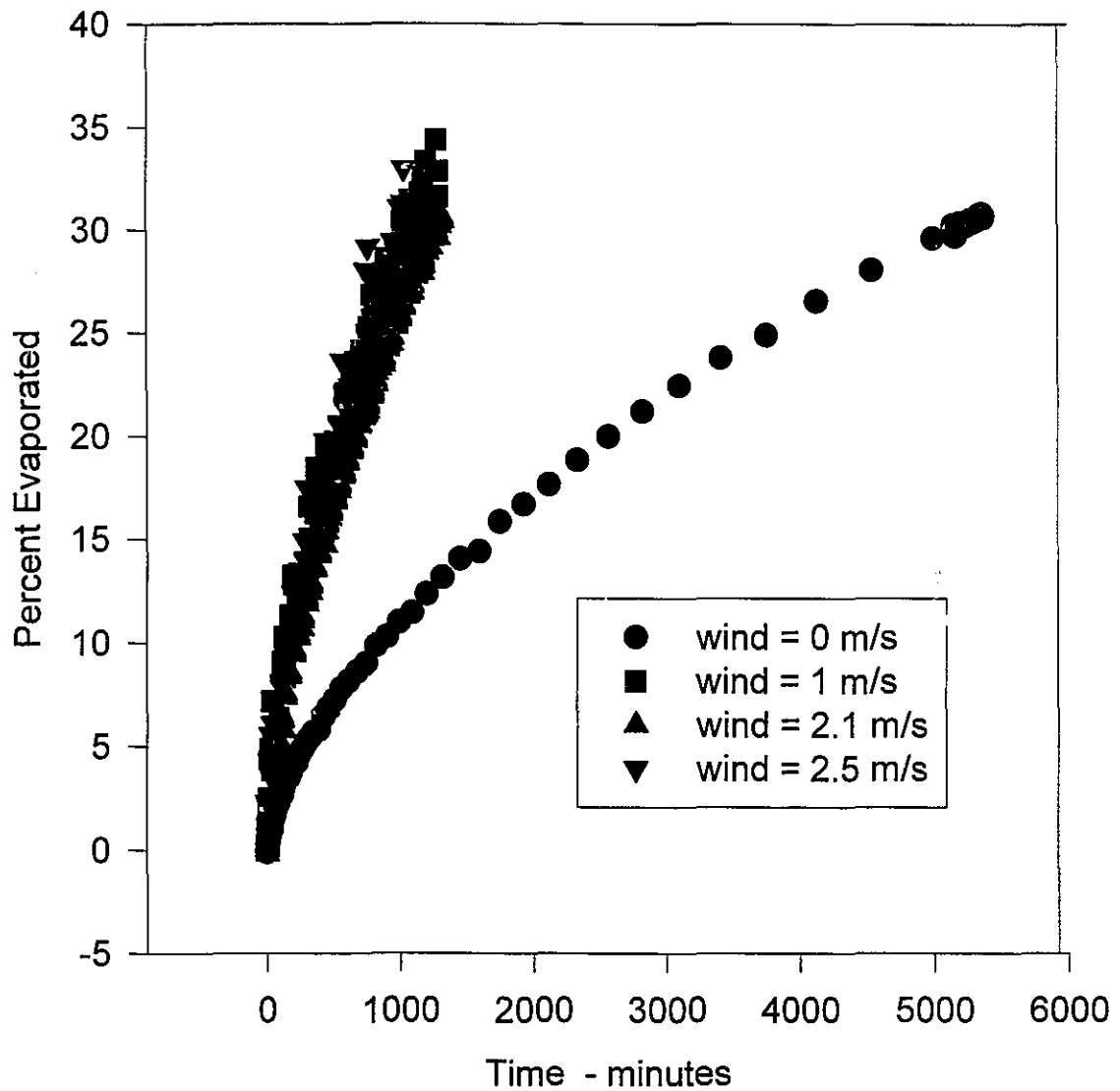


Figure 5.11

### Evaporation of Gasoline with Varying Wind Velocities

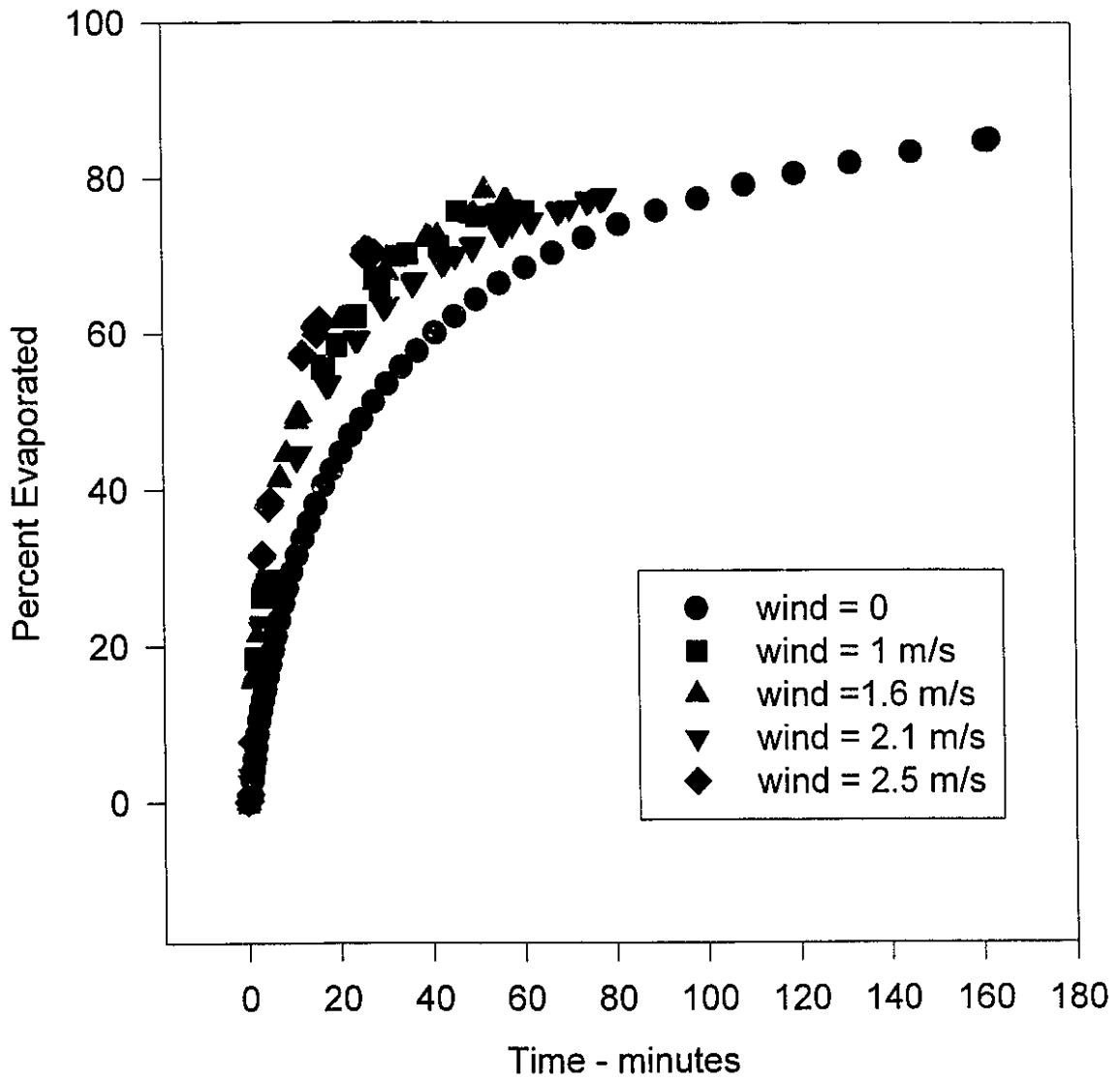


Figure 5.12

### Evaporation of Water (20g) with Varying Wind Velocities

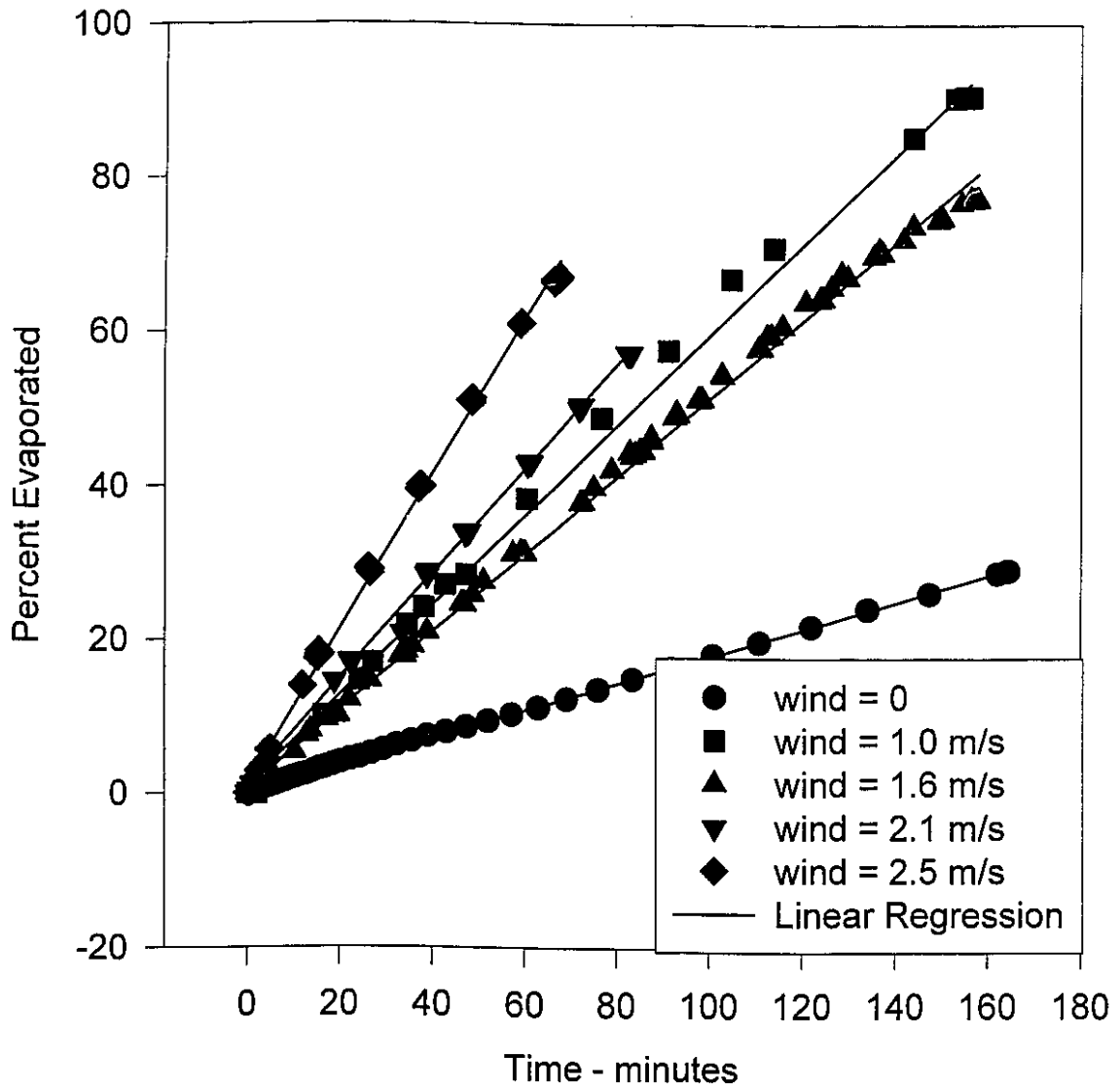
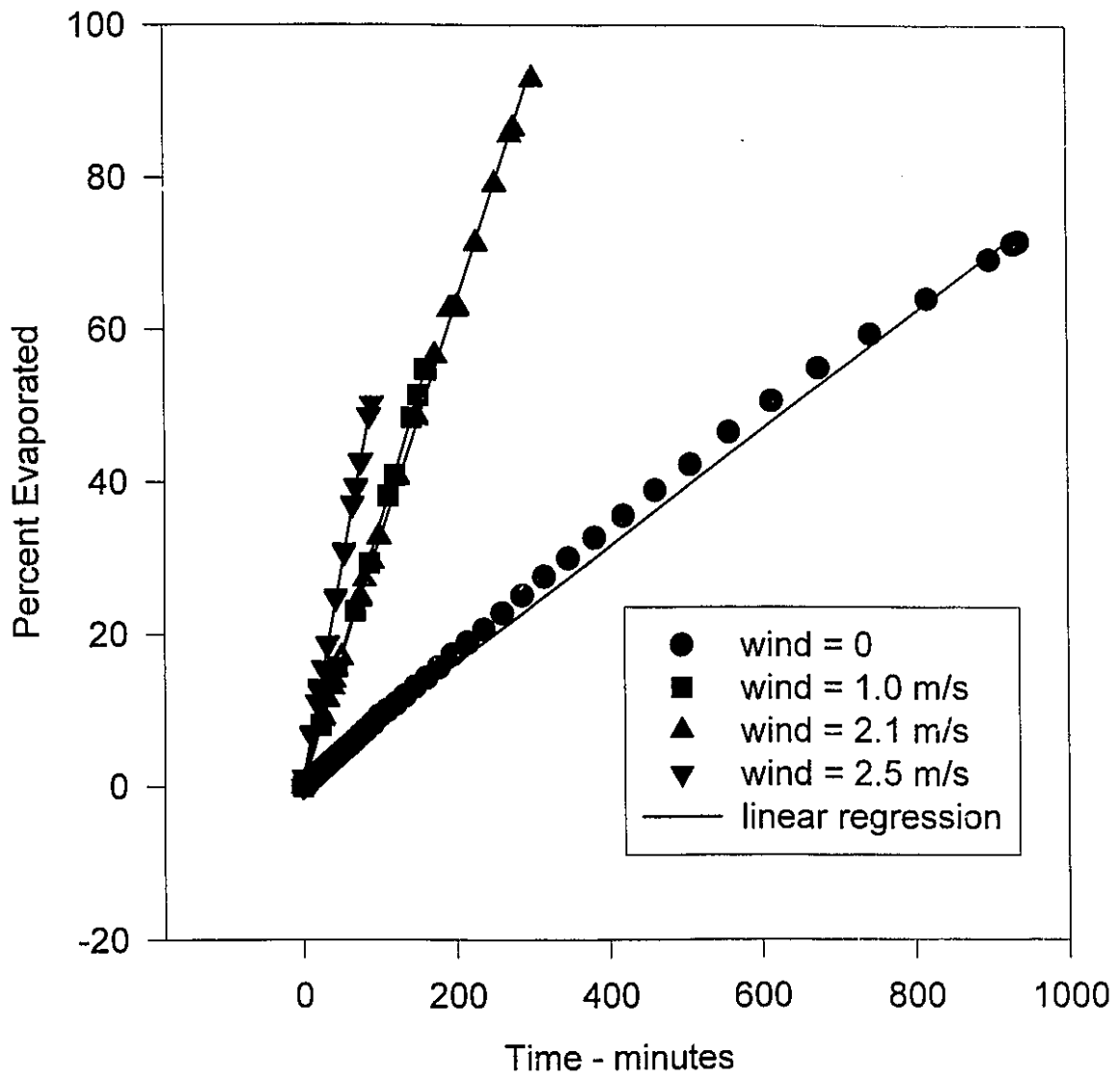


Figure 5.13

### Evaporation of Water (40g) with Varying Wind Velocities



#### 4. Study of Volume and Evaporation Rate.

Alberta Sweet Mixed Blend oil was again used to conduct a series of experiments with volume as the major variant. Alternatively thickness and area were held constant to ensure that the strict relationship between these two variables did not affect the final regression results. Table 5.6 shows the data from these experiments and Figure 5.17 illustrates the relationship between evaporation rate and volume of evaporation material (also equivalent to mass of evaporating material). Figure 5.17 illustrates a strong correlation between oil mass (or volume) and evaporation rate. This also suggests no or little boundary-layer regulation. It also shows that any tendencies observed in the area and thickness tests described above, may have been due to volume/mass factors rather than area or thickness.

#### 5. Study of the Evaporation of Pure Hydrocarbons - With and Without Wind

A study of the evaporation rate of pure hydrocarbons was conducted to confirm the classic boundary-layer evaporation theory as applied to the hydrocarbon constituents of oils. These experiments confirm the evaporation behaviour of pure hydrocarbons and relate these to that of oil, to determine to what degree these are boundary-layer regulated. The evaporation rate data are shown in Table 5.7 and are illustrated in Figure 5.18. The latter figure shows that the evaporation rates of the pure hydrocarbons have a variable response to wind. Heptane (hydrocarbon number 7) shows a large difference between evaporation rate in wind and no wind conditions. Decane (carbon number 10) shows a lesser effect and Hexadecane (carbon number 16) shows a negligible difference between the two experimental conditions. This experiment shows the extent of boundary-regulation and the reason for the small degree of boundary-regulation in crude oils and petroleum products. Crude oil contains very little material with carbon numbers less than decane, often less than 3% of its composition (Wang and Fingas, 1994). Even the more volatile petroleum products, gasoline and diesel fuel only have limited amounts of material of size less than decane, and thus are also not strongly boundary-layer regulated.

Figure 5.14

### Correlation of Evaporation Rates and Wind Velocity

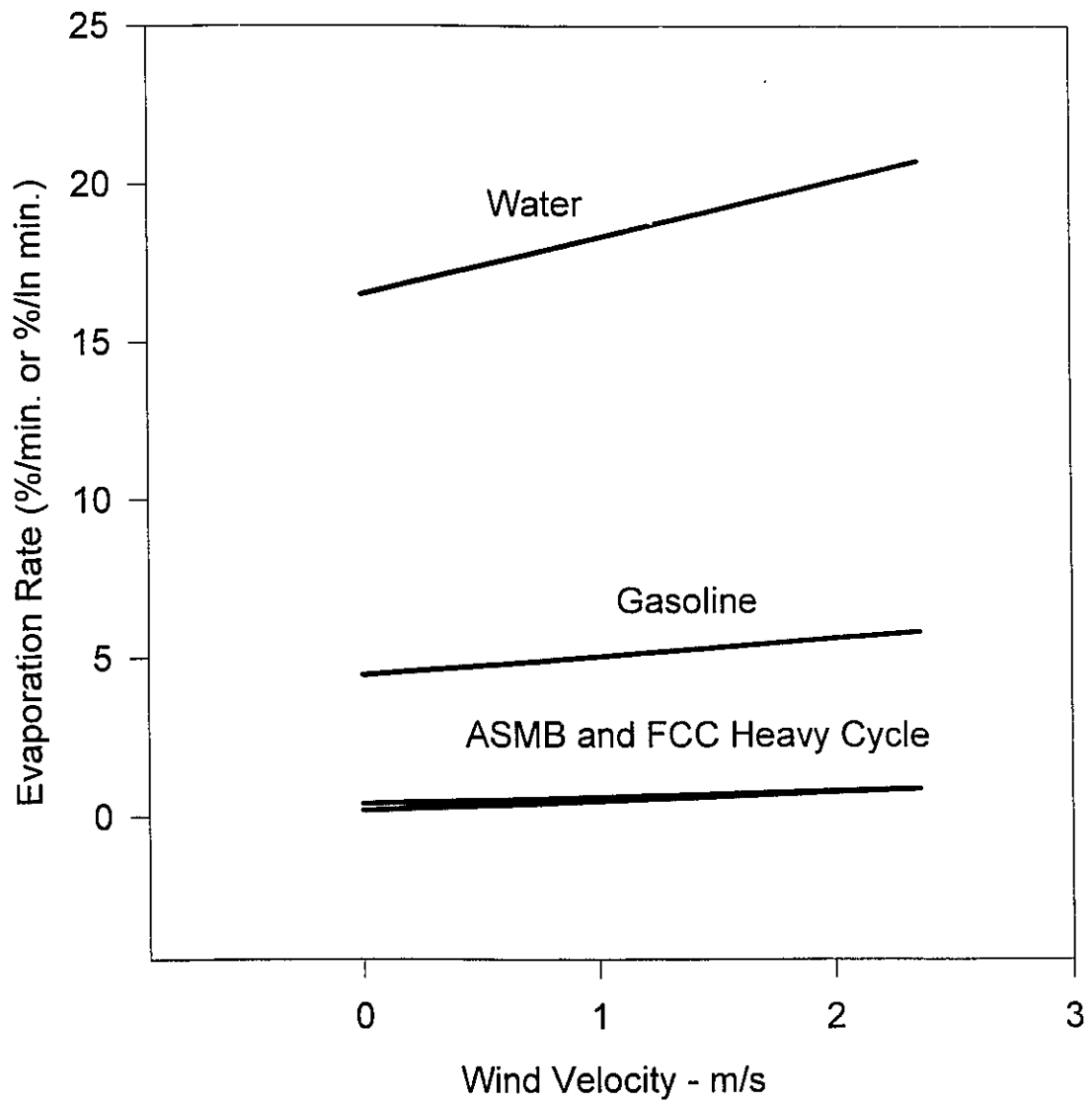


Table 5.4 Data from the Thickness Tests

Thickness (mm)	Equation Factor - %	Equation Factor - g	Thickness (mm)	Equation Factor - %	Equation Factor - g
0.79	5.23	0.0554	2.4	4.07	1.24
1.58	2.89	0.0612	2.54	4.78	1.52
3.72	3.67	0.183	2.67	3.84	1.3
7.45	2.95	0.295	2.69	4.45	1.52
0.79	4.57	0.188	2.8	4.27	1.52
1.58	4.35	0.356	2.84	3.81	1.37
1.92	3.77	0.377	2.93	4.02	1.49
3.84	3.52	0.703	2.96	3.65	1.37
0.59	5.16	0.379	2.99	3.74	1.42
0.63	5.18	0.409	3.17	3.85	1.55
0.63	4.95	0.398	3.17	3.85	1.55
0.65	5.35	0.435	3.21	3.95	1.61
0.72	4.76	0.776	4.55	4.09	2.36
1.33	4.73	0.799	5.21	3.56	2.35
1.39	5.26	0.916	5.27	4.27	2.84
1.43	5.7	1.03	6.29	3.32	2.65
1.45	4.54	0.829	7.61	3.86	3.72
1.53	4.66	0.9	9.08	3.07	3.54
1.54	4.37	0.85	9.89	3.08	3.86
1.59	4.05	0.818	0.74	4.06	0.406
1.62	4.28	0.898	0.79	4.07	0.436
1.69	4.28	0.912	1.48	3.98	0.796
1.71	4.16	0.901	1.58	3.66	0.783
1.78	4.36	0.982	2.22	4.7	1.41
1.96	4.49	1.11	3.7	3.16	1.58
1.96	5.58	1.59	1.3	4.43	1.31
1.98	4.16	1.04	0.79	5.27	0.72
2.14	4.26	1.16	1.58	3.63	1.03
2.15	4.23	1.15			

note: all runs conducted with ASMB oil  
at laboratory temperatures (~20°C)

g= grams or by weight  
%= percentage

Figure 5.15

### Correlation of Thickness With Evaporation Rate

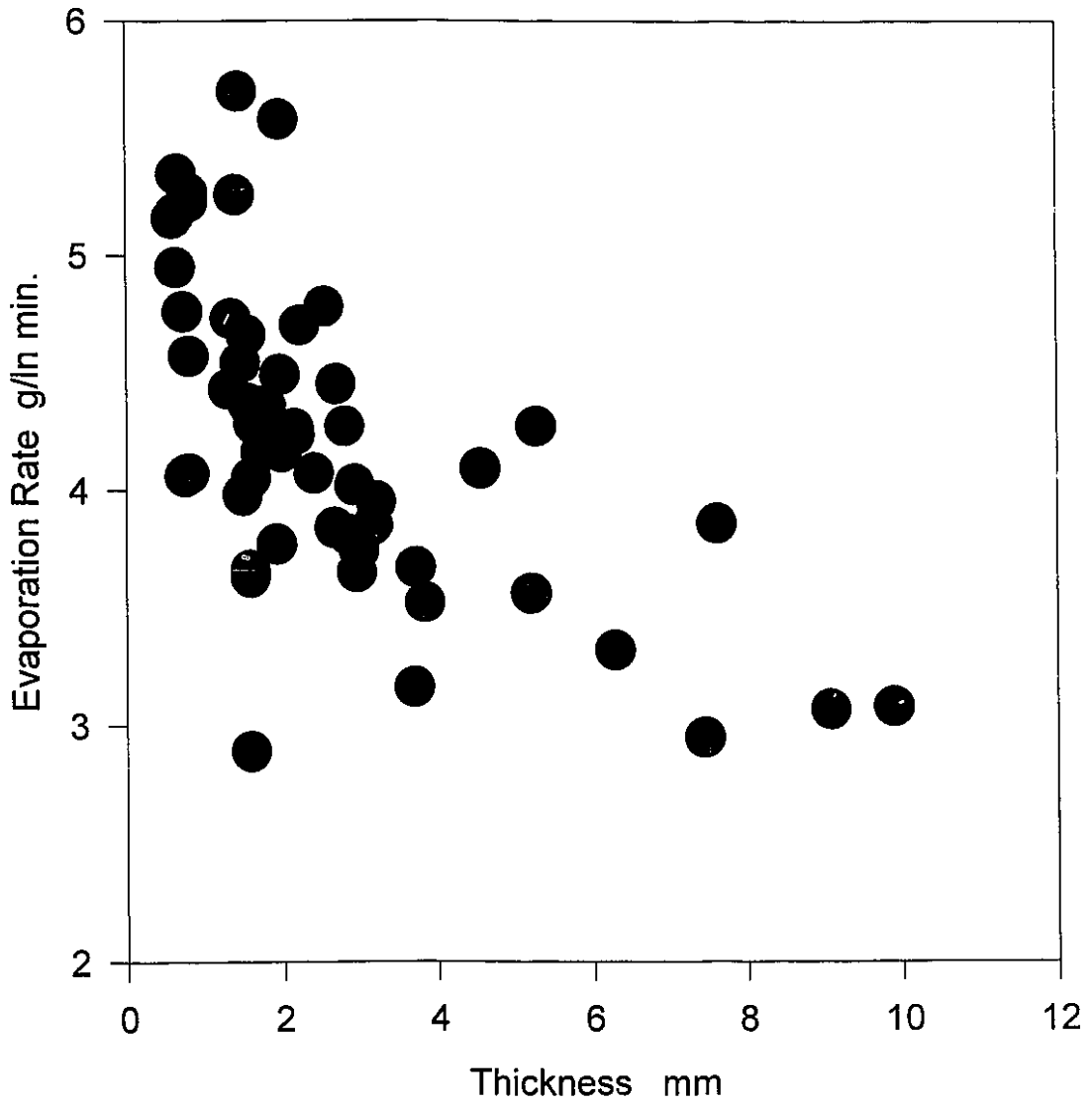


Table 5.5 Data from the Area Tests

Area (mm <sup>2</sup> )	Equation Factor - %	Equation Factor - g	Area (mm <sup>2</sup> )	Equation Factor - %	Equation Factor - g
16	5.23	0.0554	151	4.07	1.24
16	2.89	0.0612	151	4.78	1.52
16	3.67	0.183	151	3.84	1.3
16	2.95	0.295	151	4.45	1.52
62	4.57	0.188	151	4.27	1.52
62	4.35	0.356	151	3.81	1.37
62	3.77	0.377	151	4.02	1.49
62	3.52	0.703	151	3.65	1.37
151	5.16	0.379	151	3.74	1.42
151	5.18	0.409	151	3.85	1.55
151	4.95	0.398	151	3.85	1.55
151	5.35	0.435	151	3.95	1.61
151	4.76	0.776	151	4.09	2.36
151	4.73	0.799	151	3.56	2.35
151	5.26	0.916	151	4.27	2.84
151	5.7	1.03	151	3.32	2.65
151	4.54	0.829	151	3.86	3.72
151	4.66	0.9	151	3.07	3.54
151	4.37	0.85	151	3.08	3.86
151	4.05	0.818	161	4.06	0.406
151	4.28	0.898	161	4.07	0.436
151	4.28	0.912	161	3.98	0.796
151	4.16	0.901	161	3.66	0.783
151	4.36	0.982	161	4.7	1.41
151	4.49	1.11	161	3.16	1.58
151	5.58	1.59	185.5	4.43	1.31
151	4.16	1.04	206	5.27	0.72
151	4.26	1.16	206	3.63	1.03
151	4.23	1.15			

note: all runs conducted with ASMB oil  
at laboratory temperatures (~20°C)

g= grams or by weight  
%= percentage



Table 5.6 Data from the Volume/Mass Tests

Mass (g)	Equation Factor - %	Equation Factor - g	Mass (g)	Equation Factor - %	Equation Factor - g
1.06	5.23	0.0554	30.38	4.07	1.24
2.12	2.89	0.0612	32.2	4.78	1.52
5	3.67	0.183	33.87	3.84	1.3
10	2.95	0.295	34.1	4.45	1.52
4.1	4.57	0.188	35.44	4.27	1.52
8.2	4.35	0.356	35.98	3.81	1.37
10	3.77	0.377	37.15	4.02	1.49
20	3.52	0.703	37.52	3.65	1.37
7.43	5.16	0.379	37.92	3.74	1.42
7.92	5.18	0.409	40.21	3.85	1.55
8.04	4.95	0.398	40.21	3.85	1.55
8.18	5.35	0.435	40.67	3.95	1.61
16.29	4.76	0.776	57.67	4.09	2.36
16.87	4.73	0.799	66	3.56	2.35
17.56	5.26	0.916	66.82	4.27	2.84
18.06	5.7	1.03	79.69	3.32	2.65
18.32	4.54	0.829	96.41	3.86	3.72
19.35	4.66	0.9	115.03	3.07	3.54
19.46	4.37	0.85	125.3	3.08	3.86
20.16	4.05	0.818	10	4.06	0.406
20.48	4.28	0.898	10.7	4.07	0.436
21.47	4.28	0.912	20	3.98	0.796
21.67	4.16	0.901	21.4	3.66	0.783
22.52	4.36	0.982	30	4.7	1.41
24.8	4.49	1.11	50	3.16	1.58
24.82	5.58	1.59	29.49	4.43	1.31
25.07	4.16	1.04	13.65	5.27	0.72
27.15	4.26	1.16	27.3	3.63	1.03
27.26	4.23	1.15			

note: all runs conducted with ASMB oil  
at laboratory temperatures (~20°C)

g= grams or by weight  
%= percentage

Figure 5.17

### Correlation of Mass with Evaporation Rate

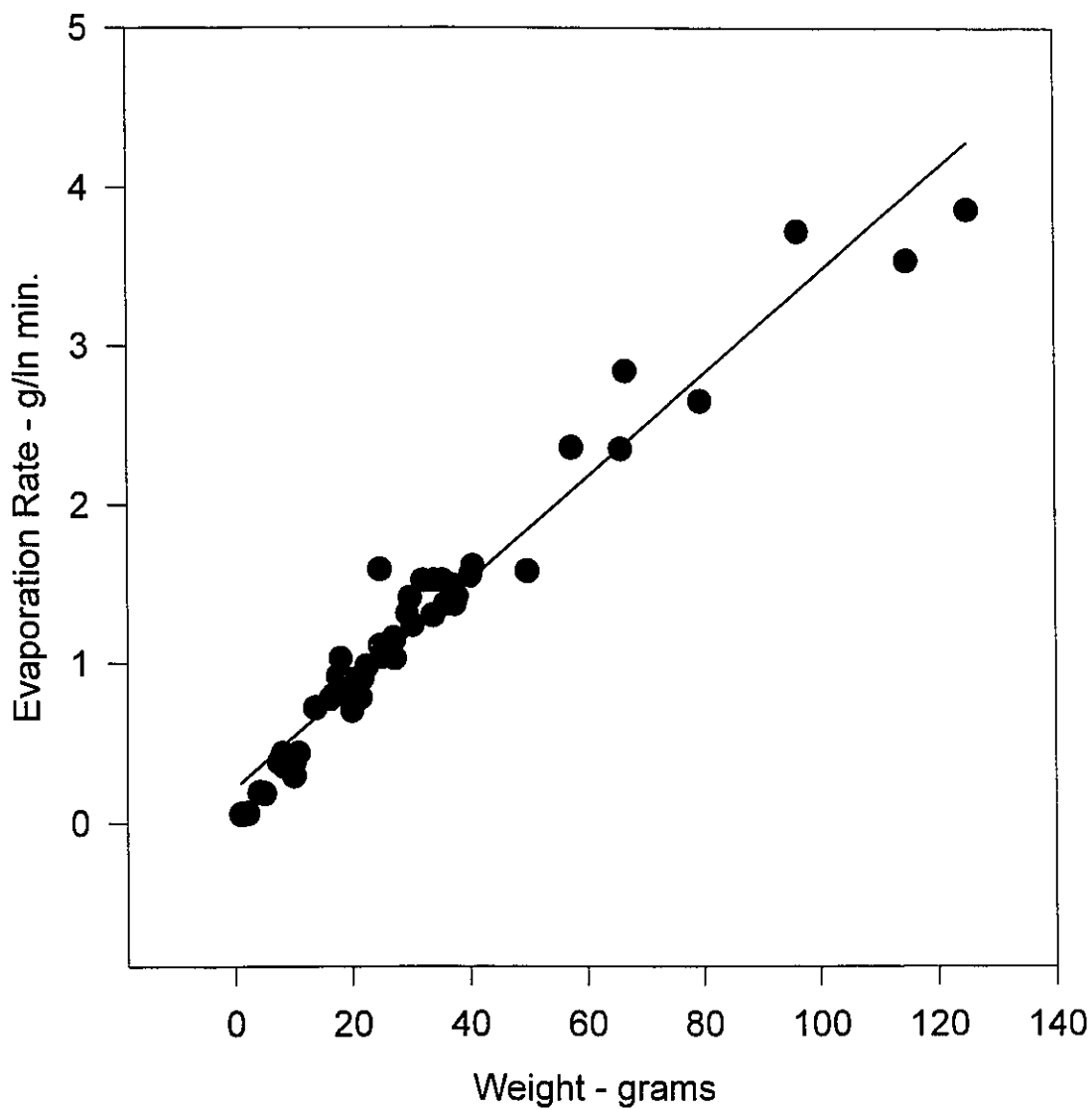


Table 5.7

**Data from the Evaporation Tests of Pure Hydrocarbons**

Hydrocarbon	Carbon Number	No Wind		Wind	
		Equation Factors Calculated by Regression			
		Wt. %	Abs. Wt.	Wt. %	Abs. Wt.
Heptane	7	0.326	0.0652	2.82	0.565
Octane	8	0.221	0.0448	1.27	0.262
Nonane	9	0.117	0.0234	0.545	0.109
Decane	10	0.0498	0.0097	0.2	0.041
Undecane	11	0.0193	0.00386	0.0586	0.0117
Dodecane	12	0.0068	0.0014	0.0245	0.00489
Tridecane	13	0.00136	0.00278	0.0078	0.00156
Hexadecane	16	0.000008	0.000002	0.000008	0.000002

Table 5.8

**Data From The Evaporation of Pure Hydrocarbons  
In A Weathered Oil Matrix**

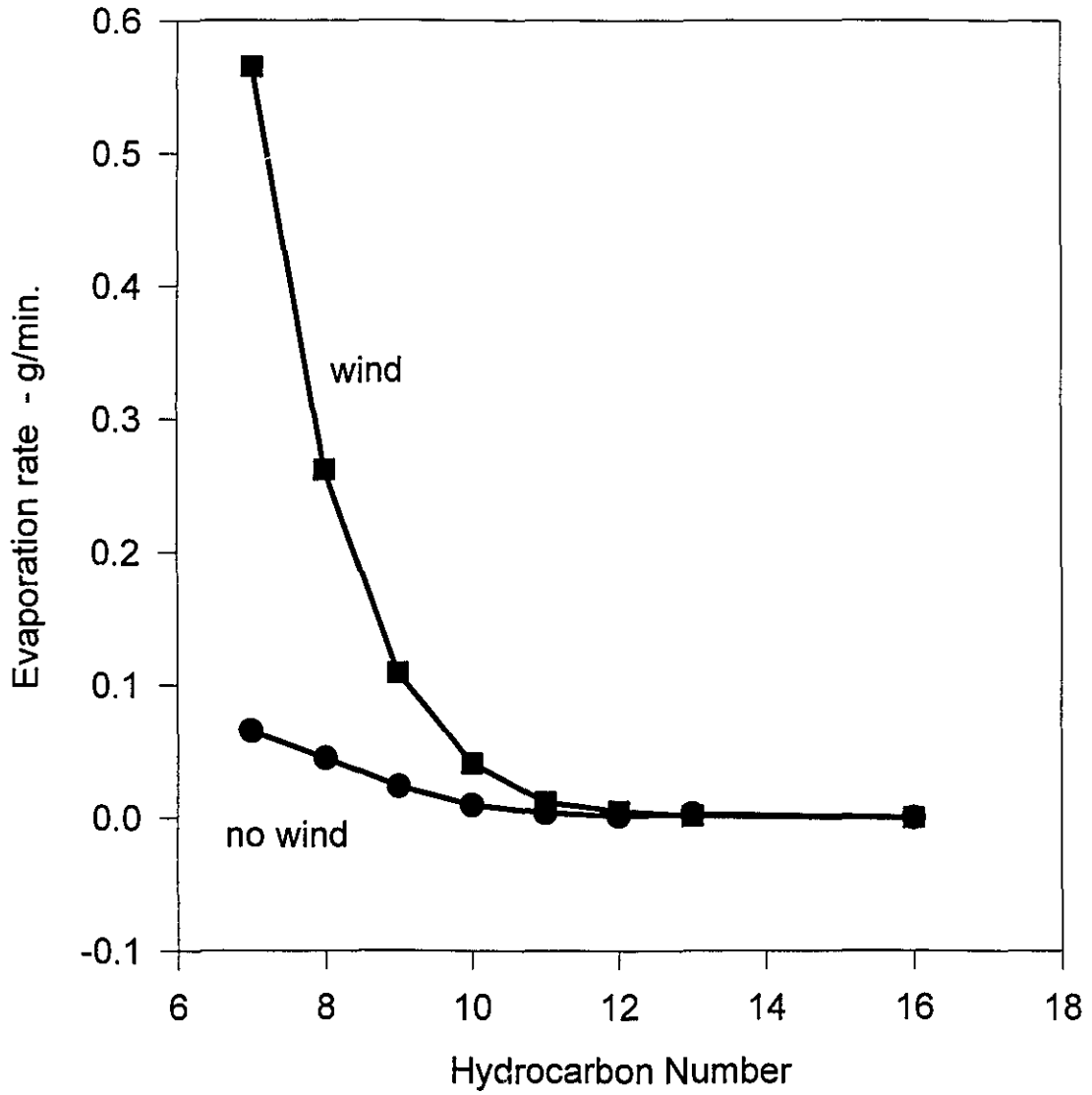
		No Wind		Wind	
Carbon Number	Equation Factors Calculated by Regression	Wt. %	Abs. Wt.	Wt. %	Abs. Wt.
		Heptane+WAS	7	0.841	0.168
Nonane+WAS	9	0.535	0.107	0.72	0.144
Decane+WAS	10	0.481	0.0718	0.597	0.119
Undecane+WAS	11	0.251	0.0502	0.414	0.0829
Dodecane+WAS	12	0.137	0.0276	0.294	0.0589
Tridecane+WAS	13	0.083	0.0166	0.2	0.0401
WAS - 34.5	16*	0.0333	0.00666	0.0967	0.0194

\*taken as the equivalent value

WAS is Weathered Alberta Sweet mixed blend oil

Figure 5.18

### Evaporation Rate of Pure Compounds



## 6. Study of the Evaporation of a Highly-Evaporated ASMB Residue, Combined with Pure Hydrocarbons - With and Without Wind.

A final set of experiments specifically designed to examine the boundary layer regulation of oils was conducted using a moderately-weathered Alberta Sweet Mixed Blend crude oil (34 % weathered by weight) and pure components. The experiment addresses the possibility of the regulation of oil evaporation by other components in the oil, a possibility suggested by several workers in the field (weathering regulation by components). This hypothesis is that certain components in oil form a film at the surface so that the evaporation of oil is regulated by a barrier that might be similar in effect to boundary regulation. This would mean that if the compounds evaporate at similar rates to those measured in the above experiment, the remaining mass of the oil does not affect the evaporation process. It would also imply that, at least for ASMB oil, the regulation by waxy or similar components is not a factor. The evaporation rate data was fit best by square root factors with time. This indicates, as noted in Chapter 4, that between 4 and 7 components are evaporating at once. The resulting data are listed in Table 5.8 and illustrated in Figure 5.19. A direct comparison of the evaporation rates is shown in Figure 5.20. It shows that the evaporation rates are not strongly affected by the oil matrix.

## 7. Other Data and Comparisons

An examination of specific evaporation rates of the products used in the previous experiments was performed. Data from the ASMB-20g loading experiments were taken for comparison. The instantaneous evaporation rate was calculated from the weight loss at each time point recorded. This rate, with units in g/min., changes constantly over the oil evaporation period. For those tests with wind higher than 1 m/s, the noise level increases because of the direct effect of the wind on the balance mechanism. As noted in the experimental section above, these data were recorded during periodic no-wind breaks. The instantaneous evaporation rates are inherently noisy. To calculate the instantaneous evaporation rate for these runs, 4 data points were averaged during the initial 15 minutes of the run and 14 data points thereafter. This then yields smoothed data that is

Figure 5.19

### Evaporation Rate of Pure Hydrocarbons in an Oil Matrix

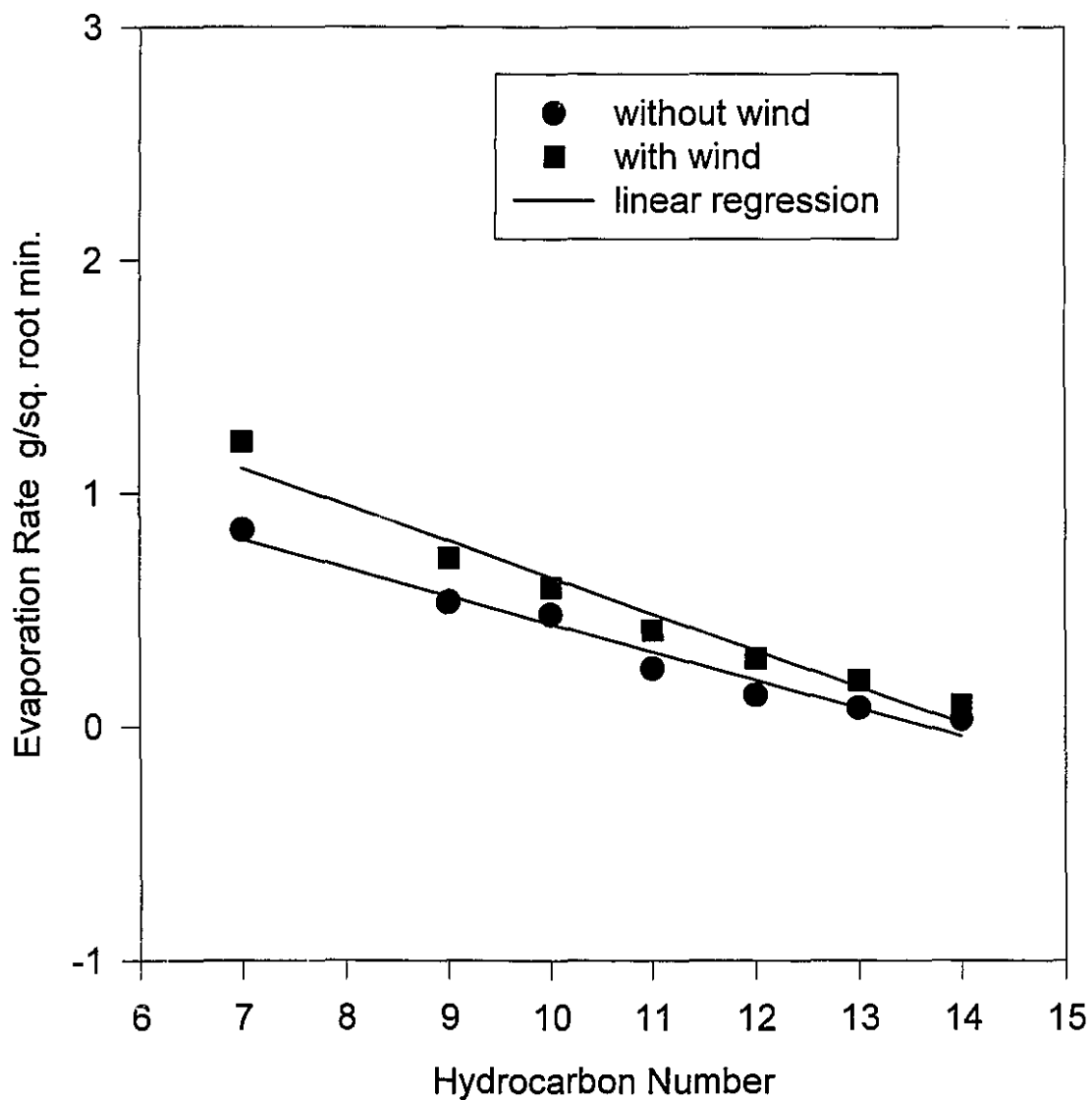
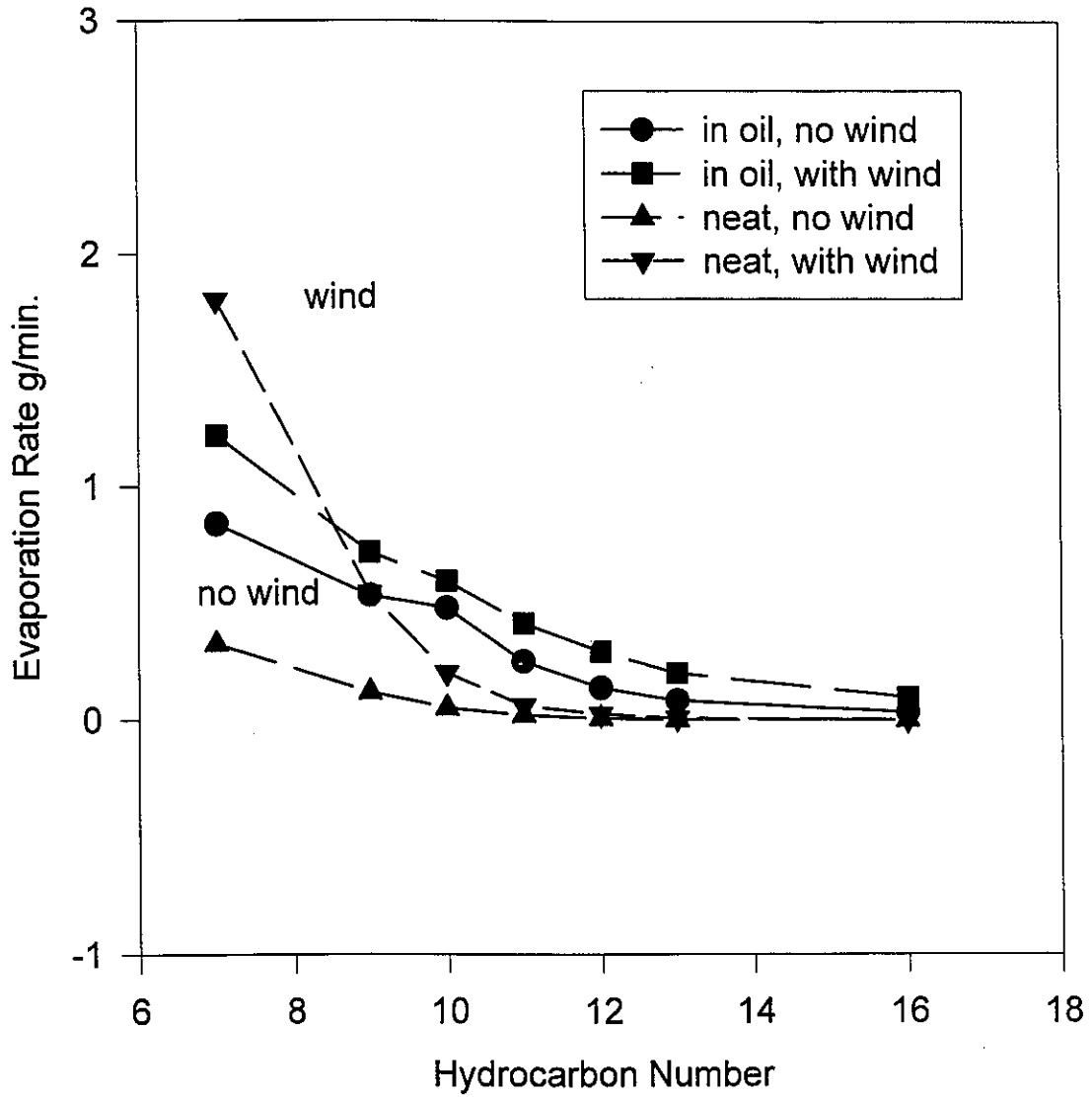


Figure 5.20

### Comparison of Evaporation Rates of Pure Hydrocarbons, Neat and in an Oil Matrix



representative of the actual evaporation. At 1 m/s wind this manipulation was not necessary, because the noise level of the data did not result in negative values. The data used for this portion of the study are given in Table 5.9, truncated to allow it to fit into one page. The full data set was, however, used to plot the data in the figures below. The maximum evaporation rate measured for each series is shown by the shaded value in Table 5.9 and the value of time and instantaneous evaporation rate after which no value is greater than 0.075 g/min is underlined. This value is of significance because it is the level after which boundary-layer regulation is insignificant; it is the evaporation rate of ASMB without wind. For the no wind situation, the evaporation rate attains the maximum value of 0.075 g/min at 2 minutes. This then is taken as the boundary-layer regulated maximum rate. At 1 m/s the value of 0.075 g/min. is not found beyond 6.2 minutes, for 1.6 m/s wind, not past 1.5 minutes and for the 2.1 m/s wind, not past 4.3 minutes. Thus it appears that ASMB oil is only boundary-layer regulated during the first 6 minutes of evaporation time. This would be the time during which the primary evaporative loss would come from components more volatile than decane, of which most light oils contain little and heavier oils, even less. In fact even gasoline, shows similar evaporative behaviour.

The instantaneous evaporation rates are illustrated in Figures 5.21 and 5.22. Figure 5.21 shows the plot of ASMB oil without wind. The evaporation rate at initial times is boundary-layer regulated for about 2 minutes, where the evaporation rate does not exceed 0.075. Figure 5.22 shows the composite evaporation rates for all four runs with varying winds from 0 to 2.1 m/s. This shows that all the rates of evaporation are below 0.075 m/s after about 5 minutes of evaporation.

A comparison of the maximum evaporation rates of ASMB oil, water, decane and heptane is shown in Figure 5.23. The figure shows that heptane has the highest evaporation rates and highest slopes. As noted above, heptane shows strong boundary-layer regulation. The maximum rates of ASMB evaporation are also shown and these show a rate below that of heptane. The water evaporation is then shown and then finally decane. This again reflects the fact that the high evaporation rates seen at the start of ASMB evaporation are in the range for boundary-layer regulation, whereas after the first

Table 5.9 Instantaneous Evaporation Rates of ASMB with Varying Winds

ASMB, Wind 0		ASMB, Wind 1		ASMB, Wind 1.6		ASMB, Wind 2.1	
Time	Rate, g/min	Time	Rate, g/min	Time	Rate, g/min	Time	Rate, g/min
0	0.05	0	0.146	0	0.213	0	0.137
2	0.075	6.2	0.115	0.2	0.515	0.2	0.288
2.2	0.062	12.2	0.031	0.4	0.311	0.4	0.425
2.4	0.033	19.1	0.015	0.6	0.311	0.6	0.474
2.6	0.042	20.5	0	1.5	0.286	0.8	0.399
3.1	0.05	31.7	0.037	1.8	0.008	1	0.318
3.4	0.054	35.8	0.026	7.7	0.087	1.8	0.26
4	0.046	43.7	0.017	8.7	0.041	1.9	0.112
4.4	0.047	52.2	0.013	10.2	0.036	4.3	0.128
5.2	0.052	71	0	15.8	0.035	4.4	0.069
5.7	0.042	92.5	0	18.5	0.035	18	0.01
6.8	0.04	106.3	0.005	19.5	0.032	18.1	0.083
7.4	0.044	113.2	0.004	32.7	0.031	24.8	0.021
9.7	0.041	123.2	0.002	33.5	0.024	32.2	0.035
11.6	0.038	135.8	0.019	43.3	0.018	37.7	0.019
12.7	0.034	151.1	0.01	45.7	0.01	49.5	0.019
15.3	0.031	167	0.005	47.2	0.02	72.6	0.009
16.8	0.029	180.5	0.005	57.6	0.038	98.7	0.077
18.4	0.034	202.9	0.005	58.3	0.029	123.2	0.012
20.2	0.03	220.1	0.002	80.2	0.029	147.7	0.09
22.2	0.027	239.9	0.003	82.5	0.028	172.2	0.035
24.4	0.03	263.5	0.003	82.8	0.014	185.2	0.004
26.8	0.027	290.4	0	107.2	0.021	221.1	0.059
29.4	0.025	318.6	0.001	132.1	0.006	244.6	0.041
32.3	0.025	357.4	0	157	9E-04	294.8	0.034
42.9	0.022	382.9	0	181.9	9E-04	295	0.012
51.9	0.022	432.2	0.005	203.2	0.009	319.3	0.076
57	0.023	462.2	0.002	207.5	0.022	346	0.06
75.8	0.023	533.5	0.002	229	0.03	392.8	0.075
83.4	0.022	558.2	0.002	256.5	0.001	410.1	8E-04
121.9	0.019	623.3	6E-04	274.3	0.001	417.9	0.074
134	0.016	691	8E-04	306.1	0.027	430.8	0.04
178.3	0.007	746.4	1E-04	307	0.024	442.5	0.034
215.7	0.004	820	7E-04	331	0.016	466.2	0.009
286.9	0.003	921.4	1E-03	353.6	0.026	491.6	0.043
315.5	0.003	995.1	6E-04	380.6	0.028	499.3	0.085
419.8	0.002	1102.2	0.002	405.5	0.013	539.7	0.009
507.8	0.001	1196.6	0	952.6	0.008	567.4	0.05
675.7	0.001	1325.7	0.013	996.5	0.02	589.5	0.024
743.2	7E-04	1406.2	0.013	1001.6	0.021	613.6	0.025
989.1	7E-04	1406.4	0	1225.5	0	625.3	0.042
1196.7	8E-04	1406.6	0.012	1250.3	0.009	637.7	0.041
1316.3	8E-04	1406.8	9E-15	1274.3	0.004	637.8	0.042
1751.8	5E-04	1407.9	0	1304.2	0.009	686.8	0.058
2119.5	4E-04	1408.2	0	1317.7	0.007	711	0.093
3048.3	0	1409	0.025	1349.3	0	720.9	0

shaded area = maximum value

line shows last point where evaporation is greater than boundary layer regulation

Figure 5.21

### Plot of ASMB Evaporation Rates Versus Time - No Wind

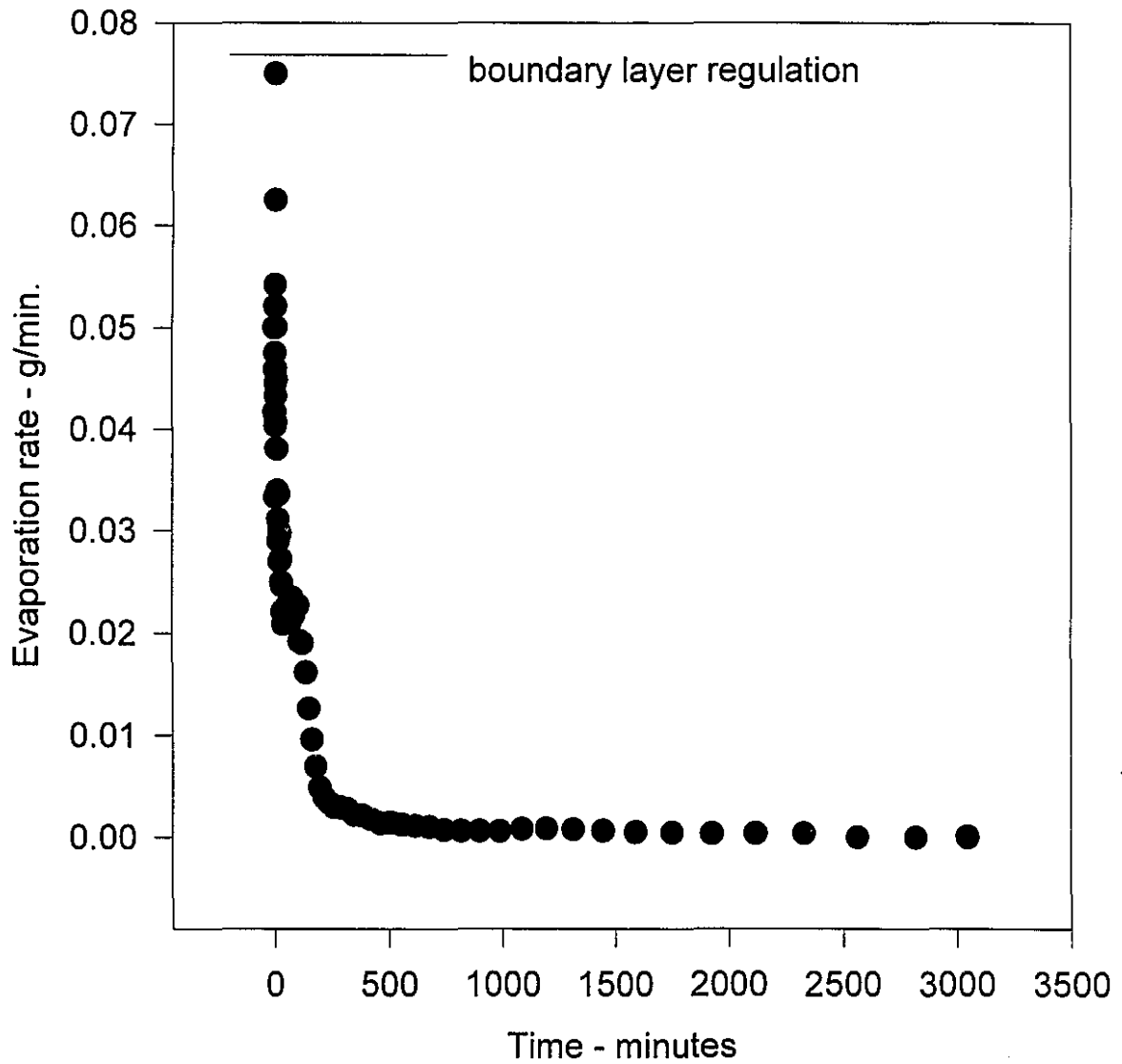


Figure 5.22

### Plot of ASMB Evaporation Versus Time- Variable Winds

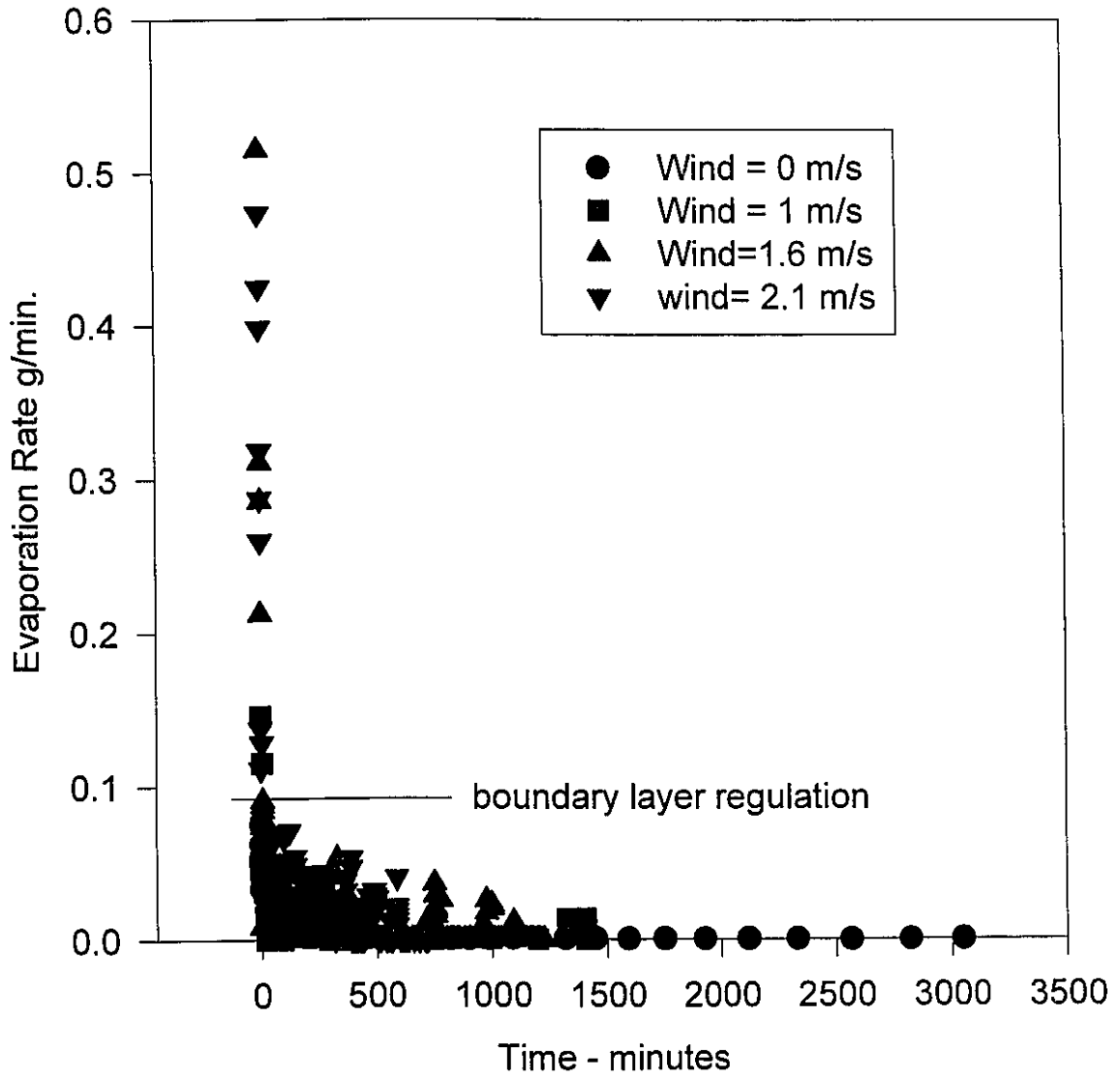
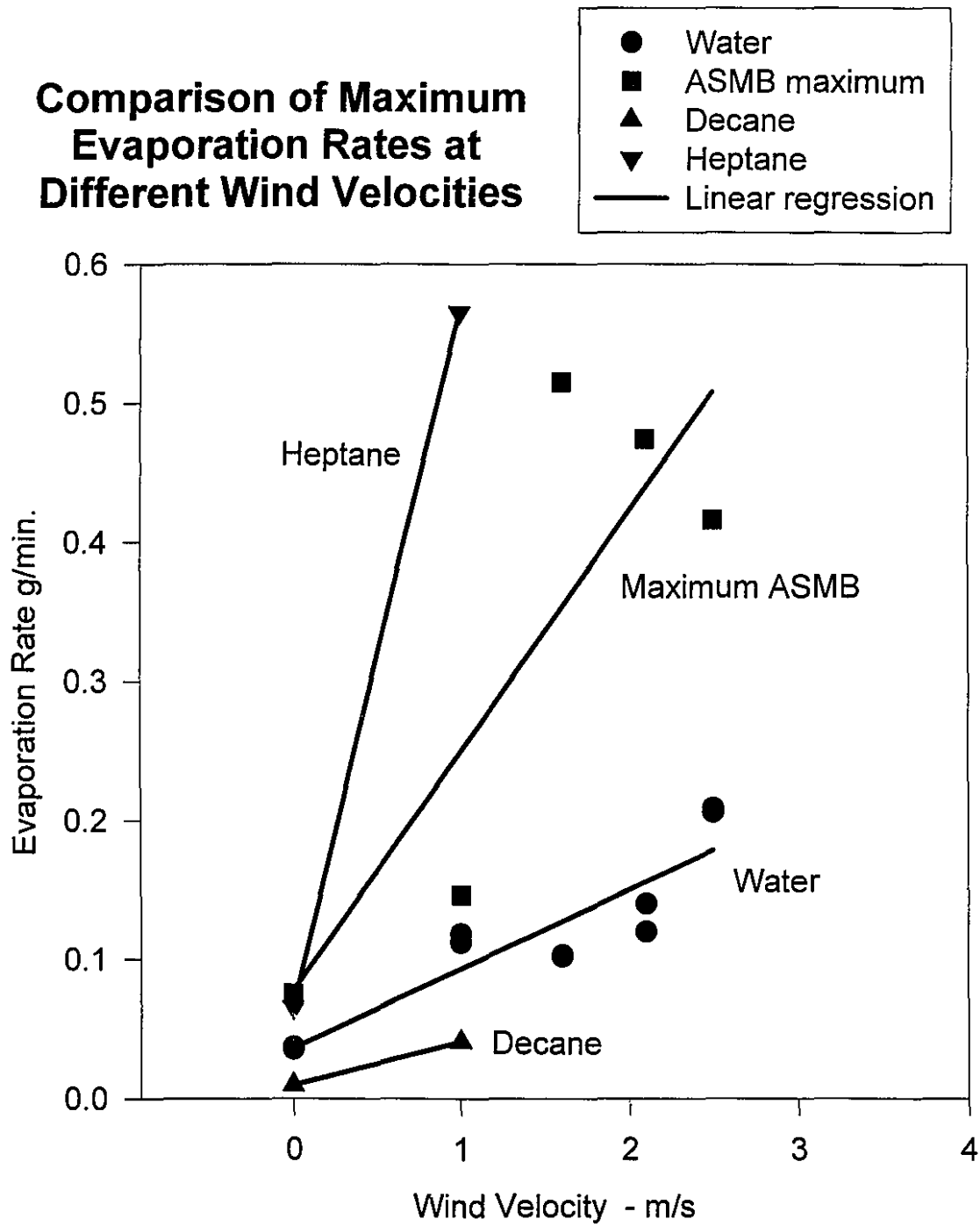


Figure 5.23



boundary-layer regulated) and thus are not boundary-layer regulated.

Table 5.10 gives a summary of rate comparisons for ASMB, gasoline and FCC Heavy Cycle. It should be noted that each of these fluids has characteristic evaporation patterns. ASMB represents a light to medium crude oil and evaporates at rates similar to many crude oils. It is thus very representative of crude oil evaporation. Gasoline is the most volatile petroleum product and represents the extreme evaporation rate behaviour. It is felt that if gasoline is not strictly boundary-layer regulated then no product will be. FCC heavy is an unusual and uncommon product that is a refinery intermediate. The "Heavy" refers not to the weight, but to the number of cycles through the refinery cracker. A "Heavy" Cycle product is highly refined and lower in density than a "Light" Cycle product. FCC is unusual in that if recycled many times consists of only a few components. FCC was included in the wind study to determine how such a product, perhaps being similar to diesel fuel, would evaporate.

Table 5.10 consists of two parts. The first sub-table shows the peak evaporation rates, the time after which the BLR or boundary-layer regulation no longer applies and the percentage of product evaporated after the evaporation rate decreases below the boundary layer regulation level. This portion of the table illustrates that all three products, gasoline, ASMB and FCC, show the same behaviour as noted repeatedly above, that an increase in evaporation rate is only noted for the step from 0-wind to the first wind level and then not thereafter. All three products, including gasoline, show non-boundary-regulated behaviour after an initial wind velocity and all three products show non-boundary regulated behaviour after a short initial time period. Even gasoline, the most volatile of the common petroleum products, exhibits the same behaviour. Table 5.10 also shows that the time period during which the evaporation rate is above that for boundary-layer regulation is less than about 5 minutes for ASMB and gasoline. For FCC Heavy, it can be as long as 46 minutes; however, in the latter case only 1.7% of the product is evaporated during this time. Only for gasoline is the volume evaporated during boundary-regulation significant - as much as 44%. Volumes for the other cases are typically less than 3%.

The second part of Table 5.10 provides another form of comparison of

The second part of Table 5.10 provides another form of comparison of evaporation rates, the length of time to evaporate a certain portion of the liquid. This table shows that after the first velocity increment (0-wind to 1 m/s), the time to evaporate the same percentage changes. The times to evaporate the same percentage extent, can be as much as 5-6 times when there is 0-wind, as opposed to when wind is present. However, this does not change after the first wind velocity increment, indicating that only the initial fractions are subject to boundary-layer regulation.

The findings are further strengthened by comparison of the maximum evaporation rates with no wind, as shown in Table 5.11. This again shows that the rate of evaporation is not the only governing factor. ASMB has an evaporation rate of 0.075 g/min at no wind, which is much higher than the no wind rate of water at 0.034, and as shown above, shows boundary regulation for only a few minutes out of several days of evaporation time. This table clearly shows that compounds having evaporation rates below about 0.01 g/min., about that of decane, will not show boundary-layer regulation. Above this, boundary layer regulation is also dependant on composition. Multi-component mixtures typically show boundary layer regulation for only a few minutes. This also shows that evaporation of a particular compound is relatively independent of the evaporation of other compounds at the same time.

Another form of comparison is that of saturation concentration, the maximum concentration soluble in air. Table 5.12 lists the saturation concentrations of water and several oil components. This table shows that saturation concentration of water is less than that of many common oil components. The saturation concentration of water is in fact, about two orders less in magnitude than the saturation concentration of volatile oil components such as pentane. This further explains why oil has a boundary layer limitation higher than that of water.

Table 5.10

## Summary of Rate Comparisons

Peak Rates, Times greater than BLR, Percentage Evaporated before BLR reached													
Oil	Boundary Layer	Wind=0			Wind=1 m/s			Wind=1.6 m/s			Wind=2.1 m/s		
		Max. Rate	t	%	Max. Rate	t	%	Max. Rate	t	%	Max. Rate	t	%
		Rate (g/min.)	(g/min.)	(min.)	Evap.	(g/min.)	(min.)	Evap.	(g/min.)	(min.)	Evap.	(g/min.)	(min.)
ASMB	0.075	0.075	2	0.5	0.145	0-6	0-3	0.515	0.2	1.4	0.47	0.6	1.1
Gasoline	0.34	0.34	3.1	2.2	1.03	3.1	26	1.02	7	44	1.38	4.7	28.7
FCC Heavy	0.008	0.008	3.1	0.1	0.089	10.2	2.5	0.196	23.7	5.6	0.356	46	1.7

BLR = Boundary Layer Regulation

## Time to The Same Evaporation Extent

Oil	Evaporation Percentage	(time in minutes)			
		Wind=0	Wind=1 m/s	Wind=1.6 m/s	Wind=2.1 m/s
ASMB	30	740	230	157	180
Gasoline	75	40*-200*	46	49	68
	50	60	10	12	15
FCC Heavy	30	830*-5000	1010	1290	1260
	15	1750	360	300	400

\*calculated from the best equation with two terms, evaporation not carried out to full extent experimentally

Table 5.11

**Comparison of Maximum Evaporation Rates**

<b>Date</b>	<b>Oil Type</b>	<b>Maximum Rate (g/min.)</b>	<b>Boundary Regulation</b>
Oct 8	Hexadecane	1.65E-05	
Oct 6	Tridecane	0.000278	
Sept 22b	Dodecane	0.001	
Sept 24	Undecane	0.00386	
Sept 28c	Decahydronaphthalene	0.00707	
several	FCC Heavy	0.008	
Sept 27	Decane	0.0097	
Sept 26b	Nonane	0.0234	m
Sept 26a	p-Xylene	0.0322	√
several	<b>Water</b>	0.034	√
Nov 14a	2-component	0.04	√
Sept 28b	Octane	0.0448	√
Sept 28a	Heptane	0.0652	√
Nov 15a	3-component	0.0705	m
several	ASMB	0.075	
Sept 22a	Benzene	0.136	√
several	Gasoline	0.34	

m=marginally

Table 5.12 **Saturation Concentration of Water and Oil Components**

<b>Substance</b>	<b>Saturation Concentration *</b> <b>in g/m<sup>3</sup> at 25°C</b>
water	20
n-pentane	1689
hexane	564
cyclohexane	357
benzene	319
n-heptane	196
methylcyclohexane	192
toluene	110
ethybenzene	40
p-xylene	38
m-xylene	35
o-xylene	29

\*Values taken from Ullman's Encyclopedia

## 5.5 Conclusions

Oil evaporation does not appear to be strictly boundary-layer regulated to any significant degree. The results of the following experimental series have shown the lack of boundary-layer regulation: 1) A study of the evaporation rate of several oils with increasing wind speed shows that the evaporation rate does not change significantly except for the initial step over 0-level wind. Water, known to be boundary-layer regulated, does show a significant increase with wind speed,  $U$  ( $U^x$ , where  $x$  varies from 0.5 to 0.78, depending on the turbulence level). 2) Increasing area does not significantly change the oil evaporation rate. This is directly contrary to the prediction resulting from boundary-layer regulation.

3) Decreasing thickness does not increase oil evaporation rate. This is a corollary to 2 above. 4) The volume or mass of oil evaporating correlates with the evaporation rate. This is a strong indicator of the lack of boundary-layer regulation because with water, volume (rather than area) and rate do not correlate. 5) Evaporation of pure hydrocarbons with and without wind (turbulence) shows that compounds larger than nonane and decane are not boundary-layer regulated. Most oil and hydrocarbon products consist of compounds larger than these two and thus would not be expected to be boundary-layer regulated. 6) Evaporation of pure hydrocarbons with a highly-weathered oil residue, with and without wind, shows that the evaporative behaviour is not boundary-layer regulated. This shows that the effect is not simply an artifact of certain oil compositions.

Having concluded that boundary-layer regulation is not applicable to oil evaporation, it remains to explain why this is so. The reason is twofold: oil evaporation, especially after an initial time period, is relatively slow compared to the threshold where it is boundary-layer regulated; and the threshold to boundary-layer regulation for oil evaporation is much higher than that for water. These two factors were highlighted by three comparisons using the experimental data:

1) A comparison of the length of time that oils exceed the boundary-layer limit, taken as the maximum evaporation rate in the absence of wind, shows that the length of time during which the evaporation rate in the presence of wind exceeds the boundary-layer

limit, can be as short as 2 minutes to a maximum of 46 minutes. This represents a very small fraction of the required time to significantly evaporate oil (in these experiments, typically 2000 to 8000 minutes). For most of the time the evaporation is far below the boundary-layer regulated rate. 2) A comparison of the maximum rates of evaporation for some oils, gasoline and water, in the absence of wind, shows that some oil rates exceed that for water by as much as an order of magnitude (water=.034 g/min, ASMB=0.075 g/min., and Gasoline=.34 g/min.; all under the specific conditions noted), and 3) The saturation concentration of several hydrocarbons in air reveals that some hydrocarbon saturation concentrations in air can be greater than that of water by as much as two orders-of-magnitude.

The explanation of oil evaporation can be illustrated by a diagram such as Figure 5.24. This illustrates evaporation of a volatile oil such as ASMB. If evaporation occurs in a turbulent atmosphere, the time that the evaporation rate exceeds the boundary-layer limited rate is very short. If no turbulence is present, evaporation will proceed at the limitation rate then drop off to a similar, but higher rate than the turbulent rate. The area under the two curves would be the same. The difference in time is a matter of minutes, as explained above and the end result will not be noticeable to an observer. Thus, it is stated that oil and petroleum evaporation is not strictly boundary-layer regulated.

The fact that oil evaporation is not strictly boundary-layer regulated implies a simplistic evaporation equation will suffice to describe the process. The following factors do not require consideration: wind velocity, turbulence level, area, thickness, and scale size. The factors important to evaporation are time and temperature.

## References

Brutsaert, W., *Evaporation into the Atmosphere*, Reidel Publishing Company, Dordrecht, Holland, 299 p., 1982.

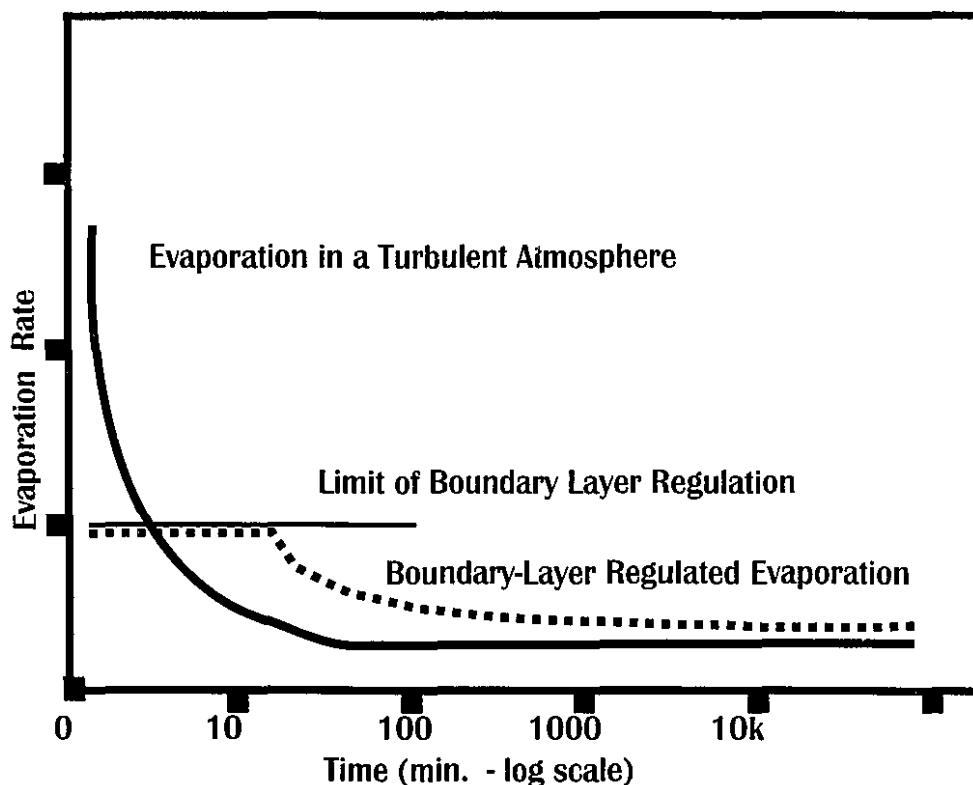
Jones, F.E., *Evaporation of Water*, Lewis Publishers, Chelsea, Michigan, 188 p., 1992.

Wang, Z., M.F. Fingas and Ken Li, "Fractionation of a Light Crude Oil and Identification and Quantitation of Aliphatic, Aromatic, and Biomarker Compounds by GC-FID and GC-MS, Part I", *Journal of Chromatographic Science*, Vol. 32, pp. 361-366, 1994.

Whiticar, S., M. Bobra, M.F. Fingas, P. Jokuty, P. Liuzzo, S. Callaghan, F. Ackerman and J. Cao, *A Catalogue of Crude Oil and Oil Product Properties (1992 Edition)*, Environment Canada Manuscript Report Number EE-144, Ottawa, Ontario, 643 p., 1993.

Yang, W.C. and H. Wang, "Modelling of Oil Evaporation in Aqueous Environments", *Water Research*, Vol. 11, Pergamon Press, Great Britain, pp. 879-887, 1977.

**Figure 5.24 Conceptual Diagram of Oil Evaporation**



## Chapter 6 The Relationship between Evaporation Rate and Temperature

### 6.1 Abstract

The relationship between oil evaporation and temperature was investigated. It was found that the evaporation rate is linear with temperature change. Although each oil or petroleum product yields a unique relationship for temperature and evaporation rate, these can be predicted using the evaporation rate at 15 °C alone or using distillation data. The slope of the distillation curve at 140 °C correlates well with the slope and intercept of the temperature curve determined empirically. These correlations were used to develop a prediction scheme for the effects of temperature on evaporation rate.

### 6.2 Introduction

The effect of temperature on the evaporation has been a matter of discussion. The most-accepted point of view is that extracted from the Mackay equation (Stiver and Mackay, 1984):

$$N = kAP/(RT) \quad (6.1)$$

where  $N$  is the evaporative molar flux (mol/s),  $k$  is the mass transfer coefficient under the prevailing wind (m/s),  $A$  is the area (m<sup>2</sup>),  $P$  is the vapour pressure of the bulk liquid, and  $T$  is temperature (K).

Most interpretations of this equation are that evaporation rate is related to temperature by  $\log T/T$ . This interpretation derives from the view that  $P$  (vapour pressure) is related to temperature as  $\log T$ . Work by Lehr (1992, 1994) assumes that this estimation is approximately correct and thus that the equations are highly sensitive to temperature. In fact, Lehr (1992) states that the change of evaporation rate with temperature is greater than linear and may be even as much as  $T^2$ .

Examination of some other theoretical material appears to indicate that the relationship of evaporation rate to temperature may be linear. Experimental work, described later in this chapter, shows that, in fact, the evaporation rate is linearly related to temperature. In Chapter 1 some thermodynamic relationships were reviewed and these showed that the evaporation rate may be linear.

The Clausius-Clapeyron equation, Maxwell's equations and the ideal gas equation show that the volume change and thus the evaporation rate is directly and linearly related to the temperature. This theoretical information will be tested experimentally and the results presented in this chapter.

### 6.3 Experimental

Details of the experimental method are given in Chapter 3. Evaporation rate was measured by weight loss using an electronic balance as previously described.

Experiments were conducted in a constant temperature chamber (room), a Constant Temperature model constructed in 1993. It can maintain temperatures from -40°C to +60°C within  $\pm 1^\circ\text{C}$ . The chamber also controls relative humidity. At relative humidities of 40 to 70%, the unit maintains set humidities within  $\pm 2\%$ , at other levels this precision decreases. The relative humidity was maintained at 40% when relative humidity was not a parameter of concern. Temperatures were confirmed using a Keithley 871 digital thermometer with a thermocouple supplied by the same firm. Temperatures were taken manually at the beginning and the end of a given experimental run to confirm the functioning of the temperature controller. A data recorder also monitored temperatures in the chamber.

A tared petri dish (Corning 139 mm diameter, ID) was loaded with a measured amount of oil. Data acquisition was started and continued until the desired time (varying from a few hours for a volatile substance to several days for a less-volatile oil). At the end of the experiment, the weathered oil was saved for chemical analysis. Vessels were cleaned and rinsed with Dichloromethane and a new experiment started.

The properties of the oils used in the tests are listed in Table 6.1 and the experiments conducted are listed in Table 6.2

Table 6.1

**Properties of the Test Liquids**

<b>Name</b>	<b>Description</b>	<b>Density g/mL</b>	<b>Viscosity mPa.s at 15°C</b>
ASMB	Alberta Sweet Mixed Blend - A common crude oil in Canada	0.839	9
Gulfaks	A common Norwegian oil - sometimes exported to Canada	0.882	13
Brent	A common British, North Sea oil, sometimes exported to Canada	0.833	6
Arabian Light	A common blend of Saudi Arabian oil exported around the world	0.867	14
Terra Nova	One of the oils from the Hibernia field off Newfoundland	0.864	17
Statfjord	A common Norwegian oil - sometimes exported to Canada	0.834	7
Bunker C Light	A variation on Bunker C, a refinery residual product, with some diesel-like diluent	0.969	10000
Diesel	Standard automotive/truck diesel fuel	0.809	2
Gasoline	Standard automotive non-leaded gasoline	0.709	0.6

Table 6.2

## Experiments Conducted to Test the Temperature Effect

Series	Date	Oil Type	Days	Total Length	Total Time (hr)	Pan (cm <sup>2</sup> ) Area	Initial Weight (g)	Initial (mm) Thickness	End Wt.	% Evap	Temp C	Wind m/s	R <sup>2</sup> Equation	Best Equation	Single Parameter
8	April 22b	ASMB	1	26	151	20	1.58	14	30	10	0	0.996	ln	3.87	
	April 23	ASMB	2	47	151	20	1.58	14	30	5	0	0.987	ln	3.48	
	April 25	ASMB	1	24	151	20	1.58	14	32	15	0	0.995	ln	4.22	
	April 26	ASMB	1	25	151	20	1.58	13	33	20	0	0.997	ln	4.28	
	April 27	ASMB	1	24	151	20	1.58	13	34	25	0	0.998	ln	4.45	
	April 28	ASMB	1	24	151	20	1.58	13	36	30	0	0.995	ln	4.88	
	April 29	ASMB	1	23	151	20	1.58	13	38	35	0	0.996	ln	5.13	
	April 30	ASMB	2	48	151	20	1.58	15	24	0	0	0.984	ln	2.76	
	May 2	ASMB	2	45	151	20	1.58	16	22	-5	0	0.894	ln	1.81	
	May 4	ASMB	3	61	151	20	1.58	15	24	-5	0	0.938	ln	2.44	
	May 6	ASMB	3	52	151	20	1.58	16	18	-10	0	0.826	ln	1.33	
	May 13	ASMB	6	143	151	20	1.58	16	18	-15	0	0.673	ln	1.06	
	May 28a	ASMB	0.5	5	151	20	1.58	13	33	40	0	0.994	ln	5.49	
	May 28b	ASMB	1	21	151	20	1.58	19	4	-15	0	0.754	ln	0.536	
	May 29	ASMB	3.5	72	151	20	1.58	17	15	-20	0	0.659	ln	0.916	
18	Feb 20	Gulfaks	4	96	151	20	1.5	15	24	10	0	0.959	ln	2.53	
	Feb 24	Gulfaks	8	188	151	20	1.5	15	25	5	0	0.975	ln	2.54	
	Mar 4	Gulfaks	6	144	151	20	1.5	15	23	0	0	0.977	ln	2.19	
	Mar 10	Gulfaks	3	72	151	20	1.5	15	26	15	0	0.984	ln	2.81	
	Mar 13	Gulfaks	3	72	151	20	1.5	15	26	20	0	0.997	ln	3	
	Mar 16	Gulfaks	2	48	151	20	1.5	15	26	25	0	0.997	ln	3.01	
	Mar 18	Gulfaks	2	46	151	20	1.5	15	27	30	0	0.972	ln	3.24	
	Mar 20	Gulfaks	2	42	151	20	1.5	14	29	35	0	0.985	ln	3.54	
19	Mar 22	Arabian Lt	5	101	151	20	1.53	14	28	15	0	0.993	ln	3.11	
	Mar 26	Bunker C Lt	4	88	151	20	1.37	19	3	15	0	0.99	sq. rt.	0.0422	
	Mar 30a	Gasoline	0.5	3	151	21.1	1.97	3.1	85	15	0	0.956	ln	16	
	Mar 30b	Gasoline	0.5	3	151	20.4	1.91	3.1	85	15	0	0.955	ln	15.8	
	Mar 30c	Diesel	4	89	151	20.3	1.66	13	38	15	0	0.991	sq. rt.	0.538	
	April 3a	Gasoline	0.5	4	151	20	1.87	5.5	73	-5	0	0.99	ln	12	
	April 3b	Gasoline	0.5	3	151	21.6	2.02	6.6	70	-5	0	0.944	ln	12.2	
	April 3c	Diesel	3	120	151	20.2	1.65	15	24	-5	0	0.997	sq. rt.	0.276	
	April 6	Bunker C Lt	3	119	151	20.2	1.38	20	1	-5	0	0.407	sq. rt.	0.003	
	April 13	Arabian Lt.	2.5	95	151	20	1.53	16	22	-5	0	0.992	ln	2.37	
	April 17	Statfjord	5	117	151	20.05	1.59	18	10	-5	0	0.747	ln	2	
	April 22	Brent	5	121	151	20	1.59	14	30	-5	0	0.956	ln	3.08	
	April 27	Terra Nova	6	137	151	21.86	1.73	19	11	-5	0	0.818	ln	0.955	
	May 3a	Gasoline	0.5	1	151	20.03	1.87	1.1	94	35	0	0.943	ln	21.5	
	May 3b	Gasoline	0.5	1	151	20	1.87	1.2	94	35	0	0.954	ln	22.3	
	May 3c	Diesel	2	41	151	20	1.64	11	47	35	0	0.984	sq. rt.	0.988	
	May 5	Brent	1.5	32	151	20	1.59	12	38	35	0	0.988	ln	5.07	
	May 6	Bunker Lt	3	70	151	20	1.37	19	7	35	0	0.999	sq. rt.	0.105	
	May 9	Arabian Lt.	3	73	151	20	1.53	14	32	35	0	0.997	ln	3.78	
	May 12	Terra Nova	3.5	88	151	20	1.58	14	30	35	0	0.991	ln	3.26	
	May 16	Statfjord	2	46	151	20	1.59	12	39	35	0	0.993	ln	4.69	
	May 19	Bunker C Lt.	9	216	151	20.02	1.37	20	0	5	0	0.85	sq. rt.	0.0031	
	May 28	Arab Light	2	49	151	20	1.53	16	22	5	0	0.998	ln	2.61	
	May 30	Statfjord	2.5	66	151	20	1.58	14	29	5	0	0.979	ln	3.3	
	June 2a	Gasoline	0.5	4	151	20	1.87	2	90	5	0	0.997	ln	14.8	
	June 2b	Gasoline	0.5	2	151	20	1.87	4.3	79	5	0	0.991	ln	15.6	
	June 2c	Diesel	3	73	151	20	1.64	15	26	5	0	0.998	sq. rt.	0.389	
	June 05	Brent	2.5	63	151	20	1.59	14	32	5	0	0.994	ln	3.67	
	June 23c	Gasoline	0.5	2	151	20	1.87	0.9	95	25	0	0.979	ln	16.9	
	June 23t	Gasoline	0.5	2	151	20	1.87	0.9	95	25	0	0.978	ln	16.9	
	June 23c	Diesel	3	70	151	20	1.64	12	39	25	0	0.99	sq. rt.	0.623	
	June 26	Terra Nova	3	50	151	11.7	0.92	8.7	26	25	0	0.99	ln	3	
	June 28	Bunker C Lt.	12	283	151	20	1.37	18	8	25	0	0.999	sq. rt.	0.061	
	July 10	Statfjord	9	220	151	20	1.59	12	39	25	0	0.996	ln	4.1	
	July 19	Brent	3	68	151	20	1.59	13	37	25	0	0.991	ln	4.44	
	July 22	Arab Light	2	51	151	20	1.53	14	28	25	0	0.997	ln	3.5	

## 6.4 Results and Discussion

Figure 6.1 shows the composite of all evaporation rates versus the temperature. The evaporation rates are the coefficients of the logarithmic equation except for diesel and Bunker C light, where they are the coefficients of the square root equation. Figure 6.1 shows that the evaporation rates (used here interchangeably with equation constant) are linear with respect to temperature. This confirms the theoretical approaches discussed in the introduction above. Figure 6.2 shows an expanded correlation of evaporation rates versus temperature, this expansion is achieved by eliminating the gasoline curve which has very high evaporation rates. The small amount of noise seen in these graphs, is possibly due to error in fitting the logarithmic or square curves. These figures indicate that most of the curves are parallel. This phenomenon is further examined in Figure 6.3 and Figure 6.4. These show the evaporation rates, with and without gasoline, with curves fit with linear regression. The curves for the light crudes, ASMB, Brent, Arabian Light, Statfjord and Gullfaks appear to be parallel. The curves for gasoline, Terra Nova crude, diesel, and Bunker C light have different slopes than those for crude oils and may be due to the unique properties of these liquids. Gasoline evaporates at a rapid rate and is composed of only lighter crude components. Terra Nova is a heavier crude with a large wax component. Diesel is a refined cut with medium to heavy components remaining. Bunker C light is a refined residual with a small amount of diesel as a diluent. The evaporation rates of the latter two products are best fit with square root equations rather than logarithmic equations.

Further examination of the temperature behaviour of oil evaporation was conducted by determining the equations by which the evaporation rates, or equation parameters, change with temperature. A series of correlations was performed, between the evaporation rates, by both percentage and weight loss, using a linear equation. The evaporation rates or equation parameters used to perform the correlations are listed in Table 6.1. Figures 6.5 to 6.13 show the correlations for ASMB, Gullfaks, Brent, Arabian Light, gasoline, Terra Nova, Statfjord, diesel and Bunker C light. Each figure shows the rank of the linear equation out of the simple equations available in the TableCurve

Figure 6.1

### The Variation of Evaporation Rates with Temperature

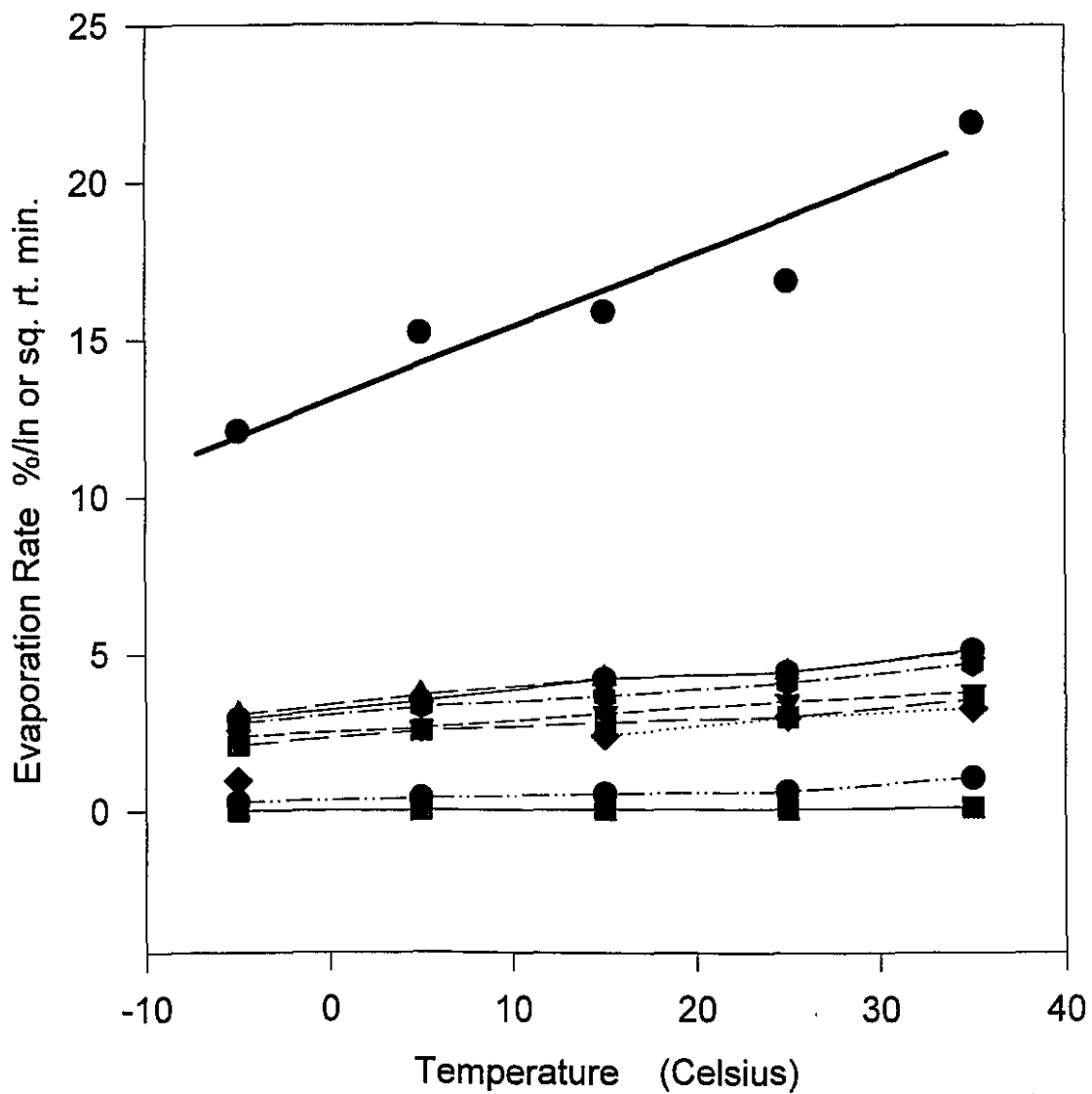
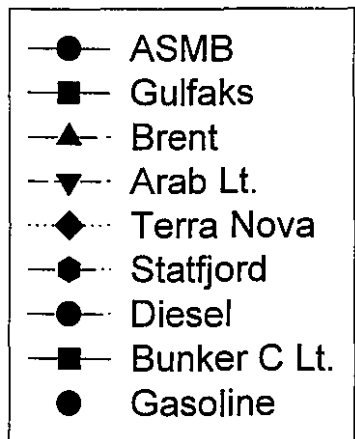


Figure 6.2

### The Variation of Evaporation Rates with Temperature - Without Gasoline

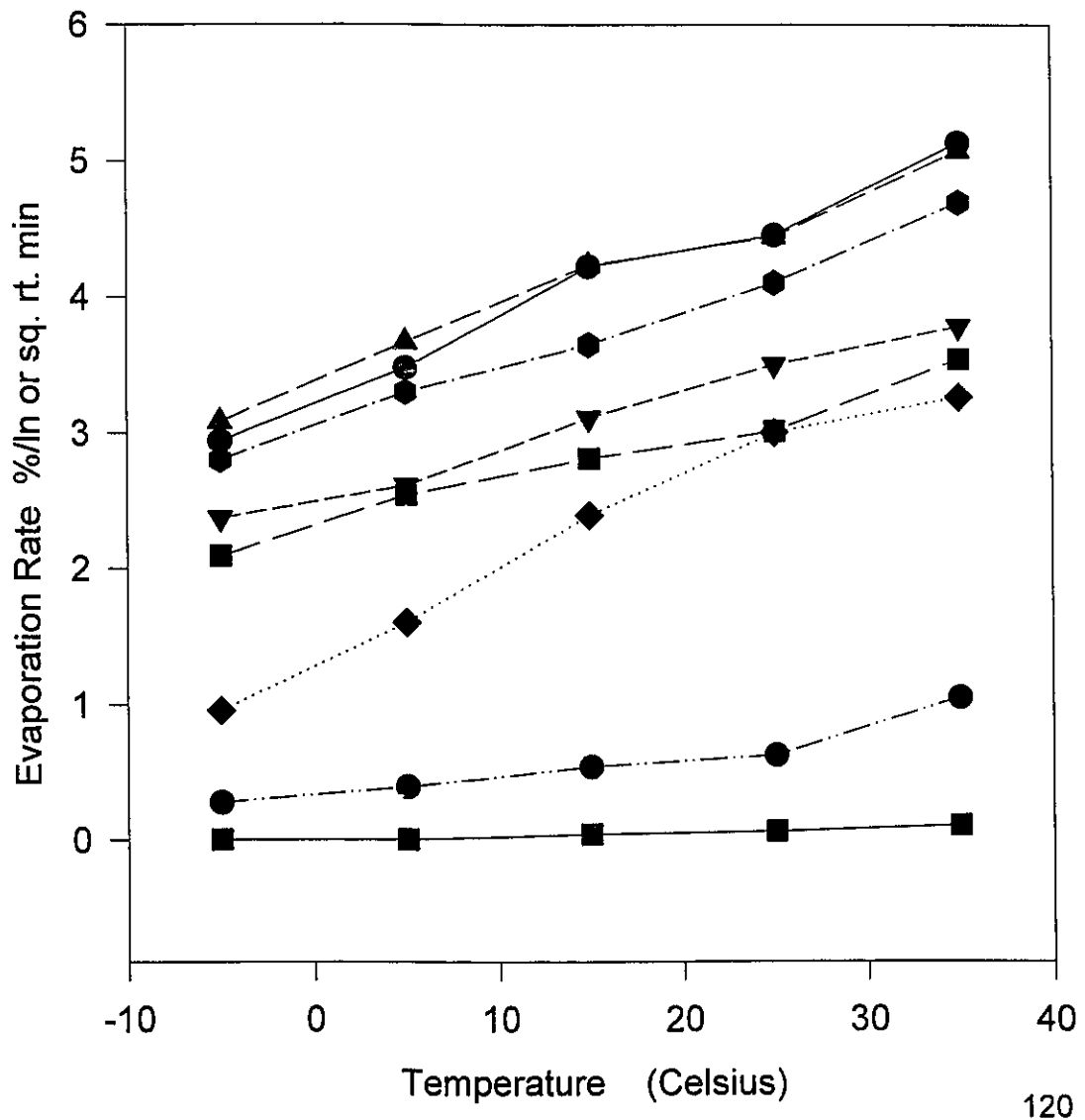
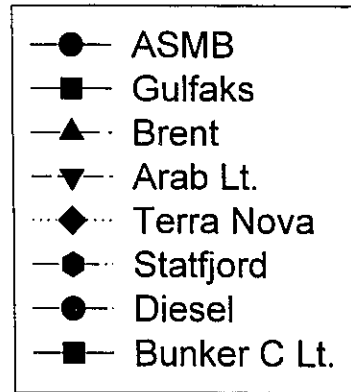


Figure 6.3

### The Variation of Evaporation Rates with Temperature - Linear Regression

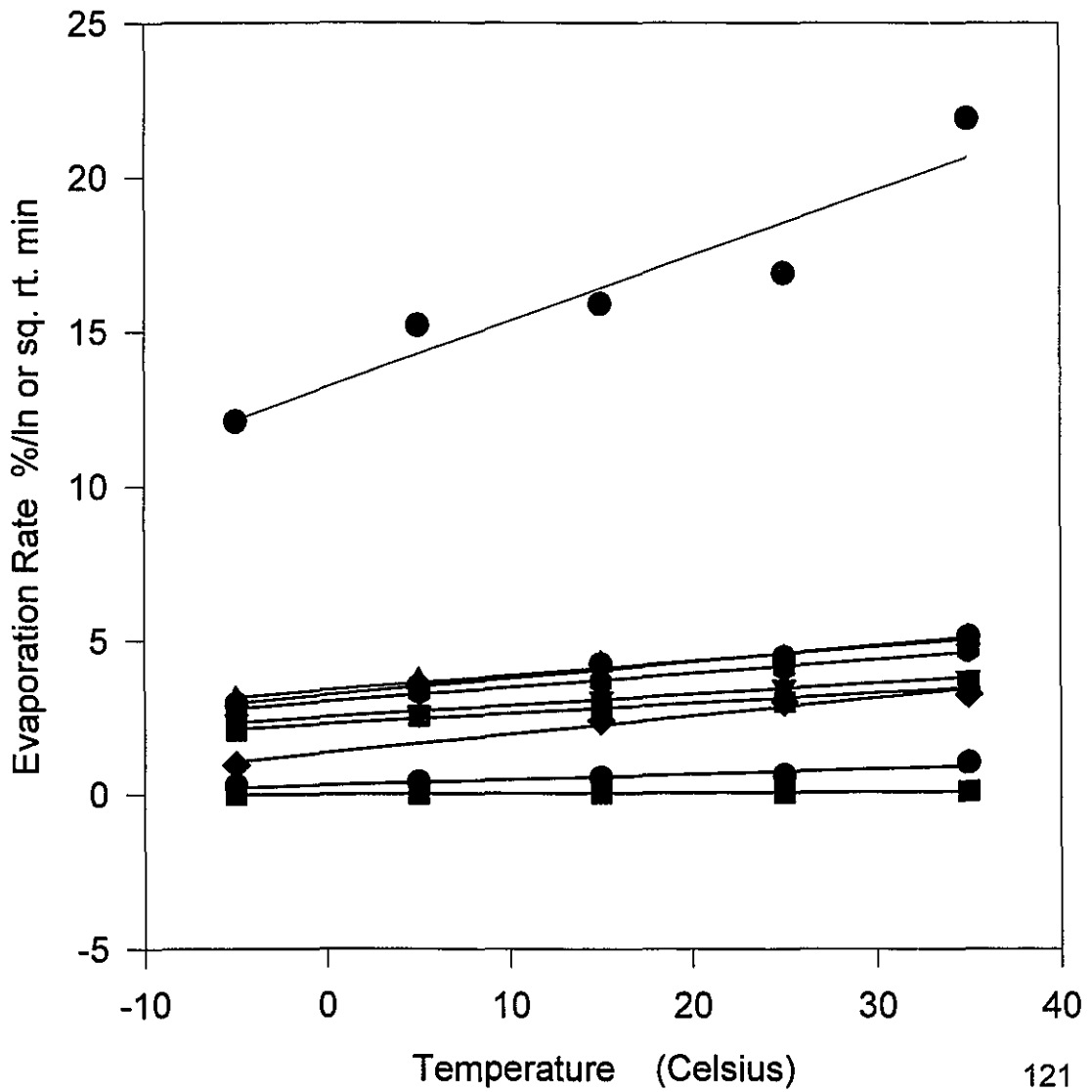
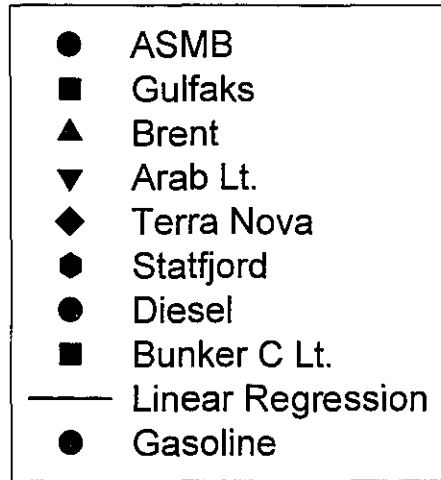


Figure 6.4

### The Variation of Evaporation Rates with Temperature - Without Gasoline - Linear Regression

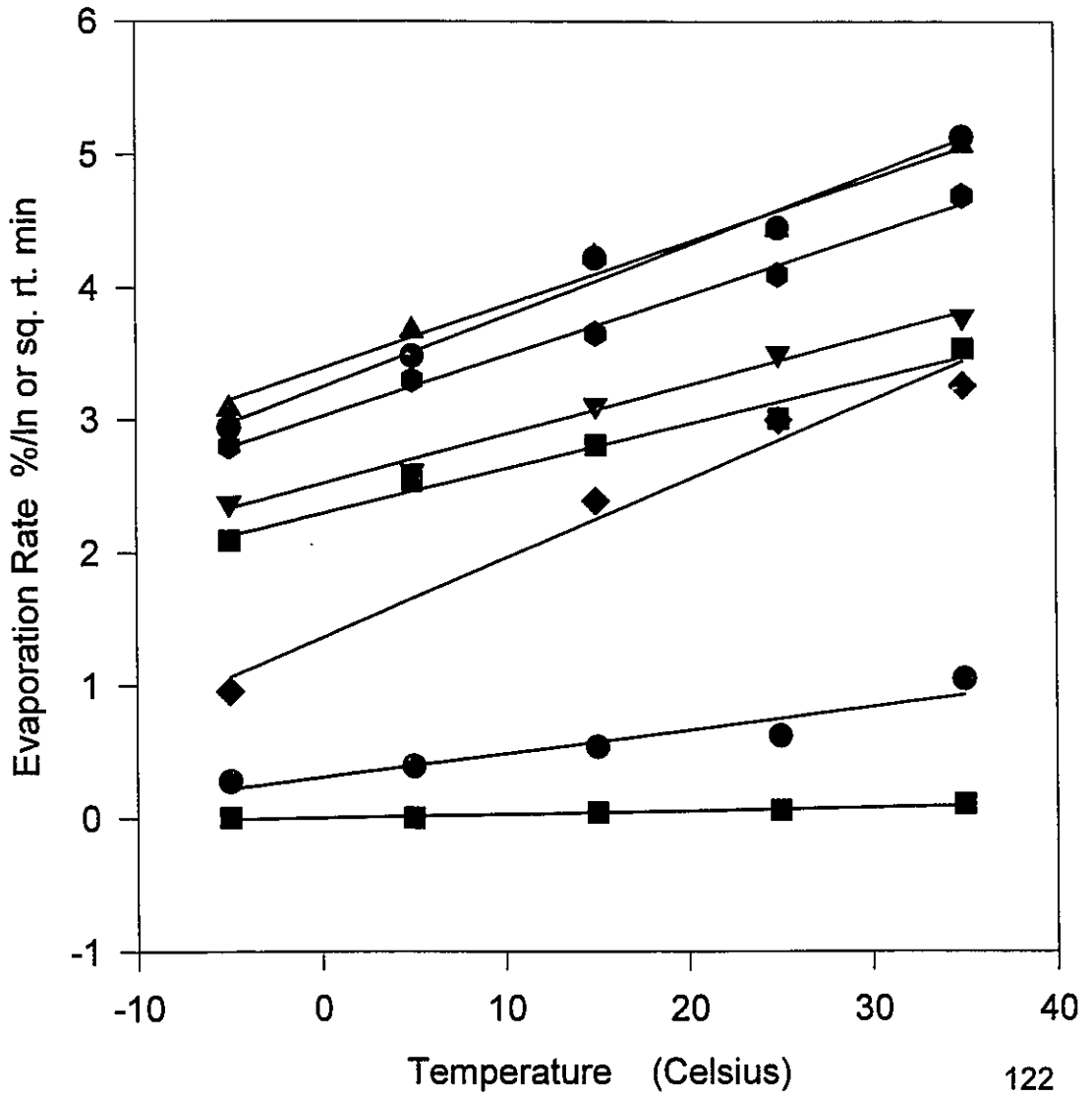
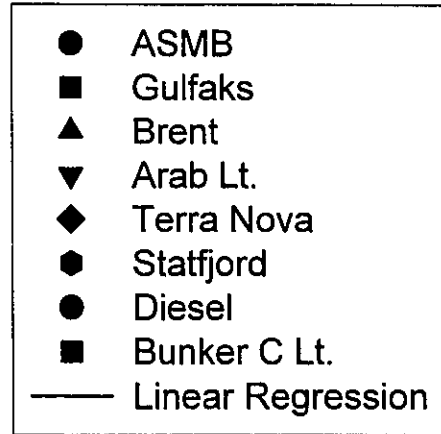


Figure 6.5

Correlation of ASMB Evaporation and Temperature

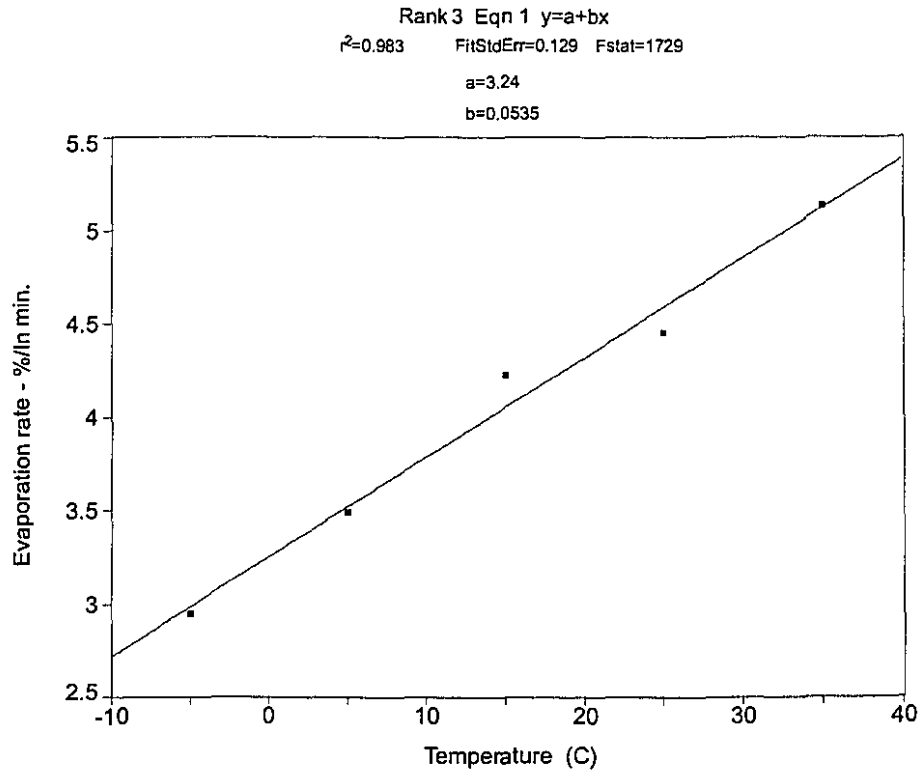


Figure 6.6

Correlation of Gullfaks Evaporation and Temperature

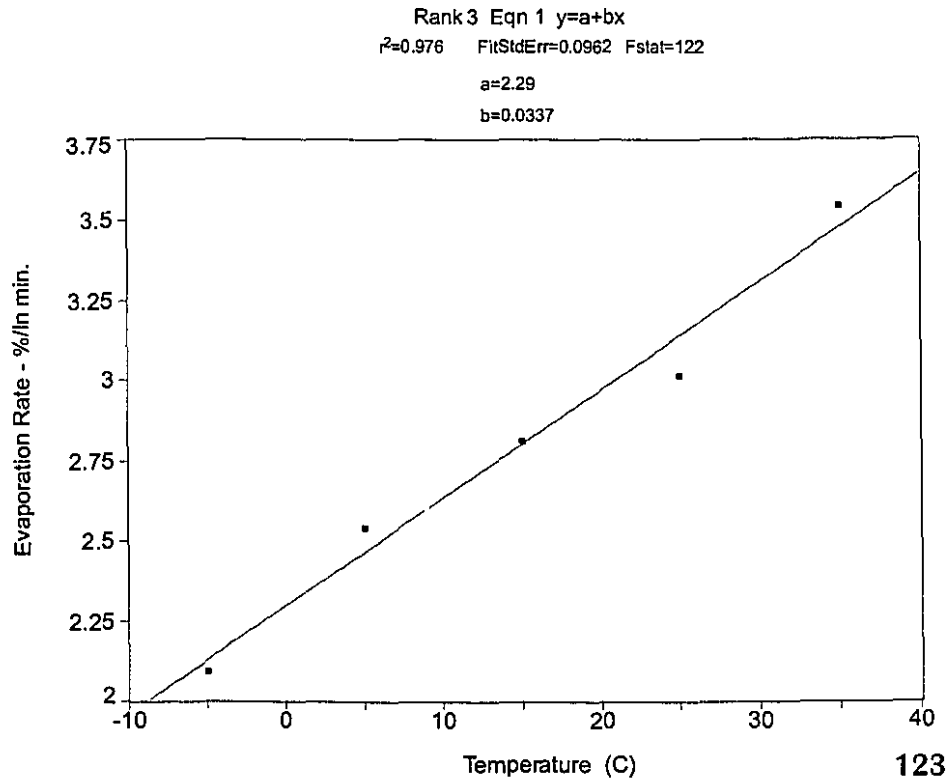


Figure 6.7

Correlation of Brent Evaporation and Temperature

Rank 4 Eqn 1  $y=a+bx$

$r^2=0.982$  FitStdErr=0.119 Fstat=160

$a=3.39$

$b=0.0475$

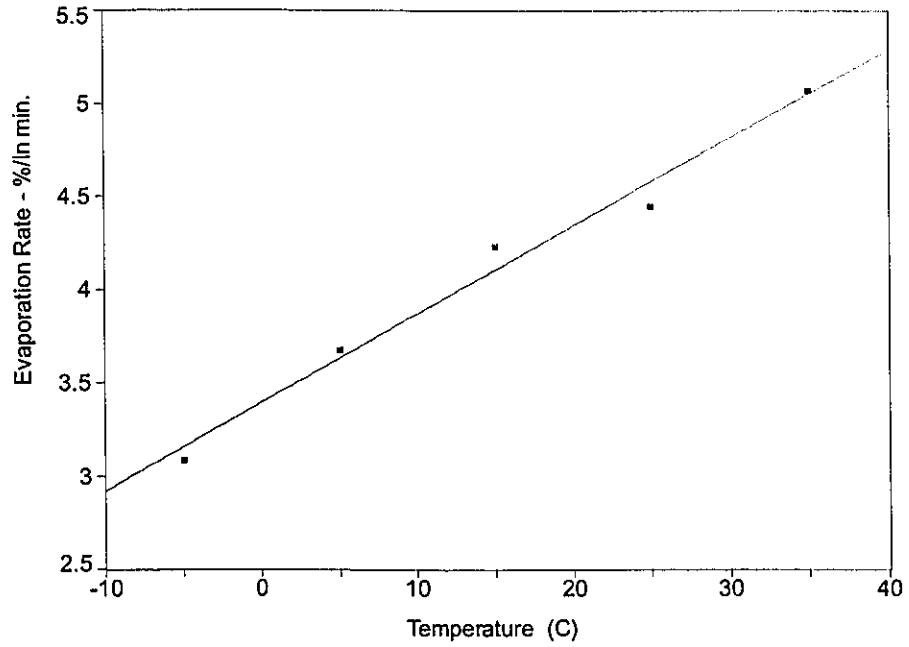


Figure 6.8

Correlation of Arabian Light Evaporation and Temperature

Rank 2 Eqn 1  $y=a+bx$

$r^2=0.989$  FitStdErr=0.0725 Fstat=263

$a=2.52$

$b=0.0371$

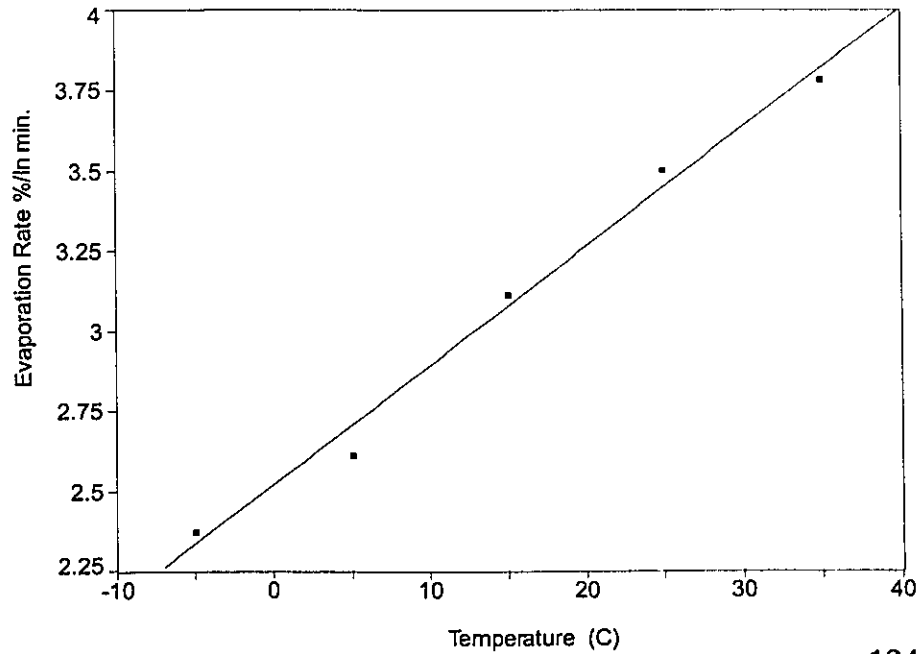


Figure 6.9 Correlation of Gasoline Evaporation and Temperature

Rank 5 Eqn 1  $y=a+bx$   
 $r^2=0.895$  FitStdErr=1.33 Fstat=25.6  
a=13.2  
b=0.213

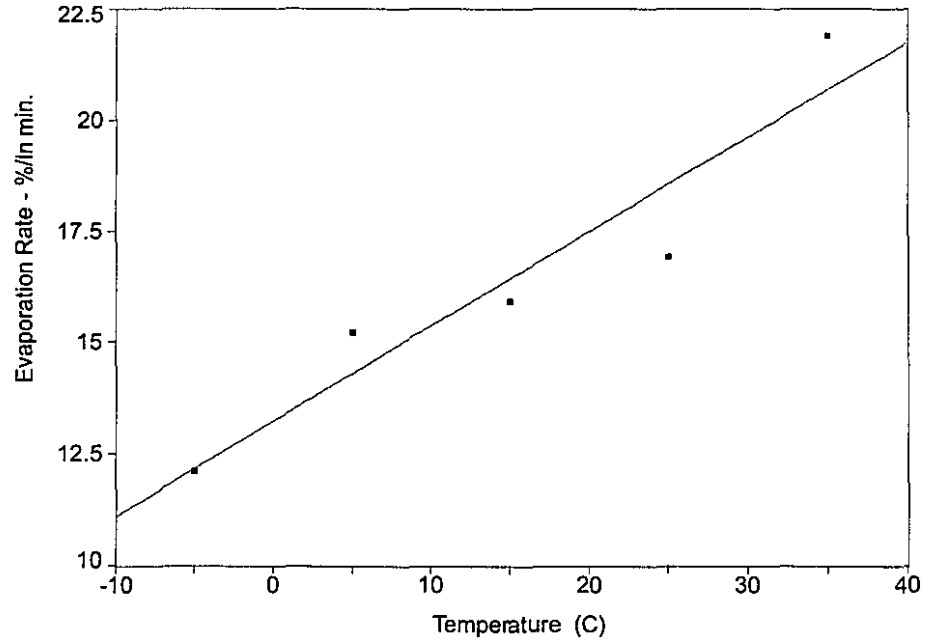


Figure 6.10 Correlation of Terra Nova Evaporation and Temperature

Rank 3 Eqn 1  $y=a+bx$   
 $r^2=0.988$  FitStdErr=0.110 Fstat=162  
a=1.69  
b=0.0473

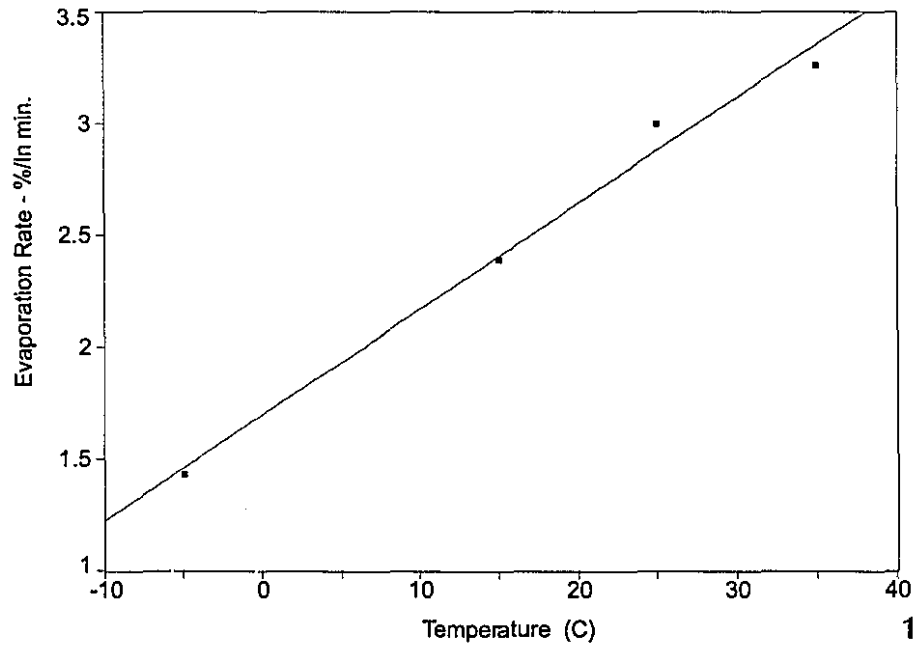


Figure 6.11

Correlation of Statfjord Evaporation and Temperature

Rank 2 Eqn 1  $y=a+bx$   
 $r^2=0.992$  FitStdErr=0.0769 Fstat=390  
 $a=2.97$   
 $b=0.048$

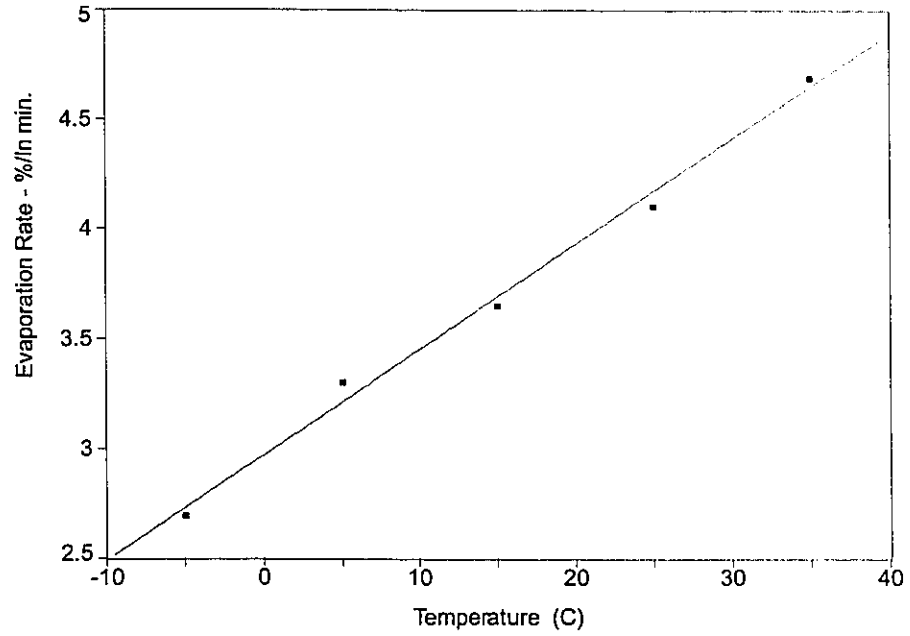
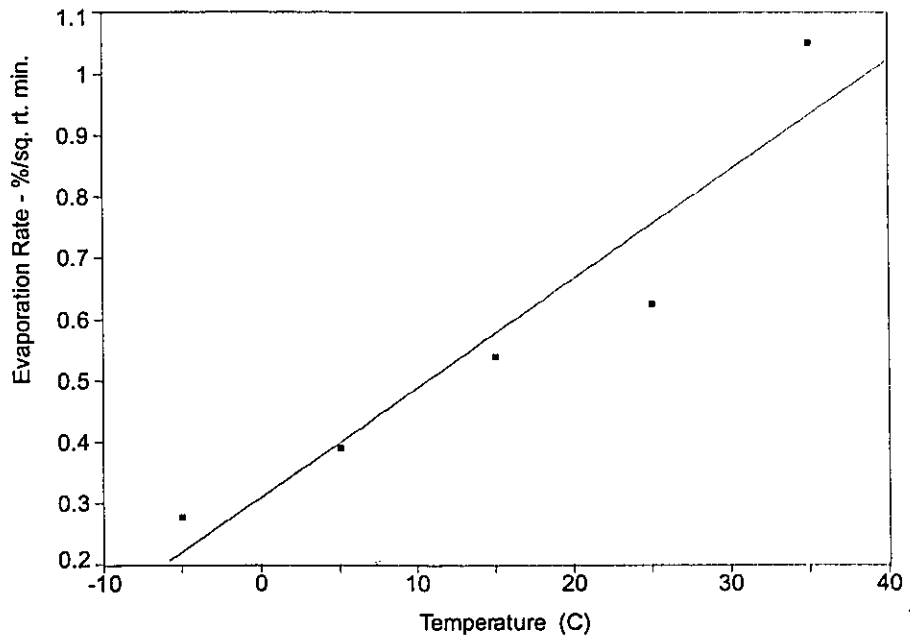


Figure 6.12

Correlation of Diesel Evaporation and Temperature

Rank 15 Eqn 1  $y=a+bx$   
 $r^2=0.899$  FitStdErr=0.109 Fstat=26.7  
 $a=0.308$   
 $b=0.0178$



program used to fit the equations. The regression coefficient ( $r^2$ ), the standard error of fit and the F statistic are given and then a and b, the equation constants. Figure 6.14 shows the same plot for the weight loss equation form of ASMB evaporation. These figures show the high correlation of the single-factor equation parameter (evaporation rate) with temperature using a linear equation. Regression coefficients range from a low of 0.90 to a typical 0.98. Table 6.4 lists the equations obtained performing these correlations. It is noted that the slopes obtained for the various equations, although slightly similar, are different enough to conclude that a unique equation is required for each oil.

The result that unique equations may be needed for each oil is of significant disadvantage to practical end use, and a way to accurately predict evaporation using other readily-available data is necessary. Two means to predict the evaporation were developed. The first data type is to use the value of the slope (fitted with one parameter) at 15°C as a basis for correlation. The assumption here is that the slopes of the temperature parameters are similar, so that they can be used as a predictor. It has already been noted that only light and medium crude oils display similar slopes. However, it will be fruitful to test such a hypothesis. The other observation noted is that the slope of the equation appears to correlate with the magnitude of the evaporation rate at 15°C. The second type of data used to study evaporation are distillation data. Distillation data are very common and often are the only data used to characterize oils. This is because the data is crucial in operating refineries. Crudes may even be priced on the basis of their distillation data. New procedures to measure distillation data are very simple, fast and repeatable (Jokuty and Fingas, 1994). Two separate ways of using the distillation data will be tried, first a portion of the curve, and second, the entire distillation curve slope.

The first method involves correlating the empirically-measured parameters at 15°C with both the slopes and the intercepts of the temperature equations. The latter data are given in Table 6.4. The equation base parameters (single-factor equation constant determined at 15 °C) used for the correlation are listed in Table 6.3. The regressions for the percentage equations are shown in Figures 6.15 (slope) and 6.16 (intercept). The regressions for the weight equations are shown in Figures 6.17 (slope) and 6.18 (intercept). These figures display fit information and the plot itself. The rank (in terms of

Figure 6.13

Correlation of Bunker C Light Evaporation and Temperature

Rank 8 Eqn 1  $y=a+bx$

$r^2=0.932$  FitStdErr=0.0130 Fstat=40.8

$a=0.0035$

$b=0.00262$

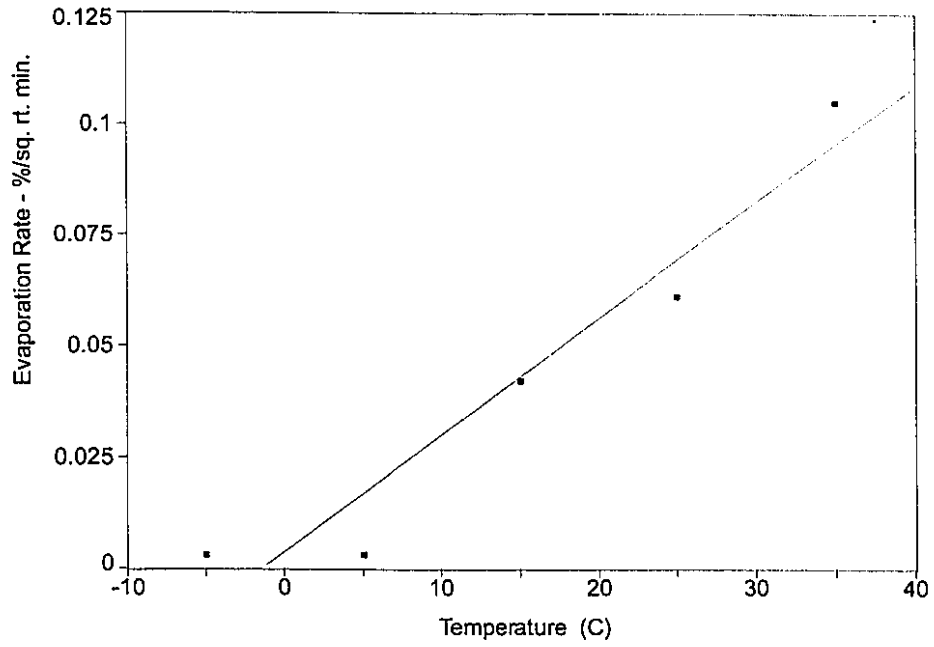


Figure 6.14

Correlation of ASMB Evaporation and Temperature  
Loss of Weight Equation

Rank 3 Eqn 1  $y=a+bx$

$r^2=0.957$  FitStdErr=0.0494 Fstat=67.0

$a=0.598$

$b=0.0128$

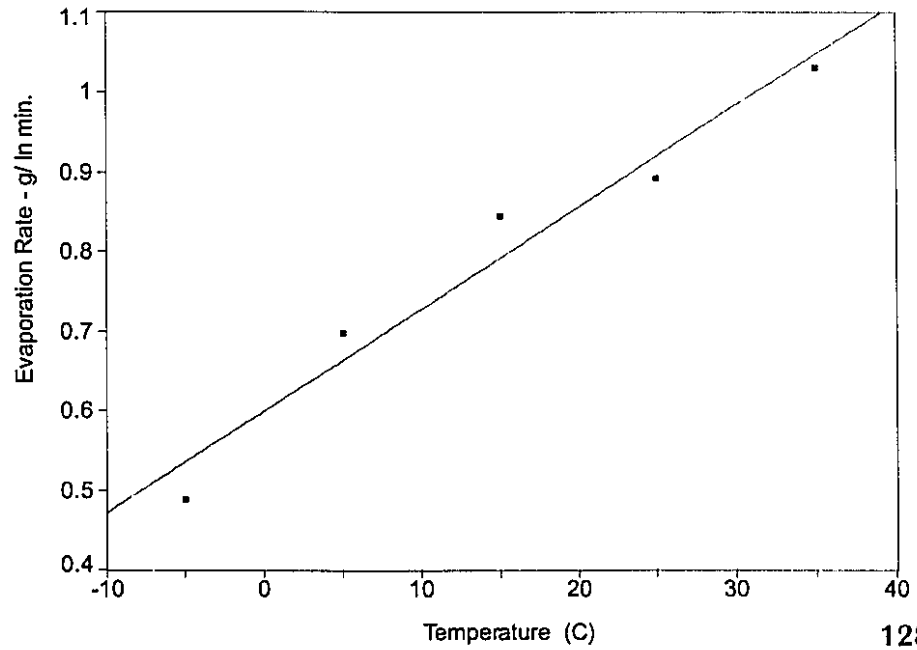


Table 6.3 Evaporation Rates or Single-Factor Equation Parameters

Weight Percent Parameters									
Temp -°C	ASMB	Gulfaks	Brent	Arab Lt.	Gasoline	Terra Nova	Statfjord	Diesel	Bunker C Lt.
-5	2.94	2.09	3.08	2.37	12.1	1.43	2.69	0.276	0.003
5	3.48	2.54	3.67	2.61	15.2	not done	3.3	0.389	0.003
15	4.22	2.81	4.23	3.11	15.9	2.39	3.65	0.538	0.042
25	4.45	3.01	4.44	3.5	16.9	3	4.1	0.623	0.061
35	5.13	3.54	5.07	3.78	21.9	3.26	4.69	1.05	0.105

Absolute Weight Parameters									
Temp -°C	ASMB	Gulfaks	Brent	Arab Lt.	Gasoline	Terra Nova	Statfjord	Diesel	Bunker C Lt.
-5	0.487	0.407	0.615	0.475	2.52	0.313	0.449	0.054	0.0006
5	0.697	0.509	0.735	0.523	3.13	not done	0.66	0.078	0.006
15	0.844	0.562	0.846	0.621	3.29	0.351	0.73	0.109	0.008
25	0.891	0.601	0.888	0.699	3.39	0.482	0.82	0.125	0.012
35	1.03	0.715	1.01	0.757	4.39	0.651	0.938	0.198	0.021

Table 6.4 Equations Relating Evaporation Rate and Temperature

Oil	Equation Parameters - %		Equation Parameters - Wt.		Parameter at 15 °C	
	Intercept	Slope	Intercept	Slope	Percent	Weight
Arab Lt.	2.52	0.0371	0.504	0.0074	3.11	0.621
ASMB	3.24	0.0535	0.598	0.0128	4.22	0.844
Brent	3.39	0.0475	0.677	0.00943	4.23	0.846
Bunker C Lt.*	0.0035	0.00262	0.0025	0.00468	0.042	0.008
Diesel*	0.308	0.0178	0.0626	0.00335	0.538	0.109
Gasoline	13.2	0.213	2.74	0.04	15.9	3.29
Gulfaks	2.29	0.0337	0.453	0.00708	2.81	0.562
Statfjord	2.67	0.06	0.499	0.0134	3.65	0.73
Terra Nova	1.36	0.0595	0.235	0.0108	2.39	0.351

\* fitted with square root equations

regression coefficient,  $r^2$ ) of the linear equation used for the regressions appears directly below the captions. Then the regression coefficient, fit standard error and the F statistic are given. Finally, the equation constants are given. The regression coefficients,  $r^2$ , are .86, .99, .76, and .99 for the four linear regressions. This indicates a very high correlation of the data and consequently, the fact that the temperature equations are relatively parallel. This is remarkable, especially since diesel and Bunker C light are best fit with square root curves rather than logarithmic ones. Gasoline was not included in this analysis because of the high rates involved (evaporation rates are an order of magnitude higher) and this skews the results, despite the increased regression coefficients with gasoline in the data set. The equations resulting from the regressions illustrated in Figures 6.15 to 6.18 were used to calculate rates. The empirical and calculated values are shown in Table 6.5. It can be seen that the calculated equation parameters are reasonable and are well within 5% of the empirical ones. This scheme could be used to estimate evaporation equations using only the rate at 15°C. The recalculation of the base equations is given in Table 6.6. The equations, in this case, were calculated using a direct linear factor in a spread sheet. The total difference squared between the calculated and the actual values was minimized. In the case of the percentage equation, the best relationship found, was 0.45 times the temperature and for the weight equation, the best relationship was 0.01 times the temperature difference plus the base found at 15°C. These might then also be described as formulae:

$$\text{percentage equation factor} = (B + 0.045(T-15)) \quad (6.2)$$

$$\text{and weight equation factor} = (B + 0.01(T-15)) \quad (6.3)$$

where B is the equation parameter at 15°C and T is temperature in Celsius.

This technique produces satisfactory results for all of the oils except for diesel and Bunker C light. These oils, as noted several times above, follow a square root equation rather than a logarithmic equation, so it is expected that correlation of logarithmic equations would not yield satisfactory results for these oils.

The second correlation noted was that of the distillation data and the equation parameters. The distillation data are taken from a standard reference work on oil (Whitcar et al., 1994). The form of the data used here is the percentage evaporated at a

Figure 6.15

Correlation of Percent Temperature Equation Slope and Base Parameter  
Rank 18 Eqn 1  $y=a+bx$   
 $r^2=0.858$  FitStdErr=0.00715 Fstat=36.3  
 $a=0.00894$   
 $b=0.0103$

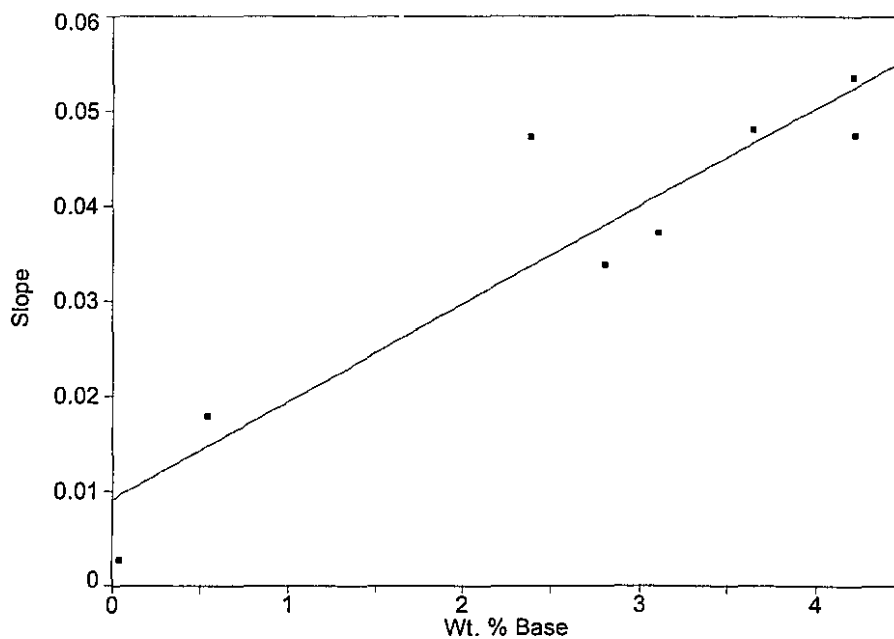


Figure 6.16

Correlation of Percent Temperature Equation Intercept and Base Parameter  
Rank 6 Eqn 1  $y=a+bx$   
 $r^2=0.994$  FitStdErr=0.106 Fstat=1030  
 $a=-0.0853$   
 $b=0.814$

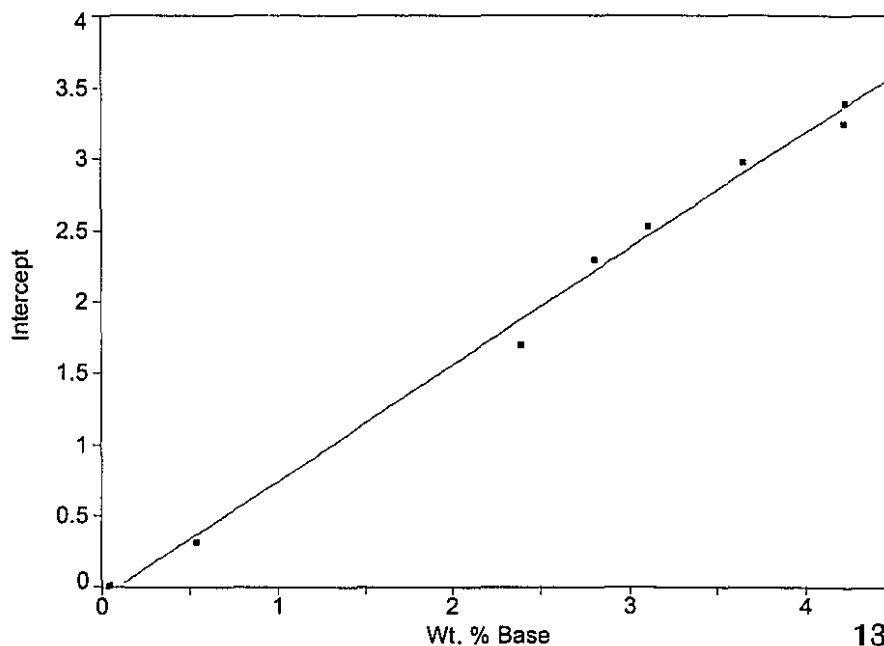


Figure 6.17  
Correlation of Weight Temperature Equation Slope and Base Parameter

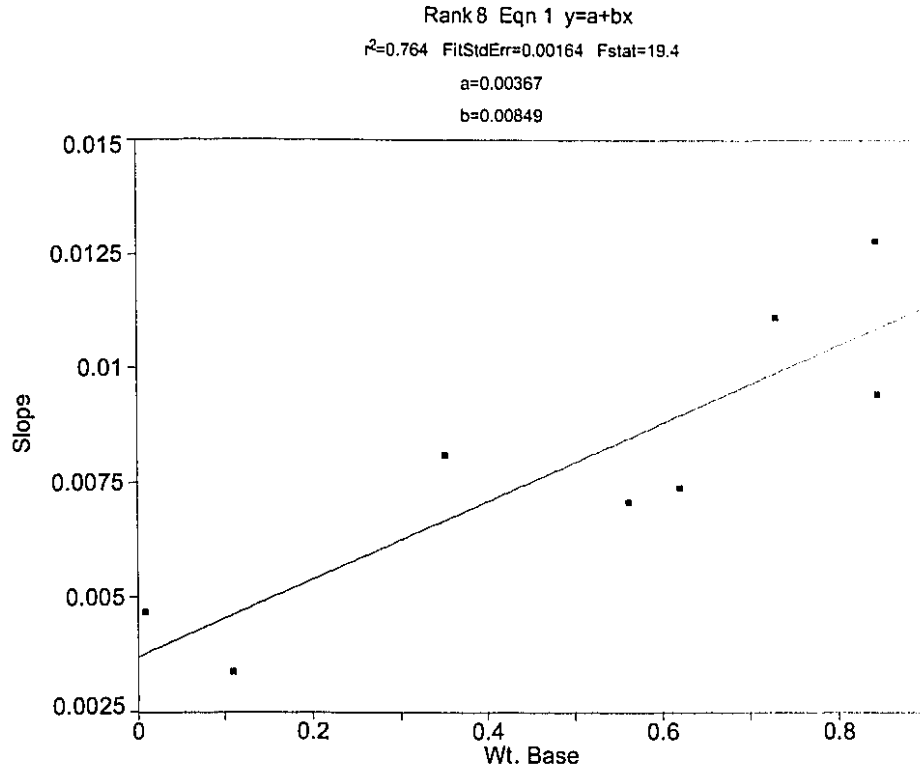


Figure 6.18 Correlation of Weight Temperature Equation Intercept and Base Parameter

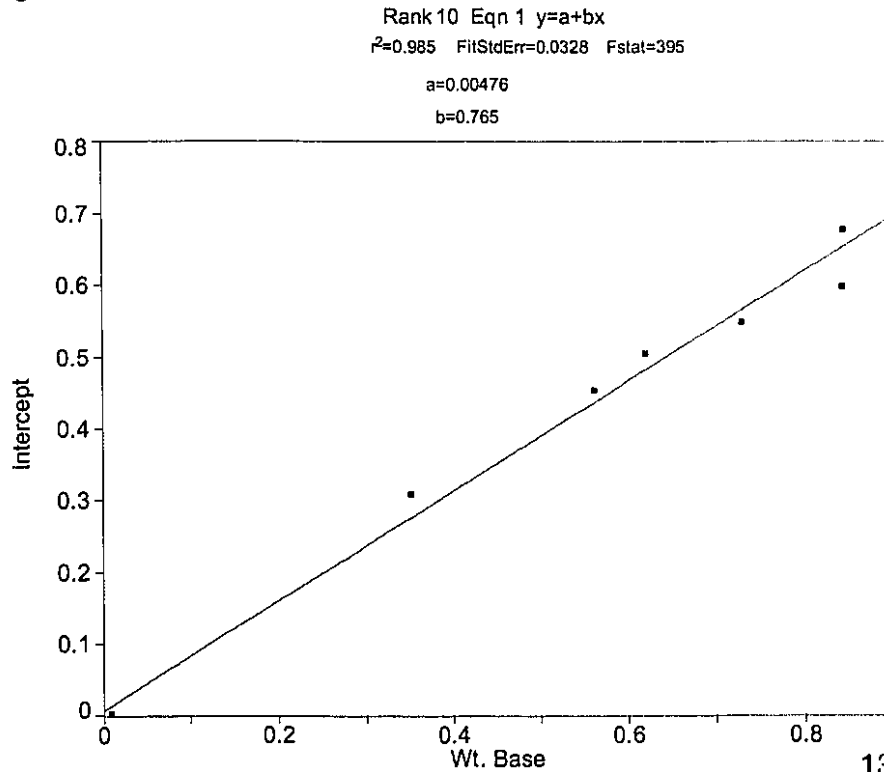


Table 6.5 Experimental and Calculated Temperature Equations

Oil	Equation Parameters - % *		Equation Parameters - Wt. *		Single-Parameter **	
	Intercept	Slope	Intercept	Slope	% Base	Wt. Base
ASMB	3.24	0.0535	0.598	0.0128	4.22	0.844
Gulfaks	2.29	0.0337	0.453	0.00708	2.81	0.562
Brent	3.39	0.0475	0.677	0.00943	4.23	0.846
Arab Lt.	2.52	0.0371	0.504	0.0074	3.11	0.621
Terra Nova	1.69	0.0473	0.308	0.0081	2.39	0.351
Statfjord	2.97	0.048	0.548	0.0111	3.65	0.73
Diesel	0.308	0.0178	0.0626	0.00335	0.538	0.109
Bunker C Lt.	0.0035	0.00262	0.0025	0.00468	0.042	0.008

\* The equation parameters consist of a slope and intercept which when combined yield a regular single-parameter equation at the given temperature

\*\* regular single parameter equations at 15°C

**Calculated Values from Regression Equations**

Oil	Equation Parameters - %		Equation Parameters - Wt.	
	Intercept	Slope	Intercept	Slope
ASMB	3.52	0.052	0.65	0.011
Gulfaks	2.37	0.038	0.435	0.008
Brent	3.53	0.053	0.652	0.011
Arab Lt.	2.62	0.041	0.48	0.009
Terra Nova	2.03	0.034	0.273	0.007
Statfjord	3.06	0.047	0.563	0.01
Diesel	0.52	0.014	0.088	0.005
Bunker C Lt.	0.12	0.009	0.011	0.004

**Equations used to Calculate the Values**

$$I = .00853 + .814 \cdot \text{base}$$

$$S = .00894 + .0103 \cdot \text{base}$$

$$I = .00476 + .765 \cdot \text{base}$$

$$S = .00367 + .00849 \cdot \text{base}$$

I = intercept S = slope

**Table 6.6 Evaporation Rates or Single-Factor Equation Parameters  
- Prediction Using Base Equations**

**Percent Parameters**

Temp -°C	ASMB	Gulfaks	Brent	Arab Lt.	Gasoline	Terra Nova	Statfjord	Diesel	Bunker C Lt.
-5	2.94	2.09	3.08	2.37	12.1	1.43	2.69	0.276	0.003
5	3.48	2.54	3.67	2.61	15.2	not done	3.3	0.389	0.003
15	4.22	2.81	4.23	3.11	15.9	2.39	3.65	0.538	0.042
25	4.45	3.01	4.44	3.5	16.9	3	4.1	0.623	0.061
35	5.13	3.54	5.07	3.78	21.9	3.26	4.69	1.05	0.105
Base	4.22	2.81	4.23	3.11	15.9	2.39	3.65	0.538	0.042

**Calculated Percent Parameters**

Temp -°C	ASMB	Gulfaks	Brent	Arab Lt.	Gasoline	Terra Nova	Statfjord	Diesel	Bunker C Lt.
-5	3.32	1.91	3.33	2.21	15	1.49	2.75	-0.36	-0.86
5	3.77	2.36	3.78	2.66	15.45	1.94	3.2	0.09	-0.41
15	4.22	2.81	4.23	3.11	15.9	2.39	3.65	0.54	0.04
25	4.67	3.26	4.68	3.56	16.35	2.84	4.1	0.99	0.49
35	5.12	3.71	5.13	4.01	16.8	3.29	4.55	1.44	0.94

*calculated using the equation value = base + .045 (T-15)*

**Absolute Weight Parameters**

Temp -°C	ASMB	Gulfaks	Brent	Arab Lt.	Gasoline	Terra Nova	Statfjord	Diesel	Bunker C Lt.
-5	0.487	0.407	0.615	0.475	2.52	0.313	0.449	0.054	0.0006
5	0.697	0.509	0.735	0.523	3.13	not done	0.66	0.078	0.006
15	0.844	0.562	0.846	0.621	3.29	0.351	0.73	0.109	0.008
25	0.891	0.601	0.888	0.699	3.39	0.482	0.82	0.125	0.012
35	1.03	0.715	1.01	0.757	4.39	0.651	0.938	0.198	0.021
Base	0.844	0.562	0.846	0.621	3.29	0.385	0.73	0.109	0.008

**Calculated Weight Parameters**

Temp -°C	ASMB	Gulfaks	Brent	Arab Lt.	Gasoline	Terra Nova	Statfjord	Diesel	Bunker C Lt.
-5	0.64	0.36	0.65	0.42	3.09	0.19	0.53	-0.09	-0.19
5	0.74	0.46	0.75	0.52	3.19	0.29	0.63	0.01	-0.09
15	0.84	0.56	0.85	0.62	3.29	0.39	0.73	0.11	0.01
25	0.94	0.66	0.95	0.72	3.39	0.49	0.83	0.21	0.11
35	1.04	0.76	1.05	0.82	3.49	0.59	0.93	0.31	0.21

*calculated using the equation value = base + .01 (T-15)*

given temperature (the alternative form is the temperature at which a fixed distillation percentage is given). Distillation data are common and are one of the few pieces of information that are routinely available for most oils because distillation data are used to rate petroleum products and feed-stock oils. The slopes of both the percentage and weight evaporation curves were correlated with the percentages of the product that distills at given temperatures. The resulting regression coefficient ( $r^2$ ) was plotted versus the temperature at which it was taken. Figures 6.19 and 6.20 show the results of these calculations. The plot of regression coefficients versus the temperatures at which the distillation data was obtained, was used in TableCurve to optimize the value at which the regression coefficient is highest. In each of Figures 6.19 and 6.20, the first ranked equation used to perform this optimization is given, then the regression coefficient of this optimization equation, the corrected regression coefficient, corrected for the degrees of freedom for this particular case, the standard error of fit, and the F statistic (all rounded to 3 significant figures). Finally the parameters of the optimization equation itself are given. Both figures show that the regression coefficient is maximum when distillation data of approximately 140 °C are used.

The distillation data at 140 °C was then correlated with the slopes and intercepts of the temperature-dependent equations to yield predictor values. The correlations are shown in Figures 6.21 to 6.24. These figures were created using TableCurve and include: the equation chosen (always a one-parameter linear one here), the regression coefficient ( $r^2$ ), the corrected regression coefficient, the standard error of fit, the F statistic, and finally, the value of the linear equation parameter, a ( $Y=ax$ ). The regression coefficient in all four cases (Figures 6.21 to 6.24, slopes and intercepts of both the percentage and weight equations) ranges from a low of 0.91 to a high of .96, indicating strong correlation. This belies the fact, however, that there is a wide-gap between the values for the crude oils and that for gasoline. When gasoline is removed, the remaining data show significant noise.

The values from this correlation were used to estimate the values of the single-parameter temperature equations. The results are given in Table 6.7. The best fit equations are:

**Figure 6.19 Optimization of Distillation and Temperature Slope - Percent Equation**

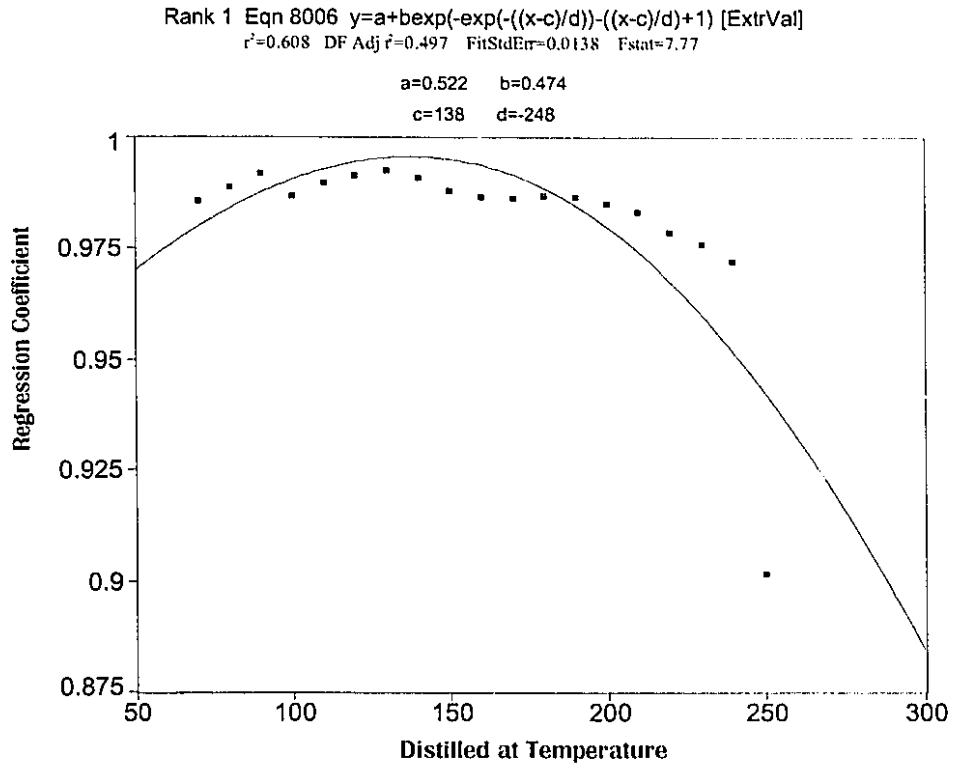


**Figure 6.20 Optimization of Distillation and Temperature Slope - Weight Equation**

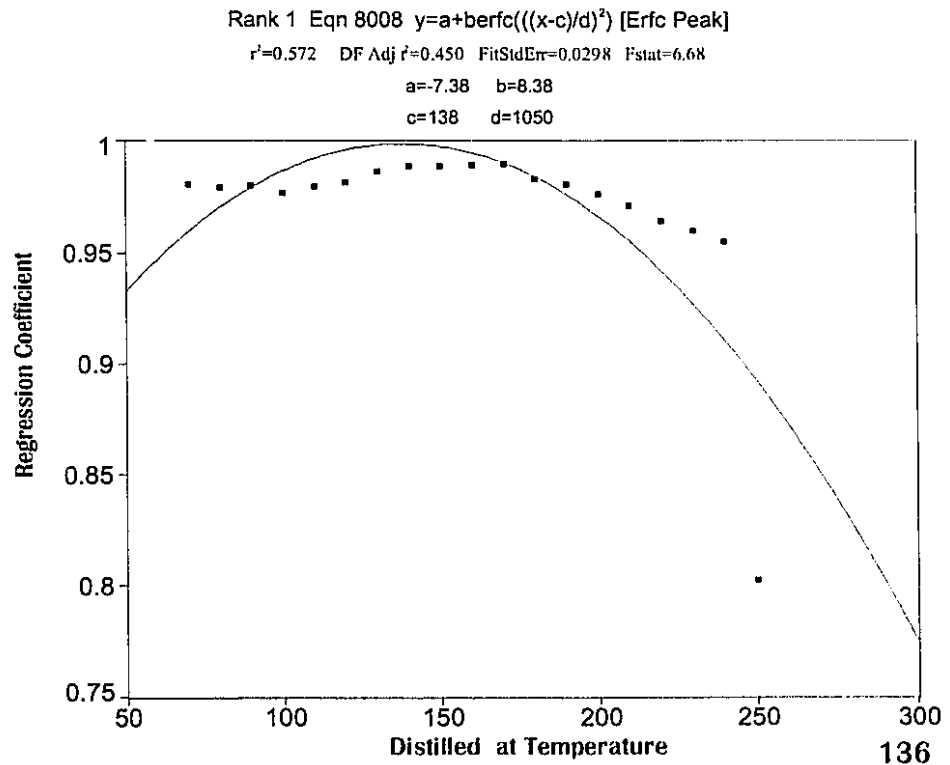


Figure 6.21 Correlation of Slope of Percent Equation and the Percent Distilled at a Given Temperature

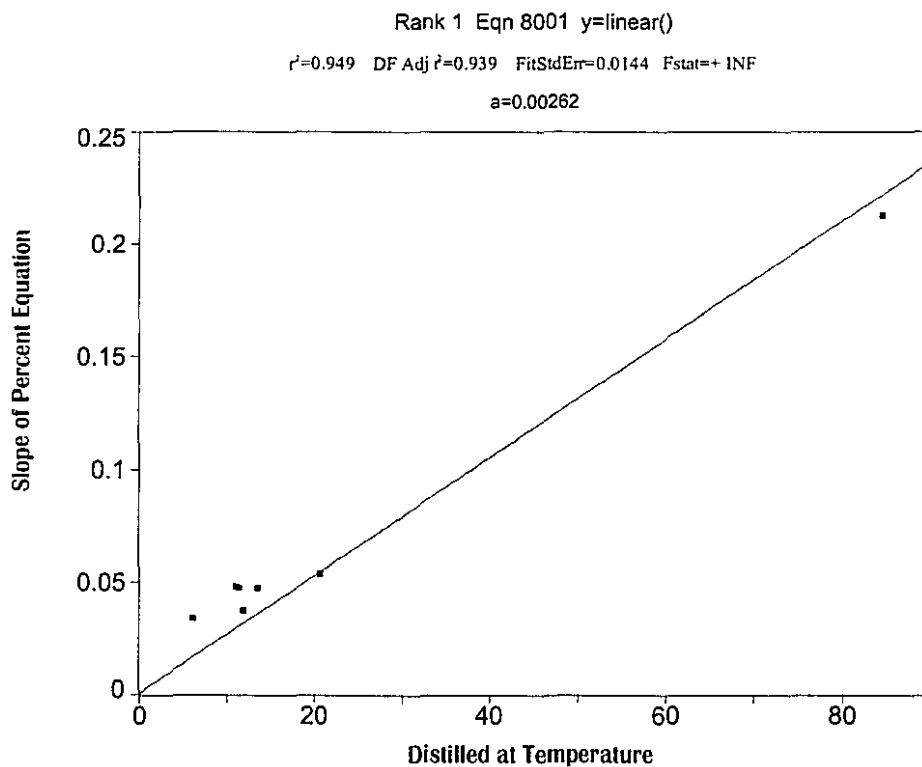


Figure 6.22 Correlation of Intercept of Percent Equation and the Percent Distilled at a Given Temperature

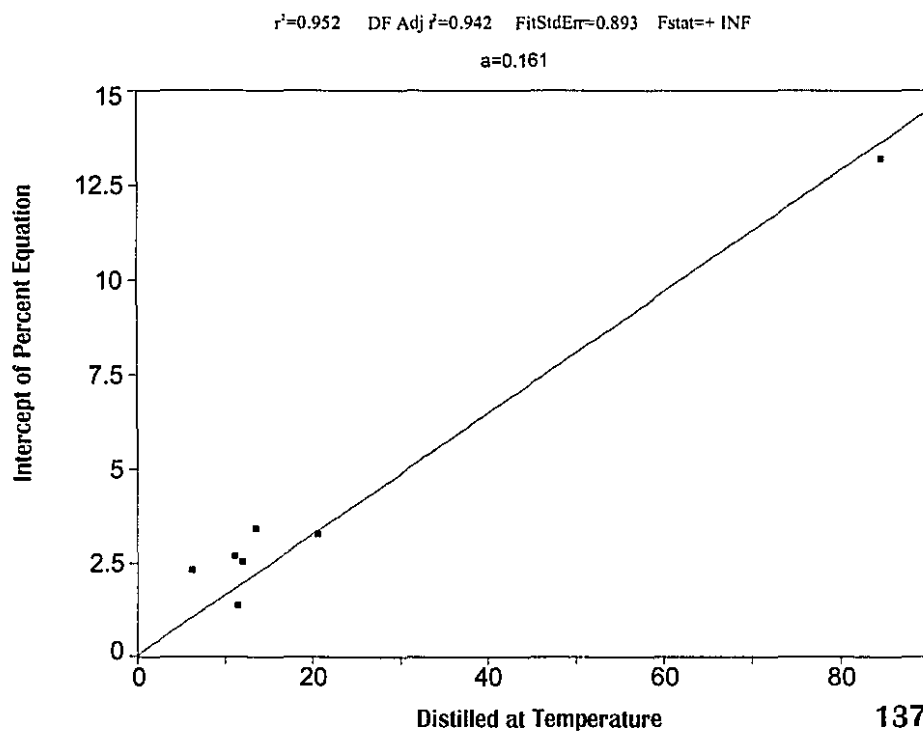


Figure 6.23 Correlation of Slope of Weight Equation and the Percent Distilled at a Given Temperature

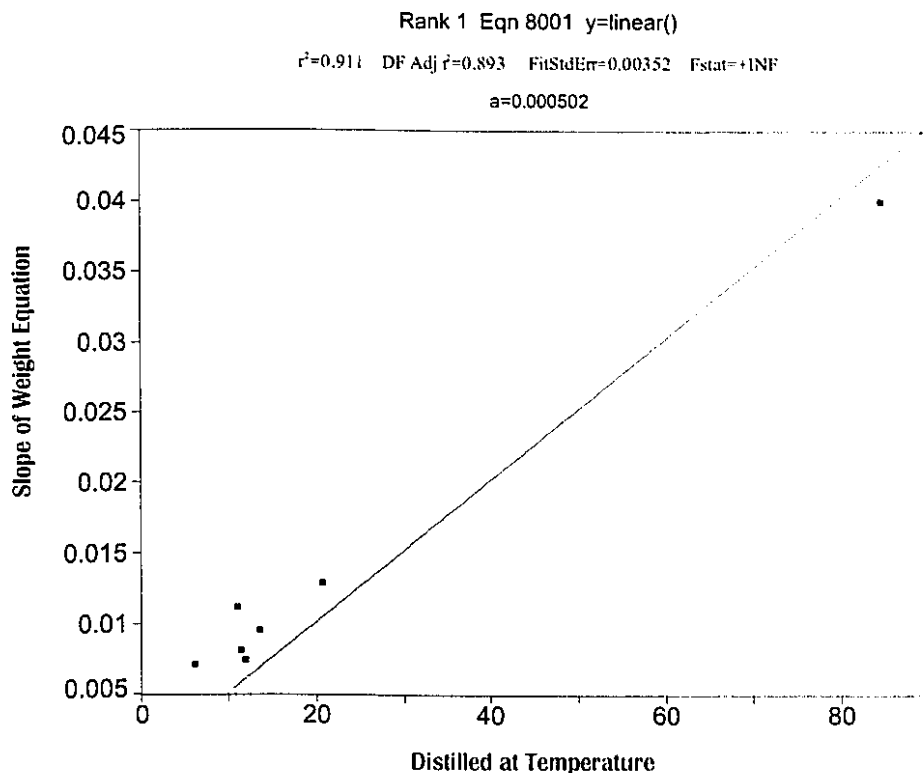
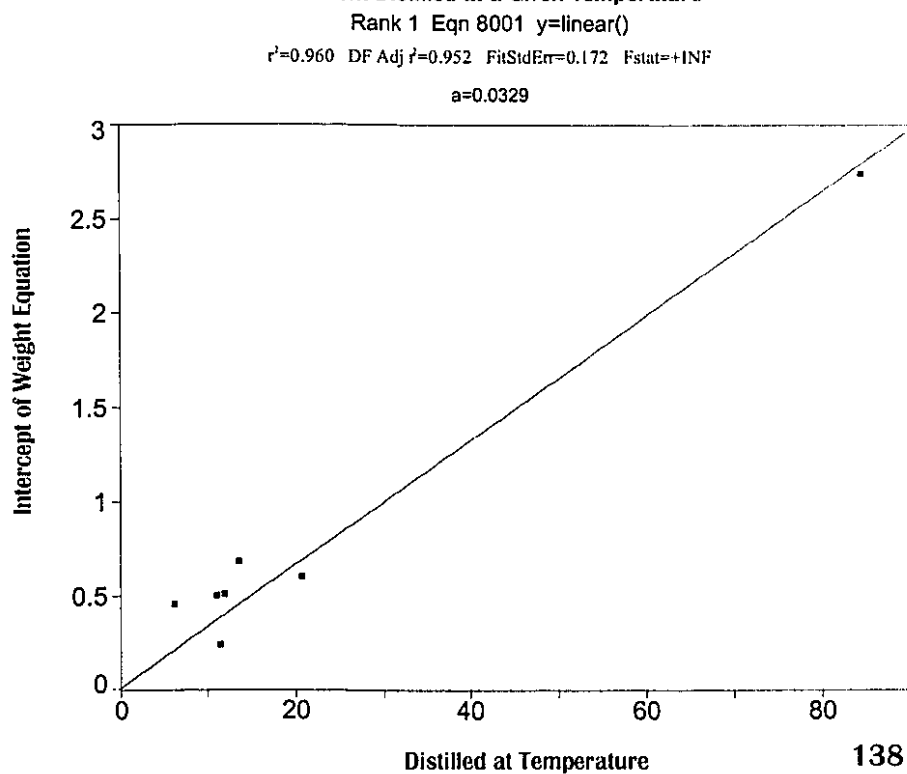


Figure 6.24 Correlation of Intercept of Weight Equation and the Percent Distilled at a Given Temperature



$$\text{percentage equation factor} = 0.161 D + 0.00262 TD \quad (6.4)$$

$$\text{and weight equation factor} = 0.329 D + 0.00502 TD \quad (6.5)$$

where D is the percent distilled at 140 °C.

Table 6.7 shows that, the results of this correlation are very good for ASMB and gasoline, but poorer for the other oils. The method could not be applied to Diesel and Bunker C light because there is no distillation data for 140 °C, however, a trial run at 160 °C, where there are data, shows that this calculation method was not successful. This is probably due to the difference in equations for these two oils (square root versus logarithmic) and a separate procedure would be needed to perform this calculation. Despite the variability in the fit qualities, the prediction of the temperature-equations using only distillation data implies that the evaporation and distillation data are indeed strongly related. In practical terms, this also implies that evaporation for oils where no evaporation data exist, can be predicted, with accuracy better than 50%, using only distillation data. No other alternatives are available at the moment.

## 6.5 Conclusions

Some researchers state that the relation of evaporation rate and temperature may be  $\log T/T$  or  $T^2$  (Stiver and Mackay, 1984). An examination of thermodynamics indicates that the relationship may be linear. Experimental evidence confirms that the relationship between evaporation rate and temperature is linear.

The rate of evaporation change with temperature is similar for the crude oils tested. Diesel fuel and Bunker C light, were fitted with square root equations, and show similar behaviour to the other test oils, all of which were best fit with logarithmic equations. Prediction methods for diesel fuel and Bunker C light would require separate analysis.

The change of evaporation rate (both as percentage and as absolute weight) can be predicted using two entirely different methods. First, the rate of temperature change correlates with the values of the evaporation rate at 15 °C. Equations deriving from this correlation yield predictions that are within about 10% of their empirical counterparts. The best fit equations are:

Table 6.7 **Evaporation Rates or Single-Factor Equation Parameters  
- Prediction By Use of Distillation Data**

**Percent Parameters**

Temp -°C	ASMB	Gulfaks	Brent	Arab Lt.	Gasoline	Terra Nova	Statfjord	Diesel	Bunker C Lt.
-5	2.94	2.09	3.08	2.37	12.1	1.43	2.69	0.276	0.003
5	3.48	2.54	3.67	2.61	15.2	not done	3.3	0.389	0.003
15	4.22	2.81	4.23	3.11	15.9	2.39	3.65	0.538	0.042
25	4.45	3.01	4.44	3.5	16.9	3	4.1	0.623	0.061
35	5.13	3.54	5.07	3.78	21.9	3.26	4.69	1.05	0.105
Distilled at 140 °C	20.6	6.6	13.5	11.9	84.7	11.4	12.2	0	0

**Calculated Percent Parameters**

Temp -°C	ASMB	Gulfaks	Brent	Arab Lt.	Gasoline	Terra Nova	Statfjord	Diesel	Bunker C Lt.
-5	3.05	0.98	2	1.76	12.53	1.69	1.8	0	0
5	3.59	1.15	2.35	2.07	14.75	1.98	2.12	0	0
15	4.13	1.32	2.7	2.38	16.97	2.28	2.44	0	0
25	4.67	1.49	3.06	2.7	19.18	2.58	2.76	0	0
35	5.21	1.67	3.41	3.01	21.4	2.88	3.08	0	0

*calculated using the equation value = .161 Distill + .00262 T Distill*

**Absolute Weight Parameters**

Temp -°C	ASMB	Gulfaks	Brent	Arab Lt.	Gasoline	Terra Nova	Statfjord	Diesel	Bunker C Lt.
-5	0.487	0.407	0.615	0.475	2.52	0.313	0.449	0.054	0.0006
5	0.697	0.509	0.735	0.523	3.13	not done	0.66	0.078	0.006
15	0.844	0.562	0.846	0.621	3.29	0.351	0.73	0.109	0.008
25	0.891	0.601	0.888	0.699	3.39	0.482	0.82	0.125	0.012
35	1.03	0.715	1.01	0.757	4.39	0.651	0.938	0.198	0.021
Distilled at 140 °C	20.6	6.1	13.5	11.9	84.7	11.4	11	0	0

**Calculated Weight Parameters**

Temp -°C	ASMB	Gulfaks	Brent	Arab Lt.	Gasoline	Terra Nova	Statfjord	Diesel	Bunker C Lt.
-5	0.63	0.2	0.41	0.36	2.57	0.35	0.37	0	0
5	0.73	0.23	0.48	0.42	3	0.4	0.43	0	0
15	0.83	0.27	0.55	0.48	3.42	0.46	0.49	0	0
25	0.94	0.3	0.61	0.54	3.85	0.52	0.55	0	0
35	1.04	0.33	0.68	0.6	4.27	0.58	0.62	0	0

*calculated using the equation value = .0329 Distill + .000502 T Distill*

$$\text{percentage equation factor} = (B + 0.045(T-15)) \quad (6.2)$$

$$\text{and weight equation factor} = (B + 0.01(T-15)) \quad (6.3)$$

where B is the equation parameter at 15°C and T is temperature in Celsius.

Second, the slopes and intercepts of the temperature equations correlate strongly with oil distillation data. These correlations yield predictions of the temperature-dependant evaporation equations that show good agreement with their empirical counterparts. The variability ranges from a high of about 50% for Gullfaks oil to a low of about 3% variance for ASMB. The equations based on distillation data are:

$$\text{Percentage equation factor} = 0.161 D + 0.00262 TD \quad (6.4)$$

$$\text{and weight equation factor} = 0.329 D + 0.00502 TD \quad (6.5)$$

where D is the percent distilled at 140 °C.

The correlations with distillation data indicate that evaporation is a similar or related process to distillation. The correlation with the evaporation data itself at 15 °C shows that the temperature effect is somewhat similar for most oils. This also indicates that the evaporation rate itself is correlated with the variance with temperature.

## REFERENCES

Lehr, W.J., R. Overstreet, R. Jones and G. Watabayashi, ADIOS-Automatic Data Inquiry for Oil Spill", *Fifteenth Arctic Marine Oilspill Program Technical Seminar*, Environment Canada, Ottawa, Ontario, pp 31-45, 1992.

Lehr, W., Private Communication, 1994.

Jokuty, P. and M.F. Fingas, "Oil Analytical Techniques for Environmental Purposes", in *Proceedings of the Seventeenth Arctic and Marine Oil Spill Program Technical Seminar*, Environment Canada, Ottawa, Ontario, pp. 245-260, 1994.

Stiver, W. and D. Mackay, "Evaporation Rate of Spills of Hydrocarbons and Petroleum Mixtures", *Environmental Science and Technology*, Vol. 18, American Chemical Society, Washington, D.C., pp 834-840, 1984.

Whiticar, S., M. Bobra, M.F. Fingas, P. Jokuty, P. Liuzzo, S. Callaghan, F. Ackerman and J. Cao, *A Catalogue of Crude Oil and Oil Product Properties (1992 Edition)*, Environment Canada Manuscript Report Number EE-144, Ottawa, Ontario, 643 p., 1993.

## **Chapter 7 Field Confirmation of Laboratory Methodology**

### **7.1 Abstract**

Three experiments were performed outdoors to confirm that laboratory conditions were representative of real conditions. The ASMB oil was evaporated from the same laboratory pans in two experiments and from a larger square pan in another case. The results are consistent with those from laboratory experiments. The field results can also be predicted using the equations where only the temperature and time are variables. Wind is not a determinant in results from outdoor experiments. This is again indicative that oil is not strictly boundary-layer regulated and that temperature and time are primary variables. These experiments were confirmation that the laboratory tests were representative of the real world.

### **7.2 Introduction**

The previous chapters presented results that showed the evaporation rates of oils and petroleum products are largely governed by temperature and time. The boundary-layer regulation as evidenced for water is not a governing factor for oil. As shown in laboratory experiments as described in Chapter 5, only during the first 5 minutes of exposure does the evaporation rate of ASMB, a typical volatile, light crude oil, exceed the rate at which the boundary layer effect is important. The experiments described in all the above work were conducted in the laboratory. It remains to be shown that similar, if not identical results could be achieved in the field. This chapter presents the results of three experiments run outdoors to verify the laboratory findings.

### **7.3 Experimental**

Experimental methodology largely followed the details described in Chapter 3. The weight loss dish for the first two outdoor experiments was a standard 139 mm diameter (ID) dish (Corning). This was the most frequently used test vessel in laboratory experiments. In the third outdoors experiment, a square metal pan was used with dimensions 212 X 212 mm with a depth of 48 mm. This was to demonstrate that pan

dimensions were not a factor in the experiments. Dimensions were measured using a Mitutoyo digital vernier caliper. Measurements were conducted in the following fashion. The tared pan was loaded with a measured amount of oil. Data acquisition was started and continued during the day. At the end of the day's experiment, the vessel was cleaned and rinsed with Dichloromethane.

Measurements were taken in a field 30 m north of the Environment Canada laboratory building. The balance and pan were sunk into the ground to ensure that the wind flow over the grass was level with the top of the pan. The predominant wind was from the northwest. There was 50 metres fetch of mowed grass, a single row of trees and another open field behind that. Behind the test plot, on both the south and east directions were the Environment Canada laboratory building at distances of 30 m. The computer and power supply were placed in plastic wraps offset one metre crosswind of the balance and weight pan.

Temperatures were measured using a Keithley 871 digital thermometer with a thermocouple supplied by the same firm. Temperatures were taken at the beginning and the end of a given experimental run, and were measured in the middle of runs at approximately 3-hour intervals. Air temperatures were taken.

Wind velocities were measured using a Taylor vane anemometer (no model number on the unit) and a Tadi, 'Digital Pocket Anemometer'. The wind velocities were measured at the same times as were the temperatures.

The experiments conducted are summarized in Table 7.1 and the measured environmental parameters in Table 7.2.

#### **7.4 Results and Discussion**

Figure 7.1 shows the fit of the October 3 data to a logarithmic curve. This figure (and the five subsequent figures) provides additional statistical data, including the rank of the particular equation chosen compared to the other 72 chosen to fit out of approximately 150 possible equations. The next value given is the regression coefficient ( $r^2$ ), which here is 0.92, the fit standard error, the F statistic and the parameters of the equation, 'a' and 'b'. The correspondence of the logarithmic curve to the data is good

Table 7.1 Summary of Outdoor Confirmation Experiments

Date	Oil Type	Days Length	Total Time (hr)	Pan Area (cm <sup>2</sup> )	Initial Loading (g)	Initial (mm) Thickness	Oil Type	End Wt.
Oct 3	ASMB	0.5	8	151	24.4	1.93	ASMB	17.8
Oct 4	ASMB	0.5	6	151	25.45	2.01	ASMB	19.67
Oct 5	ASMB	0.5	5	449	67.95	1.8	ASMB	49.52

Date	Oil Type	End Wt.	% Evap	Temp °C	Wind m/s	R <sup>2</sup> Best Equation	Best Equation	Single Parameter
Oct 3	ASMB	17.8	27	7.4	0.46	0.926	ln	3.9
Oct 4	ASMB	19.67	23	9.1	0.29	0.821	ln	2.89
Oct 5	ASMB	49.52	27	7.1	0.53	0.834	ln	3.92

Table 7.2 Temperature and Wind for Outdoors Experiments

Experiment	Time	Temperature	Wind Velocity
		°C	m/s
3-Oct	9:30	5.3	0.65
	11:45	6.5	0.58
	14:45	8.7	0.14
	17:17	8.2	0.25
	Time Weighted Average	7.4	0.46
4-Oct	8:54	6.8	0.35
	11:00	9.7	0.25
	14:45	9.4	0.28
	14:48	9.4	0.28
	Time Weighted Average	9.1	0.29
5-Oct	9:08	5.6	0.03
	11:45	8	1.01
	13:30	7.2	1.63
	13:56	7.2	1.63
	Time Weighted Average	7.1	0.53

considering the noise caused by wind on the scale. It can be seen from Figure 7.1 that the logarithmic curve over-predicts the evaporation rate at the start and then under-predicts slightly at the end of the evaporation period. This is not typical of the results presented in the thesis and may be a result of changing temperatures throughout the experiment. Figure 7.2 shows the fit of a single-parameter logarithmic equation to the data. This figure shows that the fit is degraded somewhat from the standard two-parameter equation and that the curve fits poorly at the start and end of the process.

Figure 7.3 shows the fit of the logarithmic curve to the October 4 data. The logarithmic curve has an acceptable regression coefficient ( $r^2 = .82$ ) but the trend of not fitting the start and end of the curve is more exaggerated here. Figure 7.4 shows the application of another curve from the top-ranking equations. The curve chosen here is that of the square root curve, which in this rare case fits the data better than does the logarithmic one. The regression coefficient is very high (0.98), but the upward trend at the end of the time data would yield less reliable results for long-term weathering.

Figure 7.5 shows the fit of a logarithmic curve to the October 5 data. The regression curve is similar to the October 4 case and similar trends are seen for the curve, over-predicting at the start and under-predicting at the end. Another curve of the fit set was used to correlate the data. This is illustrated in Figure 7.6. The curve is a modified logarithmic curve ( $y = a + b (\ln x)^2$ ), which fits the data with an approximate regression coefficient of 0.99. This indicates the basic form of the equation is logarithmic.

All three days' data show that the logarithmic curve fits the ASMB evaporation data acceptably, however, not as well as in the laboratory. Possible explanations for this include: 1. The slow temperature change during the day gradually increased the evaporation rate and thus a single predictive method will not fit as well. 2. The noise of wind on the electronic balance degrades the ultimate fit. 3. The lower temperatures meant that fewer components were evaporating than usual and thus the curve should actually be a square root equation or something between this and the logarithmic equation. 4. Different physics are operative in the field than in the laboratory. It will be shown here that the results are, in fact, that close to the laboratory findings that hypothesis 4 can be discarded and 1 is the primary effect. To re-emphasise, the outdoors

**Figure 7.1** Log Curve Fit of October 3 Data

Rank 12 Eqn 13  $y=a+b\ln x$   
 $r^2=0.945$   $DFAdj\ r^2=0.944$   $FitStdErr=1.97$   $Fstat=2460$

$a=4.72$   
 $b=5.03$

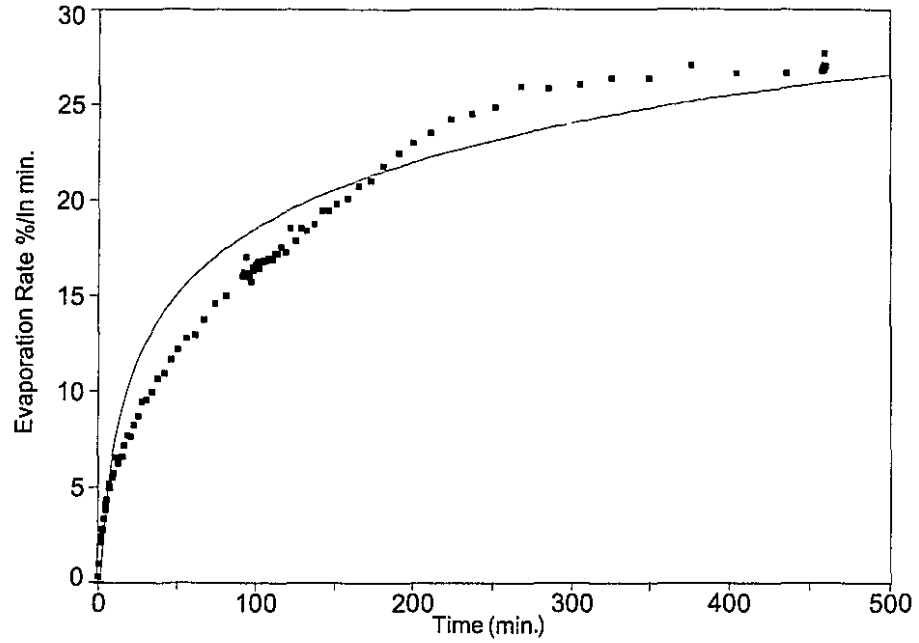


**Figure 7.2** Single-Factor Log Curve Fit of October 3 Data

Rank 2 Eqn 8001  $y=simlog()$   
 $r^2=0.913$   $DFAdj\ r^2=0.913$   $FitStdErr=2.46$   $Fstat=INF$

$a=4.15$

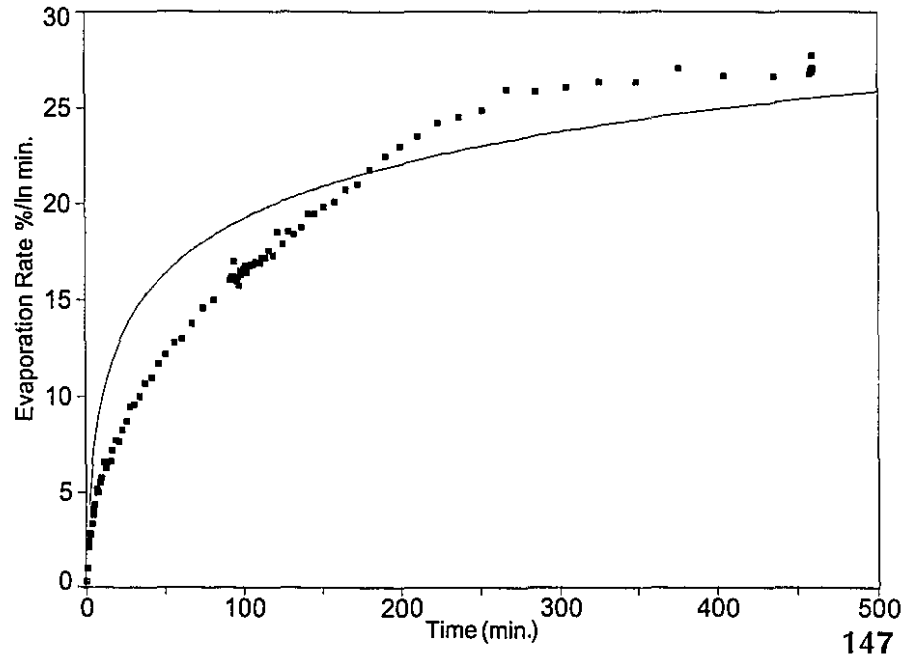


Figure 7.3

Log Curve Fit of October 4 Data

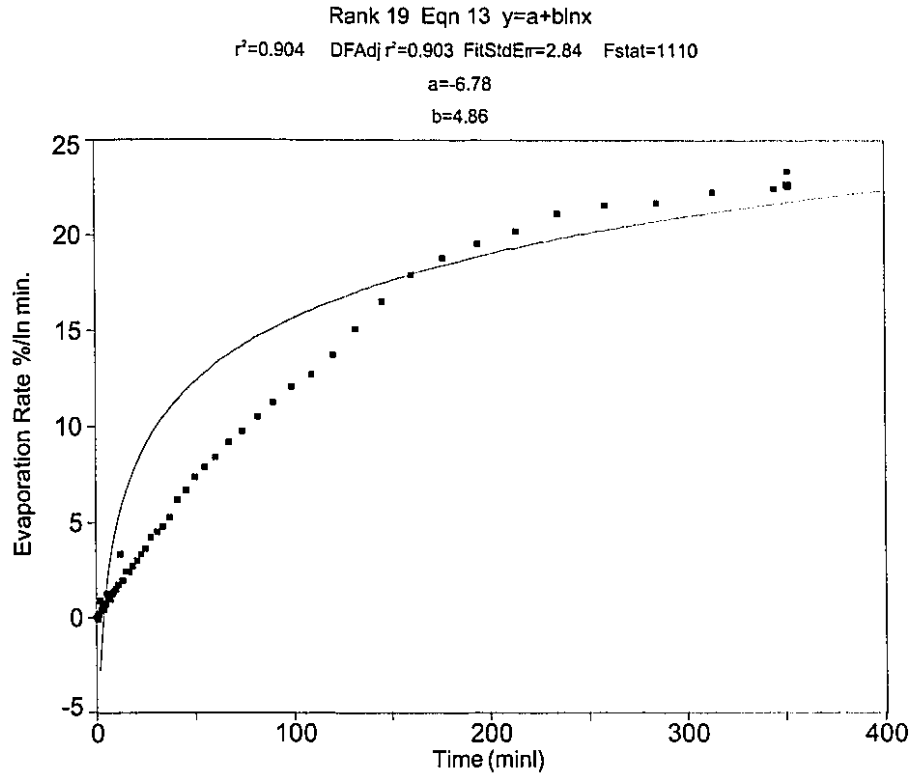


Figure 7.4

Square Root Curve Fit of October 4 Data

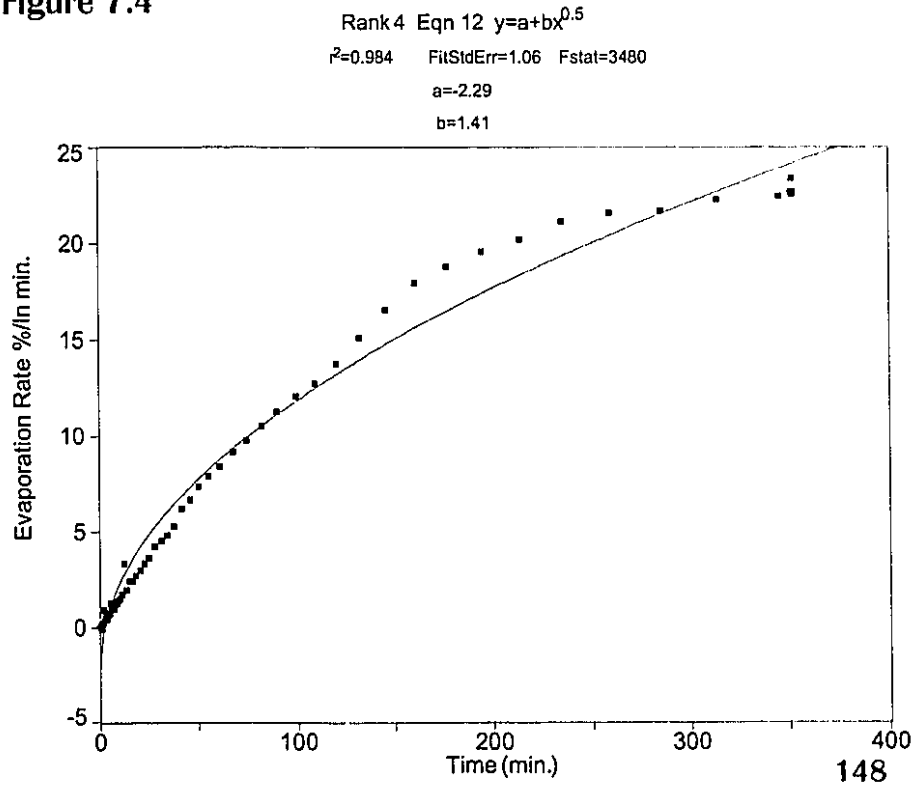


Figure 7.5

Log Curve Fit of October 5 Data

Rank 29 Eqn 13  $y=a+b\ln x$

$r^2=0.887$  DF Adj  $r^2=0.884$  FitStdErr=2.55 Fstat=590

$a=-5.43$

$b=5.56$

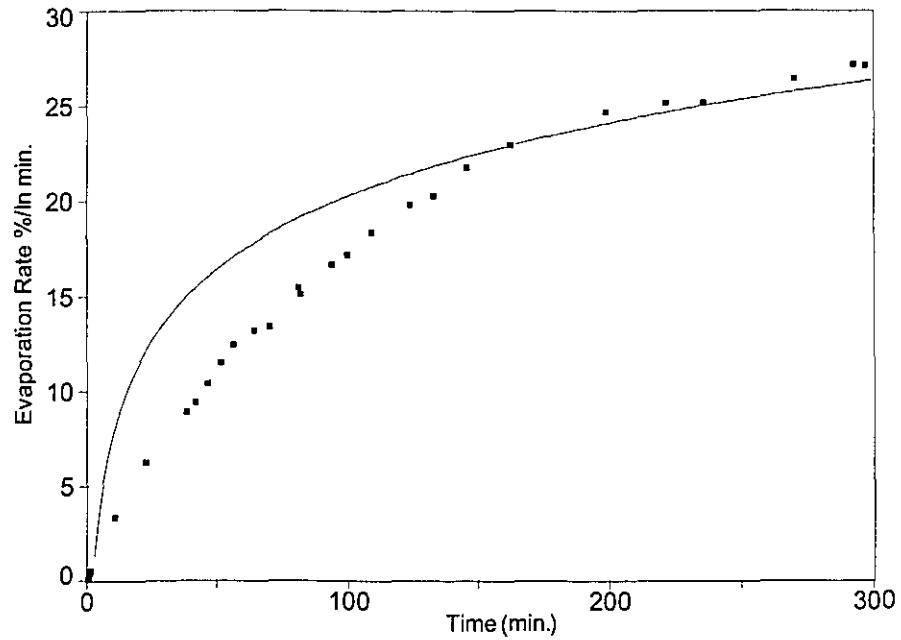


Figure 7.6

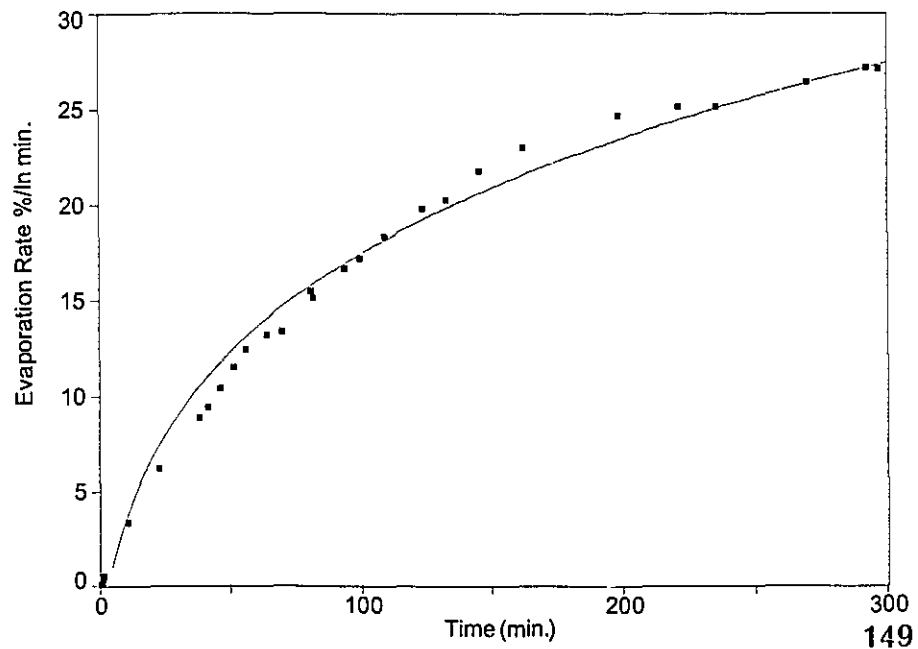
Modified Log Curve Fit of October 5 Data

Rank 6 Eqn 10  $y=a+b(\ln x)^2$

$r^2=0.986$  FitStdErr=1.01 Fstat=1820

$a=-1.38$

$b=0.884$



experiments yield results that compare in overall magnitude to those found indoors and the poorer data fits from the outdoors experiments will be shown to be largely due to outdoor temperature variations.

During the outdoors experiments, temperatures were measured with an air probe, and it was noted that the substrate (eg. pan) temperatures were less than that of the air - especially in the early morning when each experiment was started. Table 7.2 shows that the air temperatures typically started at 5 °C and then rose to about 10 °C at noon and then fell to about 7 °C by the experiment's end at the close of the day. This rate increase could account for a changing evaporation rate throughout the day and thus the poorer logarithmic curve fit.

The major purpose in conducting the outdoors experiments was to test the hypothesis that the factors of influence noted during the indoor experiments are also operative outdoors. In particular, it was a test of the numerous findings in the laboratory such as the finding that oil evaporation is not strictly boundary layer regulated and thus the wind can be ignored. Furthermore, a test of the temperature equations found in Chapter 6 above is in order.

Figures 7.7 to 7.9 present the results of fitting the prediction equations to the data from October 3, 4 and 5. A "standard calculation" is presented which uses the one-term logarithmic equation calculated from the predictive equation for ASMB calculated in Chapter 6 above (from Table 6.5) where the equation for ASMB oil is given as:  $(3.52 + 0.052 \times \text{temperature}) \times \ln(t)$ . The temperature taken in each case is the average calculated in Table 7.2. A "cumulative calculation" was also done to examine the effects of a different form of calculation where the temperature at the time was used rather than the average. The temperature was calculated to be a linear variation between measurements. The evaporation between each time interval was calculated using the same basic equation as for the standard calculation,  $\text{fraction evaporated} = (3.52 + .052 \times \text{temperature}) \times (\ln(t) - \ln(t-1))$ . This calculation was performed to see if the effect of averaging the temperature data is significant. As can be seen from Figures 7.7 to 7.9, both types of calculations predict the end point (at the end of the time period) very well and that the cumulative calculation generally yields a slightly better result. The curves of

Figure 7.7

### Prediction of October 3 Results

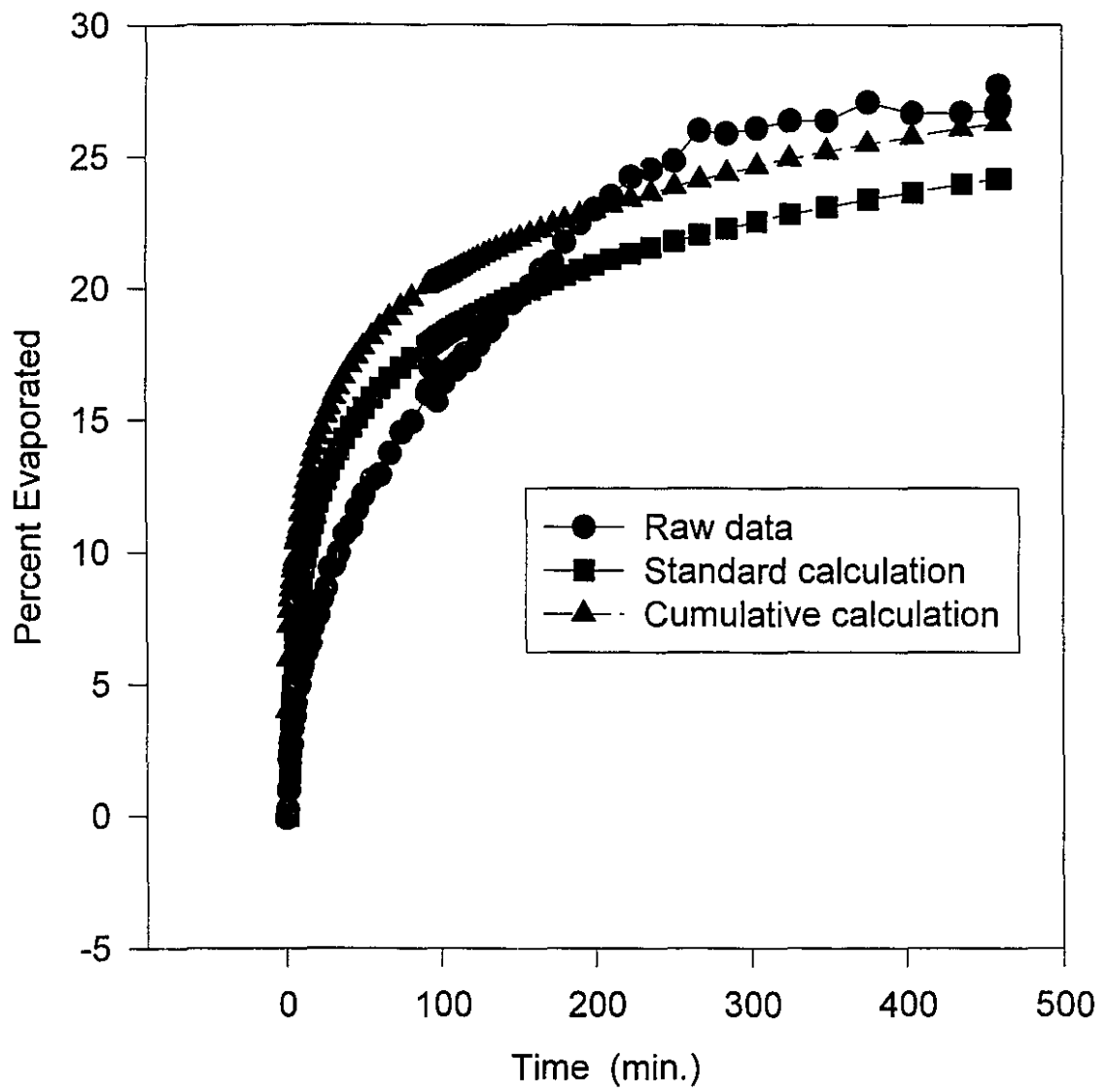


Figure 7.8

### Prediction of October 4 Results

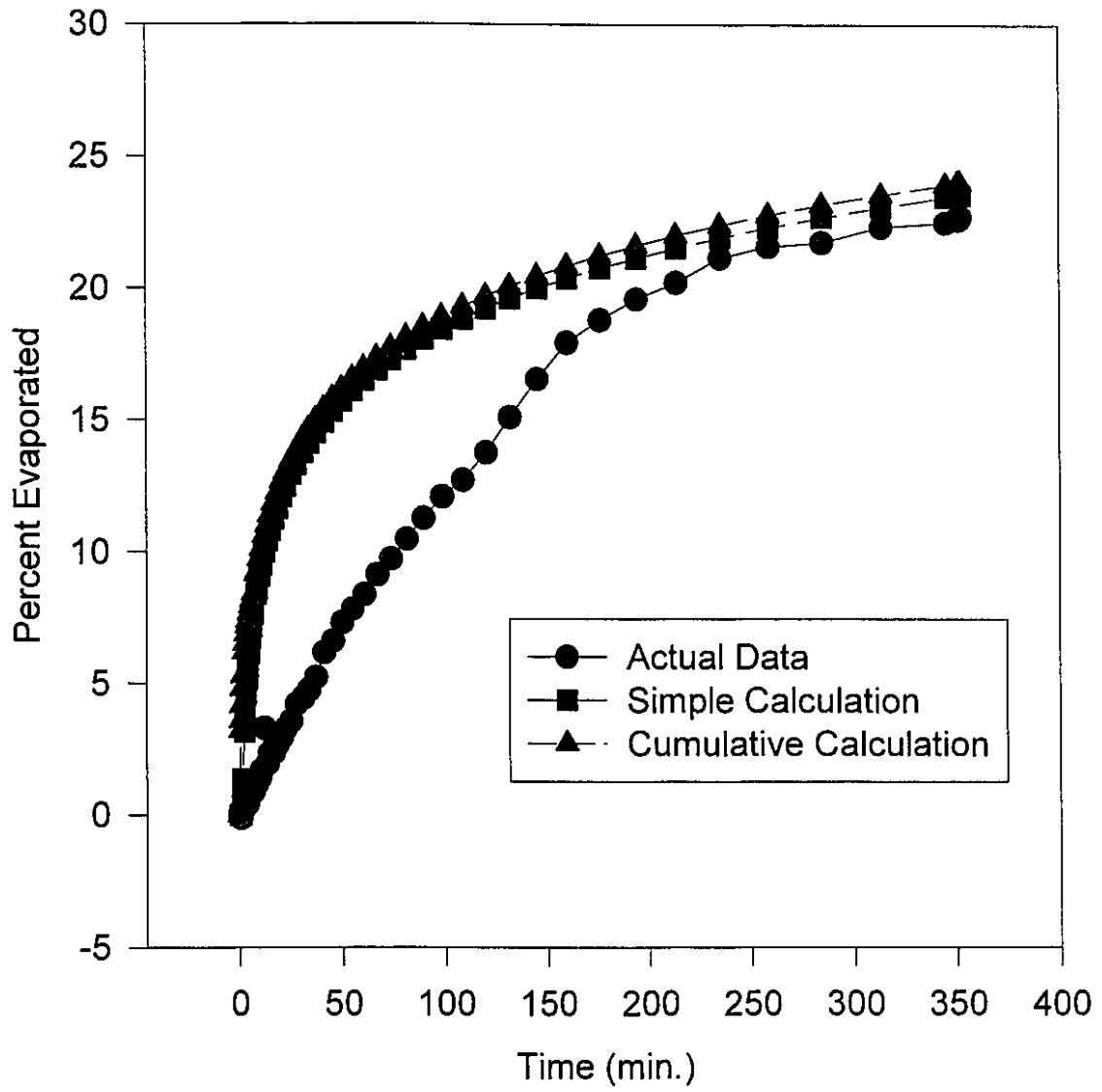
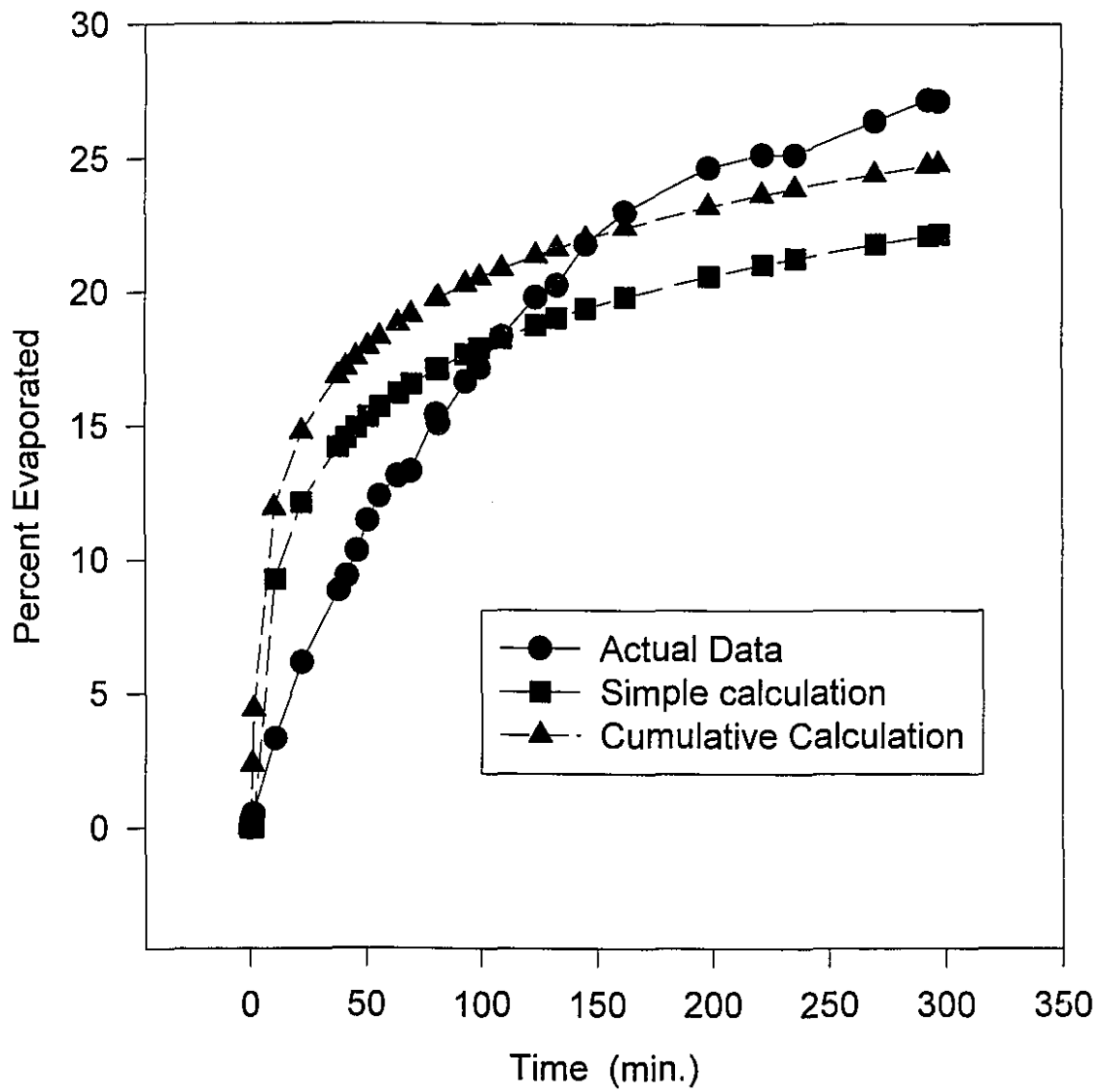


Figure 7.9

### Prediction of October 5 Results



the actual data in these figures rise slower than predicted at the start, especially for the October data. This is most likely a result of a cold evaporation pan at the start of the experiment.

The ability of the predicted evaporation curves to fit the outdoor data suggests that the wind is not a prime factor in the evaporation of the oil and that the laboratory conditions adequately simulate the conditions in the outdoors. This is true for the conditions prevalent in the laboratory and outdoor experiments. Furthermore, the use of a larger, square pan for the October 5 experiments and that fact that the results from these tests were compatible to other results, reinforces the previous statement.

In the outdoors experiments, the wind profiles would be governed by the upstream surface roughness, ie. grass. The internal boundary layers produced by a discontinuity in air flow between grass-covered ground and an aerodynamically smooth oil surface might be different.

## **7.5 Conclusions**

The results from the outdoors experiments are not dissimilar to those achieved under laboratory conditions. This confirms that the methods and conditions in the laboratory are consistent with those outdoors. The outdoors results can be predicted using equations developed in the laboratory with only temperature and time as variables. Wind in the outdoors experiment does not change the evaporation rate. This also confirms that the oil evaporation is not strictly boundary-regulated.

## **Chapter 8 - Development of Evaporation Prediction Equations**

### **8.1 Abstract**

A study of the evaporative characteristics of 19 different crude oils and petroleum products was conducted. Best-fit equation parameters were determined for both percentage loss by time and absolute weight loss. All oils except for three (diesel fuel, FCC Heavy Cycle and Bunker C light) were found to fit logarithmic curves. The exceptions noted, fit square root curves with time. The equation constants were correlated with oil distillation data. The equation constants correlated highly with the percentage distilled at 180 °C ( $r^2$  ranged from 0.98 to 0.74). Using this correlation, equations were developed by which the oil evaporation can be predicted using the distillation data alone.

### **8.2 Introduction**

The previous chapters presented results that showed the evaporation rates of oils and petroleum products are largely governed by temperature and time. Equations were derived which correlated the temperature changes to the equations with both, the empirical findings themselves and with distillation data. This work still left the basic parameter of the evaporation rate at 15 °C to be determined empirically. The experiments to determine these empirical parameters involve experiments lasting several days. Obviously, means to predict these equations would be convenient for users of the data. Furthermore, it is necessary for full understanding of the evaporation process to determine if there are relationships between the evaporation parameters and other properties of oil.

### **8.3 Experimental**

Details of experimental methodology are given in Chapter 3. Experiments were conducted both in a fume hood at laboratory temperatures or in a constant temperature chamber. These were also described in Chapter 3.

The experiments conducted are summarized in Table 8.1 The properties of the test

liquids are given in Table 8.2.

Distillation data are used for correlations. All Data are taken from an oil properties collection by Environment Canada (Whiticar et al., 1993). Data used in this study are summarized in Table 8.3.

#### **8.4 Results and Discussion**

Distillation data were directly correlated to the evaporation rates determined by experimentation. Empirical rates, given as a percentage evaporated, are listed in Table 8.1. In addition, evaporation rates as absolute weight (in grams) were also calculated and used in these studies. The latter data are generally not available in as accurate form as the former and to interpret them, total mass of the oil evaporating must be divided by the amount used in the experiment, typically 20 g. Thus, the more accurate form is used here. The distillation data are available in two forms, percent evaporated at a given temperature value (as used here) and as temperature at which a fixed amount of material is lost. The distillation curves are illustrated in Figure 8.1. Several trends are evident. Gasoline, the most volatile of the petroleum products, shows this volatility as a distinct curve on the left of the other curves. Diesel and FCC Heavy Cycle show a narrow boiling point range between about 160 and 260 degrees. It is interesting that these two products, of all those listed here, show best-fit evaporation equations with the square root of time, rather than the logarithm. This was shown in Chapter 4 to be the result of the number of components evaporating. This conclusion is confirmed by the distillation curve, which indicates that the products in question consist of a few components over a narrow boiling point range. Figure 8.1 shows that most crude oil distillation curves are similar. Two curves which are slightly different than the others and pass through the bulk of the other curves are: Amauligak and Issungnak, both waxy, but light, Beaufort Sea crude oils. Bunker C and Bunker C light show the typical expected behaviour of heavy residual products.

The percentage distilled at each temperature was correlated with the equation parameter (sometimes referred to here as the evaporation rate). An example of such a correlation is shown in Figure 8.2. This figure shows the correlation of the percentage

Table 8.1

Summary Table of Experiments Involving Different Oils

Series-year-93	Date	Oil Type	Days Total Length	Total Time (hr)	Pan (cm <sup>2</sup> ) Area	Initial Load (g)	Initial (mm) Thickness	End Wt.	% Evap	Temp C	Wind m/s	R <sup>2</sup> Best Equation	Best Equation	Single Parameter
2	July 2	ASMB	1	15	151	20.2	1.59	14	30	22.4	0	0.937	In	4.05
3	Sept 22	ASMB	3	71	151	24.8	1.96	16	37	23.1	0	0.976	In	4.49
4	Nov 1	ASMB	2	51	151	20.5	1.62	14	32	20.9	0	0.994	In	4.28
5	Dec 8	ASMB	2	46	151	19.5	1.54	13	35	17	0	0.998	In	4.37
	Dec 10	ASMB	2.5	65	151	21.5	1.69	14	34	20.2	0	0.967	In	4.28
6	Dec 24	Bunker	4	99	151	252	17.13	250	1	11.8	0	0.687	In	0.048
	Dec 29b	Gasoline	0.5	2	151	20	1.81	2.3	89	19.5	0	0.889	In	15.9
	Dec 29c	Bunker	3	72	151	20.1	1.37	19	6	19.6	0	0.875	In	0.473
94	Jan 1	Prudhoe	2	49	151	20	1.49	17	15	21.5	0	0.993	In	1.65
	Jan 3	Prudhoe	3	71	151	20	1.49	16	19	21.3	0	0.997	In	2.17
	Jan 10	Brent	1	27	151	20	1.59	12	38	21.6	0	0.991	In	4.06
	Jan 12	Brent	3	67	151	30	2.38	20	35	19.5	0	0.991	In	4.03
	Jan 15	Brent	3	74	151	50	3.97	33	33	18.1	0	0.986	In	3.97
	Jan 18	Ericcott	2	42	151	50	3.62	46	9	20.1	0	0.972	In	0.926
	Jan 20c	Issungnak	2	47	151	20	1.56	16	22	19	0	0.947	In	2.23
	Jan 22	Terra Nova	2	43	151	20	1.54	17	17	18.8	0	0.971	In	1.93
	Jan 28b	Prudhoe Bay	8	190	151	30	2.23	23	24	11.2	0	0.986	In	2.36
	Feb 5	Santa Clara	2	48	151	20	1.44	16	18	24.1	0	0.967	In	2.3
8	April 14	FCC heavy	2	46	151	20	1.46	16	18	24	0	0.986	sq. rt.	0.31
	April 25	ASMB	1	24	151	20	1.58	14	32	15	0	0.995	In	4.22
16	Dec 23	Komineft	5	121	151	12.9	1.02	8.8	32	23.3	0	0.995	In	3.4
95	Jan 3	Federated	4	95	151	20	1.58	13	34	15	0	0.985	In	3.99
	Jan 11	Avalon	3	70	151	20	1.56	18	9	15	0	0.96	In	2.08
	Jan 14	Gulfaks	4	89	151	20	1.61	15	26	15	0	0.983	In	2.89
	Jan 18	Brent	3	79	151	20	1.58	13	36	15	0	0.995	In	4.23
	Jan 21	Amaulgak	5	120	151	20.1	1.5	15	24	15	0	0.952	In	2.3
17	Jan 26	Terra Nova	4	96	151	20	1.54	15	23	15	0	0.927	In	2.39
	Feb 15	Statfjord	5	118	151	20	1.59	13	33	15	0	0.983	In	3.65
18	Mar 10	Gulfaks	3	72	151	20	1.5	15	26	15	0	0.984	In	2.81
19	Mar 22	Arabian Lt	5	101	151	20	1.53	14	28	15	0	0.993	In	3.11
	Mar 26	Bunker C lt	4	88	151	20	1.37	19	3	15	0	0.99	sq. rt.	0.0422
	Mar 30a	Gasoline	0.5	3	151	21.1	1.97	3.1	85	15	0	0.956	In	16
	Mar 30b	Gasoline	0.5	3	151	20.4	1.91	3.1	85	15	0	0.955	In	15.8
	Mar 30c	Diesel	4	89	151	20.3	1.66	13	38	15	0	0.991	sq. rt.	0.538

Table 8.2

**Properties of the Test Liquids**

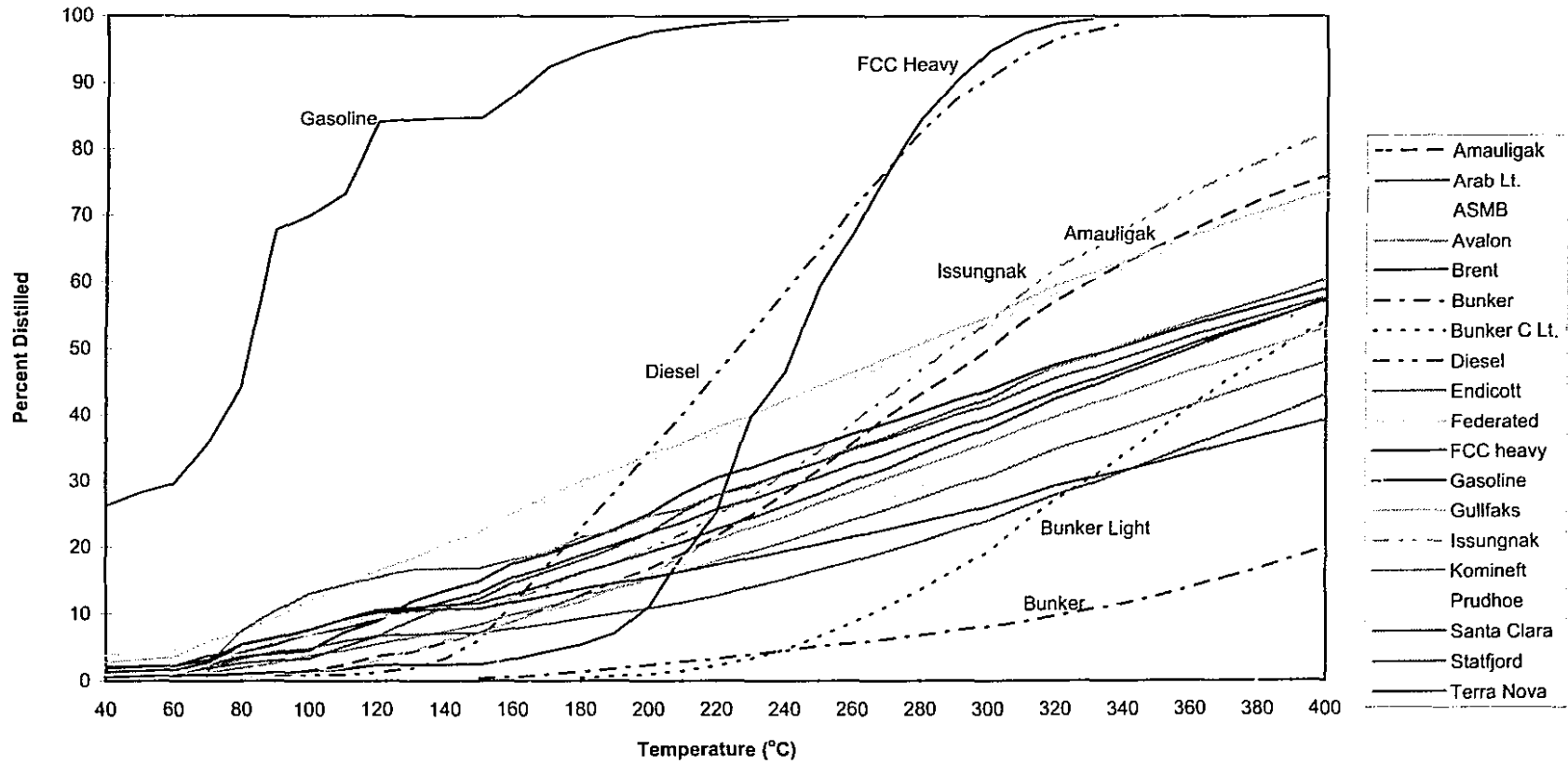
Name	Description	Density	Viscosity
		g/mL at 15°C	mPa.s at 15°C
Amaligak	A light crude oil from Canada's Beaufort Sea	0.871	14
Arabian Light	A common blend of Saudi Arabian oil exported around the world	0.867	14
Avalon	One of the test crude oils from Newfoundland's Hibernia field	0.871	15
ASMB	Alberta Sweet Mixed Blend - A common crude oil in Canada	0.839	9
Brent	A common British, North Sea oil, sometimes exported to Canada	0.833	6
Bunker C	A heavy residual fuel containing distillation residuals	0.98	48000
Bunker C Light	A variation on Bunker C, a refinery residual product, with some diesel-like diluent	0.969	10000
Diesel	Standard automotive/truck diesel fuel	0.809	2
Endicott	Oil from one of the smaller fields on Alaska's North Slope	0.915	84
Federated	A light, sweet Alberta crude that forms the primary feed of Edmonton's refineries	0.826	5
FCC Heavy	A light refinery intermediate product, the "heavy" refers to the number of times the product is re-cycled	0.908	3
Gasoline	Standard automotive non-leaded gasoline	0.709	0.6
Gullfaks	A common Norwegian oil - sometimes exported to Canada	0.882	13
Issungnak	Oil from the Canadian Beaufort Sea, a very light oil	0.849	4
Komineft	Crude oil from the Russian Komi republic	0.85	14
Prudhoe Bay	Oil from the largest field on Alaska's North slope	0.905	26
Santa Clara	A heavy crude oil from Southern California	0.92	300
Statfjord	A common Norwegian oil - sometimes exported to Canada	0.834	7
Terra Nova	One of the oils from the Hibernia field off Newfoundland	0.864	17

Table 8.3 Distillation Data on Oil Used in Study  
(data are percentages boiled off at the specified temperature)

Temp	Amullgak	Arab Lt.	ASMB	Avalon	Brent	Bunker	Bunker C L	Diesel	Endicott	Federated	FCC heavy	Gasoline	Gullfaks	Issungnak	Komineft	Prudhoe	Santa Clara	Statfjord	Terra Nova
40		2.1	3.80						1.00	2.8	0.60	26.2				0.90	1.90		1.40
50		2.2	4.20						1.00	3.2	0.70	28.2				1.00	2.10		1.50
60		2.3	4.70	0.7					1.10	3.6	0.90	29.6				1.10	2.30		1.70
70		3.8	6.60	1.3	2.5				2.00	5.9	0.90	35.6	0.6	1.60	2.6	2.50	3.20	1.9	2.80
80		4.3	8.40	2	3.6				3.30	7.4	1.10	44.4	0.6	4.60	7.5	4.70	5.50	2.7	5.40
90	1	5.4	10.30	2.7	4.1			0.8	4.40	9.4	1.30	67.9	1	5.80	10.5	6.00	6.50	3.1	6.40
100	1.6	7	12.70	3.9	4.6			0.9	4.90	12	1.40	70.1	1.2	7.00	13.1	7.00	7.70	3.4	7.60
110	2.4	7.8	14.20	4.5	7.2			0.9	5.90	14.1	1.80	73.2	2	8.50	14.3	8.40	9.20	5.1	9.20
120	3.7	9.2	16.30	5.5	8.9			1.3	6.70	16.4	2.40	84.1	3	9.70	15.4	9.50	10.20	6.6	10.60
130	4.4	10.6	18.20	6.5	11.9			1.9	7.00	18.3	2.50	84.5	4.6	10.40	16.7	10.00	10.60	9.1	11.00
140	5.8	11.9	20.60	7.4	13.5			3.4	7.10	20.6	2.50	84.7	6.1	10.60	16.8	10.20	10.80	11	11.40
150	7.1	13.1	22.30	8.4	14.8	0.4		6.1	7.10	22.3	2.50	84.7	6.9	10.80	16.8	10.30	10.80	12.2	11.60
160	8.9	15.4	24.80	10	17.5	0.60		11	7.80	25.2	3.30	88.3	9	12.30	18.1	11.30	11.80	14.6	12.90
170	10.9	16.9	27.00	11.1	19	1.00		17	8.50	27.6	4.40	92.5	10.5	13.90	19.3	12.40	12.70	16.3	14.40
180	12.7	18.8	29.20	12.6	20.8	1.40	0.4	23	9.30	30	5.40	94.6	11.8	16.00	21.5	13.70	13.70	18	16.10
190	14.7	20.4	30.90	13.7	22.6	1.80	0.7	28	10.00	31.6	7.10	96.2	13.7	17.60	22.4	14.80	14.50	19.9	17.50
200	16.7	22.2	33.10	15.1	25	2.40	1	34	10.90	34.1	11.10	97.7	15.7	19.90	24.7	16.20	15.40	22.2	19.30
210	19.1	23.7	34.80	16.4	28.1	2.90	1.5	40	11.70	35.7	18.60	98.4	18.7	22.00	25.7	17.40	16.30	25.3	20.80
220	21.7	25.7	37.20	17.9	30.5	3.30	2.3	46	12.70	38.2	25.30	98.9	21.2	24.90	27.9	18.90	17.40	27.9	22.70
230	24.8	27.2	39.10	19.4	32.1	4.00	3.4	53	14.00	40.1	39.90	99.3	23	27.60	29.2	20.50	18.40	29.5	24.40
240	28.1	29	41.20	20.9	33.9	4.50	4.7	59	15.20	42.4	46.50	99.5	24.6	31.20	31.4	22.10	19.50	31.2	26.30
250	31.7	30.6	43.20	22.5	35.4	5.20	6.6	65	16.60	44.4	59.40		26.7	34.50	32.9	23.80	20.50	32.9	28.10
260	35.7	32.5	45.30	24.1	37.2	5.60	8.7	71	17.90	46.4	67.40		28.4	38.90	35.1	25.60	21.60	34.8	30.20
270	39.8	34.1	47.50	25.7	38.8	6.20	11.1	77	19.40	48.7	76.80		30.4	42.70	36.7	27.30	22.70	36.4	31.90
280	43.2	36	49.40	27.4	40.5	6.80	13.6	83	20.90	50.8	84.80		32.2	46.70	38.8	29.10	23.80	38.2	34.10
290	46.2	37.9	51.50	29.2	42.2	7.50	16.4	88	22.50	52.8	90.30		33.9	50.50	40.8	31.00	24.90	40	36.10
300	49.9	39.5	53.40	30.7	43.7	8.1	19.4	91	24.00	54.7	94.90		35.8	53.80	42.4	32.70	26.10	41.5	37.90
310	53.9	41.5	55.90	32.8	45.7	8.80	23.5	94	26.00	57.2	97.50		37.9	58.30	45	34.80	27.70	43.6	40.20
320	57.2	43.5	58.20	34.8	47.6	9.70	27.2	97	27.90	59.5	98.90		39.8	62.00	47.2	36.90	29.30	45.5	42.50
330	60.1	45.1	60.30	36.4	48.9	10.60	30.3	98	29.50	61.2	99.50		41.6	64.70	48.7	38.60	30.40	47	44.20
340	62.8	46.9	61.90	38	50.4	11.50	33.9	99	31.40	63.1			43.2	67.90	50.6	40.50	31.60	48.6	46.20
350	65.3	48.8	63.90	39.7	51.9	12.60	37.6		33.30	65.1			44.9	70.80	52.3	42.40	32.80	50.2	48.10
360	67.7	50.6	65.80	41.4	53.4	13.80	41.3		35.20	66.9			46.6	73.50	53.9	44.30	34.10	51.8	50.00
370	70	52.3	67.60	43.1	54.9	15.30	44.9		37.20	68.8			48.2	76.00	55.6	46.10	35.40	53.3	52.00
380	72.2	53.9	69.40	44.7	56.2	16.70	48		39.00	70.4			49.8	78.10	57.1	47.80	36.70	54.8	53.70
390	74.2	55.5	71.00	46.2	57.5	18.30	51.2		40.90	72			51.3	80.30	58.6	49.60	37.90	56.2	55.50
400	76	57.2	72.60	47.9	58.9	19.90	53.9		43.00	73.7			52.9	82.30	60.3	51.40	39.20	57.7	57.40

Figure 8.1

Plot of Distillation Curves



equation factor versus the distillation percentage at 150, 180 and 200 °C. As can be seen by the regression line, the correlation is high. This same correlation was repeated for both the percentage and weight equation factors and for several different temperatures. The regressions were also repeated without gasoline, which has a higher evaporation rate than the other values and could possibly skew the results. The data are referred to in figures and tables as “full set” when gasoline is included and “partial set” when gasoline is not. The regression coefficients ( $r^2$ ) are listed in Table 8.4. This table shows that regression is highest when the distillation data are near 200 °C. This is illustrated by a plot of the regression coefficients versus temperature as shown in Figure 8.3. This figure shows that the regression coefficient peaks when the distillation temperature is about 180 °C, irrespective of whether the data is for the percentage or weight equations or whether gasoline is included or not. The optimal point, or point at which the regression coefficient is maximum, was found to be 180 °C by using peak functions. These functions were also applied using the program, TableCurve. The results are shown in Figures 8.4 to 8.7. These figures include the rank of the peak equation selected by the program based on the highest regression coefficient, the regression coefficient ( $r^2$ ), the standard error of fit, the F statistic and the constants for the equation.

The percent mass distilled at 180 degrees was used to calculate the relationship between the distillation values and the equation parameters. The equations used were derived from correlations of the data. Figures 8.6 to 8.9 show the correlations for the distillation data (percent distilled) at 180 °C. These figures include the rank of the linear equation selected for this exercise, the regression coefficient ( $r^2$ ), the corrected regression coefficient for the current degrees of freedom, the standard error of fit, the F statistic and the constants for the equation.

The data from those oils which were better fitted with square root equations, diesel, Bunker C light and FCC Heavy Cycle, were separated and calculated separately. Since there are only three data points, the reliability and accuracy are lower than for the other set. Table 8.5 shows the equation parameters determined experimentally and those calculated using the function obtained from the regression. Table 8.6 shows the same data for the square-root equation products.

Figure 8.2

### Correlation of Evaporation Parameters with Distillation Data

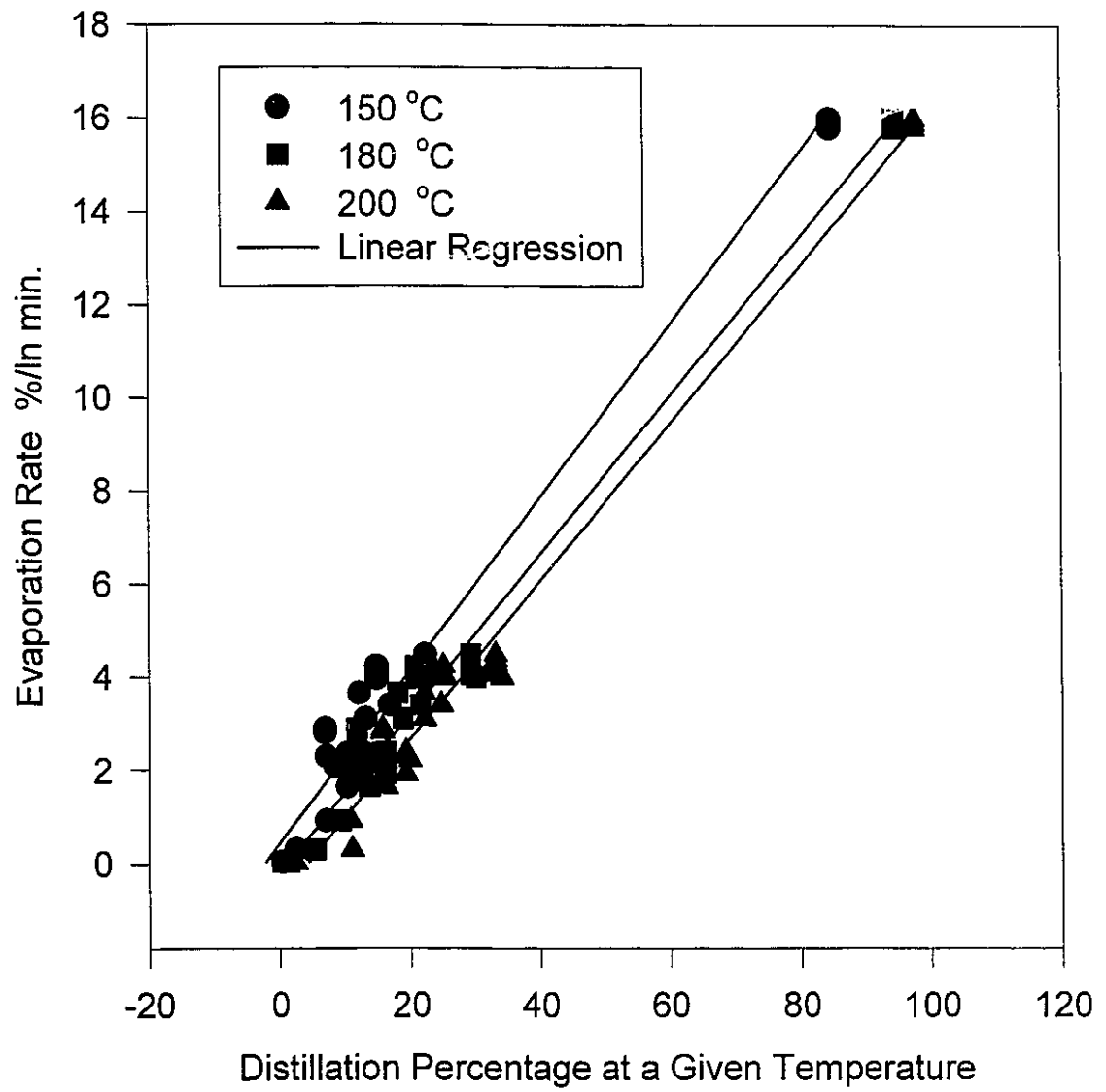


Figure 8.3

### Distillation Regression Coefficients versus Temperature

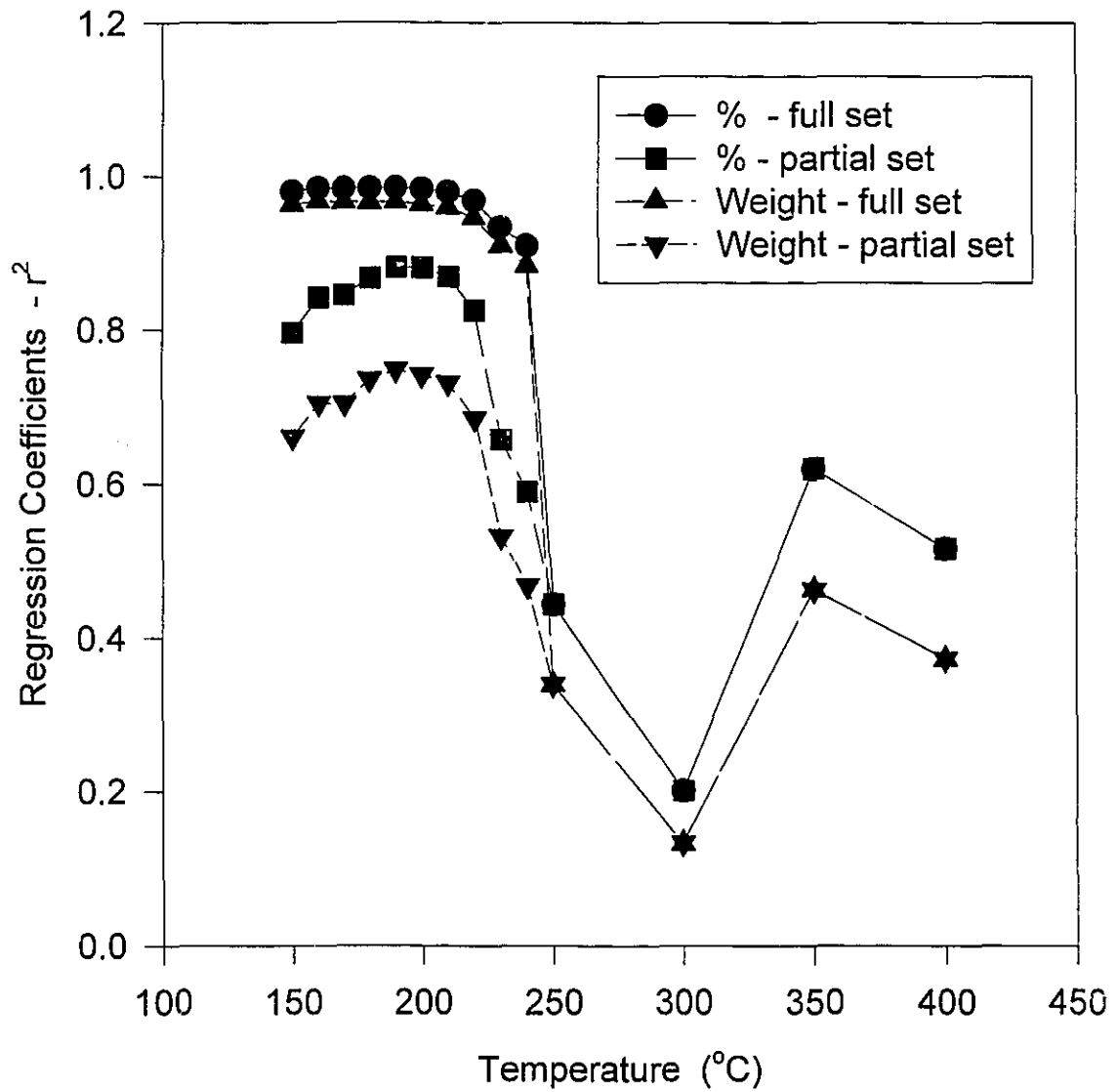


Table 8.4 **Correlation Between Distillation Data and Evaporation**

Boiling Temperature	Percentage		Weight	
	r <sup>2</sup> Percent Full Set	r <sup>2</sup> Percent Partial Set	r <sup>2</sup> Percent Full Set	r <sup>2</sup> Percent Partial Set
150	0.9796	0.7958	0.9626	0.6605
160	0.9839	0.8414	0.9668	0.7043
170	0.984	0.8448	0.9662	0.7037
180	0.9838	0.8665	0.9652	0.7352
190	0.9847	0.8805	0.9659	0.7477
200	0.9828	0.8803	0.9628	0.7413
210	0.9792	0.8684	0.9588	0.7309
220	0.9678	0.825	0.9456	0.6845
230	0.9327	0.6565	0.9089	0.5309
240	0.9085	0.5894	0.8829	0.4673
250	0.4432	0.4432	0.3398	0.3398
300	0.2011	0.2011	0.1332	0.1332
350	0.6194	0.6194	0.4615	0.4615
400	0.5158	0.5158	0.3732	0.3732

Figure 8.4

Comparison of Regression Coefficients  
and Temperatures at Which These Occur  
- Percentage Curves and Full Set

Rank 1 Eqn 8007  $y=a+b*4n/(1+n)^2$   $n=\exp(-(x-c)/d)$  [Logistic]  
 $r^2=0.939$  FitStdErr=0.00797 Fstat=310  
 $a=-73.2$   $b=742$   
 $c=179$   $d=-944$

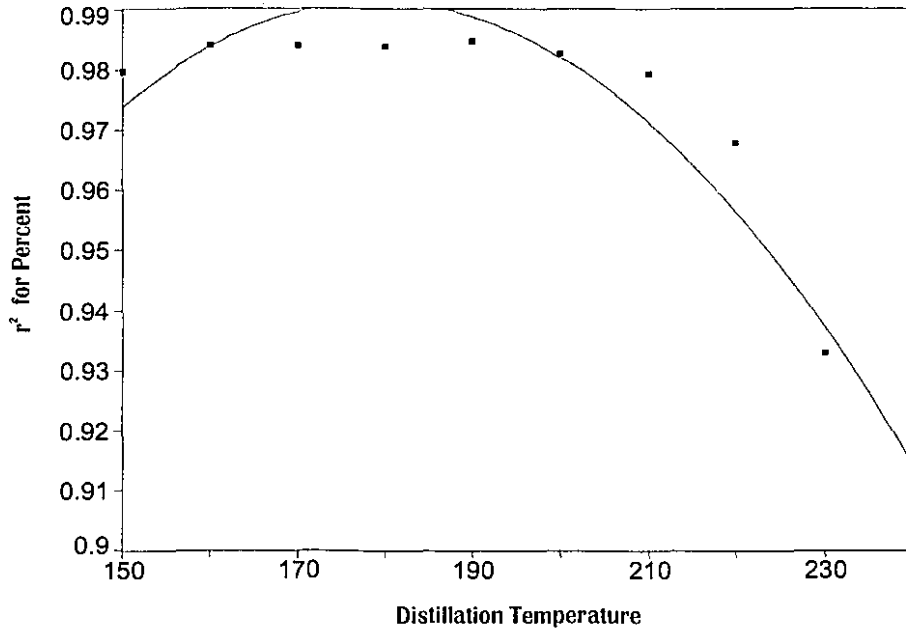


Figure 8.5

Comparison of Regression Coefficients  
and Temperatures at Which These Occur  
- Percentage Curves and Partial Set

Rank 1 Eqn 8008  $y=a+berfc(((x^2-c)/d))$  [Erfc Peak]  
 $r^2=0.917$  FitStdErr=0.0354 Fstat=22.1  
 $a=-8.49$   $b=9.39$   
 $c=185$   $d=327$

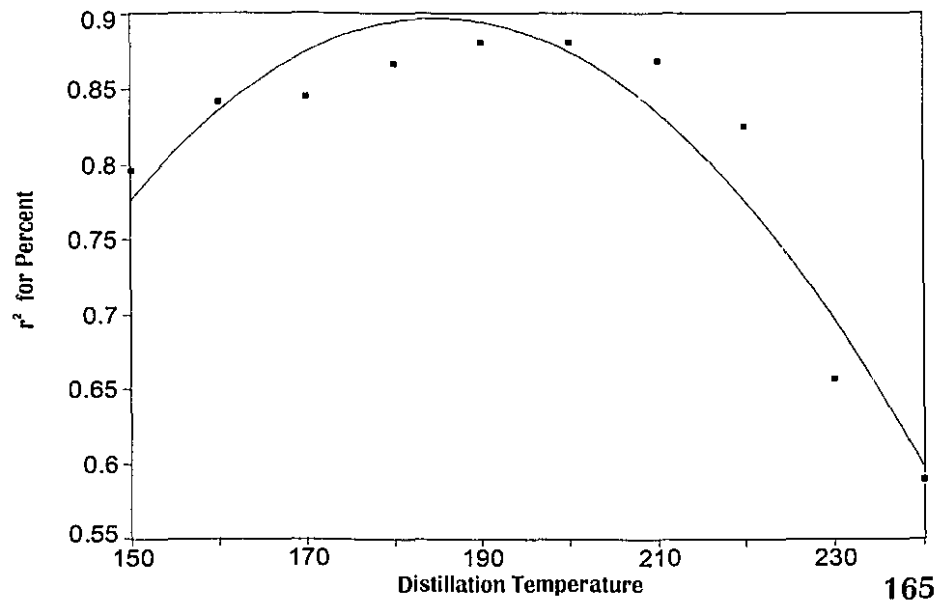


Figure 8.6

Correlation of Percent Equation and  
the Percent Distilled at 180 °C

Rank 1 Eqn 8001 y=linear()

$r^2=0.983$  DF Adj  $r^2=0.982$  FitStdErr=0.533 Fstat=+INF

a=0.165

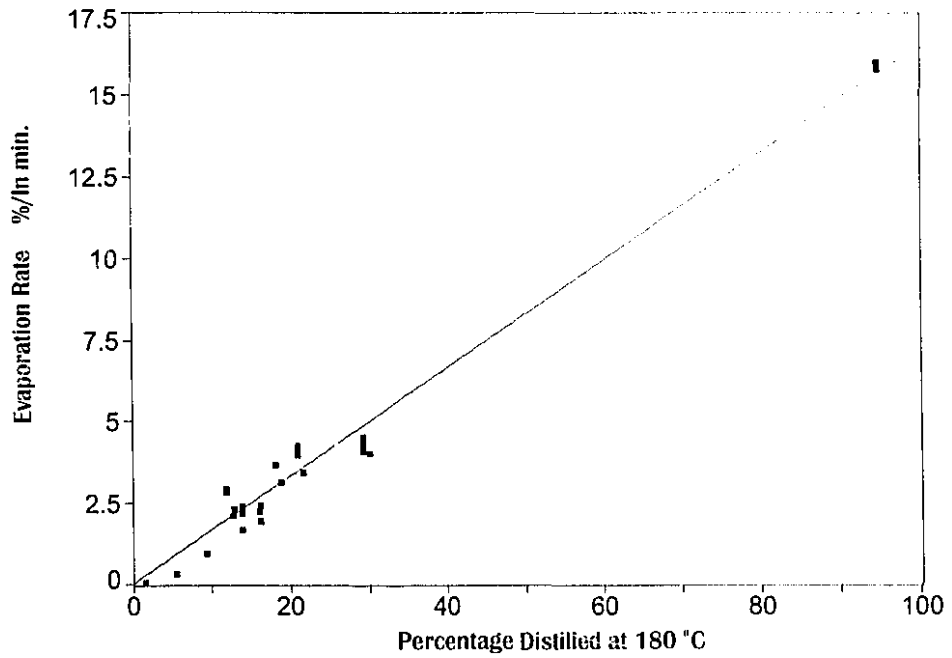


Figure 8.7

Correlation of Weight Equation and  
the Percent Distilled at 180 °C

$r^2=0.964$  DF Adj  $r^2=0.963$  FitStdErr=0.157 Fstat=+INF

a=0.0341

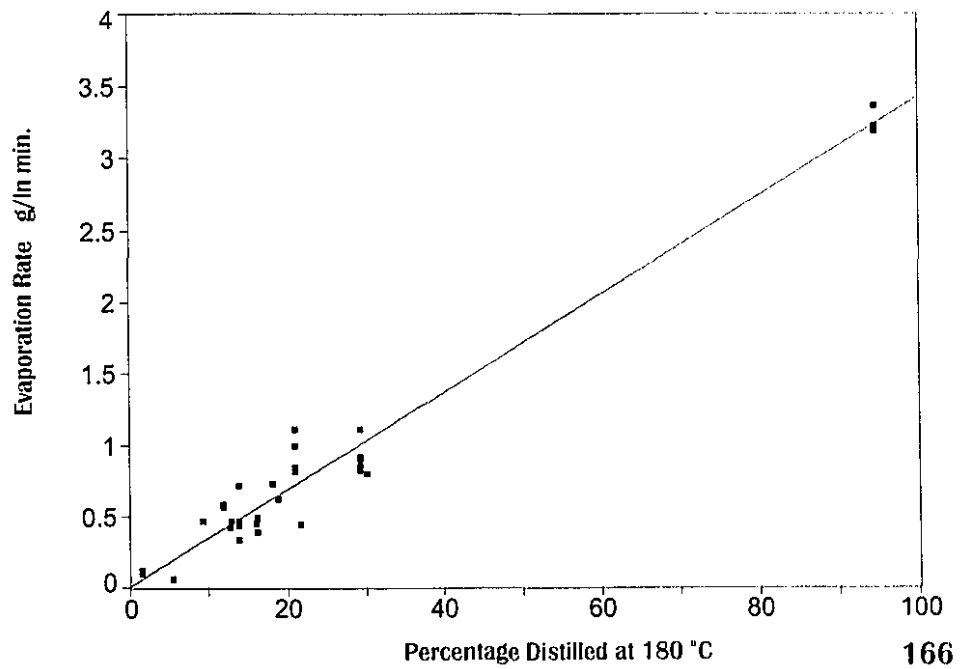


Figure 8.8

Correlation of Percent Equation and the Percent Distilled at 180 °C - Narrow-cut Products

Rank 2 Eqn 8001 y=linear()

$r^2=0.735$  DF Adj  $r^2=0.471$  FitStdErr=0.128 Fstat=+INF

a=0.0254

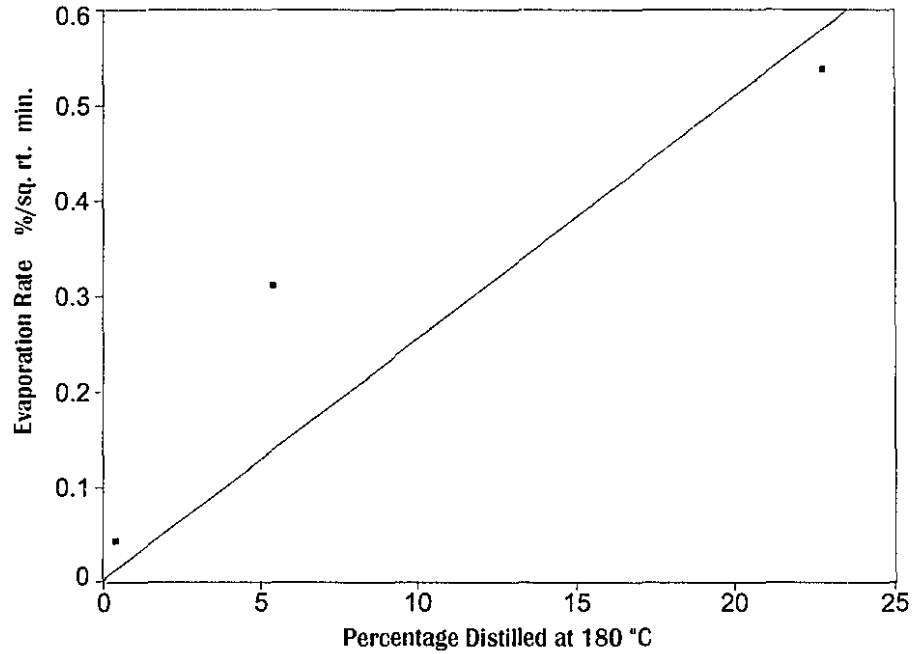
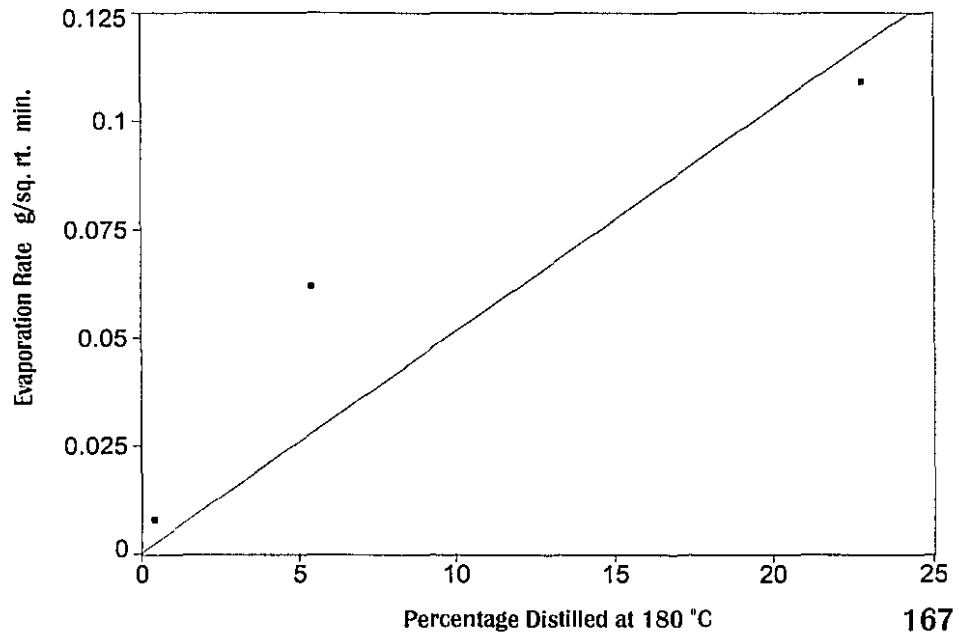


Figure 8.9

Correlation of Weight Equation and the Percent Distilled at 180 °C - Narrow Cut Products

$r^2=0.750$  DF Adj  $r^2=0.501$  FitStdErr=0.0252 Fstat=+INF

a=0.00514



The equations derived from the regressions (parameters from Figures 8.6 to 8.9) are as follows:

For oils that follow a logarithmic equation:

$$\text{Percentage evaporated} = 0.165(\%D) \ln(t) \quad (8.1)$$

$$\text{Weight evaporated} = 0.0341(\%D) \ln(t) \quad (8.2)$$

For oils that follow a square root equation:

$$\text{Percentage evaporated} = 0.0254(\%D)\sqrt{t} \quad (8.3)$$

$$\text{Weight evaporated} = 0.00514(\%D)\sqrt{t} \quad (8.4)$$

where the weight evaporated is in grams per 20 grams evaporated and %D is the percentage (by weight) distilled at 180°C.

These equations can be combined with the equations generated in Chapter 6 to account for the temperature variations:

For oils that follow a logarithmic equation:

$$\text{Percentage evaporated} = [.165(\%D) + .045(T-15)]\ln(t) \quad (8.5)$$

For oils that follow a square root equation:

$$\text{Percentage evaporated} = [.0254(\%D) + .01(T-15)]\sqrt{t} \quad (8.6)$$

where %D is the percentage (by weight) distilled at 180°C.

The distillation data correlates well with the evaporation rate equations except for one or two select oils. The data shown in Table 8.5 and 8.6 show an average variance of calculated equations parameters (or evaporation rates) from the experimental values of 3% for the percent equations and 1.5% for the weight equations. The maximum value is 66% for the percent equation for Endicott oil. Some variance like this is expected by examination of the distillation curves in Figure 8.1. It can be seen here that the slopes of the distillation curves are not constant and furthermore contain some anomalies due to unique blends of constituents. Despite this, most oil evaporation can be predicted much more accurately using this method than by the methods noted in the literature search covered in Chapter 2. The prediction scheme historically used only the slope of a nonstandard boiling curve and historically resulted in errors as large as several hundred percent.

Table 8.5 **Experimental and Calculated Evaporation Rates**

Date	Oil Type	Single % Parameter	Single Wt. Parameter	Distillation 180°C	Calculated Rates			
					Percentage	% Variation	Weight	% Variation
Jan 21	Amauligak	2.3	0.464	12.7	2.1	9	0.43	7
Mar 22	Arabian Lt	3.11	0.621	18.8	3.11	0	0.64	-3
July 2	ASMB	4.05	0.818	29.20	4.82	-19	1	-22
Sept 22	ASMB	4.49	1.11	29.20	4.82	-7	1	10
Nov 1	ASMB	4.28	0.898	29.20	4.82	-13	1	-11
Dec 8	ASMB	4.37	0.85	29.20	4.82	-10	1	-18
Dec 10	ASMB	4.28	0.912	29.20	4.82	-13	1	-10
April 25	ASMB	4.22	0.844	29.20	4.82	-14	1	-18
Jan 11	Avalon	2.08	0.416	12.6	2.08	0	0.43	-3
Jan 10	Brent	4.06	0.812	20.8	3.44	15	0.71	13
Jan 12	Brent	4.03	1.11	20.8	3.44	15	0.71	36
Jan 15	Brent	3.97	0.99	20.8	3.44	13	0.71	28
Jan 18	Brent	4.23	0.846	20.8	3.44	19	0.71	16
Dec 24	Bunker	0.28	0.12	1.40	0.231	18	0.05	58
Dec 29c	Bunker	0.23	0.095	1.40	0.23	0	0.05	47
Jan 18	Endicott	0.926	0.463	9.30	1.54	-66	0.32	31
Jan 3	Federated	3.99	0.797	30	4.96	-24	1.02	-28
Dec 29b	Gasoline	15.9	3.18	94.6	15.63	2	3.23	-2
Mar 30a	Gasoline	16	3.36	94.6	15.63	2	3.23	4
Mar 30b	Gasoline	15.8	3.22	94.6	15.63	1	3.23	0
Jan 14	Gulfaks	2.89	0.58	11.8	1.95	33	0.4	31
Mar 10	Gulfaks	2.81	0.562	11.8	1.95	31	0.4	29
Jan 20c	Issungnak	2.23	0.448	16.00	2.64	-18	0.55	-23
Dec 23	Komineff	3.4	0.438	21.5	3.55	-4	0.73	-67
Jan 1	Prudhoe	1.65	0.33	13.70	2.26	-37	0.47	-42
Jan 3	Prudhoe	2.17	0.434	13.70	2.26	-4	0.47	-8
Jan 28b	Prudhoe Bay	2.36	0.707	13.70	2.26	4	0.47	34
Feb 5	Santa Clara	2.3	0.461	13.70	2.26	2	0.47	-2
Feb 15	Statfjord	3.65	0.73	18	2.97	19	0.61	16
Jan 22	Terra Nova	1.93	0.385	16.10	2.66	-38	0.55	-43
Jan 26	Terra Nova	2.39	0.482	16.10	2.66	-11	0.55	-14

Table 8.6 **Experimental and Calculated Rates For Narrow-Cut Products**

Date	Oil Type	Single % Parameter	Single Wt. Parameter	Distillation 180 °C
March 26	Bunker C Light	0.0422	0.008	0.4
March 30c	Diesel	0.538	0.109	22.8
April 14	FCC heavy	0.31	0.062	5.40

Date	Oil Type	Calculated Rates			
		Percentage	% Variation	Weight	% Variation
March 26	Bunker C Light	0.01	76	0	100
March 30c	Diesel	0.58	-8	0.12	-10
April 14	FCC heavy	0.14	55	0.03	52

The high correlation of distillation data and evaporation data suggest a strong relationship between the processes. Distillation does not involve the influence of environmental relationships such as boundary-layer regulation. This is suggestive that the evaporation of oil follows similar processes and that the evaporation process is largely (if not exclusively) governed by oil properties rather than environmental properties.

The utility of the calculation scheme is illustrated by taking two sets of data at random (chosen were ASMB and gasoline, taken respectively on December 8, 1993, and March 20, 1995). The actual data, the best curve fit, using a single logarithmic equation and the predicted data using the distillation values were plotted as shown in Figures 8.10 and 8.11. Figure 8.10 shows the gasoline data, which were recent data and where the test run was performed in a constant temperature chamber. The actual data, curve fit and the predicted values are very close. Figure 8.11 shows the ASMB data. The fit is also good.

## 8.5 Conclusions

The equation parameters found experimentally for the evaporation of oils can be related to commonly-available distillation data for the oil. Specifically, it has been found that the distillation percentage at 180 °C correlates well with the equation parameters. Regression coefficients ( $r^2$ ) range from 0.74 to 0.98, depending on the type of equation and the selection of data. Relationships enabling calculation of evaporation equations directly from distillation data have been developed:

For oils that follow a logarithmic equation:

$$\text{Percentage evaporated} = 0.165(\%D) \ln(t) \quad (8.1)$$

$$\text{Weight evaporated} = 0.0341(\%D) \ln(t) \quad (8.2)$$

For oils that follow a square root equation:

$$\text{Percentage evaporated} = 0.0254(\%D)\sqrt{t} \quad (8.3)$$

$$\text{Weight evaporated} = 0.00514(\%D)\sqrt{t} \quad (8.4)$$

where the weight evaporated is in grams per 20 grams evaporated and %D is the

Figure 8.10

### Comparison of Gasoline Evaporation- Data Taken March 20, 1995

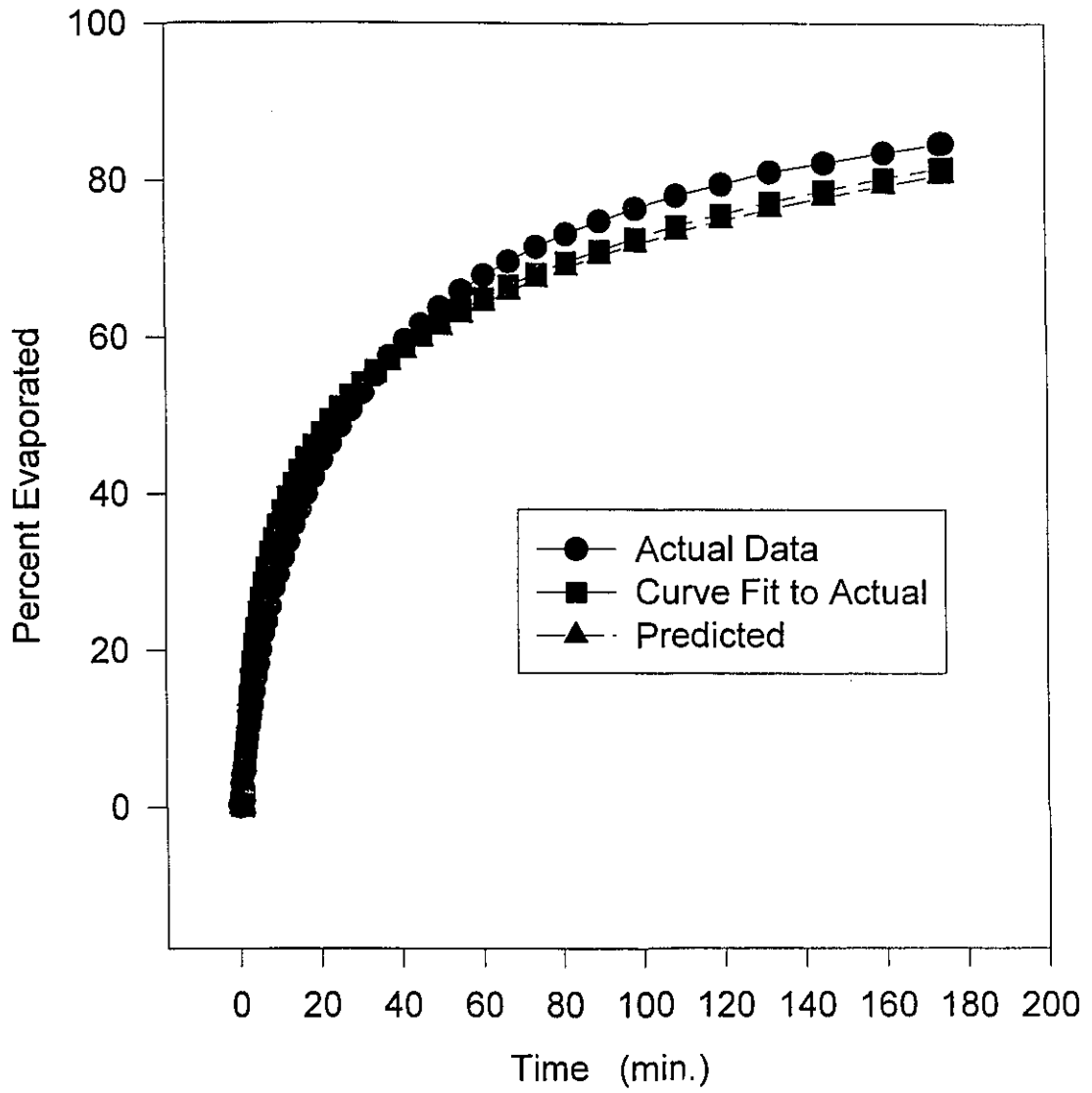
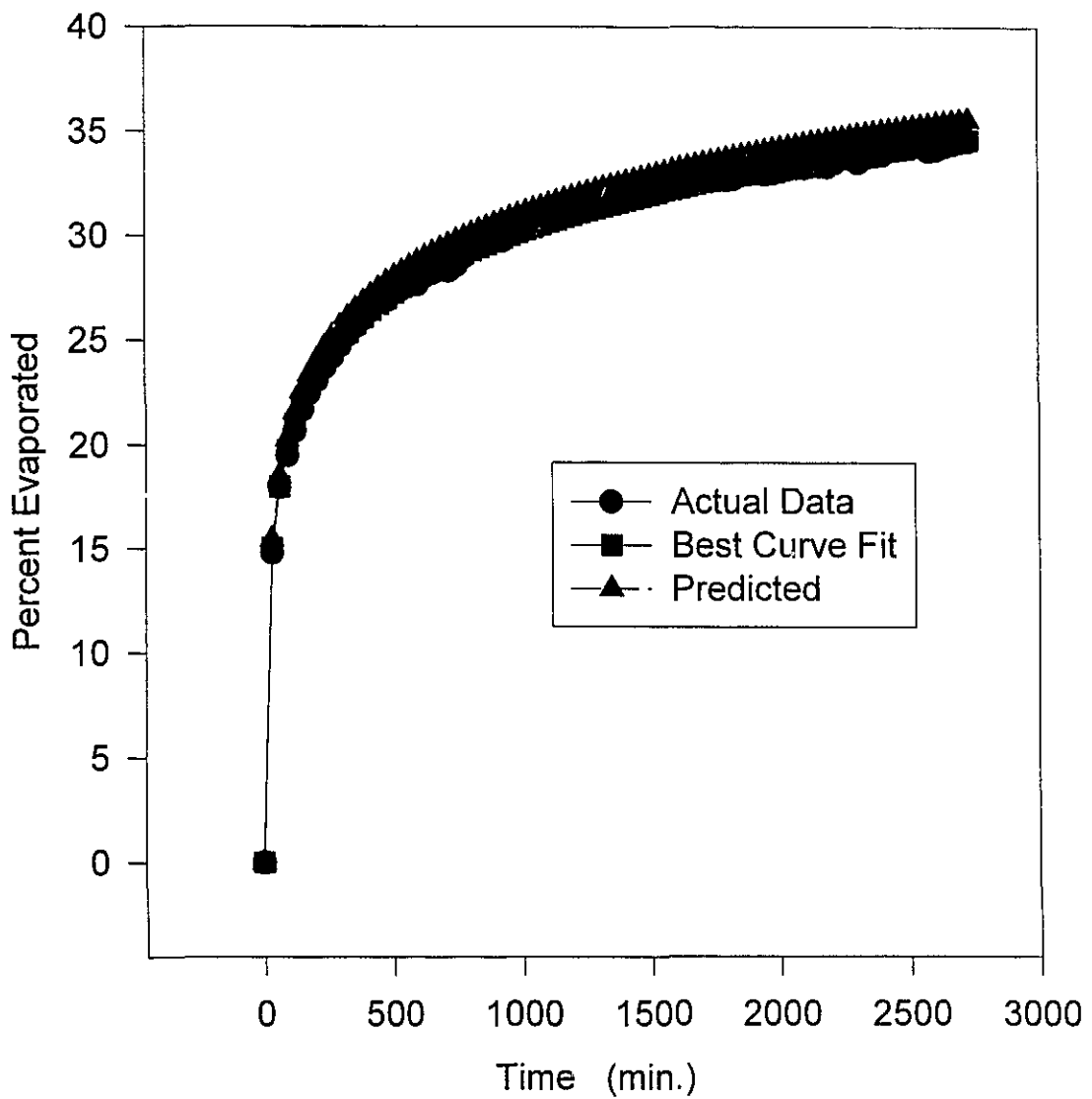


Figure 8.11

### Comparison of ASMB Evaporation-Data Taken December 8, 1993



percentage (by weight) distilled at 180°C.

These equations were combined with the equations generated to account for the temperature variations:

For oils that follow a logarithmic equation:

$$\text{Percentage evaporated} = [.165(\%D) + .045(T-15)]\ln(t) \quad (8.5)$$

For oils that follow a square root equation:

$$\text{Percentage evaporated} = [.0254(\%D) + .01(T-15)]\sqrt{t} \quad (8.6)$$

The high correlation of distillation data and evaporation data suggests that the two processes are analogous and that evaporation, like distillation, is largely governed by intrinsic oil properties rather than environmental properties such as boundary-layer factors.

### References

Whiticar, S., M. Bobra, M.F. Fingas, P. Jokuty, P. Liuzzo, S. Callaghan, F. Ackerman and J. Cao, *A Catalogue of Crude Oil and Oil Product Properties (1992 Edition)*, Environment Canada Manuscript Report Number EE-144, Ottawa, Ontario, 643 p., 1993.

## Chapter 9 Overall Conclusions

### Overall Conclusions

An examination of thermodynamic literature shows that the volume change and thus the evaporation rate is directly related to the temperature and the vapour pressure, and inversely to saturation vapour pressure.

Literature on the physics and mathematical modelling of oil spill evaporation has been reviewed (Fingas, 1995). Two basic approaches to the mechanism of evaporation are proposed in the literature, first-order decay and boundary-layer limited. Some workers propose a first-order decay process which yields a logarithmic decrease in evaporation with time. Most workers use boundary-layer equations adapted from water evaporation work. These equations predict a constant evaporative mass-transfer rate dependent on scale size and wind turbulence levels.

The most common approach in the literature is the use of the Mackay equations (Mackay and Matsugu, 1973; Stiver and Mackay, 1984) derived from earlier water evaporation work by Sutton (Sutton, 1934):

$$K_m = 0.0292 U^{0.78} X^{-0.11} Sc^{-0.67} \quad (9.1)$$

where  $K_m$  is the mass transfer coefficient in units of mass per unit time,  $U$  is wind speed,  $Sc$  is the Schmidt number and  $X$  is the scale size of evaporating area.

Mackay and Matsugu noted that for hydrocarbon mixtures the evaporation process is more complex, being dependent on the liquid diffusion characteristics, a liquid phase diffusion resistance being present. The mass transfer rate shown in (9.1) above is used in the following to calculate the molar evaporative flux:

$$N = KAP/(RT) \quad (9.2)$$

where  $N$  is the evaporative molar flux,  $A$  is the area,  $K$  is the mass transfer coefficient under the prevailing wind,  $P$  is the vapour pressure of the bulk liquid,  $R$  is the universal gas constant and  $T$  is the temperature (K).

This equation is not used frequently in actual practice, and a logarithmic equation was proposed to have the same form as (9.2) above:

$$F_v = (T/K_1) \ln (1 + K_1\theta/T) \exp(K_2 - K_3/T) \quad (9.3)$$

where  $F_v$  is the fraction evaporated,  $\theta$  is the evaporative exposure or  $Kat/V_o$  and  $K_{1,2,3}$  are empirical constants.

Variations of all the above equations have been used extensively by many other experimenters and for model application. Tests of this equation show deviations from empirical results, however, explanations for such deviations vary. The equations developed by Mackay and co-workers can be implemented in a variety of ways. No extensive empirical studies of oil evaporation are published in the literature.

Extensive experimentation was conducted on oil evaporation in this study. Results show that pure compounds evaporate in a linear manner. Most crude oils evaporate in a logarithmic manner, that is the loss of mass is logarithmic with time. The study of the nature of the evaporative curve shows that 'best' fit largely depends on the number of components evaporating simultaneously. Pure compounds evaporate in a direct linear fashion, as has been known. Mixtures of components between about 3 and 7 evaporate as a square root with time. Logarithmic equations result when approximately 10 or more components evaporate simultaneously.

The results of the experiments described below, show that oil is not strictly boundary-layer regulated:

- 1) A study of the evaporation rate of several oils with increasing wind speed shows that, unlike water, the evaporation rate does not change significantly except for the initial step over 0-level wind.
- 2) Increasing area does not significantly change oil evaporation rate. This is directly contrary to the prediction resulting from boundary-layer regulation.
- 3) Decreasing thickness does not increase oil evaporation rate.
- 4) The volume or mass of oil evaporating correlates with the evaporation rate. This is a strong indicator of the lack of boundary-layer regulation because with water, volume and rate do not correlate.
- 5) Evaporation of pure hydrocarbons with and without wind (turbulence) shows that compounds larger than nonane and decane are not boundary-layer regulated. Most oil and hydrocarbon products consist of compounds larger than these two and thus would not

be expected to be boundary-layer regulated.

6) Evaporation of pure hydrocarbons with a highly-weathered oil residue, with and without wind, shows that the evaporative behaviour is not boundary-layer regulated. This shows that the effect is not simply an artifact of oil composition.

Having concluded that boundary-layer regulation is not applicable to oil evaporation, it remains to explain why this is so. The reason is twofold: oil evaporation, especially after an initial time period, is relatively slow compared to the threshold where it is boundary-layer regulated; and the threshold to boundary-layer regulation for oil evaporation is much higher than that for water. These two factors were highlighted by three comparisons using the experimental data:

- 1) A comparison of the length of time that oils exceeds the boundary-layer limit, taken as the maximum evaporation rate when there is no wind, shows that the length of time during which evaporation rate in the presence of wind exceeds the boundary-layer limit, can be as short as 2 minutes to a maximum of 46 minutes. This represents a very small fraction of time to significantly evaporate an oil (in these experiments, typically 2000 to 8000 minutes). For most of the time, the evaporation rate is below the boundary-layer regulated rate.
- 2) A comparison of the maximum rates of evaporation for some oils, gasoline and water, in the absence of wind, shows that the oil rates exceed that for water by as much as an order of magnitude (water=.034 g/min, ASMB=0.75 g/min., and gasoline=.34 g/min.; all under the specific conditions noted), and
- 3) The saturation concentration of several hydrocarbons in air reveals that some hydrocarbon saturation concentrations in air can be greater than that of water by as much as two orders-of-magnitude.

Oil evaporation can be explained as follows: If evaporation occurs in a turbulent atmosphere, the time that the evaporation rate exceeds the boundary-layer limited rate is very short. In the absence of turbulence, evaporation will proceed at the limitation rate then drop off to a similar, but higher rate than the turbulent rate. The difference in time is a matter of minutes, as explained above, and the end result will not be noticeable to an observer. Thus, it is stated that oil and petroleum evaporation is not strictly boundary-

layer regulated.

The fact that oil evaporation is not strictly boundary-layer regulated implies a simplistic evaporation equation will suffice to describe the process. The following processes do not require consideration: wind velocity, turbulence level, area, thickness, and scale size. The factors important to evaporation are time and temperature.

Literature indicates that the relation of evaporation rate and temperature to be  $\log T/T$  or possibly  $T^2$  (Stiver and Mackay, 1984). An examination of thermodynamics reveals that the relationship may be linear. Experimental evidence confirms that the relationship between evaporation rate and temperature is linear.

The rate of evaporation change with temperature is similar for the crude oils tested. Data from Diesel fuel and Bunker C light were fitted with square root equations, and show similar behaviour than the other test oils, all of which were best fit with logarithmic equations. Prediction methods for diesel fuel and Bunker C light would require separate analysis.

The change of evaporation rate (both as percentage and as absolute weight) can be predicted using two entirely different methods. First, the rate of temperature change correlates with the values of the evaporation rate at 15 °C. Equations derived from this correlation yield predictions that are within about 10% of their empirical counterparts. The best fit equations are:

$$\text{percentage equation factor} = (B + 0.045(T-15)) \quad (9.4)$$

and  $\text{weight equation factor} = (B + 0.01(T-15)) \quad (9.5)$

where B is the equation parameter at 15°C and T is temperature in Celsius.

Second, the slopes and intercepts of the temperature equations correlate strongly with oil distillation data. These correlations yield predictions of the temperature-dependant evaporation equations that show good agreement with their empirical counterparts. The variability of agreement ranges from a high of about 50% for Gullfaks oil to a low of about 3% variance for ASMB. The equations derived from this correlation are:

$$\text{percentage equation factor} = 0.161 D + 0.00262 TD \quad (9.6)$$

and  $\text{weight equation factor} = 0.329 D + 0.00502 TD \quad (9.7)$

where D is the percent distilled at 140 °C.

The correlations with distillation data indicate that evaporation is a similar or related process to distillation. The correlation with the evaporation data itself at 15 °C shows that the temperature effect is somewhat similar for most oils. This also indicates that the evaporation rate itself is correlated with the variance with temperature, that is, the higher the evaporation rate, the higher the change with temperature.

Experiments were conducted outdoors to test the laboratory simulation. The results from the outdoors experiments are very close to those achieved under laboratory conditions. This confirms that the methods and conditions in the laboratory are consistent with those outdoors. The outdoors results can be predicted using equations developed in the laboratory with only temperature and time as variables. Wind in the outdoors experiment does not significantly change the evaporation rate. This also confirms that the oil evaporation is not strictly boundary-regulated.

The equation parameters found experimentally for the evaporation of oils can be related to commonly-available distillation data for the oil. Specifically, it has been found that the distillation percentage at 180 °C correlates well with the equation parameters. Regression coefficients ( $r^2$ ) range from 0.74 to .98, depending on the type of equation and the selection of data. Relationships enabling calculation of evaporation equations directly from distillation data have been developed:

For oils that follow a logarithmic equation:

$$\text{Percentage evaporated} = 0.165(\%D) \ln(t) \quad (9.8)$$

$$\text{Weight evaporated} = 0.0341(\%D) \ln(t) \quad (9.9)$$

For oils that follow a square root equation:

$$\text{Percentage evaporated} = 0.0254(\%D)\sqrt{t} \quad (9.10)$$

$$\text{Weight evaporated} = 0.00514(\%D)\sqrt{t} \quad (9.11)$$

where the weight evaporated is in grams per 20 grams evaporated, %D is the percentage (by weight) distilled at 180°C and t is the time in minutes.

These equations were combined with the equations generated to account for the temperature variations:

For oils that follow a logarithmic equation:

$$\text{Percentage evaporated} = [0.165(\%D) + 0.045(T-15)]\ln(t) \quad (9.12)$$

For oils that follow a square root equation:

$$\text{Percentage evaporated} = [0.0254(\%D) + 0.01(T-15)]\sqrt{t} \quad (9.13)$$

The high correlation of distillation data and evaporation data suggests that the two processes are analogous and that evaporation, like distillation, is largely governed by intrinsic oil properties rather than environmental properties such as boundary-layer factors.

The results have practical application in oil spill prediction and modelling. The simple equations presented here can be applied using readily-available data such as sea temperature and time. Old equations required oil vapour pressure, specialized distillation data, spill area, wind speed and mass transfer coefficients, all of which are difficult to obtain.

## References

Fingas, M.F., "The Evaporation of Oil Spills", *Journal of Hazardous Materials*, Vol 42, pp. 157-175, 1995.

Mackay, D., and R.S. Matsugu, "Evaporation Rates of Liquid Hydrocarbon Spills on Land and Water", *Canadian Journal of Chemical Engineering*, Vol. 51, Canadian Society for Chemical Engineering, Ottawa, pp 434-439, 1973.

Stiver, W., and D. Mackay, "Evaporation Rate of Spills of Hydrocarbons and Petroleum Mixtures", *Environmental Science and Technology*, Vol. 18, American Chemical Society, Washington, D.C., pp 834-840, 1984.

Sutton, O.G., "Wind Structure and Evaporation in a Turbulent Atmosphere", *Proceedings of the Royal Society of London*, A 146, pp. 701-722, 1934.

## Recommendations for Further Research

Specific recommendations for further research include:

### 1. Studies into boundary layer regulation

a) It was concluded that oil was not strictly boundary-layer regulated. However, there should be a thickness at which boundary-layer regulation becomes important. Studies on what this thickness is for varying types of oil and how this relates to oil properties, might be interesting. Such research would not specifically useful for oil prediction but would be informative from a physics point of view.

b) The thesis showed that the saturation concentration of substances in air was not exclusive. It is not known if the overall saturation concentration is additive or not. This information would be useful in understanding the evaporation of multi-component liquids.

c) The boundary-layer regulated limits of oil and petroleum change with each component mixture, as illustrated by the very different saturation concentrations of the pure components. Further work on this aspect, including modelling of the specific boundary-layer regulation level past the initial evaporation phase, could shed light on the processes involved.

### 2. Studies into oil evaporation in general

a) A study of long-term evaporation can be done to ascertain how components evaporate on the very long term. Several experiments were conducted with evaporation times of 5 to 9 days, however, it would be instructive to see if times greater than 30 days affect the curvature of the evaporation rate or if the curves deviate from logarithmic or square root functions.

b) Studies of the application of the thesis findings to oil spill models, might be instructive. Although, the data has already been used by Environment Canada to predict the behaviour of actual spills, extensive use would yield insight about applying equations in real time.